



Industria Textilă

ISSN 1222-5347

2/2021

ISI rated journal, included in the ISI Master Journal List of the Institute of Science Information, Philadelphia, USA, starting with vol. 58, no. 1/2007, with impact factor 0.504 and AIS 0.046 in 2018.

The journal is indexed by CrossRef, starting with no. 1/2017 having the title DOI: <https://doi.org/10.35530/IT>.

Edited in 6 issues per year, indexed and abstracted in:
Science Citation Index Expanded (SCIE), Materials Science Citation Index®, Journal Citation Reports/Science Edition, World Textile Abstracts, Chemical Abstracts, VINITI, Scopus, Toga FIZ teknik, EBSCO, ProQuest Central, Crossref
Edited with the Romanian Ministry of Research, Innovation and Digitalization support

INDUSTRIA TEXTILĂ EDITORIAL BOARD:

Dr. Eng. CARMEN GHITULEASA
GENERAL MANAGER
National R&D Institute for Textiles and Leather,
Bucharest, Romania

Dr. Eng. SABINA OLARU
CS II, EDITOR IN CHIEF
National R&D Institute for Textiles and Leather,
Bucharest, Romania

Dr. Eng. EMILIA VISILEANU
CS I, HONORIFIC EDITOR
National R&D Institute for Textiles and Leather,
Bucharest, Romania

Prof. XIANYI ZENG
Ecole Nationale Supérieure des Arts et Industries
Textiles (ENSAIT), France

Prof. Dr. Eng. LUIS ALMEIDA
University of Minho, Portugal

Prof. Dr. STJEPANOVIĆ ZORAN
University of Maribor, Faculty of Mechanical
Engineering, Department of Textile Materials
and Design, Maribor, Slovenia

Lec. ALEXANDRA DE RAEVE
HOGENT University of Applied Science
and Arts, Belgium

Prof. LUBOS HES
PhD, MSc, BSc, Department of Textile Evaluation,
Technical University of Liberec, Czech Republic

Prof. Dr. Eng. ERHAN ÖNER
Marmara University, Turkey

Prof. Dr. S. MUGE YUKSELOGLU
Marmara University, Turkey

Dr. MAZARI ADNAN
ASSISTANT PROFESSOR
Department of Textile Clothing, Faculty of Textile
Engineering, Technical University of Liberec
Czech Republic

Dr. AMINODDIN HAJI
PhD, MSc, BSc, Textile Chemistry and Fiber Science
ASSISTANT PROFESSOR
Textile Engineering Department
Yazd University, Yazd, Iran

Prof. Dr. Eng. CARMEN LOGHIN
PRO-RECTOR
Faculty of Industrial Design and
Business Management, Technical University
"Gh. Asachi", Iași, Romania

Associate Prof. Dr. Eng. MARIANA URSACHE
DEAN
Faculty of Industrial Design and
Business Management, Technical University
"Gh. Asachi", Iași, Romania

Prof. Dr. GELU ONOSE
CS I
"Carol Davila" University of Medicine
and Pharmacy, Bucharest, Romania

Prof. Dr. DOINA I. POPESCU
The Bucharest University of Economic Studies,
Bucharest, Romania

Prof. Dr. MARGARETA STELEA FLORESCU
The Bucharest University of Economic Studies,
Bucharest, Romania

JIE HONG

Research on sound absorption properties of hydrogenated carboxyl nitrile rubber/four-hole hollow polyester fibre composites 117–125

ALPTEKIN ULUTAŞ, CAN BÜLENT KARAKUŞ

Location selection for a textile manufacturing facility with GIS based on hybrid MCDM approach 126–132

ANA M. RODES-CARBONELL, JOSUÉ FERRI, EDUARDO GARCIA-BREIJO, EVA BOU-BELDA

A preliminary study of printed electronics through flexography impression on flexible substrates 133–137

ELENA-CORNELIA MITRAN, IRINA-MARIANA SANDULACHE, LUCIA-OANA SECAREANU, MIHAELA CRISTINA LITE,

OVIDIU GEORGE IORDACHE, ELENA PERDUM, GABRIEL-LUCIAN RADU
Assessing the presence of pesticides in modern and contemporary textile artifacts using advanced analysis techniques 138–143

FANGTAO RUAN, CHENGLONG XIA, LI YANG, ZHENZHEN XU, FEIYAN TAO

Effect of filaments diameter on the mechanical properties of wrap hybrid CFRP 144–148

RALUCA MARIA AILENI, LAURA CHIRIAC, DOINA TOMA

Statistical analysis of the 3D electroconductive composites based on copper and graphene 149–155

MIHA POZDEREC, DUNJA ŠAJN GORJANC

Permeability properties of woven fabrics containing two-ply fancy yarns 156–167

FREDERICK FUNG, LUBOS HES, ROSHAN UNMAR, VLADIMIR BAJZIK

Thermal and evaporative resistance measured in a vertically and a horizontally oriented air gap by Permetest skin model 168–174

MUHAMMAD ZAHID NAEEM, CRISTI SPULBAR, ABDULLAH EJAZ, RAMONA BIRAU, TIBERIU HORAȚIU GORUN, CRISTIAN REBEGEA

Measuring the effectiveness of signals approach in an early warning system for crises and its impact on textile industry: a case study for South-East Asia 175–190

QIAN XU, HUA CHENG, YABIN YU

Analysis and forecast of textile industry technology innovation capability in China 191–197

IVAN MILOJEVIĆ, SNEŽANA KRSTIĆ, MIHAILO ĆURČIĆ

Optimisation of accounting model of inventory management in the textile industry 198–202

CENGIZ ONUR ESER, ARZU YAVAS

Effect of silk sericin pre-treatment on dyeability of woollen fabric 203–209

STEFAN-CLAUDIU CAESCU, FLORINA BOTEZATU, RALUCA-GIORGIANA CHIVU, IONUT-CLAUDIU POPA, MARGARETA STELA FLORESCU

The impact of online marketing on the use of textile packaging: an approach to consumer behaviour 210–216

YANG YANG, YU XIN, WANG XUNGAI, LIU XIN, ZHANG PEIHUA

Thermal comfort properties of cool-touch nylon and common nylon knitted fabrics with different fibre fineness and cross-section 217–224

RIADH ZOUARI, SONDES GARGOUBI, EMILIA VISILEANU

Effect of plasma grafting with Hexamethyldisiloxane on comfort and flame resistance of cotton fabric 225–230

Scientific reviewers for the papers published in this number:

- Assoc. Prof.* Qionxia Qin, University of Kentucky, School of Agriculture Economics, United States of America
Assist. Prof. Shi Jian, Akita Prefectural University, Faculty of Systems Science and Technology, Japan
Assoc. Prof. PhD Msc. Bsc. Aminoddin Haji, Yazd University, Textile Engineering Department, Iran
PhD. Zhu Chunhong, Shinshu University, Faculty of Textile Science and Technology, Japan
Prof. Dr. Lubos Hes, Technical University of Liberec, Faculty of Textile Engineering, Czech Republic
Prof. Jose Ivan Medeiros, Federal University of Rio Grande do Norte, Departamento de Engenharia Têxtil Natal, Brazil
Assoc. Prof. Andreja Rudolf, University of Maribor, Department of Textile Materials and Design, Faculty of Mechanical Engineering, Slovenia
Prof. Wu Hailiang, Xi'an Polytechnic University, China
Dr. Hamza Ajmal, University of Waikato, New Zealand
Assoc. Prof. Dragana Kopitar, University of Zagreb, Department of Textile Design and Management, Croatia
Prof. Marmarali Arzu, EGE University, Turkey
Assoc. Prof. Jiang Hui, University of Finance and Administration Prague, Czech Republic
PhD. Bogdana Mitu, National Institute for Lasers, Plasma and Radiation Physics, Romania
Assoc. Prof. Dr. Jatin Trivedi, Amity University Mumbai, Faculty of Finance, India
Assoc. Prof. Dragisa Stanujkic, University of Belgrade, Technical Faculty in Bor, Serbia
Assoc. Prof. Liliana Indrie, The University of Oradea, Faculty of Energy Engineering, Department of Textiles, Romania
Dr. Bal Kausik, University of Kolkata, India
Assoc. Prof. Darjan Karabasevic, University Business Academy in Novi Sad, Faculty of Applied Management, Economics and Finance, Serbia
PhD. Goran Buturac, The Institute of Economics, Croatia
Senior Lec. Yordanka Angelova, Technical University of Gabrovo, Bulgaria
Assoc. Prof. Gabrijele Popovic, Megatrend University in Belgrade, Faculty of Management in Zajecar, Serbia
PhD. Dragomir Djordjević, University of Business Studies, Bosnia and Herzegovina
Assoc. Prof. Dr. Muhammad Mohsin, University of Engineering and Technology Lahore, Textile Engineering Department, Pakistan

EDITORIAL STAFF

- General Manager:** Dr. Eng. Carmen Ghițuleasa
Editor-in-chief: Dr. Eng. Sabina Olaru
Onorific editor: Dr. Eng. Emilia Visileanu
Graphic designer: Florin Prisecaru
Translator: Cătălina Costea
Site administrator: Constantin Dragomir
e-mail: industriatextila@incdtp.ro

INDUSTRIA TEXTILA journal, edited by INCDTP BUCHAREST, implements and respects Regulation 2016/679/EU on the protection of individuals with regard to the processing of personal data and on the free movement of such data ("RGPD"). For information, please visit the Personal Data Processing Protection Policy link or e-mail to DPO rpd@incdtp.ro

Aknowledged in Romania, in the Engineering sciences domain, by the National Council of the Scientific Research from the Higher Education (CNCSIS), in group A
Journal edited in collaboration with **Editura AGIR**, 118 Calea Victoriei, sector 1, Bucharest, tel./fax: 021-316.89.92; 021-316.89.93; e-mail: editura@agir.ro, www.edituraagir.ro

Research on sound absorption properties of hydrogenated carboxyl nitrile rubber/four-hole hollow polyester fibre composites

DOI: 10.35530/IT.072.02.1547

JIE HONG

ABSTRACT – REZUMAT

Research on sound absorption properties of hydrogenated carboxyl nitrile rubber/four-hole hollow polyester fibre composites

A series composite was prepared by adding hydrogenated carboxyl nitrile rubber (abbreviated HXNBR) as the matrix and four-hole hollow polyester (abbreviated FHHPF) as the reinforcement. The sound absorption properties of these composites were studied. The results show that with the increasing of FHHPF quantity, the storage modulus increases and the loss factor decreases gradually. On the contrary, the sound absorption performance of the composite was improved continuously. Composite with 40% FHHPF in 1 mm thickness is the best. The sound absorption coefficient reached to 0.651 at 2500 Hz and the effective frequency range of absorption coefficient above 0.2 was 1750–2500 Hz. When the amount of FHHPF increased to 50%, negative effects of overuse shown up, that led to the decreasing of the sound absorption property. With a constant mass ratio 70/30 of HXNBR/FHHPF composite, the sound absorption performance can be enhanced by changing its thickness. However, the improvement was smaller after the thickness increased to 2 mm. When increasing the thickness above 2 mm, the improvement of sound absorption performance tended to move to the middle and low frequency. In the meantime, the tensile mechanical properties of the composite were significantly improved by adding FHHPF. Tensile tenacity was improved greatly and the breaking elongation is significantly decreased. The deformation of the composite was smaller and more stable, which was beneficial for the actual engineering practice.

Keywords: hydrogenated carboxyl nitrile rubber, hollow polyester, sound absorption, damping, composite

Cercetări privind proprietățile de absorbție acustică a cauciucului carboxil nitril hidrogenat/compozitelor din fibre de poliester cu miez cu patru orificii

Un compozit de serie a fost preparat prin adăugarea de cauciuc carboxil nitril hidrogenat (prescurtat HXNBR) ca matrice și poliester cu miez cu patru orificii (prescurtat FHHPF) ca armătură. Au fost studiate proprietățile de absorbție acustică a acestor compozite. Rezultatele arată că odată cu creșterea cantității de FHHPF, modulul de stocare crește și factorul de pierdere scade treptat. În plus, performanța de absorbție acustică a compozitului a fost îmbunătățită continuu. Compozitul cu 40% FHHPF cu grosimea de 1 mm este cel mai performant. Coeficientul de absorbție acustică a ajuns la 0,651 la 2500 Hz, iar gama de frecvență efectivă a coeficientului de absorbție de peste 0,2 a fost de 1750–2500 Hz. Când cantitatea de FHHPF a crescut la 50%, au apărut efecte negative ale utilizării excesive, ceea ce a dus la scăderea proprietății de absorbție acustică. Cu un raport de masă constant 70/30 al compozitului HXNBR/FHHPF, performanța de absorbție acustică poate fi îmbunătățită prin modificarea grosimii sale. Cu toate acestea, îmbunătățirea a fost mai puțin semnificativă dacă grosimea a crescut la 2 mm. La creșterea grosimii la peste 2 mm, îmbunătățirea performanței de absorbție acustică a avut tendința de a se deplasa la frecvența medie și joasă. Între timp, proprietățile mecanice de tracțiune ale compozitului au fost semnificativ îmbunătățite prin adăugarea de FHHPF. Rezistența la tracțiune s-a îmbunătățit foarte mult, iar alungirea la rupere a scăzut semnificativ. Deformarea compozitului a fost mai redusă și mai stabilă, ceea ce a fost benefic pentru ingineria reală practică.

Cuvinte-cheie: cauciuc carboxil nitril hidrogenat, poliester cu miez, absorbție acustică, amortizare, compozit

INTRODUCTION

Fiber material with its diverse categories and abundant sources, especially the hollow fiber was widely used in the field of sound absorption materials [1–3], but mostly in the form of nonwovens [4–6]. Rubber, as a viscoelastic polymer material, can absorb the energy and well transform to heat, especially synthetic rubber, can be used as sound-absorbing material [7, 8]. Research of rubber as the matrix and hollow fiber blended composites for sound absorption is less. Jiang et al. used CPE as the matrix, Zhou et al. used R-Rubber as the matrix, blend with seven-hole

polyester to make the CPE/SHPF and R-Rubber/SHPF, respectively. Their studies showed that the material got the best sound absorption property when use 20% SHPF ratio with 1mm thickness. Meantime, the tensile mechanical properties of the material were also well improved, and increased the material thickness can further improve its sound performance [9–11]. In addition, few such studies can be found in the published document.

According to the study of Jiang and Zhou et al., the maximum fiber content was 20% and the thickness was 3 mm. For such materials, will continuously

increase the fiber quantity and thickness be helpful to improve the damping and sound absorption performance? What is the changing rule? In this study, using hydrogenated carboxyl nitrile rubber (abbreviated HXNBR) as matrix and four-hole hollow polyester staple fiber (abbreviated FHHPF) as reinforcements, HXNBR/FHHPF composites in 1 mm thickness with different mass ratio and fixed mass ratio with different thickness were made, the influence of FHHPF content and material thickness on the sound absorption properties and its mechanism actions were studied. Furthermore, the influence on tensile properties of the material was also studied.

MATERIAL FABRICATION

The rubber matrix HXNBR used in preparation of the HXNBR/FHHPF composites marked Therban XT VP KA 8889 was manufactured by LANXESS Deutschland GMBH. The FHHPF used with fineness of 0.833 tex and length of 60 mm was produced by Sinopec Yizheng Chemical Fiber Co., Ltd., China. The ordinary polyester staple fiber (referred to as PF) used with fineness of 0.156 tex and length of 38 mm is from the same manufacturer. The cross-sectional morphology amplified 2000 of these two kind fibers were acquired by using fiber microtome and CU-2 fiber fineness tester (Beijing UVTEC Science and Technology Ltd., China) is shown in figure 1.

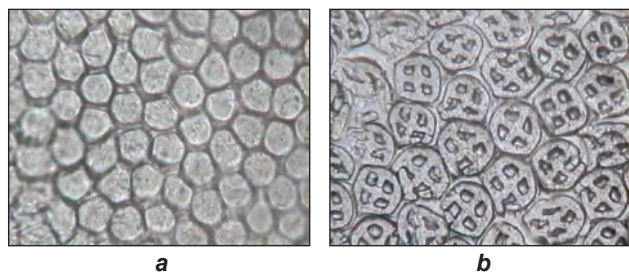


Fig. 1. Cross-sectional shape of PF and FHHPF, amplified 2000: a – PF; b – FHHPF

The material preparation process is as follows:

1. Mixing, when the roller temperature of the X(S) K-460 double roll mill (Wuxi Chuangcheng Rubber and Plastic Machinery Co., Ltd., China) raised to 30°C, the HXNBR was added into the machine for 5 min treatment, and then the weighed fibres was added in several times to make sure the materials were well mixed. The mixing time was from 20–40 min, which was depended on the fibre quantity added. A cutting knife was used to enhance the homogeneity of the composite.
2. Vulcanization, the homogenized HXNBR/polyester fibre mixture was placed in a mould, the mould was hold by a 30 cm×30 cm and 5 mm thickness stainless steel plate, and between the mould and steel plate,

a layer of thermostable PTFE cloth with a layer of anti-sticky thermostable PET film was put on it. Then the mould was put into QLB-50D/Q type plate vulcanizing press (Wuxi Chuangcheng Rubber and Plastic Machinery Co., Ltd., China), which was preheated at 1–2 MPa pressure and 140°C for 5 min. Then the pressure of the machine was adjusted to 10 MPa and the material was pressed at 140°C for 20 min. Release the pressure and take the mould out. Let it cool down and demould it, obtain the required material with a smooth surface.

Refer to research of Jiang, Zhou et al. and myself pre-research [10, 11], six kinds of 1mm thickness of HXNBR/FHHPF composite in mass ratio of 100/0, 90/10, 80/20, 70/30, 60/40 and 50/50 were made respectively. Fixed mass ratio of 70/30 in thickness of 0.5 mm, 2 mm, 3 mm, 4 mm and 5 mm were made respectively. HXNBR/PF material with 1 mm thickness was also prepared for comparison.

MATERIAL TESTING

The degree of hollowness of the used FHHPF fiber was tested. The thermodynamic performance, sound absorption properties, morphology and tensile properties of the prepared materials were tested.

Paper-cut weighing method was used for hollowness test. The cross-sectional morphology graph of the FHHPF, refer to figure 1, b, was printed on the uniform thickness white paper, the average value was calculated from 100 fiber cross-sections randomly chosen. The test result of the hollowness of FHHPF was 22.9%.

The sound absorption performance of composite was tested according to the standard of ISO 10534-2 by SW230 series impedance tube manufactured by BSWA Technology Co., Ltd., China (figure 2).

Dynamic mechanical analysis (DMA) measurements of the composites were carried out using a dynamic mechanical analyser (DMA7e, Perkin Elmer. USA) in a tension mode at a constant frequency of 1 Hz with a heating rate of 5°C/min. The sample size was 12 mm (length) × 4 mm (width) × 1 mm (thickness). Fractured surface morphology of the HXNBR/FHHPF composite was conducted by using a Quanta-250 environment scanning electron microscope (ESEM)

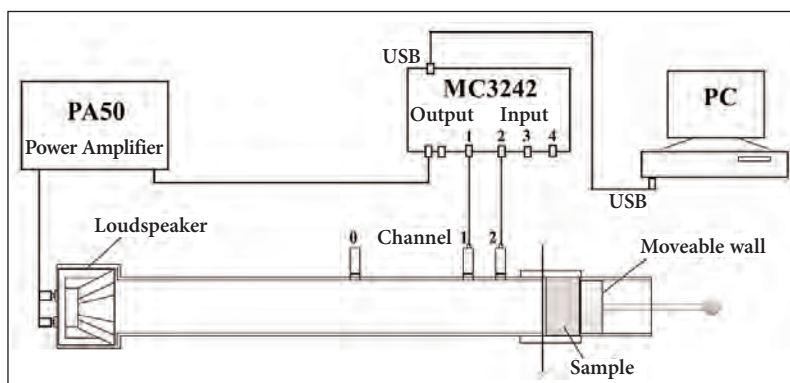


Fig. 2. Assembled diagram of measured sound absorption coefficient with an impedance tube

(FEI Company, USA). The material samples were immersed in liquid nitrogen for a period in order to achieve brittle fracture, and then the fractured surfaces were sputter coated with gold before examination. The surface morphology of the composite was conducted by TM3000 desktop electronic scanning microscope (Hitachi, Japan). The composite surface was also sputter coated with gold before examination.

The tensile property test was conducted according to GB/T 528-2009, the test equipment was YG065 electronic fabric strength tester (Laizhou Electron Instrument Co., Ltd., Shandong, China). The tested samples were cut into dog-bone shape with 115 mm in length and 25 mm in width. The width of the narrow section was 6mm. The gauge length was 25 mm. The instrument was set at a speed of 500 mm/min for testing.

RESULTS AND DISCUSSION

1 mm thickness HXNBR/FHHPF composites with different mass ratio were tested for DMA, sound absorption, SEM and tensile property. The sound absorption performance of HXNBR/FHHPF materials with mass ratio of 70/30 and different in thickness was tested. The results were analysed and studied.

Influence of FHHPF content on sound absorption properties of material

The DMA performance of different mass ratio with 1 mm thickness HXNBR/FHHPF composites was shown in figure 3. From figure 3, *a*, it shows that the storage modulus of HXNBR/FHHPF increased with the increasing of the FHHPF fibre content, and the transition temperature moved toward to a higher temperature. Meanwhile, in figure 3, *b*, at the initial only 10% FHHPF was added, the loss factor decreased in a large amplitude, but the glass transition temperature (T_g) had a significant movement toward to the higher temperature direction. With the increasing of the FHHPF content, the loss factor of the material continued to decrease and the T_g moved toward to

the higher temperature direction, but the changing was relatively small.

Adding FHHPF in the material to change the damping properties of HXNBR/FHHPF was due to the high modulus of the fibre itself and the storage modulus of the material can be increased based on its reinforcing effect. At the same time, the interaction between the fibre and the matrix restrains the movement of the HXNBR molecular chain, which promoted the decreasing of the loss factor [12, 13]. With the increasing of the FHHPF content, the interfacial interaction between fibre and matrix was strengthened, and the motion of HXNBR molecular chain segment was restricted more. In the meanwhile, the decreasing of HXNBR content led to the decreasing of the total molecular segment motion. Furthermore, undergone the mixing and vulcanization process, from the cross-section SEM of the material in figure 4, *a*, it can be found that the gradually increased fibres were evenly dispersed in the matrix to form a fibre web, which were entangled with each other and further restricted the movement of the HXNBR molecular chain segment [11–13]. The material storage modulus was improved, but at the same time, the material loss factor decreased and the T_g moved toward to the higher temperature.

The sound absorption performance of HXNBR/FHHPF with different mass ratio of 1 mm thickness is shown in figure 5. It can be found that pure HXNBR has a certain sound absorption capacity, and the sound absorption coefficient is 0.245 at 2500 Hz. Generally, material with sound absorption coefficient greater than 0.2 can be called sound-absorption material [14], so the frequency range with the sound absorption coefficient not less than 0.2 can be used to determine the material's sound absorption capacity. For pure HXNBR, the frequency range with sound absorption coefficient greater than 0.2 is merely 2300–2500 Hz. With reference to the damping property of the pure HXNBR in figure 3, sound absorption capacity is resulted from its excellent viscoelastic internal damping characteristics. From figure 5, it can be found that the sound absorption has been improved to a certain extent by adding PF.

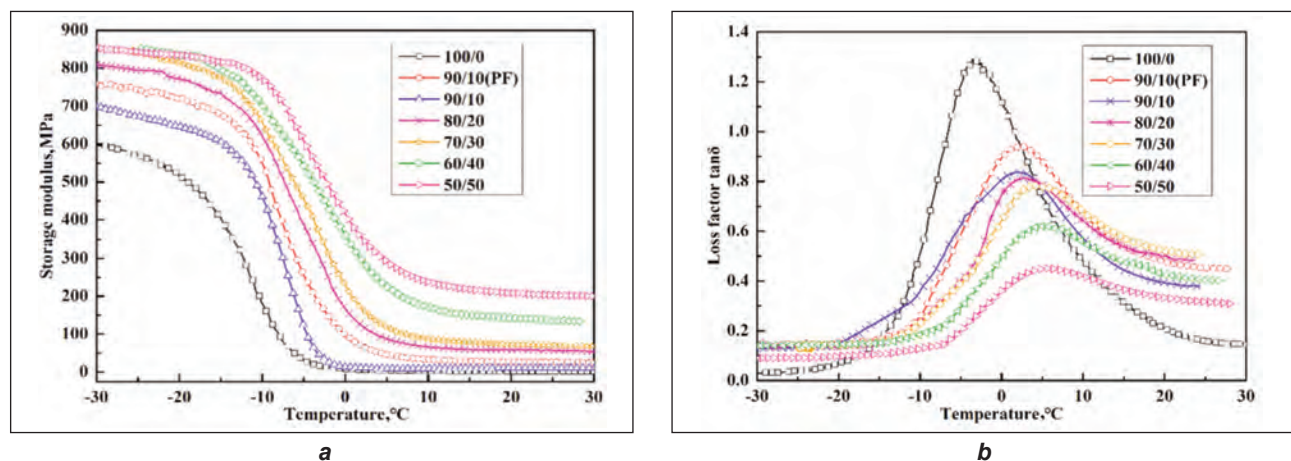


Fig. 3. Damping property of HXNBR/FHHPF composites: *a* – storage modulus-temperature curve; *b* – loss factor-temperature curve

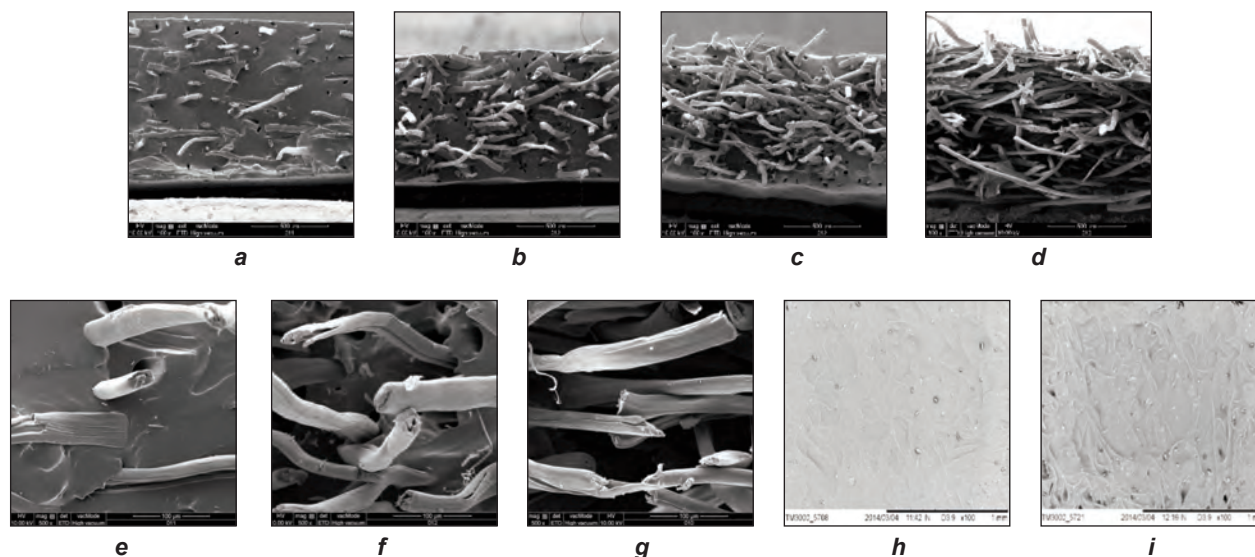


Fig. 4. SEM of HXNBR/FHHPF materials: *a* – cross section 90/10, amplified 100; *b* – cross section 80/20, amplified 100; *c* – cross section 70/30, amplified 100; *d* – cross section 50/50, amplified 100; *e* – cross section 90/10, amplified 500; *f* – cross section 70/30, amplified 500; *g* – cross section 50/50, amplified 500; *h* – surface 70/30, amplified 100; *i* – surface 50/50, amplified 100

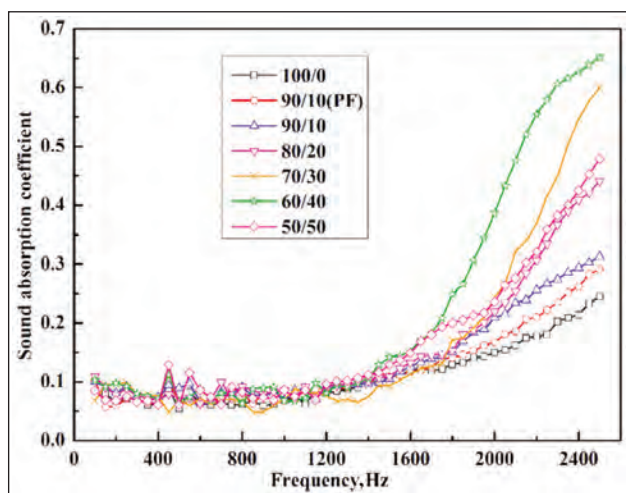


Fig. 5. Sound absorption property of HXNBR/FHHPF composites

The sound absorption coefficient of HXNBR/PF is 0.291 at 2500 Hz and the frequency range of sound absorption coefficient greater than 0.2 is slightly widened to 2150–2500 Hz. Combined with figure 3, the material storage modulus increases by adding of 10% PF, but with a substantial declining of the loss factor, so the energy consumption sound absorption capacity that based on the damping characteristic of the material decreased. However, overall sound absorption performance has improved, which can be concluded that other sound absorption energy dissipation mechanism played a role. It is believed that this is mainly based on the adding of fine short PF, which is evenly distributed in the matrix and interacts with the matrix. The sound absorption of HXNBR/PF is extended from the original single HXNBR viscoelastic damping energy dissipation to the viscoelastic damping energy consumption, fibre viscosity and heat conduction, the friction between fibre

itself vibration and matrix generated under the combined effect of energy consumption [9, 10].

Therefore, the use of PF to improve the sound absorption capacity of HXNBR/PF makes up for the reduction of the rubber matrix that resulted in the decreasing of the viscoelastic damping energy consumption of sound-absorbing performance, the general performance has been improved. However, as far as the frequency range of sound absorption coefficient greater than 0.2 and the corresponding sound absorption coefficient at every frequency point, the use of PF in the material has limited effect in improving the sound absorption performance.

Therefore, use 10% FHHPF to instead PF, the corresponding figure 5 shows that the sound absorption has been further improved, the sound absorption coefficient reached to 0.313 at 2500 Hz, and the frequency range of sound absorption coefficient greater than 0.2 is 2000–2500 Hz. When consider figure 3, the storage modulus and loss factor of PF is higher than FHHPF. Therefore, based on the sound absorption mechanism of used PF, there are other sound absorption energy dissipation mechanism effects that further improved the sound absorption performance of used FHHPF. From figure 1 of the fibre cross-section we can see the FHHPF is four-hole hollow, the hollowness testing result is 22.9%. With this characteristic, there are many pores and static air in the HXNBR/FHHPF. Meanwhile, as FHHPF is evenly distributed in the matrix and the cutting effect prompts more gaps in the matrix. When the sound wave enters the material, the air vibrates in the pore, the viscosity of the air and the friction between the air and cavity wall cause the increasing of energy consumption. Therefore, the sound absorption performance of the composite material has been greatly improved [9, 10, 15].

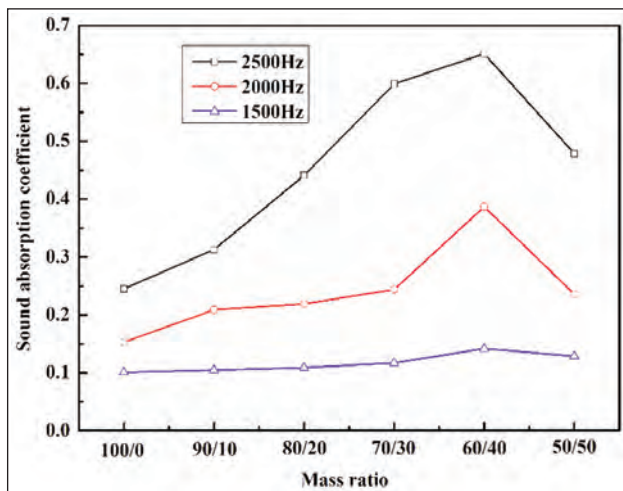


Fig. 6. Sound absorption coefficient of HXNBR/FHHPF material in main frequency point

Continue to increase the FHHPF content, from figure 5, it can be found that when the FHHPF content is less than 40%, the sound absorption performance of the HXNBR/FHHPF material was improved with the increasing of the FHHPF quantity. It is shown consistent sound absorption characteristics with porous material, the sound absorption property was improved with the increasing of frequency [16], and effect that is more significant was found especially when the frequency is above the 1600 Hz. The change trend of sound absorption coefficient in the main frequency point was shown in figure 6. At the same time, the frequency range of the sound absorption coefficient greater than 0.2 was also gradually broadened, which broadened from the high frequency of 2000 Hz above to medium frequency of 2000 Hz below. When the FHHPF reached to 40%, the sound absorption coefficient at 2500 Hz was up to 0.651, the frequency of sound absorption coefficient greater than 0.2 frequency range from 1750 Hz to 2500 Hz. This change of the sound absorption performance is due to the increasing of porosity because of the increasing of the FHHPF content, the air layer gradually penetrate, the interaction between the fibre and the matrix, and the gradual formation of the fibre web so the interaction between fibres also strengthens the ability to consumption sound energy [9, 10].

with different FHHPF contents was calculated according to the equation:

$$K = 1 - \rho \times \sum_{i=1}^n \frac{c_i}{\rho_i} \quad (1)$$

where K is porosity of composite, ρ – the material density, c_i – the volume density of each composite, ρ_i – the volume density of each material [15, 17].

The volume density of the HXNBR/FHHPF is in table 1. The volume density of FHHPF was tested by density gradient method. After getting the volume density of the material, the calculated porosity of the materials are shown in table 2.

From table 2, it can be seen that when the mass ratio of HXNBR/FHHPF is 90/10, the porosity of the material is 6.375%, and the cross-sectional SEM of the material in figure 4 shows that the fiber is less and evenly distributed and solidified in the matrix, the pores does not exert its best energy-absorbing sound absorption. When the fiber content increased to 20%, the porosity of the material is 10.688%, in contrast to the cross-sectional SEM observation from figure 4, it can be seen that more fibers come into contact with each other, but a perfect fiber web has not yet been formed. In this composite, part of the air layers in the pores are interpenetrated with each other, meanwhile there has vibration friction between fibers, coupled with the enhancement of the friction between the fiber and the matrix, the sound absorption performance has been greatly improved. The sound absorption coefficient at 2500 Hz increased to 0.441. Refer to table 2, further increasing the FHHPF quantity to 30%, the porosity increases to 14.514%. From figure 4, it can be found that a relatively complete fiber network is formed, so that the existence of air in the pores interpenetrated with each other and showed a good energy consumption sound absorption property. Vibration friction between fiber-fiber and fiber-matrix is also much stronger, so the energy consumption of the material raised and the sound absorption property is improved. The sound absorption coefficient at 2500 Hz reaches to 0.599. When the quantity of FHHPF is 40%, the porosity attains the maximum of 16.089%, the web between fibers is more perfect, and more air exists and penetrates each other. The vibration friction between fiber-fiber and fiber-matrix promoted more energy consumption

Table 1

VOLUME DENSITY OF HXNBR/FHHPF MATERIAL							
Ratio	100/0	90/10	80/20	70/30	60/40	50/50	0/100
Density (g/cm ³)	0.97	0.929	0.907	0.889	0.894	0.938	1.25

For porous sound absorption material, the porosity has an important influence on the sound absorption performance. Based on the use of FHHPF, the existence of voids in HXNBR/FHHPF composites and air content will have an influence on the sound absorption performance. The porosity of HXNBR/FHHPF

Table 2

POROSITY OF HXNBR/FHHPF MATERIAL					
Ratio	90/10	80/20	70/30	60/40	50/50
Porosity (%)	6.375	10.688	14.514	16.089	14.126

sound absorption. The composite has achieved the best sound absorption property.

According to figure 5 and figure 6, the sound absorption performance increases with the increasing of FHHPF content especially obvious at higher frequency area. That is because the higher frequency sound wave can more easily cause vibration after it gets into the material and the energy consumption of the material increased under various sound absorption effect. The fiber web formed by FHHPF in the HXNBR/FHHPF can be regarded as a kind of microstructure of the porous material which is good at absorbing higher frequency sound wave. The more FHHPF in the material, the better sound absorption capability at high frequency area will be [5]. However, further increasing the ratio of FHHPF to 50%, the sound absorption performance of the material decreased in a large extent. The sound absorption coefficient at 2500 Hz is 0.479 and the frequency range of sound absorption coefficient larger than 0.2 is also slightly narrowed to 1800–2500 Hz. From table 2, it can be found that the porosity of the material decreased to 14.126%, which indicates that the negative effects begin to appear when FHHPF content reached to a certain value. The cross-section and surface SEM of HXNBR/FHHPF composite with 50% FHHPF content in figure 4 shows that the fiber web is too dense and the FHHPF entangled with each other, and the material was compressed under plate compression, so the porosity of the material decreased. The vibration friction between fibers and the elastic deformation of HXNBR has been greatly limited, so the internal damping viscoelastic loss effect of the material decreased. The loss factor-temperature curve of HXNBR/FHHPF composite with the FHHPF content 50% in figure 3 is also confirmed above analysis. Besides, the entanglement of the excess fiber depressed the friction-energy consumption between FHHPF and HXNBR. Therefore, the sound absorption property of the material turned worse.

Influence of material thickness on sound absorption property

From the above analysis of the sound absorption properties of HXNBR/FHHPF composites with different ratio of FHHPF, we can see that the improvement of the sound absorption performance is mainly in the high-frequency region above 1600 Hz, almost no improvement in the low frequency sound absorption performance. According to the research report, the sound absorption performance of the material can also be improved by increasing the thickness of the material [10, 11, 18]. For this purpose, the HXNBR/FHHPF composites with mass ratio of 70/30 was made into different thickness for study, the thickness of these materials are 0.5 mm, 1 mm, 2 mm, 3 mm, 4 mm and 5 mm respectively. The sound absorption property of these composites can be seen in figure 7. HXNBR/FHHPF material with thickness in 0.5 mm already has good sound absorption performance.

The sound absorption coefficient at 2500 Hz is 0.329, the frequency range of sound absorption coefficient larger than 0.2 is 2000–2500 Hz. When the thickness of the material increased to 1 mm and 2 mm, the sound absorption performance improved significantly at 2000 Hz and above. The sound absorption coefficient at 2500 Hz increased to 0.599 and 0.795 respectively. The frequency range of sound absorption coefficient larger than 0.2 of the two materials is widened to 1900–2500 Hz and 1850–2500 Hz respectively. However, for the middle and low frequency that below 2000 Hz, there is almost no improvement. This is because low frequency sound wave induces small vibration that cannot effectively cause the energy consumption of the rubber matrix and FHHPF, which are consistent with the sound absorption mechanism of the porous sound-absorbing material [19]. When increasing the thickness from 2 mm to 3 mm, 4 mm, 5 mm, it is hard to improve the sound absorption coefficient of the high-frequency region, the sound absorption coefficient at 2500 Hz is 0.802, 0.806 and 0.811 respectively. However, the improvement in the middle and low frequency direction is gradually significant, especially in 1200–2000 Hz range. From figure 7, we can find that the frequency ranges of sound absorption coefficient larger than 0.2 of the three kinds of thickness material are widened to 1800–2500 Hz, 1700–2500 Hz, and 1450–2500 Hz, respectively.

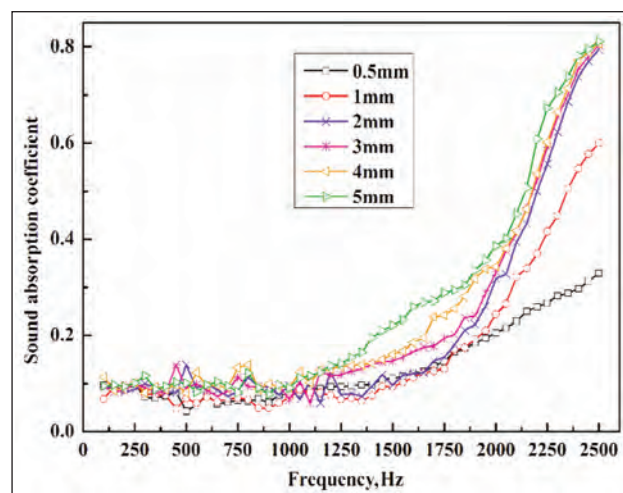


Fig. 7. Effect of thickness of HXNBR/FHHPF composites with 30% FHHPF on sound absorption property

This shows that the increasing of the composite thickness can effectively improve the sound absorption properties of the material, but when the thickness increased to a certain value, the improvement is small. In considering the economic applicability, appropriate thickness of the material should be chosen. Improving the sound absorption performance of the material by increasing its thickness is mainly because of the increasing of the propagation distance. The sound waves through HXNBR viscoelastic damping energy dissipation, the vibration energy dissipation between FHHPF, the air viscous effect of the sound wave caused by the presence of pores of

the FHHPF, and the relative increased energy dissipation caused by the friction between the air and the cavity wall. All the above lead to more energy being absorbed by the material and the sound absorption property of the material is improved [20]. Continue to increase the thickness above 2 mm, the sound absorption improvement tends to move to the low and medium frequency direction which is consistent with other document [16, 18, 21]. This is because of the better penetrating power of the lower frequency sound wave. When increasing the material to certain thickness, all kinds of sound absorption mechanism in the material can be fully exerted that more low frequency sound energy is attenuated, so the sound absorption performance in the middle-low region is largely improved. In the high-frequency region, due to the increasing of the material thickness, the acoustic impedance increases accordingly. In this situation, the reflective ability of the material to the sound waves is enhanced, and the high-frequency acoustic waves which get into the material are reduced. Therefore, when the thickness increases to a certain level, sound absorption performance of high-frequency is no longer significant, the increasing of the sound absorption coefficient is relatively small [19].

The tensile mechanical property of the material

From the above analysis, it can be concluded that the use of FHHPF can significantly improve the sound absorption performance of the 1 mm thickness HXNBR/FHHPF composites for frequency over 1600 Hz, and whether the material has excellent mechanical properties is important for practical application in the engineering field. Tensile mechanical properties of HXNBR/FHHPF composites with different mass ratios are shown in figure 8. The influence of FHHPF content on the tensile properties of the material is shown in figure 9.

It can be seen from figure 8 that the strain of pure HXNBR matrix is very large, and it can produce great deformation under very small stress. The tensile breaking tenacity of the pure HXNBR matrix is only 6.3 MPa, and the elongation at break is as high as

100.5%. The mechanical properties are improved significantly after adding FHHPF. With the increasing of the fiber content gradually up to 50%, the strain of the material gradually decreases, especially when the fiber content over 30%, the tensile strain of the material is greatly decreased and its strength is greatly improved. Figure 9 clearly shows the influence of the FHHPF ratio on the mechanical properties of the materials.

Pure HXNBR material is subjected to external force alone when the material is being stretched. The stress-strain characteristic of the rubber is shown in figure 8. When add a small amount of FHHPF, the FHHPF is homogeneously dispersed in the HXNBR matrix after mixing and vulcanizing. From the SEM of the material in figure 4, a we can find that the fibers are not continuous. When the material is subjected to external tensile force, the external force is transmitted to the fiber through the fiber matrix interface and the interfacial bonding between the FHHPF and the HXNBR matrix enables the fiber and the substrate to bear the external stress effectively and limit the deformation of the rubber matrix simultaneously [22]. In addition, compared with the pure HXNBR, when the HXNBR/FHHPF composite is under external force, besides the fracture of the original HXNBR matrix, the pull out friction between the fiber and the matrix during the pulling process and some fibers ruptured, under the combine action, the tensile strength of the material is improved. However, the HXNBR matrix still plays the main role in strength property of material in this situation, so although the elongation at break is lower, but the material deformation is still large [22–24]. With the further increasing of FHHPF content, the fibers were evenly distributed in the matrix and a dense fiber web was formed gradually. From the SEM in figure 4, it can be found that the FHHPF is in bending and twisting state in HXNBR matrix. The three-dimensional fiber crimp also helps to strengthen the interface binding force between the fiber and matrix which improved the ability of bearing external force. The breaking strength of the material is further improved when the content of FHHPF is

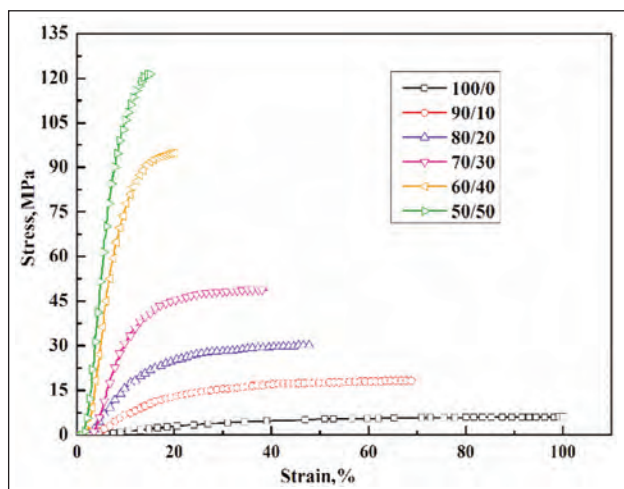


Fig. 8. Tensile stress-strain curves of the composites

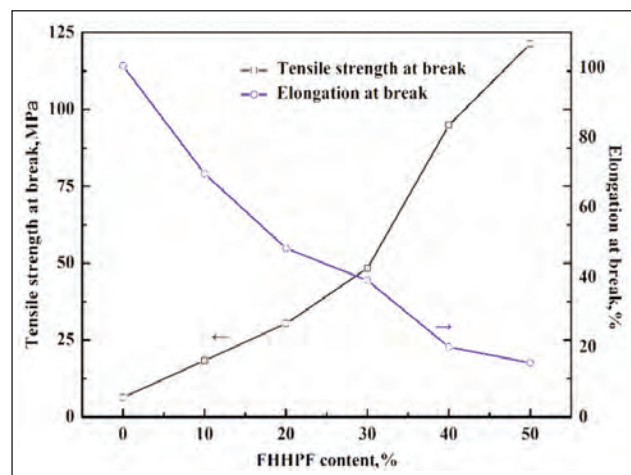


Fig. 9. Effect of FHHPF content on tensile mechanical properties of composites

increased to 30% and above. Meanwhile, the increasing of FHHPF fiber can restrain the elastic deformation of HXNBR and the material is more stable. The main role bear external force is gradually transferred to FHHPF fiber, more fibers ruptured when under external force, the pull-off of the fibers make a lot of tiny cracks and holes in the material that will lead to earlier breakage of the HXNBR. The material elongation at breakage is gradually decreased especially significant when the content reaches to 30% and above [25].

CONCLUSIONS

A series of HXNBR/FHHPF composites were prepared. After the study of the sound absorption properties and the tensile properties of these materials, the following conclusions are drawn.

- The storage modulus of HXNBR/FHHPF increased with the increasing of FHHPF, but the loss factor gradually decreased and the corresponding T_g moved to the higher temperature region, which is based on the use of FHHPF to make its energy storage increased. In addition, the interaction of the fiber-matrix and the gradually formed fiber web limit the motion of HXNBR molecular chain segment. This effect is enhanced by the increasing use of FHHPF, so the peak value of the material loss factor decreases, the corresponding T_g moves to the higher temperature direction.
- The sound absorption performance of HXNBR/FHHPF composite is characterized as porous sound-absorbing material. The higher the frequency is, the higher the sound absorption coefficient is, and both increases with the increasing of FHHPF content. It gains the best sound absorption property at 40% FHHPF. The coefficient peak value is 0.651, and the effective frequency domain with sound absorption coefficient greater than 0.2 is 1750–2500 Hz. The excellent sound absorption performance of the material is due to the use of

FHHPF. With the increasing of the FHHPF content in the material, the porosity of the material increases, the air layer penetrates gradually, the friction between the fiber and the matrix increases, and the friction between the fibers increases after forming as a web. That enhances the consuming of the sound energy. Continue to increase the FHHPF content to 50%, due to the excessive entanglement between fiber web, it suppresses the vibration of the friction between the fibers and the elastic deformation of the HXNBR. Meanwhile, through vulcanizing press process, the porosity of the material also decreased. In combined aspects, the sound absorption performance decreased after the FHHPF reaching to 50%.

- Keep the 30% ratio of FHHPF, and gradually increase the thickness of the HXNBR/FHHPF composite from 0.5 mm to 5 mm, the sound absorption coefficient of the material increases while the effective frequency domain of the sound absorption coefficient greater than 0.2 also be widened. However, when continue increasing the thickness from 2 mm to 3 mm and above, there is limit improvement in the sound absorption performance in high-frequency region while relatively significant improvement in low-frequency.
- Adding the FHHPF to HXNBR is not only improving the sound absorption of the material over the frequency range of 1600 Hz, but also improves the tensile properties. With the increase of FHHPF content, the tensile strength of the material gradually increases and the strain gradually decreases. This contributes to the practical application of materials in engineering.

ACKNOWLEDGEMENTS

We would like to thank the financial support of Top-notch Academic Programs Project of Jiangsu Higher Education Institutions (No. PPZY2015A093), Qing Lan Project in Jiangsu Province (2020).

REFERENCES

- [1] Xiang, H.F., Zhao, N., Xu, J., *Recent progress in sound absorption materials based on polymer fibers*, In: Polymer Bulletin, 2011, 5, 1–9
- [2] Xiang, H.F., Wang, D., Liu, H.C., et al., *Investigation on sound absorption properties of kapok fibers*, In: Chinese Journal of Polymer Science, 2013, 31, 3, 521–529
- [3] Liu, X.T., Yan, X., Li, L., et al., *Sound-absorption properties of kapok fiber nonwoven fabrics at low frequency*, In: Journal of Natural Fibers, 2015, 12, 4, 311–322
- [4] Gliscinska, E., Michalak, M., Krucinska, I., *Sound absorption property of nonwoven based composites*, In: AUTEX Research Journal, 2013, 13, 4, 150–155
- [5] Hassanzadeh, S., Hasani, H., Zarrebini, M., *Analysis and prediction of the noise reduction coefficient of lightly-needled Estabragh/polypropylene nonwovens using simplex lattice design*, In: Journal of the Textile Institute, 2014, 105, 3, 256–263
- [6] Santhanam, S., Bharani, M., Temesgen, S., et al., *Recycling of cotton and polyester fibers to produce nonwoven fabric for functional sound absorption material*, In: Journal of Natural Fibers, 2018, 1, 1–7
- [7] Zhou, H., Huang, G.S., Chen, X.R., et al., *Advances in sound absorption polymers*, In: Rubber & Plastics Resources Utilization, 2004, 16, 3, 450–455
- [8] Chen, R.J., *Rubber sound absorption material and their application*, In: China Rubber Industry, 2008, 55, 2, 122–125
- [9] Jiang, S., Yan, X., *Acoustical absorption property of elastomer composites consisting of chlorinated polyethylene and seven-hole hollow polyester fibers*, In: Journal of Textile Research, 2010, 31, 3, 32–35

- [10] Jiang, S., Xu, Y.Y., Zhang, H.P., et al., *Seven-hole hollow polyester fibers as reinforcement in sound absorption chlorinated polyethylene composites*, In: Applied Acoustics, 2012, 73, 3, 243–247
- [11] Zhou, X.O., Jiang, S., Yan, X., et al., *Damping acoustic properties of reclaimed rubber/seven-hole hollow polyester fibers composite materials*, In: Journal of Composite Materials, 2014, 48, 26, 3249–3254
- [12] Jin, Z., Wu, X.Y., Luo, Z., et al., *Complex modification of polyamide fiber and the research of polyamide fiber reinforced natural rubber composites*, In: New Chemical Materials, 2015, 43, 4, 149–151
- [13] Xia, Z.L., Luo, Z., Lou, J.F., et al., *Study on the properties of aramid fiber reinforced natural rubber*, In: Special Purpose Rubber Products, 2013, 34, 6, 15–20
- [14] Su, W., Li, X.Y., Liu, S.S., *Influence of thickness and density on sound-absorption capability of nonwoven sound-absorbing material*, In: Journal of Tianjin Polytechnic University, 2009, 28, 3, 34–36
- [15] Jiang, S., *Structure and properties of hollow fiber as reinforcement in acoustics absorption wasted rubber composites*, In: Polymer Materials Science and Engineering, 2015, 31, 12, 73–77
- [16] Lou, C.W., Lin, J.H., Su, K.H., *Recycling polyester and polypropylene nonwoven selvages to produce functional sound absorption composites*, In: Textile Research Journal, 2005, 75, 5, 390–394
- [17] Yilmaz, N.D., Banks-Lee, P., Powell, N.B., et al., *Effects of porosity, fiber size, and layering sequence on sound absorption performance of needle-punched nonwovens*, In: Journal of Applied Polymer Science, 2011, 1215, 3056–3069
- [18] Lee, Y.E., Joo, C.W., *Sound absorption properties of thermally bonded nonwovens based on composing fibers and production parameters*, In: Journal of Applied Polymer Science, 2004, 92, 4, 2295–3302
- [19] Shen, Y., Jiang, G.M., Ji, T., et al., *Analysis of sound absorbing properties of activated carbon fiber materials*, In: Journal of Textile Research, 2013, 34, 3, 1–4
- [20] Seddeq, H.S., Aly, N.M., Ali, M.A., et al., *Investigation on sound absorption properties for recycled fibrous materials*, In: Journal of Industrial Textiles, 2013, 43, 1, 56–73
- [21] Wang, C.N., Tornø, J.H., *Experimental study of the absorption characteristics of some porous fibrous materials*, In: Applied Acoustics, 2001, 62, 4, 447–459
- [22] Manaila, E., Stelescu, M.D., Doroftei, F., *Polymeric composites based on natural rubber and hemp fibers*, In: Iranian Polymer Journal, 2015, 24, 2, 135–148
- [23] Leny, M., Narayanankutty, S., *Cure characteristics and mechanical properties of HRH bonded nylon-6 short fiber-nanosilica-acrylonitrile butadiene rubber hybrid composite*, In: Polymer-Plastics Technology and Engineering, 2008, 48, 1, 75–81
- [24] Zainudin, E.S., Yan, L.H., Haniffah, W.H., et al., *Effect of coir fiber loading on mechanical and morphological properties of oil palm fibers reinforced polypropylene composites*, In: Polymer Composites, 2014, 35, 7, 1418–1425
- [25] Han, Z., Qi, S., Wei, L., et al., *Surface-modified polyimide fiber-filled ethylenepropylenediene monomer insulations for a solid rocket motor: processing, morphology, and properties*, In: Industrial & Engineering Chemistry Research, 2013, 52, 3, 1284–1290

Authors:

JIE HONG^{1,2}

¹Jiangsu College of Engineering and Technology, Nantong, Jiangsu, China

²Jiangsu Advanced Textile Engineering Technology Center, Nantong, Jiangsu, China

Corresponding author:

JIE HONG

e-mail: 85391392@qq.com

Location selection for a textile manufacturing facility with GIS based on hybrid MCDM approach

DOI: 10.35530/IT.072.02.1736

ALPTEKIN ULUTAŞ

CAN BÜLENT KARAKUŞ

ABSTRACT – REZUMAT

Location selection for a textile manufacturing facility with GIS based on hybrid MCDM approach

The establishment of a textile manufacturing facility in any city of a country is a very significant decision since it will have a significant positive effect on the economy of both the city and the country and reduce unemployment in the city. Even though it is a very important decision to establish a textile manufacturing facility, there are very few studies on the location selection of the textile manufacturing facility. This study aims to propose a new integrated MCDM model including FUCOM and PIV-F with GIS to fill this research gap. The criteria used in this study are as follows; Proximity to Airport (PA), Proximity to Highway (PH), Proximity to Shopping Centre (PSC), Proximity to Railway (PR), Proximity to Retailer Centre (PRC), Proximity to Supplier Centre (PSCT), Slope of Land (SL) and Distance to Population Density (DPD). FUCOM was used to obtain criteria weights. PR criterion was designated as the most important criterion with respect to the results of FUCOM. PIV-F method was used to rank suitable areas for a textile manufacturing facility in Sivas province of Turkey. According to the results of PIV-F, Area-4 was determined as the most suitable area for the establishment of a textile manufacturing facility in Sivas province. This study aims to make two contributions to the literature. First, the fuzzy extension of the PIV method is newly developed. Second, a new integrated MCDM-GIS model is used to select the location for the textile manufacturing facility.

Keywords: MCDM, location selection, GIS, PIV-F, FUCOM

Selecția locației pentru o companie textilă cu GIS bazată pe abordarea modelului hibrid MCDM

Înființarea unei companii textile în orice oraș al unei țări este o decizie foarte importantă, deoarece va avea un efect pozitiv semnificativ atât asupra economiei orașului, cât și a țării și va reduce șomajul. Chiar dacă este o decizie foarte importantă de a înființa o companie textilă, există foarte puține studii privind selectarea locației. Acest studiu are ca obiectiv propunerea unui nou model integrat MCDM, inclusiv FUCOM și PIV-F cu GIS pentru a umple acest gol în cercetare. Criteriile utilizate în acest studiu sunt următoarele: apropierea de aeroport (PA), apropierea de autostradă (PH), apropierea de centrul comercial (PSC), apropierea de calea ferată (PR), apropierea de centre de vânzare (PRC), apropierea de centrul de furnizare (PSCT), panta terenului (SL) și distanța față de densitatea populației (DPD). FUCOM a fost utilizat pentru a obține ponderile criteriilor. Criteriul PR a fost desemnat drept cel mai important în ceea ce privește rezultatele FUCOM. Metoda PIV-F a fost utilizată pentru a clasifica zonele adecvate pentru o companie textilă din provincia Sivas din Turcia. Conform rezultatelor PIV-F, Zona-4 a fost determinată drept cea mai potrivită pentru înființarea unei companii textile în provincia Sivas. Acest studiu își propune să aducă două contribuții la cercetarea științifică. În primul rând, extensia fuzzy a metodei PIV este recent dezvoltată. În al doilea rând, se utilizează un nou model integrat MCDM-GIS pentru a selecta locația pentru unitatea de producție a produselor textile.

Cuvinte-cheie: MCDM, selectarea locației, GIS, PIV-F, FUCOM

INTRODUCTION

The establishing of a new facility is considered as an important and strategic decision problem since the establishment will have long-term effects on the sustainability, availability, and profitability of the facility. One of the most important of these decision processes is choosing the appropriate location for the facility. Improper location choices in today's competitive globe can trigger irrecoverable results for any sector [1]. A methodological, analytical and planned approach to the selection of suitable areas for the facilities will minimize the possibility of inaccurate location selection to a very low level. Although there are many approaches having these attributes in the literature, multi-criteria decision making (MCDM)

methods can be used more effectively in solving this problem since there are multiple alternatives in the location selection problem and these alternatives are evaluated under more than one criteria. MCDM as part of operational research is increasingly being utilized to address a range of problems [2]. Nowadays, different MCDM methods have been used to solve different problems [3–5]. In addition to MCDM methods, the GIS (geographic information systems) can be used to solve the location selection problem as the GIS can capture, store, manipulate, handle and, most significantly, evaluate geographic data [1].

In recent years, many different location selection problems have been solved using MCDM methods and GIS in the literature. For instance, the problem of energy-related facility location [6–10], the problem of

logistics and warehouse related location selection [11, 12] and the problem of waste-related location selection [13, 14] were analysed by using GIS and MCDM methods.

The textile sector is so important for the economy of Turkey in terms of employment and exports [15]. In August 2019, the share in Turkey's total exports of textiles and raw materials constituted to 5.5% of its overall exports [16]. Turkey's total textile and raw material exports between January 2019 and August 2019 were approximately \$ 6.5 billion [16]. As a result, it can be said that the textile sector is the backbone of the Turkish economy.

The establishment of a textile manufacturing facility in any city of a country is a very significant decision since it will have a significant positive effect on the economy of both the city and the country and reduce unemployment in the city. Although the establishment of a textile manufacturing facility is a very important decision, there are very few studies on the selection of textile manufacturing facility location [1]. This study aims to propose a new integrated MCDM model including FUCOM (Full Consistency Method) and PIV-F (Fuzzy Proximity Indexed Value) with GIS to fill this research gap. This study aims to make two contributions to the literature. First, the fuzzy extension of the PIV method is newly developed. Second, a new integrated MCDM-GIS model is used to select the location for the textile manufacturing facility.

METHODOLOGY

FUCOM

FUCOM method developed by Pamučar et al. [17], is used to determine criteria weights as the developers of this method claimed that this method is better than Best Worst Method and Analytic Hierarchy Process. In recent years, successful applications of FUCOM method have been performed [18–22]. This method is summarized as described in Pamučar et al. [17], Nunić [18], Zavadskas et al. [19].

Step 1: Criteria are ranked with respect to their significance level.

Step 2: Ranked criteria are compared to obtain the priorities ($\vartheta_{C_j(k)}$) of them and the comparative priority ($\omega_{k/k+1}$) of them is identified.

$$\varpi = (\omega_{1/2}, \omega_{2/3}, \dots, \omega_{k/k+1}) \quad (1)$$

In equation 1, k is the rank of the criteria.

Step 3: In the final step, criteria weights are calculated; however, weights should fulfil the following 2 conditions.

- The comparative priority is equal to the ratio of weights of criteria. Equation 2 indicates this condition.

$$\omega_{k/k+1} = \frac{w_k}{w_{k+1}} \quad (2)$$

- Criteria weights should fulfil the condition of mathematical transitivity, i.e. $\omega_{k/k+1} \cdot \omega_{k+1/k+2} = \omega_{k/k+2}$.

As $\omega_{k/k+1} = \frac{w_k}{w_{k+1}}$ and $\omega_{k+1/k+2} = \frac{w_{k+1}}{w_{k+2}}$, $\frac{w_k}{w_{k+1}} \cdot \frac{w_{k+1}}{w_{k+2}} =$

$\frac{w_k}{w_{k+2}}$ is determined. Equation 3 indicates this formula:

$$\frac{w_k}{w_{k+2}} = \omega_{k/k+1} \cdot \omega_{k+1/k+2} \quad (3)$$

The final model is formed to obtain final weights of criteria. Equation 4 presents the final model:

$$\begin{aligned} & \text{Min } \chi \\ & \text{s.t.} \\ & \left| \frac{w_{j(k)}}{w_{j(k+1)}} - \omega_{k/k+1} \right| \leq \chi, \forall j \\ & \left| \frac{w_{j(k)}}{w_{j(k+2)}} - \omega_{k/k+1} \right| \cdot \omega_{k+1/k+2} \leq \chi, \forall j \\ & \sum_{j=1}^n w_j = 1, \forall j \\ & w_j \geq 0, \forall j \end{aligned} \quad (4)$$

In equation 4, χ indicates a deviation from full consistency and this value should be between 0 and 0.025. These weights will be transferred into PIV-F method.

PIV-F

PIV method (developed by Mufazzal and Muzakkir [23] to minimize rank reversal problem) is used to rank alternatives. Since the PIV method is newly developed, there are very few studies on the application of the PIV method [24, 25]. In this study, the aim of developing PIV-F method is to handle uncertain values and minimize the rank reversal problem. This method consists of 6 steps.

Step 1: A fuzzy decision matrix (\tilde{S}) is formed. When forming fuzzy decision matrix, experts use linguistic values indicated in table 1. These linguistic values are converted into fuzzy values by aiding of table 1.

$$\tilde{S} = [\tilde{s}_{ij}]_{m \times n} \quad (5)$$

Table 1

LINGUISTIC AND FUZZY VALUES	
Linguistic values	Fuzzy values
Very Low	(0, 1, 3)
Low	(1, 3, 5)
Fair	(3, 5, 7)
High	(5, 7, 9)
Very High	(7, 9, 10)

Step 2: This matrix is normalized as

$$\tilde{t}_{ij} = (t_{ij}^l, t_{ij}^m, t_{ij}^u) = \frac{\tilde{s}_{ij}}{\sqrt{\sum_{i=1}^m \tilde{s}_{ij}^2}} = \left(\frac{s_{ij}^l}{\sqrt{\sum_{i=1}^m [(s_{ij}^l)^2 + (s_{ij}^m)^2 + (s_{ij}^u)^2]}}, \frac{s_{ij}^m}{\sqrt{\sum_{i=1}^m [(s_{ij}^l)^2 + (s_{ij}^m)^2 + (s_{ij}^u)^2]}}, \frac{s_{ij}^u}{\sqrt{\sum_{i=1}^m [(s_{ij}^l)^2 + (s_{ij}^m)^2 + (s_{ij}^u)^2]}} \right) \quad (6)$$

In equation 6, $\tilde{t}_{ij} = (t_{ij}^l, t_{ij}^m, t_{ij}^u)$ is the fuzzy normalized value of \tilde{s}_{ij} and a member of fuzzy normalized decision matrix (T).

Step 3: Fuzzy normalized values are multiplied by criteria weights.

$$\tilde{k}_{ij} = \tilde{t}_{ij} \times w_j \quad (7)$$

Step 4: Fuzzy weighted proximity index (\tilde{v}_{ij}) is computed as. Equation 8 and 9 are used for beneficial and cost criteria respectively.

$$\begin{aligned} \tilde{v}_{ij} &= (v_{ij}^l, v_{ij}^m, v_{ij}^u) = \max(\tilde{k}_{ij}) - \tilde{k}_{ij} = \\ &= (\max(k_{ij}^u) - k_{ij}^u, \max(k_{ij}^u) - k_{ij}^m, \max(k_{ij}^u) - k_{ij}^l) \end{aligned} \quad (8)$$

$$\begin{aligned} \tilde{v}_{ij} &= (v_{ij}^l, v_{ij}^m, v_{ij}^u) = \tilde{k}_{ij} - \min(\tilde{k}_{ij}) = \\ &= (k_{ij}^l - \min(k_{ij}^l), k_{ij}^m - \min(k_{ij}^l), k_{ij}^u - \min(k_{ij}^l)) \end{aligned} \quad (9)$$

Step 5: Fuzzy overall proximity index (\tilde{d}_i) is computed as

$$\tilde{d}_i = \sum_{j=1}^n \tilde{v}_{ij} = (\sum_{j=1}^n v_{ij}^l, \sum_{j=1}^n v_{ij}^m, \sum_{j=1}^n v_{ij}^u) \quad (10)$$

Step 6: Fuzzy overall proximity index ($\tilde{d}_i = (d_i^l, d_i^m, d_i^u)$) for each alternative is converted into crisp overall proximity index (d_i).

$$d_i = \frac{d_i^l + d_i^m + d_i^u}{3} \quad (11)$$

The alternative with the smallest crisp overall proximity index is determined as the best alternative.

DATA ACQUISITION AND APPLICATION

In this study, suitable areas for the establishment of the textile manufacturing facility will be determined in Sivas province. These suitable areas will be ranked from the most appropriate area to the most inappropriate area. All data used in the study were taken from the expert team consisting of managers working in the textile sector and academicians studying on the problem of location selection. Eight criteria were determined for use in the assessment in this study. These criteria are Proximity to Airport (PA), Proximity to Highway (PH), Proximity to Shopping Centre (PSC), Proximity to Railway (PR), Proximity to Retailer Centre (PRC), Proximity to Supplier Centre (PSCT), Slope of Land (SL) and Distance to Population Density (DPD). Expert opinions and literature [1] were used in determining the criteria. Only one criterion (SL) was determined as cost criterion and others were determined as beneficial criteria. The data, data source, data format, and analysis method (in GIS) related to the criteria used in the study are shown in table 2.

The application of FUCOM

Expert team ranked criteria based on the consensus: PR > PH > PSC > PA > PRC > PSCT > SL > DPD. Then experts compared criteria based on the scale [1,9] to obtain the priorities of criteria ($\vartheta_{C_j(k)}$). These values are indicated in table 3.

After performing the other steps of FUCOM method (equations 1–4), criteria weights are computed. Criteria weights are presented in table 4.

Table 2

THE CRITERIA USED IN THE STUDY AND THE ANALYSIS APPLIED FOR THESE CRITERIA				
Criteria	Data	Data Source	Data Format	Analysis
Proximity to railway (PR)	Railway	Environment and Urban Ministry/Landscaping Plan	Vector-line layer	Euclidean distance
Proximity to highway (PH)	Highway	Environment and Urban Ministry/Landscaping Plan	Vector-line layer	Euclidean distance
Proximity to shopping centre (PSC)	Shopping Centre	Google Earth Mapping	Vector-point layer	Euclidean distance
Proximity to airport (PA)	Airport	Environment and Urban Ministry/Landscaping Plan	Vector-polygon layer	Euclidean distance
Proximity to retailer centre (PRC)	Industry	Environment and Urban Ministry/Landscaping Plan	Vector-polygon layer	Euclidean distance
Proximity to supplier centre (PSCT)	Supplier Centre	Google Earth Mapping	Vector-point layer	Euclidean distance
Slope of land (SL)	Slope	U.S. Geological Survey/Digital Elevation Model	Raster (Elevation layer)	Slope
Distance to population density (DPD)	Districts	Turkish Statistical Institution	Vector-point layer	Point density

Table 3

PRIORITIES OF CRITERIA								
Criteria	PR	PH	PSC	PA	PRC	PSCT	SL	DPD
$\vartheta_{C_j(k)}$	1	1.7	1.9	2.3	2.7	3.1	3.2	3.4

CRITERIA WEIGHTS								
Criteria	PR	PH	PSC	PA	PRC	PSCT	SL	DPD
w_j	0.260	0.153	0.137	0.113	0.096	0.083	0.081	0.071

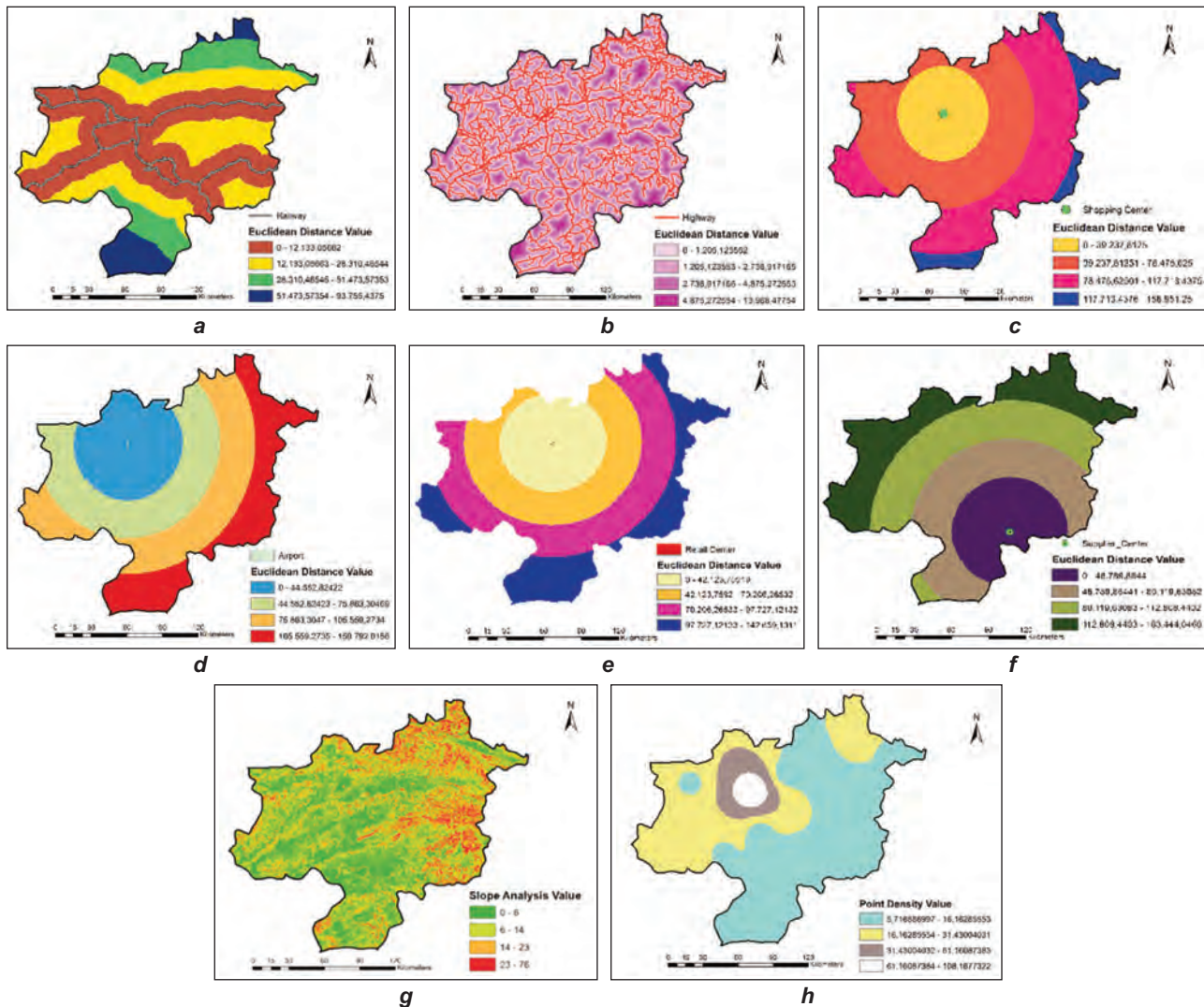


Fig. 1. Criteria maps created according to analysis methods applied in the study: a – proximity to railway; b – proximity to highway; c – proximity to shopping centre; d – proximity to airport; e – proximity to retail centre; f – proximity to supplier centre; g – slope of land; h – proximity to population density

PR criterion was designated as the most important criterion with respect to the results of FUCOM. According to the results of FUCOM, the deviation from full consistency is 0.021 and this indicates that results are consistent. After FUCOM method, the raster data are obtained with respect to Euclidean Distance Analysis, Slope Analysis and Point Density Analysis that were indicated in table 2. Maps are formed with respect to these data. Figure 1 indicates these maps.

These raster data are reclassified by using table 5. Table 5 presents a number system 1 to 4 (new values (scores)) to reclassify raster data.

With the aid of reclassified raster data and criteria weights (obtained in FUCOM), the suitable areas for the textile manufacturing facility are determined. These areas are indicated in figure 2.

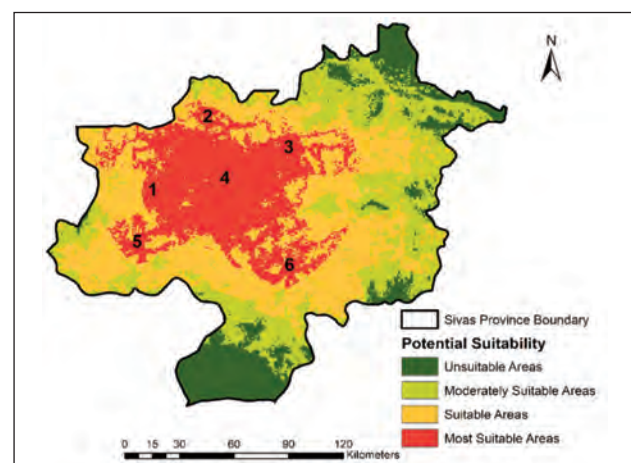


Fig. 2. Suitable areas for textile manufacturing facility

Table 5

THE SCORES AND SUB-CRITERION VALUES OBTAINED ACCORDING TO THE ANALYSIS METHODS APPLIED FOR THE CRITERIA USED IN THE STUDY		
Criteria	Old values	New values (Scores)
Proximity to railway (m)	0–12.133,056	4
	12.133,056–28.310,465	3
	28.310,465–51.473,573	2
	51.473,573–93.755,43	1
Proximity to highway (m)	0–1.205,123	4
	1.205,123–2.738,917	3
	2.738,917–4.875,272	2
	4.875,272–13.968,47	1
Proximity to shopping centre (m)	0–39.237,8125	4
	39.237,8125–78.475,625	3
	78.475,625–117.713,4375	2
	117.713,4375–156.951,25	1
Proximity to airport (m)	0–44.552,824	4
	44.552,824–75.863,304	3
	75.863,304–105.559,273	2
	105.559,273–159.792,01	1
Proximity to retailer centre (m)	0–42.123,75919	4
	42.123,75919–70.206,26532	3
	70.206,26532–97.727,12132	2
	97.727,12132–142.659,1311	1
Proximity to supplier centre (m)	0–46.789,8644	4
	46.789,8644–80.119,63082	3
	80.119,63082–112.808,4402	2
	112.808,4402–163.444,0469	1
Slope of land (Degree)	0–6	4
	6–14	3
	14–23	2
	23–76	1
Proximity to population density (person/km ²)	5,71–16,16	1
	16,16–31,43	2
	31,43–61,16	3
	61,16–108,16	4

The application of PIV-F

Expert team evaluated suitable areas, which are indicated in figure 2, by using table 1 to obtain fuzzy decision matrix. This matrix is presented in table 6.

With the use of equation 6 and 7, normalized and weighted normalized matrices are obtained respectively. By using equation 8 and 9, fuzzy weighted proximity index values are determined. These values are indicated in table 7.

With the aid of equation 10 and 11, fuzzy overall proximity index and crisp overall proximity index are calculated respectively. Table 8 indicates the results of PIV-F including fuzzy and crisp overall proximity indexes and rankings of areas.

According to the results of PIV-F, areas are sorted as follows: Area-4, Area-3, Area-1, Area-5, Area-2, and Area-6. PIV-F method is compared with the other fuzzy MCDM methods (fuzzy ARAS, fuzzy MOORA and fuzzy MABAC) to determine whether the PIV-F method has reached the accurate results. The rankings of areas according to the results of PIV-F and other fuzzy MCDM methods are presented in table 9. Spearman correlation coefficients between PIV-F method and other fuzzy MCDM methods are as follows. PIV-F-fuzzy ARAS, PIV-F-fuzzy MOORA, and PIV-F-fuzzy MABAC correlation coefficients are 0.943, 1.000 and 0.943, respectively. The correlations between the methods have been observed to be very high and therefore it can be concluded that the PIV-F method achieves accurate results.

CONCLUSIONS

Establishing a textile manufacturing facility in any city of a country is a very important judgment as it will have an important beneficial impact on both the city and the country's economy and will decrease unemployment in the city. Even though it is a very important decision to establish a textile manufacturing facility, there are very few studies on the location selection of the textile manufacturing facility [1]. This study aims to propose a new integrated MCDM model including FUCOM and PIV-F with GIS to fill this research gap. The criteria used in this study are as follows; PA, PH, PSC, PR, PRC, PSCT, SL and DPD. FUCOM was used to obtain criteria weights. PR criterion was designated as the most important criterion with respect to the results of FUCOM. PIV-F

Table 6

FUZZY DECISION MATRIX								
Criteria	PA	PH	PSC	PR	PRC	PSCT	SL	DPD
Area-1	(5, 7, 9)	(5, 7, 9)	(5, 7, 9)	(3, 5, 7)	(3, 5, 7)	(1, 3, 5)	(3, 5, 7)	(5, 7, 9)
Area-2	(5, 7, 9)	(5, 7, 9)	(5, 7, 9)	(1, 3, 5)	(5, 7, 9)	(0, 1, 3)	(5, 7, 9)	(5, 7, 9)
Area-3	(5, 7, 9)	(5, 7, 9)	(5, 7, 9)	(3, 5, 7)	(7, 9, 10)	(1, 3, 5)	(3, 5, 7)	(5, 7, 9)
Area-4	(7, 9, 10)	(7, 9, 10)	(7, 9, 10)	(7, 9, 10)	(7, 9, 10)	(3, 5, 7)	(3, 5, 7)	(7, 9, 10)
Area-5	(3, 5, 7)	(5, 7, 9)	(3, 5, 7)	(3, 5, 7)	(1, 3, 5)	(1, 3, 5)	(1, 3, 5)	(3, 5, 7)
Area-6	(1, 3, 5)	(5, 7, 9)	(1, 3, 5)	(3, 5, 7)	(1, 3, 5)	(7, 9, 10)	(3, 5, 7)	(1, 3, 5)

Table 7

FUZZY WEIGHTED PROXIMITY INDEX VALUES				
Criteria	PA	PH	PSC	PR
Area-1	(0.004, 0.012, 0.020)	(0.005, 0.014, 0.024)	(0.005, 0.014, 0.024)	(0.032, 0.053, 0.074)
Area-2	(0.004, 0.012, 0.020)	(0.005, 0.014, 0.024)	(0.005, 0.014, 0.024)	(0.053, 0.074, 0.095)
Area-3	(0.004, 0.012, 0.020)	(0.005, 0.014, 0.024)	(0.005, 0.014, 0.024)	(0.032, 0.053, 0.074)
Area-4	(0, 0.004, 0.012)	(0, 0.005, 0.014)	(0, 0.005, 0.014)	(0, 0.010, 0.032)
Area-5	(0.012, 0.020, 0.028)	(0.005, 0.014, 0.024)	(0.014, 0.024, 0.034)	(0.032, 0.053, 0.074)
Area-6	(0.020, 0.028, 0.036)	(0.005, 0.014, 0.024)	(0.024, 0.034, 0.043)	(0.032, 0.053, 0.074)
Criteria	PRC	PSCT	SL	DPD
Area-1	(0.011, 0.018, 0.025)	(0.020, 0.028, 0.036)	(0.007, 0.014, 0.021)	(0.003, 0.008, 0.014)
Area-2	(0.004, 0.011, 0.018)	(0.028, 0.036, 0.040)	(0.014, 0.021, 0.028)	(0.003, 0.008, 0.014)
Area-3	(0, 0.004, 0.011)	(0.020, 0.028, 0.036)	(0.007, 0.014, 0.021)	(0.003, 0.008, 0.014)
Area-4	(0, 0.004, 0.011)	(0.012, 0.020, 0.028)	(0.007, 0.014, 0.021)	(0, 0.003, 0.008)
Area-5	(0.018, 0.025, 0.032)	(0.020, 0.028, 0.036)	(0, 0.007, 0.014)	(0.008, 0.014, 0.019)
Area-6	(0.018, 0.025, 0.032)	(0, 0.004, 0.012)	(0.007, 0.014, 0.021)	(0.014, 0.019, 0.024)

Table 8

THE RESULTS OF PIV-F			
Results	\tilde{d}_i	d_i	Rankings
Area-1	(0.087, 0.161, 0.238)	0.1620	3
Area-2	(0.116, 0.190, 0.263)	0.1897	5
Area-3	(0.076, 0.147, 0.224)	0.1490	2
Area-4	(0.019, 0.065, 0.140)	0.0747	1
Area-5	(0.109, 0.185, 0.261)	0.1850	4
Area-6	(0.120, 0.191, 0.266)	0.1923	6

Table 9

THE RESULTS OF FUZZY MCDM METHODS				
Results	PIV-F	Fuzzy ARAS	Fuzzy MOORA	Fuzzy MABAC
Area-1	3	3	3	3
Area-2	5	6	5	4
Area-3	2	2	2	2
Area-4	1	1	1	1
Area-5	4	4	4	5
Area-6	6	5	6	6

method was used to rank suitable areas for a textile manufacturing facility in Sivas province. According to the results of PIV-F, Area-4 was determined as the most suitable area for the establishment of a textile manufacturing facility in Sivas province. PIV-F method was compared with the other fuzzy MCDM methods (fuzzy ARAS, fuzzy MOORA and fuzzy MABAC) to determine whether the PIV-F method has reached the accurate results. The correlations

between the methods have been observed to be very high and therefore it can be concluded that the PIV-F method achieves accurate results. This study aimed to make two contributions to the literature. First, the fuzzy extension of the PIV method was newly developed. Second, a new integrated MCDM-GIS model was used to select the location for the textile manufacturing facility. Future studies may use new PIV-F method to solve different MCDM methods.

REFERENCES

- [1] Onden, I., Eldemir, F., *GIS and f-AHP integration for locating a new textile manufacturing facility*, In: *Fibres & Textiles in Eastern Europe*, 2015, 5, 113, 18–22
- [2] Karabasevic, D., Maksimovic, M., Stanujkic, D., Brzakovic, P., Brzakovic, M., *The evaluation of websites in the textile industry by applying ISO/IEC 9126-4 standard and the EDAS method*, In: *Industria Textila*, 2018, 69, 6, 489–494, <https://doi.org/10.35530/IT.069.06.1520>
- [3] Chatterjee, P., Stević, Ž., *A two-phase fuzzy AHP-fuzzy TOPSIS model for supplier evaluation in manufacturing environment*, In: *Operational Research in Engineering Sciences: Theory and Applications*, 2019, 2, 1, 72–90
- [4] Naeini, A.B., Mosayebi, A., Mohajerani, N., *A hybrid model of competitive advantage based on Bourdieu capital theory and competitive intelligence using fuzzy Delphi and ism-gray Dematel (study of Iranian food industry)*, In: *International Review*, 2019, 1–2, 21–35
- [5] Karabasevic, D., Popovic, G., Stanujkic, D., Maksimovic, M., Sava, C., *An approach for hotel type selection based on the single-valued intuitionistic fuzzy numbers*, In: *International Review*, 2019, 1–2, 7–14

- [6] Villacreses, G., Gaona, G., Martínez-Gómez, J., Jijón, D.J., *Wind farms suitability location using geographical information system (GIS), based on multi-criteria decision making (MCDM) methods: The case of continental Ecuador*, In: *Renewable Energy*, 2017, 109, 275–286
- [7] Vasileiou, M., Loukogeorgaki, E., Vagiona, D.G., *GIS-based multi-criteria decision analysis for site selection of hybrid offshore wind and wave energy systems in Greece*, In: *Renewable and sustainable energy reviews*, 2017, 73, 745–757
- [8] Wang, C.N., Nguyen, V., Thai, H., Duong, D., *Multi-criteria decision making (MCDM) approaches for solar power plant location selection in Vietnam*, In: *Energies*, 2018, 11, 6, 1504
- [9] Pamučar, D., Gigović, L., Bajić, Z., Janošević, M., *Location selection for wind farms using GIS multi-criteria hybrid model: An approach based on fuzzy and rough numbers*, In: *Sustainability*, 2017, 9, 8, 1315
- [10] Gigović, L., Pamučar, D., Božanić, D., Ljubojević, S., *Application of the GIS-DANP-MABAC multi-criteria model for selecting the location of wind farms: A case study of Vojvodina, Serbia*, In: *Renewable Energy*, 2017, 103, 501–521
- [11] Özceylan, E., Erbaş, M., Tolon, M., Kabak, M., Durğut, T., *Evaluation of freight villages: A GIS-based multi-criteria decision analysis*, In: *Computers in Industry*, 2016, 76, 38–52
- [12] Kabak, M., Keskin, İ., *Hazardous materials warehouse selection based on GIS and MCDM*, In: *Arabian Journal for Science and Engineering*, 8, 43, 6, 3269–3278
- [13] Yildirim, V., Memisoglu, T., Bediroglu, S., Colak, H.E., *Municipal solid waste landfill site selection using Multi-Criteria Decision Making and GIS: case study of Bursa province*, In: *Journal of Environmental Engineering and Landscape Management*, 2018, 26, 2, 107–119
- [14] Danesh, G., Monavari, S.M., Omrani, G.A., Karbasi, A., Farsad, F., *Compilation of a model for hazardous waste disposal site selection using GIS-based multi-purpose decision-making models*, In: *Environmental monitoring and assessment*, 2019, 191, 2, 122
- [15] Ertuğrul, İ., Öztaş, T., *The application of sewing machine selection with the multi-objective optimization on the basis of ratio analysis method (MOORA) in apparel sector*, In: *Tekstil ve Konfeksiyon*, 2015, 25, 1, 80–85
- [16] İstanbul Tekstil ve Hammaddeleri İhracatçıları Birliği, Available at: <https://www.ithib.org.tr/tr/bilgi-merkezi-raporlar-aylik-ihracat-degerlendirme-bilgi-notlari-2019.html> [Accessed on August 2019]
- [17] Pamučar, D., Stević, Ž., Sremac, S., *A new model for determining weight coefficients of criteria in MCDM models: Full consistency method (fucm)*, In: *Symmetry*, 2018, 10, 9, 393
- [18] Nunić, Z., *Evaluation and selection of the PVC carpentry Manufacturer using the FUCOM-MABAC model*, In: *Operational Research in Engineering Sciences: Theory and Applications*, 2018, 1, 1, 13–28
- [19] Zavadskas, E.K., Nunić, Z., Stjepanović, Ž., Prentkovskis, O., *A novel rough range of value method (R-ROV) for selecting automatically guided vehicles (AGVs)*, In: *Studies in Informatics and Control*, 2018, 27, 4, 385–394
- [20] Prentkovskis, O., Erceg, Ž., Stević, Ž., Tanackov, I., Vasiljević, M., Gavranović, M., *A new methodology for improving service quality measurement: Delphi-FUCOM-SERVQUAL model*, In: *Symmetry*, 2018, 10, 757
- [21] Fazlollahtabar, H., Smailbašić, A., Stević, Ž., *FUCOM method in group decision-making: Selection of forklift in a warehouse*, In: *Decision Making: Applications in Management and Engineering*, 2018, 2, 1, 49–65
- [22] Bozanic, D., Tešić, D., Kočić, J., *Multi-criteria FUCOM–Fuzzy MABAC model for the selection of location for construction of single-span bailey bridge*, In: *ations in Management and Engineering*, 2019, 2, 1, 132–146
- [23] Mufazzal, S., Muzakkir, S.M., *A new multi-criterion decision making (MCDM) method based on proximity indexed value for minimizing rank reversals*, In: *Computers & Industrial Engineering*, 2018, 119, 427–438
- [24] Khan, N.Z., Ansari, T.S.A., Siddiquee, A.N., Khan, Z.A., *Selection of E-learning websites using a novel Proximity Indexed Value (PIV) MCDM method*, In: *Journal of Computers in Education*, 2019, 6, 2, 241–256
- [25] Yahya, S.M., Asjad, M., Khan, Z.A., *Multi-response optimization of TiO₂/EG-water nano-coolant using entropy based preference indexed value (PIV) method*, In: *Materials Research Express*, 2019, 6, 8, 0850a1

Authors:

ALPTEKİN ULUTAŞ¹, CAN BÜLENT KARAKUŞ²

¹Sivas Cumhuriyet University, Faculty of Economics and Administrative Sciences, Department of International Trade and Logistics, 58000, Sivas, Turkey

²Sivas Cumhuriyet University, Faculty of Architecture-Fine Arts and Design, 58000, Sivas, Turkey
e-mail: cbkarakus@gmail.com

Corresponding author:

ALPTEKİN ULUTAŞ
e-mail: aulutas@cumhuriyet.edu.tr

A preliminary study of printed electronics through flexography impression on flexible substrates

DOI: 10.35530/IT.072.02.202024

ANA M. RODES-CARBONELL
JOSUÉ FERRI

EDUARDO GARCIA-BREIJO
EVA BOU-BELDA

ABSTRACT – REZUMAT

A preliminary study of printed electronics through flexography impression on flexible substrates

The work is framed within Printed Electronics, an emerging technology for the manufacture of electronic products. Among the different printing methods, the roll-to-roll flexography technique is used because it allows continuous manufacturing and high productivity at low cost. Apart from the process parameters, the ink and the substrate properties are some of the variables associated with the flexographic printing. Specifically, this study investigates the ink penetration, the print uniformity, the adhesion, the fastness, and the electrical behaviour of the same conductive silver ink printed on different flexible substrates through the flexography process. In addition to polymeric and siliconized paper substrates, which are typical used in printed electronics, two substrates were also chosen for the study: woven and nonwoven fabric. Optical, scanning electronic microscope (SEM), 4-point Kelvin and colour fastness to wash and rubbing analyses have been performed. The results concluded that, regarding the conductivity behaviour, porous substrates like textiles and nonwoven fabrics without pre and post treatments do not present acceptable results, whereas polymers or silicone papers do. Nevertheless, woven and nonwoven fabrics are a suitable early option regarding colour fastness to wash instead of thin polymeric and paper substrates that tear at the wash machine. A solution for an optimal printing on textiles would be the surface substrates pre-treatment by applying different chemical compounds that increase the adhesion of the ink on the fabric.

Keywords: smart textile, wearable, printed-electronics, conductivity, flexography

Studiu preliminar privind electronicele imprimate prin flexografie pe suporturi flexibile

Lucrarea este încadrată în domeniul electronicelor imprimate, o tehnologie emergentă pentru obținerea produselor electronice. Printre diferitele metode de imprimare, se folosește tehnica de flexografie directă, deoarece permite fabricarea continuă și productivitatea ridicată la un cost redus. În afară de parametrii procesului, cerneala și proprietățile substratului sunt câteva dintre variabilele asociate cu imprimarea flexografică. Mai exact, acest studiu investighează penetrarea cernelii, uniformitatea imprimării, aderența, rezistența culorii și comportamentul electric al aceleiași cerneli conductoare pe bază de argint imprimată pe diferite substraturi flexibile, prin procesul de flexografie. În plus față de substraturile de hârtie polimerice și siliconate, care sunt utilizate în mod tipic în electronica imprimată, au fost selectate pentru studiu două substraturi: materialele textile țesute și materialele textile nețesute. Au fost efectuate analize microscopice optice, cu scanare electronică (SEM), Kelvin în 4 puncte și rezistența culorii la spălare și frecare. Rezultatele au arătat că, în ceea ce privește comportamentul de conductivitate, substraturile poroase, cum ar fi materialele textile țesute și nețesute fără pre și post-tratament, nu prezintă rezultate acceptabile, în timp ce hârtia polimerică și cea siliconată prezintă rezultate bune. Cu toate acestea, materialele textile țesute și nețesute reprezintă o opțiune adecvată în ceea ce privește rezistența culorii la spălare, în locul substraturilor subțiri polimerice și de hârtie care au tendința de sfâșiere la mașina de spălat. O soluție pentru o imprimare optimă pe materiale textile ar fi pretratarea substraturilor de suprafață prin aplicarea diferiților compuși chimici, care cresc aderența cernelii pe materialul textil.

Cuvinte-cheie: textile inteligente, purtabile, electronice imprimate, conductivitate, flexografie

INTRODUCTION

The technology that allows the fabrication of electronic devices through a printing process is known as printed electronics (PE). It is one of the fastest growing technologies in the world as it provides different printing techniques for fabricating low-cost and large-area flexible electronic devices [1]. In recent years, the technology of flexible electronics has attracted considerable attention as it is applicable to wearable devices including flexible displays, flexible batteries and flexible sensors [2] in different areas such as aerospace and automotive, biomedical, robotics, and

health applications [3]. Among them, wearable electronic textiles (e-textiles) are of great significance, as they provide better comfortability, durability and lighter weight as well as maintaining the desirable electrical property [4].

The PE printing technique selection shall be according to the type of electronic application (e.g., small, thin, lightweight, flexible, and disposable, etc.) to be fabricated, the production cost and volume. Also, the materials (inks/pastes and substrates) must meet certain requirements, depending on the type of printing technology being used and the final application.

PE technologies are divided in contact techniques (e.g., flexography, gravure printing and soft lithography techniques), in which the printing plate is in direct contact with the substrate and, non-contact techniques (e.g., screen printing, aerosol printing, inkjet printing, laser direct writing), where only the inks get in contact with the substrate [5, 6]. Those techniques suitable for roll-to-roll (R2R) processing, such as flexography, are especially attractive as they offer continuous production and high productivity [7].

Flexographic printing is known for depositing a wide range of thicknesses with the same resolution. Impression cylinder, plate cylinder, anilox roller, doctor blade and inking unit are the main parts of the flexographic printing [1]. Variables associated with the flexographic printing process include print speed, print force/engagement, anilox cell volume, anilox force/engagement as well as the ink and substrate properties. [8] Those variables have a direct impact on the prints' morphological and electrical behaviour, as well as the print uniformity has a considerable influence on the final functionality of the device [9]. It must be highlighted in the context of printed electronics on fabrics, the challenge of durability and withstanding bending, stretching, abrasion and washing [10].

Numerous reviews and books have been already published considering printed electronics on substrates that are usually used on electronic devices

MATERIALS AND METHODS

Materials

In addition to polymeric and siliconized paper substrates, which are typical used in printed electronics [3, 7], two substrates were also chosen for the study: woven and nonwoven fabric. The four flexible substrates are characterized in table 1.

Same aqueous flexo-printable conductive ink, PFI-600 – Silver ink from Novacentrix, has been used in all prints to ensure comparable results. The ink contains silver nanoparticles and has been formulated for high conductivity, fast curing, and improved levelling at lower printing speeds.

Methods

Flexography is a roll-to-roll direct printing technology, where an anilox roller, covered with micro-cavities on its surface, allows the collection of ink, and then is transferred to the printing plate cylinder. At the study, the one-layer flexography printing process has been performed using flexography experimental plants (Flexo VCML Lab from RK and Lambda from Edale) for printing the samples. Different test drawings for the pattern of the printing plate cylinder were designed specifically for the study. Details of the process are described in table 2.

Printed layers were dried using an in-line air flow convection dryer with temperatures within 80–150°C.

Table 1

SUBSTRATES CHARACTERIZATION						
Code	Substrate	Material	Structure	Mass per unit area*	Color	Protector
SA	Woven fabric	100% Cotton	Plain	300 g/m ²	Greige	No
SB	Spunbonded Nonwoven fabric	100% Polypropylene	Nonwoven	50 g/m ²	White	No
SC	Paper	Siliconized paper	-	140 g/m ²	White	No
SD	Polymeric	100% Thermoplastic Polyurethane	-	94 gr/m ²	Transparent	Yes (white paper)

Note: *Mass per unit area determined according to the standard ISO 3801

such as glass, metal, paper or polymers [3, 7]. However, the incorporation of the flexography printing technique for printed electronics in the textile field is still very recent and there are not enough studies for its application. As a result, the authors have proposed to analyse this printing methodology for conductive inks on textiles regarding their electronic performance.

In order to compare the results of the impression carried out on different laminar substrates, printed samples were characterized using the optimal microscope and the scanning electron microscope (SEM). The behaviour of the impression is evaluated before maintenance actions such as washing and rubbing.

Table 2

PRINTING PROCESS VARIABLES			
Code	Ink	Anilox volume (cm ³ /m ²)	Print speed (m/min)
SA	PFI-600	12	6–22
SB	PFI-600	12	6–22
SC	PFI-600	11	5
SD	PFI-600	12	6–22

RESULTS AND DISCUSSION

Ink uniformity

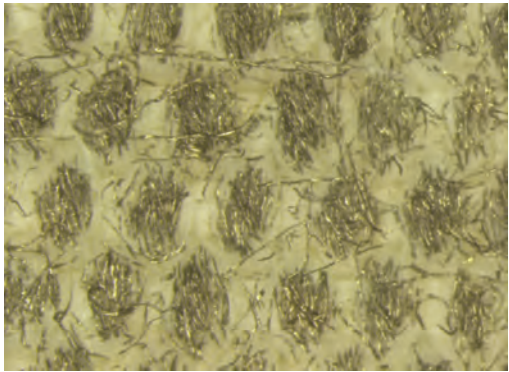
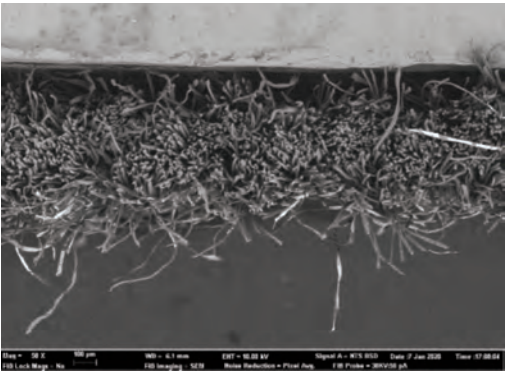
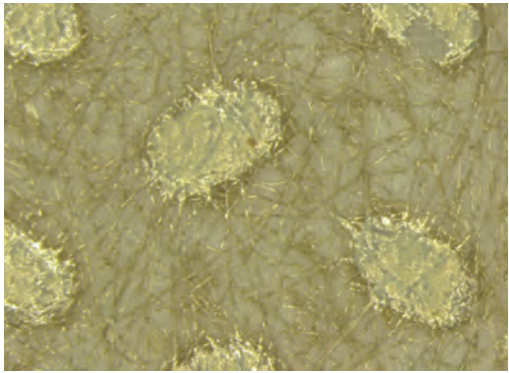
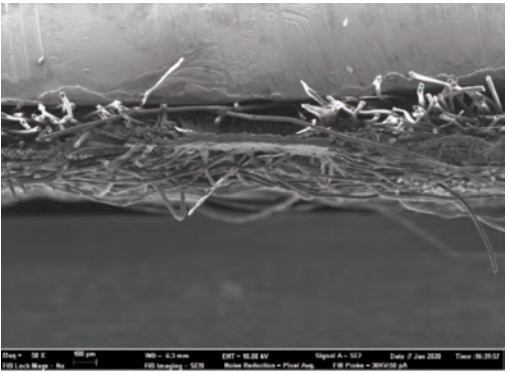
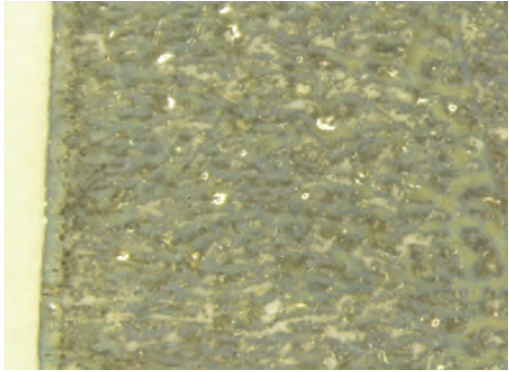
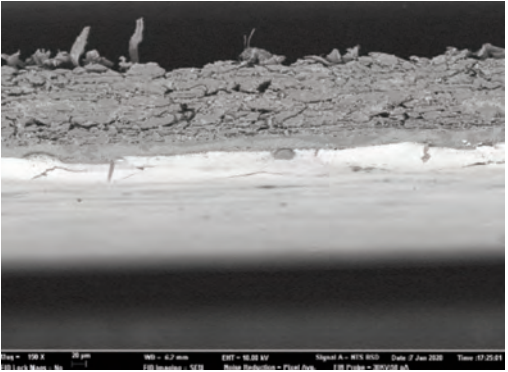
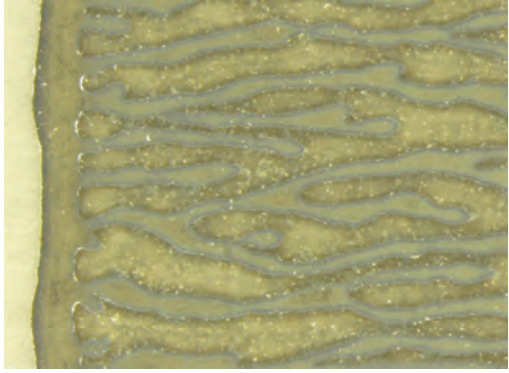
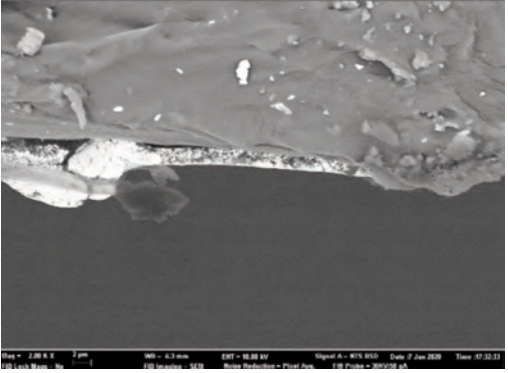
The optical macroscopic images were taken with a LEICA MZ APO stereomicroscope. It was used to analyse the print uniformity of each layer of the electronic

printed samples. Magnifications from 20 to 80 were used. Table 3 shows images of the 20× results. It is observed that both woven and non-woven fabric do not present uniformity at the print, due to the porous surface. Printing electronics with low viscosity inks onto a rough and porous textile surface is of great challenge, due to the orientation of fibres or yarns and the change of fibre morphology constantly [4].

Ink penetration

High-resolution topographic images by SE (secondary electrons) and maps of crystalline and textural orientations by EBSD (electron backscatter diffraction) were taken with a ZEISS ULTRA 55 Scanning Electron Microscope Field Emission Gun (field emission scanning electron microscopy (FE-SEM)). They were used to analyse the ink penetration

Table 3

OPTICAL MACROSCOPIC IMAGES OF THE STUDIED SUBSTRATES		
Substrate	Optical microscope 20×	FE-SEM
(SA) Woven fabric		
(SB) Nonwoven fabric		
(SC) Siliconized paper		
(SD) Polymeric film		

and the adhesion in each substrate. Table 3 shows the FE-SEM images obtained.

These images confirm that the continuity of the ink does not appear on the woven and non-woven fabrics, being able to observe a space between the ink and the surface of the fabric, not being completely adhered to the substrate. This does not observed when the ink is deposited on the paper, as it is much more uniform, the ink is completely in contact with the surface.

Conductivity

To measure the electrical behaviour a usual two-terminal sensing unit was firstly considered.

Nevertheless, a two-wire system does not provide correct output due to variation in ambient temperature, as the resistance of the lead wires (both sides) changes unpredictably. Meanwhile, Four-Wire Kelvin resistance measurement makes it possible to accurately measure resistance values less than 0.1 Ω while eliminating the inherent resistance of the lead wires connecting the measurement instrument to the component being measured [11]. For that reason, 4-wire system measurements were made Resistance measurements were made with a FLUKE 8845A multimeter from FLUKE CORPORATION (Everett, Washington, USA). Table 4 shows the results obtained for each substrate.

Table 4

KELVIN (4-WIRE) RESISTANCE MEASUREMENT		
Code	Substrate	Resistance (Ω)
SA	Woven fabric	-
SB	Spunbonded nonwoven fabric	-
SC	Paper	1.2450
SD	Polymeric	1.9747

Whereas the results for paper and polymeric substrates indicate that the printing is conductive, neither the woven nor the nonwoven fabrics present electrical conductivity. This is because poor uniformity limits the conductivity of a print, leading to functional variation and short circuits. In order to address these challenges, surface pre-treatment onto rough and porous substrates or coating and lamination processes should be done in order to produce continuous conductive pathway onto textiles [4, 6].

Colour fastness

The grade of colour fastness to wash and rubbing of the electronic flexo printed samples were evaluated and presented in the table 5. Neither the siliconized paper (SC) nor the polymeric substrate (SD) could stand the washing test and were torn at the wash machine. Furthermore, the SD was not capable of withstanding the rubbing test, crashing with the pressure of the crockmeter.

The overall results of colour fastness to rubbing of samples showed poor fastness properties in terms of discharge, which was harmonious with previous studies of other printing techniques [12]. SA and SB showed an improved grade in the rubbing degradation possibly due to the large amount of ink deposited on the surface although wet rubbing properties are lower than dry. In order to address these challenges, surface pre-treatment onto rough and porous substrates should be done in order to improve the ink adhesion and therefore the electrical behaviour [4].

On the other hand, the overall results of colour fastness to wash of woven (SA) and nonwoven (SB) fabrics samples were very good to excellent. According to a previous review [13], an increment of ink volume improves the ink coverage, upgrading in this case the conductivity, nevertheless it enhances the ink wash-out effect. For this reason, the ink volume transferred to the substrate should be optimized when conductivity and colour fastness to washing are the objectives. In addition, coating and lamination processes could be done in order to ensure the continuous conductive pathway on textiles [10].

CONCLUSIONS

By a comparison of the same ink printed on different flexible substrates it has been concluded that the roll-to-roll flexography printing process is an effective technique to produce conductive tracks on silicone paper and polymer flexible substrates. Nevertheless, it has been demonstrated that the same silver ink printings do not present uniformity, ink penetration and electrical conductivity onto textile and non-woven fabrics. For this reason, future work will explore different surface pre-treatments, such as hydrophobic and oleophobic treatments, in order to improve ink uniformity and then produce continuous conductive pathway through flexography on textiles and non-woven fabrics.

Table 5

COLOR FASTNESS TO WAS AND RUBBING RESULTS						
Code	Rubbing				Washing	
	Degradation		Discharge		Degradation	Discharge
	Dry	Wet	Dry	Wet		
SA	4-5	3-4	1	1	4	5
SB	4	1-2	3	2	4	5
SC	2	1	3	1	-	-
SD	-	-	-	-	-	-

On the other hand, woven and nonwoven fabrics are a suitable early option regarding colour fastness to wash instead of thin polymeric and paper substrates that tear at the wash machine. The ink volume transferred to the substrate should be optimized when conductivity and colour fastness to washing are the objectives. Future work will also explore several coatings that could also be applied after the printing to protect the circuits and then improve the electronic behaviour after washing. Concerning colour fastness

to rubbing, even better than for thin polymeric and paper substrates, poor results were obtained for woven and nonwoven fabrics. For this reason, future work will be focused on surface pre-treatment onto rough and porous substrates in order to improve the ink adhesion and therefore the electrical behaviour.

ACKNOWLEDGEMENTS

This research is part of HYBRID project that is funded by the Conselleria d'Economia Sostenible, Sectors Productius i Treball, through IVACE. Application No.: IMAMCI/2020/1.

REFERENCES

- [1] Avuthu, S.G., Gill, M., Ghalib, N., Sussman, M.R., Wable, G., Richstein, J.Ph., Jabil, D., *An introduction to the process of printed electronics*, 2016
- [2] Kim, C., Jeon, S., Kim, C.-H., *Reduction of Linearly Varying Term of Register Errors Using a Dancer System in Roll-to-Roll Printing Equipment for Printed Electronics*, In: International Journal of Precision Engineering and Manufacturing, 2019, <https://doi.org/20.1007/s12541-019-00157-2>
- [3] Cruz, S., Rocha, L., Viana, J., *Printing Technologies on Flexible Substrates for Printed Electronics*, 2018, <https://doi.org/10.5772/intechopen.76161>
- [4] Karim, N., Afroj, S., Novoselov, K., Yeates, S., *All Inkjet-Printed Graphene-Silver Composite Ink on Textiles for Highly Conductive Wearable Electronics Applications*, In: Scientific Reports, 2019, 8035, 1–10, <https://doi.org/10.1038/s41598-019-44420-y>
- [5] Cano-Raya, C., Denchev, Z., Cruz, S., Viana, J., *Chemistry of solid metal-based inks and pastes for printed electronics – A review*, In: Applied Materials Today, 2019, 15, 416-430, <https://doi.org/10.1016/j.apmt.2019.02.012>
- [6] Yang, K., Torah, R., Wei, Y., Beeby, S., Tudor, J., *Waterproof and durable screen printed silver conductive tracks on textiles*, In: Textile Research Journal, 2013, 83, 2023-2031, <https://doi.org/10.1177/0040517513490063>
- [7] Søndergaard, R., Hosel, M., Krebs, F., *Roll to roll fabrication of large area functional organic materials*, In: Journal of Polymer Science, 2012, 51, 16–34
- [8] Mogg, B., Claypole, T., Deganello, D., Phillips, C.O., *Flexographic printing of ultra-thin semiconductor polymer layers*, In: Translational Materials Research, 2016, 3, 015001, <https://doi.org/10.1088/2053-1613/3/1/015001>
- [9] Davide, D., *Control of morphological and electrical properties of flexographic printed electronics through tailored ink rheology*, In: Organic Electronics, 2019, 73, 212–218
- [10] Yang, K., Torah, R., Wei, Y., Beeby, S., Tudor, J., *Waterproof and durable screen printed silver conductive tracks on textiles*, In: Textile Research Journal, 2013, 83, 19, 2023–2031
- [11] Revuelta, P., Litrán, S., Thomas, J., *Electrical Power Terms in the IEEE Std 1459 Framework*, 2016, <https://doi.org/10.1016/B978-0-12-803216-9.00002-X>
- [12] Vasić, J., Kasikovic, N., Delic, G., Đurđević, M., *Impact of type of ink and substrate on colorimetric values of inkjet prints*, 2018, 365–372, <https://doi.org/10.24867/GRID-2018-p44>
- [13] Kasikovic, N., Vladić, G., Milic, N., Novaković, D., Milošević, R., Dedijer, S., *Colour fastness to washing of multi-layered digital prints on textile materials*, In: Journal of the National Science Foundation of Sri Lanka, 2018, 46, 381, <https://doi.org/10.4038/jnsfsr.v46i3.8489>

Authors:

ANA M. RODES-CARBONELL¹, JOSUÉ FERRI¹, EDUARDO GARCIA-BREIJO²,
EVA BOU-BELDA³

¹Textile Research Institute (AITEX), Alcoy 03801, Spain

²Instituto Interuniversitario de Investigación de Reconocimiento Molecular y Desarrollo Tecnológico (IDM),
Universitat Politècnica de València, Valencia 46022, Spain
e-mail: egarciab@eln.upv.es

³Department of Textile and Paper Engineering, Universitat Politècnica de València,
Plaza Ferrándiz y Carbonell s/n. 03801, Alcoy, Spain
e-mail: evbobel@upvnet.upv.es

Corresponding author:

ANA M. RODES-CARBONELL
e-mail: arodes@aitex.es

Assessing the presence of pesticides in modern and contemporary textile artifacts using advanced analysis techniques

DOI: 10.35530/IT.072.02.1828

ELENA-CORNELIA MITRAN
IRINA-MARIANA SANDULACHE
LUCIA-OANA SECAREANU
MIHAELA CRISTINA LITE

OVIDIU GEORGE IORDACHE
ELENA PERDUM
GABRIEL-LUCIAN RADU

ABSTRACT – REZUMAT

Assessing the presence of pesticides in modern and contemporary textile artifacts using advanced analysis techniques

The examination of contemporary textiles continuously offers amazing perspectives of the past for anyone who explores them. The ethnographic textile pieces are complex, both from the perspective of the component materials and regarding the techniques used for their manufacture. The action of conserving the cultural and artistic patrimony is firstly a matter of scientific research and then of technical execution. However, the possible health effects on the personnel, which are directly involved in the actions of sampling, conservation or restoration of the textile art objects, must always be taken into consideration. Textile objects can be contaminated with various toxic residues (e.g., pesticides). When investigating archaeological, modern and contemporary textiles it is very important to maintain the integrity of the artifacts, as they cannot be replaced, and the consumption or damage of even a small part of them for analytical purposes should be undertaken only if the data cannot be obtained differently. For determining the presence of pesticides in the samples they must be subjected to processes such as: extraction, enrichment of samples, isolation, identification, and quantification.

Given the above, the most common methods of extraction and determination of pesticides present in textile artifacts were briefly discussed. Punctually, the analytical techniques used in the case of three selected pesticides (malathion, methoxychlor and permethrin) were evaluated.

Keywords: GC-MS, SPME, malathion, methoxychlor, permethrin

Evaluarea prezenței pesticidelor în artefactele textile moderne și contemporane prin utilizarea tehnicilor analitice avansate

Examinarea produselor textile contemporane oferă perspective asupra trecutului într-un continuum care uimește pe oricine îl explorează. Piese textile etnografice sunt complexe, atât din punctul de vedere al materialelor componente, cât și din acela al tehnicilor folosite pentru realizarea lor. Acțiunea de conservare a patrimoniului cultural și artistic este în primul rând o problemă de cercetare științifică și apoi de execuție tehnică. Însă, trebuie luate în considerare întotdeauna eventualele efecte asupra sănătății personalului implicat direct în acțiunile de prelevare, conservare sau restaurare a obiectelor textile de artă. Obiectele textile pot fi contaminate cu diferite reziduuri toxice (de exemplu pesticide). În cazul analizei materialelor arheologice, moderne și contemporane este foarte importantă păstrarea intactă a artefactelor, întrucât acestea nu pot fi înlocuite, iar consumul sau deteriorarea chiar și a unei mici părți a acestora în scopuri analitice trebuie să fie întreprinsă numai în cazul în care datele nu pot fi altfel obținute. În vederea determinării prezenței pesticidelor în probele pe care dorim să le analizăm, acestea trebuie să treacă prin procese precum: extracție, îmbogățirea probelor, izolarea acestora, identificarea și cuantificarea acestora.

Având în vedere cele menționate anterior, în continuare s-a discutat pe scurt despre cele mai frecvent utilizate metode de extracție și determinare a pesticidelor prezente în artefacte textile, dar și punctual, prin evaluarea tehnicilor analitice utilizate în cazul a trei pesticide selectate: malation, metoxiclor și permethrin.

Cuvinte-cheie: GC-MS, SPME, malation, metoxiclor, permethrin

INTRODUCTION

Undoubtedly, textiles are a reflection of both present and past cultures. The possible effects on the health of the personnel, which are directly involved in the sampling, conservation or restoration of the textile art objects, must always be considered.

The quality of the air (temperature, humidity, light, fungal contamination) can influence the textile materials exposed in museums, as well as the human

health [1, 2]. Textiles can be contaminated with various toxic residues (e.g., pesticides). Pesticides are chemical compounds used to remove pests. They can enter the pest's body through their skin, mouth or airways.

Pesticides can have both natural and synthetic origin. Also, in the class of pesticides, hormonal regulators that inhibit the maturation of insects are sometimes mentioned.

Within museum collections, different types of pesticides or fumigants have been used over time, about which not much is known. Thus, they became dangerous even for humans, when coming into contact with textiles treated with such substances.

It is very important to use advanced techniques for identifying/quantifying these hazardous substances in order to develop protection plans for museum staff. Over time, scientists have tried to develop and optimize such analysis techniques. This paper proposes to review the main analytical procedures for identifying and quantifying the pesticides that may be present in modern and contemporary textiles.

GENERAL METHODS

Frequently, the analytical method is preceded by a process of extraction of the analyte of interest. Liquid-liquid extraction (LLE) is a common extraction method based on the different solubility of chemicals in two different liquid solvents [3]. Two phases will be formed: an aqueous phase (in which water-miscible compounds will be separated) and an organic phase (in which the pesticides will be extracted). The first successful commercial liquid-liquid extraction operation was developed for the oil industry in 1909, when Edeleanu's process was used to remove aromatic hydrocarbons from kerosene, using liquid sulfur dioxide as solvent [4]. However, this type of method is less used for the analysis of environmental samples, due to high solvent consumption and low recovery rates [3].

Another common extraction is solid-liquid extraction (SLE). The process consists in extracting the compounds of interest from a solid sample with a suitable solvent.

Supercritical Fluid Extraction (SFE) is a method that processes both solid and semi-solid samples. The difference between SFE and SLE is that, in the case of SFE, the extraction solvent is a supercritical fluid. The first recognition of the analytical potential of supercritical fluids probably came in a note made by James Lovelock in 1958 [5]. However, the first supercritical chromatographic separation was reported in 1962 by Klesper [6].

A very commonly used extraction method in the case of heritage samples is solid-phase micro-extraction (SPME)-absorption/desorption technique. The principle consists in immersing a fiber covered with silica in the sample. SPME was introduced in 1989 and it attracts more and more attention due to its simplicity and ease of use [7–9]. The sample can either be directly desorbed from the fiber in a chromatographic injection port or it can be desorbed from the fiber using a solvent [10]. Both methods have been used in various studies for pesticide analysis [11–16].

Solid phase micro-extraction in combination with gas chromatography coupled with mass spectrometry (GC-MS) offers a simple and sensitive option for analyzing art textiles that are contaminated with volatile or semi-volatile organic pesticides [17].

Liquid-liquid dispersant micro-extraction (DLLME) is also a technique that is sometimes used to analyze contaminants in heritage samples. This technique consists in dissolving a water-insoluble extract in a water-miscible solvent, followed by centrifugation of this mixture. By centrifugation, the contact surface between the phases increases, achieving a faster extraction, compared to the liquid-liquid extraction [18, 19].

A relatively new extraction technique is one-drop micro-extraction (SDME) – a miniaturized solvent micro-extraction technique. In this type of extraction, a single micro-drop of organic solvent suspended at the tip of the micro-syringe needle is used and the sample solution can be pre-concentrated directly by D-SDME (direct SDME) or by SDME headspace (HS-SDME) [20].

One of the most common methods for determining pesticides is QuEChERS (Quick, Easy, Cheap, Effective, Rugged, Safe). The name of this procedure comes from its advantages: fast, easy, cheap, efficient, robust and safe. It consists of extracting the analyte with an organic solvent, removing the water and analyzing by a suitable technique [10].

The most used methods for the analysis of toxic substances in textiles are liquid chromatography coupled with mass spectrometry (LC-MS) [21] and gas chromatography coupled with mass spectrometry (GC-MS) [21, 22–25]. GC-MS is a widely used method due to the ability to combine both the retention time of each analyte and the correct matching of the library with reference mass spectra, which provides a high degree of certainty for identification. The use of a spectrometric mass detector also allows the identification of unexpected pesticides or possible degradation products. In a study conducted in 2017 by Salmo and his collaborators on nine artifacts belonging to the Karuk Tribe, they identified 3 types of pesticides: p-dichlorobenzene, naphthalene and DDT [2].

Palmer et al. analyzed 17 heritage objects belonging to the Hupa Tribe of California and identified the presence of 5 pesticides: p-dichlorobenzene, naphthalene, thymol, lindane and DDT [27]. Another type of detector used in GC analysis is the flame ionization detector (FID). Glastrup was one of the first researchers to use GC-FID to analyze pesticides in modern and contemporary heritage samples [28].

Direct analysis by real-time mass spectrometry (DART-MS) is a method that allows the analysis of solid samples without the need for prior preparation and can be used to determine substances known to have a negative effect on human health and which may be present in textiles [29, 30].

Once a method for determining the pesticides has been established and implemented, any subsequent analysis of a sample can be completed in less than one hour and modern data systems can be used to automate the identification and quantification of compounds.

PESTICIDE ASSEMENT VIA GC-MS – MALATHION, METHOXYCHLOR AND PERMETHRIN

In order to exemplify a pesticide assessment method three pesticides were subjected to GC-MS analysis: malathion, methoxychlor and permethrin.

The chronological evolution of the three selected pesticides is shown in figure 1 and their chemical structures are presented in table 1.

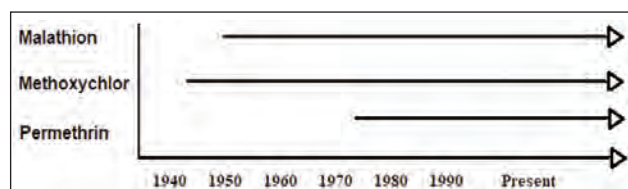


Fig. 1. Chronological evolution of the three pesticides [31]

Malathion is a compound from the class of organophosphate pesticides and it is found in liquid form, colorless or at most up to amber color, with a smell similar to garlic [32].

Physical-chemical properties:

- vapour pressure [33]: 1.78×10^{-4} mmHg at 25°C or 5.3 mPa at 30°C; also 1.2×10^{-4} to 8×10^{-6} mmHg at 20°C;

- water-octanol partition coefficient (log KOW) [34]: 2.75, 2.36–2.89;

- molecular weight [35]: 330.4 kg/kmol;

- water solubility [35]: 145 mg/l.

Malathion is toxic, thus it is recommended to avoid exposure through inhalation, skin contact or ingestion [35]. The exposure of humans to malathion can give various symptoms such as excessive sweating, pupil contraction, tearing, salivation, abdominal cramps, diarrhea, vomiting, changes in blood pressure (rapid increase or decrease of the heart rate), headache, insomnia [36–38]. Exposure to high doses of malathion can lead to the development of Intermediate Syndrome, which is manifested by acute coronary insufficiency, pre-infarction etc. [39, 40].

Some regulations and recommendations for malathion include the following [42]:

- Occupational Safety and Health Administration (OSHA) has set an occupational malathion exposure limit of 15 mg/m³ for a working day of 8 hours, 40 hours per week. National Institute for Occupational Safety and Health (NIOSH) recommends that workers should not be exposed to more than 10 mg/m³ malathion on a working day of 10 hours, 40 hours per week. NIOSH also recommends that a level of 250 mg/m³ of malathion in the air can be considered immediately dangerous to life and health.
- The Food and Drug Administration (FDA) and the Environmental Protection Agency (EPA) allow a maximum of 8 ppm of malathion to be present as residues on specific crops used as food.

Methoxychlor is an organochlorine pesticide, in the form of pale yellow powder with a slightly fruity or musty smell [42].

Physical-chemical properties:

- vapour pressure [43]: 5.56×10^{-3} Pa at 25°C;

- water-octanol partition coefficient (log KOW) [45]: 5.67;

- molecular weight: 345.65 kg/kmol;

- water solubility [43]: 0.302 mg/l at 25°C.

Methoxychlor is a pesticide proven to be an endocrine disruptor [44].

EPA limits the amount of methoxychlor that may be present in drinking water to 0.04 parts of methoxychlor to one million parts of water (0.04 ppm). The EPA has also set limits of 1–100 ppm on the amount of methoxychlor that may be present in various agricultural products (fruits, vegetables, grains, meat, milk and animal food). FDA limits the amount of methoxychlor in bottled water at 0.04 ppm. The EPA restricts the amount of methoxychlor that can be released into the environment during combustion or by disposal in landfills. OSHA has set Permissible Exposure Limit (PEL) of 15 mg/m³ of air to the average amount of methoxychlor that may be present in the air during a working day of 8 hours [45].

Table 1

STRUCTURE OF THE THREE SELECTED PESTICIDES		
Malathion	Methoxychlor	Permethrin (cis and trans-isomer)
		<p>cis-Permethrin</p> <p>trans-Permethrin</p>

Permethrin is a pyrethroid pesticide. Permethrin is a mixture of two stereoisomers (cis- and trans-permethrin) [46]. Permethrin varies in appearance, from a colorless crystal to a yellowish or brown viscous liquid [46, 47].

Physical-chemical properties:

- vapour pressure [47]: 2.15×10^{-8} mmHg;
- water-octanol partition coefficient (log KOW) [21]: 6.1;
- molecular weight: 391.3 kg/kmol;
- water solubility [46, 47]: 5.5×10^{-3} mg/l, 6×10^{-3} mg/l.

Permethrin causes damages to the nervous system of insects. It interferes with sodium channels to disrupt the function of neurons and causes muscle spasm, culminating in paralysis and death [48, 49].

The World Health Organization (WHO) recommended that the level of permethrin in drinking water should not exceed 20 µg/l. OSHA has set a level of pyrethroids in the air at work. Occupational exposure limits for a working day of 8 hours and 40 hours of work per week are 5 mg per cubic meter (mg/m^3). The EPA has recommended daily oral exposure limits for 10 different types of pyrethroids. These limits are between 0.005 and 0.05 mg/kg/day [48].

Due to the many negative effects on humans and the environment, it is important and still necessary to develop precise, sensitive and robust extraction and analysis methods to determine the amount of pesticides and to maintain them in accordance with the laws. Considering all these aspects, the most commonly used method for the extraction and determination of the three pesticides of interest was briefly discussed below.

In general, sampling techniques mostly involve swab of wipe-based surface sampling or removing a portion of the object.

GC-MS is one of the most widely used analytical methods for the analysis of organic compounds at the trace level. The MS detector ensures excellent sensitivity, the LODs frequently having values close to the picogram (10^{-12} grams) [49]. Unlike TCD (Thermal Conductivity Detector), FID (Flame Ionization Detector) and ECD (Electron Capture Detector), wherein a peak from the resulting chromatogram simply indicates a response to a particular compound exiting the column, the MS detector provides three dimensions of information: the m/z ratio, the intensity and the retention time.

Zhou et al. developed a method for the determination of 77 pesticides from textile materials by GC-MS. They analyzed a mixture of 12 pyrethroids (including permethrin), 26 organochlorines (including methoxychlor), 30 organophosphorus (including malathion), 8 carbamates and an organic nitrogen pesticide [50].

Another method for determining organophosphorus pesticides in textiles was proposed by Hu et al. They used solid phase microextraction (SPME) and GC as the method of analysis. Malathion was among the pesticides analyzed. The detection limit for the 11 selected pesticides was in the range of 0.03 µg/l – 0.5 µg/l [51].

18 objects from the Cook-voyage collections at the Pitt Rivers Museum, University of Oxford were analyzed by GC-MS for the evaluation of pesticide residues (including permethrin) by Charlton et al. [52]. The sampling method used by them was swab surface sampling: they used cotton pads moistened with distilled water and evaluated how appropriate this method is. They chose this procedure because water is considered to be the only safe solvent to use, but a disadvantage is that most pesticides have low solubility in water. These cotton pads (35–40 pads taken) were weighed and extracted with ethyl acetate. The resulting solutions were analyzed by GC-MS.

Rushworth et al. [53] developed a new method of sampling and a non-invasive analysis to assess the volatile pesticides that may be present in heritage collections. They performed a vapor phase sampling using sampling tubes loaded with Tenax-TA™, capturing the analytes in these tubes. Subsequently, they performed the analysis of the resulting vapors using thermal desorption coupled with GC-MS (TD-GC-MS). Another innovative method is the analysis of pesticides from aqueous samples by using a sampling device coupled with GC-MS [54].

Advanced analytical methods and techniques are an essential tool in the field of cultural heritage, as they provide the means to understand the studied objects [55, 56].

CONCLUSIONS

There is a major necessity of precise, selective and reproducible analytic techniques for evaluating and quantifying the presence of pesticides in modern and contemporary textile artifacts. The general methods for assessing the presence of pesticides in textile materials and specific methods for three types of pesticides which have been used to treat textiles against the attack of pests have been presented in this paperwork.

ACKNOWLEDGEMENTS

This work was elaborated through Nucleu Program, conducted with MCI support, project no. 4N/2019/PN 19 17 05 01. The publication fee of the paper is funded by the Ministry of Research and Innovation within Program 1 – Development of the national RD system, Subprogram 1.2 – Institutional Performance – RDI excellence funding projects, Contract no. 6PFE/2018.

REFERENCES

- [1] Indrie, L., Oana, D., Ilies, M., Ilieş, D.C., Lincu, A., Ilieş, A., Baias, S., Herman, G.V., Onet, A., Costea, M., Marcu, F., Burta, L., Oana, I., *Indoor air quality of museums and conservation of textiles art works. Case study: Salacea Museum House, Romania*, In: Industria Textila, 2019, 70, 1, 88–93, <http://doi.org/10.35530/IT.070.01.1608>

- [2] Zahra, Q., Mangat, A.E., Fraz, A., Hussain, S., Abbas, M., Mukhtar, U., *Air, moisture and thermal comfort properties of woven fabrics from selected yarns*, In: *Industria Textila*, 2018, 69, 3, 177–182, <http://doi.org/10.35530/IT.069.03.1447>
- [3] Peake, B.M., Braund, R., Tong, A.Y.C., Tremblay, L.A., *Detection and presence of pharmaceuticals in the environment*, In: Barrie, M.P., Rhiannon, B., Alfred, Y.C.T., Louis, A.T. (Eds.), *The Life-Cycle of Pharmaceuticals in the Environment*, Woodhead Publishing Inc., Cambridge, 2016, 77–107
- [4] Brandt, R.L., *The Edeleanu Process for Refining Petroleum*, In: *Ind. Eng. Chem.*, 1930, 22, 3, 218–223
- [5] White, C.M., *Modern supercritical fluid chromatography*, Hu^{thig}, Heidelberg, 1988, 6
- [6] Klesper, E., Corwin, A.H., Turner, D.A., *J. Org. Chem.*, 1962, 27, 700
- [7] Pawliszyn, J., *Solid-phase Microextraction: Theory and Practice*, John Wiley & Sons, New York, 1998, 264
- [8] Pawliszyn, J., *Applications of Solid-phase Microextraction*, The Royal Society of Chemistry, Cambridge, UK., 1999, 520
- [9] Vas, G., Vekey, K., *Solid-phase microextraction: A powerful sample preparation tool prior to mass spectrometric analysis*, In: *Journal of Mass Spectrometry*, 2004, 39, 233–254
- [10] Sehrish, N., Nazia, R., Karam, A., *Comparative Evaluation of Extraction Procedures and Chromatographic Techniques for Analysis of Multiresidue Pesticides in Honey*, In: *Int J Nutr Sci & Food Tech*, 2017, 3, 2, 43–49
- [11] Lee, J.H., Hwang, S.M., Lee, D.W., Heo, G.S., *Determination of volatiles organic compounds (VOCs) using Tedlar bag/solid-phase microextraction/gas chromatography/mass spectrometry (SPME/GC/MS) in ambient and workplace air*, In: *Bulletin of the Korean Chemical Society*, 2002, 23, 3, 488–496
- [12] Musshoff, F., Junker, H., Madea, B., *Simple determination of 22 organophosphorous pesticides in human blood using headspace solid-phase microextraction and gas chromatography with mass spectrometric detection*, In: *Journal of Chromatographic Science*, 2002, 40, 29–34
- [13] Sanusi, A., Ferrari, F., Millet, M., Montury, M., *Pesticide vapours in confined atmospheres. Determination of dichlorvos by SPME-GC/MS at the microgram m³ level*, In: *Journal of Environmental Monitoring*, 2003, 5, 574–577
- [14] Ferrari, F., Sanusi, A., Millet, M., Monturyl, M., *Multiresidue method using SPME for the determination of various pesticides with different volatility in confined atmospheres*, In: *Analytical and Bioanalytical Chemistry*, 2004, 379, 3, 476–483
- [15] Sakamoto, M., Tsutumi, T., *Applicability of headspace solid-phase microextraction to the determination of multi-class pesticides in water*, In: *Journal of Chromatography*, 2004, A, 1028, 63–74
- [16] Supelco, *Solid-phase Microextraction Application Guide CD*, 5th ed. Supelco, Bellefonte, Pennsylvania, 2004
- [17] Ormsby, M., Johnson, J.S., Heald, S., Chang, A., Bosworth, J., *Investigation of Solid Phase Microextraction Sampling for Organic Pesticide Residues on Museum Collections*, In: *Collection Forum*, 2006, 20, 1–2, 1–12
- [18] Bashiri-Juybari, M., Mehdiinia, A., Jabbari, A., Yamini, Y., *Determination of Amitraz in the Honey Samples by Dispersive Liquid-Liquid Microextraction Followed by Gas Chromatography-Flame Ionization Detection*, In: *Am. J. Analyt. Chem.*, 2011, 2, 632–637
- [19] Kujawski, M.W., Pinteaux, E., Namieśnik, J., *Application of dispersive liquid-liquid microextraction for the determination of selected organochlorine pesticides in honey by gas chromatography-mass spectrometry*, In: *Eur. Food Res. Technol.*, 2012, 234, 223–230
- [20] Amvrazi, E.G., Martini, M.A., Tsiropoulos, N.G., *Headspace singledrop microextraction of common pesticide contaminants in honey: method development and comparison with other extraction methods*, In: *Int. J. Environ. Anal. Chem.*, 2012, 92, 450–465
- [21] Brigden, K., Hetherington, S., Wang, M., Santillo, D., Johnston, P., *Hazardous chemicals in branded luxury textile products on sale during 2013*, Greenpeace Research Laboratories Technical Report 01, 2014, Available at: <http://www.greenpeace.org/international/Global/international/publications/toxics/2014/Technical-Report-01-2014.pdf> [Accessed on January 26, 2016]
- [22] Cioni, F., Bartolucci, G., Pieraccini, G., Meloni, S., Moneti, G., *Development of a solid phase microextraction method for detection of the use of banned azo dyes in coloured textiles and leather*, In: *Rapid Commun. Mass Spectrom.*, 1999, 13, 1833–1837
- [23] Luongo, G., Thorsén, G., Östman, C., *Quinolines in clothing textiles — a source of human exposure and wastewater pollution?*, In: *Anal. Bioanal. Chem.*, 2014, 406, 27, 47–56
- [24] Zhang, S.X., Chai, X.S., Huang, B.X., Mai, X.X., *A robust method for determining water-extractable alkylphenol polyethoxylates in textile products by reaction-based headspace gas chromatography*, In: *J. Chromatogr. A.*, 2015, 1406, 94–98
- [25] Lv, G., Wang, L., Liu, S., Li, S., *Determination of perfluorinated compounds in packaging materials and textiles using pressurized liquid extraction with gas chromatography-mass spectrometry*, In: *Anal. Sci.*, 2009, 25, 425–429
- [26] Salmo, R., Palmer, P.T., Tribe, K., *Fast, nondestructive and cost-effective methods to detect pesticide residues: a case study of several repatriated Karuk Tribe artefacts*, In: *Collection Forum*, 2017, 31, 1, 23–33
- [27] Palmer, P., Martin, M., Wentworth, G., Caldararo, N., Davis, L., Kane, S., Hostler, D., *Analysis of Pesticide Residues on Museum Objects Repatriated to the Hupa Tribe of California*, In: *Environ. Sci. Technol.*, 2003, 37, 1083–1088
- [28] Glastrup, J., *Stud. Conserv.*, 1987, 32, 59
- [29] Borbála, A., Ákos, K., Lajos, N., Tibor, N., Miklós, Z., Sándor, K., *Rapid detection of hazardous chemicals in textiles by direct analysis in real-time mass spectrometry (DART-MS)*, In: *Anal. Bioanal. Chem.*, 2016, 408, 5189–5198
- [30] Cody, R.B., Laramée, J.A., Durst, H.D., *Versatile new ion source for the analysis of materials in open air under ambient conditions*, In: *Anal. Chem.*, 2005, 77, 2, 297–302
- [31] Pool, M., Odegaard, N., Huber, M.J., *Identifying pesticides: pesticide names, classification and use history*, In: *Book – Old Poisons, new problems* by Nancy Odegaard and Alyce Sadongei, Altamira Press Editure, 2014, 5
- [32] Hazardous Substances Databank (HSDB), Malathion; U.S. Department of Health and Human Services, National Institutes of Health, National Library of Medicine
- [33] Tomlin, C.D.S., *The Pesticide Manual, A World Compendium*, 14th ed.; British Crop Protection Council: Alton, Hampshire, UK, 2006, 642–643

- [34] Roberts, T.R., *Metabolic Pathways of Agrochemicals – Part 2: Insecticides and Fungicides*, The Royal Society of Chemistry: Cambridge, UK, 1998, 360–367
- [35] Tomlin, C.D.S., *The Pesticide Manual, A World Compendium*, 14th ed.; British Crop Protection Council: Alton, Hampshire, UK, 2006, 642–643
- [36] Reigart, J.R., Roberts, J.R., *Organophosphate Insecticides. Recognition and Management of Pesticide Poisonings*, 5th ed., U.S Environmental Protection Agency, Office of Prevention, Pesticides and Toxic Substances, Office of Pesticide Programs, U.S. Government Printing Office: Washington, DC, 1999, 34–47
- [37] Toxicological Profile for Malathion, U.S. Department of Health and Human Services, Agency for Toxic Substances and Disease Registry: Atlanta, 2008
- [38] Wagner, S.L., *Diagnosis and treatment of organophosphate and carbamate intoxication*, In: *Occup. Med.: State of the Art Rev.*, 1997, 12, 2, 239–249
- [39] Udakin, D.L., Mullins, M.E., Horowitz, B.Z., Abshier, V., Letzig, L., *Intermediate syndrome after malathion ingestion despite continuous infusion of pralidoxime*, In: *Clin. Toxicol.*, 2000, 38, 1, 47–50
- [40] Lee, P., Tai, D.Y.H., *Clinical features of patients with acute organophosphate poisoning requiring intensive care*, In: *Intensive Care Med.*, 2001, 27, 694–699
- [41] ATSDR (2003): Public health statement – malathion, Available at: <https://www.atsdr.cdc.gov/phs/phs.asp?id=520&tid=92> [Accessed on January 2016]
- [42] ATSDR (2002): Toxicological Profile for Methoxychlor, U.S. Department of Health and Human Services, Public Health Service. Agency for Toxic Substances and Disease Registry. September 2002. Report, 290 pages, Available at: <http://www.atsdr.cdc.gov/ToxProfiles/tp.asp?id=778&tid=151> [Accessed on January 2016]
- [43] US EPA (2012): Estimation Programs Interface Suite™ for Microsoft® Windows, v 4.11, United States Environmental Protection Agency, Washington, DC, USA
- [44] Cummings, A.M., *Methoxychlor as a Model for Environmental Estrogens.*, In: *Crit. Rev. Toxicol.*, 1997, 27, 367–379
- [45] ATSDR (2002): Public health statement – methoxychlor, Available at: <https://www.atsdr.cdc.gov/phs/phs.asp?id=776&tid=151> [Accessed on January 2016]
- [46] Tomlin, C.D.S., *The Pesticide Manual: A World Compendium*, 14th ed., British Crop Production Council: Alton, England, 2006, 813–814
- [47] Reregistration Eligibility Decision (RED) for Permethrin, U.S. Environmental Protection Agency, Office of Prevention, Pesticides and Toxic Substance, Office of Pesticide Programs, U.S. Government Printing Office: Washington, DC, 2007
- [48] ATSDR (2003): *Public Health Statement for Pyrethrins and Pyrethroids.*, Available at: <https://www.atsdr.cdc.gov/phs/phs.asp?id=785&tid=153> [Accessed on January 2016]
- [49] Palmer, P.T., *A Review of Analytical Methods for the Determination of Mercury, Arsenic, and Pesticide Residues on Museum Objects*, In: *Collection Forum*, 2001, 16, 1–2, 25
- [50] Xiao, Z., Mingtai, W., Zhe, S., Aijun, L., Liming, X., Jun, M., Lijun, L., *Multiresidue Determination of 77 Pesticides in Textiles by Gas Chromatography–Mass Spectrometry*, In: *Journal of Chromatographic Science*, 2007, 45, 375
- [51] Xianlei, H., Mingqiu, Z., Wenhong, R., Fang, Z., Gangfeng, O., *Determination of organophosphorus pesticides in ecological textiles by solid-phase microextraction with a siloxane-modified polyurethane acrylic resin fiber*, In: *Analytica Chimica Acta*, 2012, 736, 62–68
- [52] Charlton, A., Domoney, K., Uden, J., *Pesticide residues on the Cook-voyage collections at the Pitt Rivers Museum*, University of Oxford, ICOM-CC – 17th Triennial Conference, Melbourne, 2014
- [53] Rushworth, I.D., Higgitt, C., Smith, M., Gibson, L.T., *Non-invasive multiresidue screening methods for the determination of pesticides in heritage collections*, In: *Heritage Science*, 2014, 2, 3
- [54] Ramos, T.D., Cassella, R.J., de la Guardia, M., Pastor, A., Esteve-Turrillas, F.A., *Use of a versatile, easy, and rapid atmospheric monitor (VERAM) passive samplers for pesticide determination in continental waters*, In: *Anal. Bioanal. Chem.*, 2016, 408, 8495–8503
- [55] Adriaens, A., *European actions to promote and coordinate the use of analytical techniques for cultural heritage studies*, In: *Trac, Trends Anal. Chem.*, 2004, 23, 8, 583–586
- [56] Adriaens, A., Demortier, G., *COST Actions G1 and G8: EU programs on the use of radiation in art and archaeometry*, In: *Nucl. Instrum. Methods*, 2004, B, 226, 3–9

Authors:

ELENA-CORNELIA MITRAN^{1,2}, IRINA-MARIANA SANDULACHE¹, LUCIA-OANA SECAREANU¹,
 MIHAELA CRISTINA LITE¹, OVIDIU GEORGE IORDACHE¹,
 ELENA PERDUM¹, GABRIEL-LUCIAN RADU²

¹The National Research & Development Institute for Textiles and Leather,
 16 Lucretiu Patrascanu, 030508, Bucharest, Romania

²Faculty of Applied Chemistry and Materials Science, University POLITEHNICA of Bucharest, Romania

Corresponding author:

ELENA-CORNELIA MITRAN
 e-mail: cornelia.mitran@incdtp.ro

Effect of filaments diameter on the mechanical properties of wrap hybrid CFRP

DOI: 10.35530/IT.072.02.1733

FANGTAO RUAN
CHENGLONG XIA
LI YANG

ZHENZHEN XU
FEIYAN TAO

ABSTRACT – REZUMAT

Effect of filaments diameter on the mechanical properties of wrap hybrid CFRP

In this paper, the vine-like structure of carbon bundles was designed through polyester fibre wrapping for better mechanical properties. The effect of wrapped hybrid structure and diameters of polyester fibre on the mechanical properties of carbon-polyester fibre/epoxy unidirectional composites was investigated experimentally. Five kinds of specimens with different polyester filament diameters were produced. The impact, tensile and unidirectional compressive properties of WHC (Wrap Hybrid Composite) were measured. Experimental results show that: it can be developed with strength and toughness properties far superior to those of their constituents, the compressive fracture morphology of specimens indicated that the fracture patterns of composites depend on wrapped hybrid structure, polyester fibres with higher tensile strengths provide better impact resistance, while thinner wrapping fibres enhance the compression properties of the composite material more effectively. The diameter of the wrapping fibre should be optimized as per the application of the composite material. The vine-like structure can provide a new design method for the structural design of continue fibre reinforced composite materials.

Keywords: fibre reinforced polymer, wrapped hybrid, compression failure, impact energy

Influența diametrului filamentelor asupra proprietăților mecanice ale CFRP hibrid înfășurat

În această lucrare, structura asemănătoare viței-de-vie a fasciculelor de carbon a fost proiectată prin înfășurarea fibrei de poliester pentru proprietăți mecanice superioare. Influența structurii hibride înfășurate și a diametrelor fibrelor de poliester asupra proprietăților mecanice ale compozitelor unidirecționale din fibră de carbon-poliester/epoxidice a fost investigată experimental. Au fost produse cinci tipuri de probe cu diferite diametre de filament de poliester. Au fost determinate rezistența la impact, rezistența la tracțiune și proprietățile de compresie unidirecționale ale WHC (Wrap Hybrid Composite – compozit hibrid înfășurat). Rezultatele experimentale arată că: poate fi dezvoltat cu proprietăți de rezistență mult superioare constituenților lor, morfologia compresivă a specimenelor a indicat faptul că modelele de formare ale compozitelor depind de structura hibridă înfășurată, fibrele de poliester cu rezistențe la tracțiune mai ridicate oferă o rezistență la impact superioară, în timp ce fibrele înfășurate mai subțiri sporesc mai eficient proprietățile de compresie ale materialului compozit. Diametrul fibrei înfășurate trebuie optimizat conform aplicației materialului compozit. Structura asemănătoare viței-de-vie poate oferi o nouă metodă de proiectare pentru proiectarea structurală a materialelor compozite armate cu fibre.

Cuvinte-cheie: polimer armat cu fibre, hibrid înfășurat, eșec de compresie, energie de impact

INTRODUCTION

Carbon fibre reinforced polymer composites (CFRP) have been widely used in aircraft and aerospace engineering industries for a long time due to their high specific strength to weight ratio and excellent corrosion resistance property, making it be ideal materials for designing on road and in air vehicles with less fuel consumption [1–4]. The design-ability of mechanical properties for CFRP is prominent due to it is an anisotropic composite material with a fibre arrangement structure. The reinforced fibres are usually papered as textile prefabs, such as plain weave, stitching, knitting, and three-dimensional textile structure. Apart from the textile structure design, the hybrid structure, which made of two different types of high strength fibre composed with the same resin

matrix to meet specific strength requirements, has been recognized as an important design method for many engineering applications [5]. They are generally used to reduce the costs of composites that have a combination of the best mechanical, wear, thermal or other properties. Many studies have been done on the development of carbon nanotube reinforced composites. But there are many problems with the way these materials are produced, including the problems of irregularity and the accumulation of nanotubes in one place [6]. Belle and colleagues showed that by applying the chemical vapour deposition process, a smooth thin layer of carbon nanotubes can be created on the outer surface of the fibre optic. They showed that the mechanical and electrical properties

of such a layer improved due to the growth of carbon nanotubes on the surface of alumina fibre.

Some researchers have investigated the hybrid composite with different hybrid structures. Hung et. al [7] have studied the impact response of layer hybrid carbon, glass or basalt fibre reinforced polymer composites to obtain a structure strong enough, relatively low-cost composite material. Zheng [8] co-braided hybrid structure on the tensile response of carbon/aramid hybrid braided composites. The compromise optimization of strength and toughness can be achieved by carbon-aramid hybrid composites. Liu [9] investigated the erosion characteristics of hybrid fabric reinforced polyetherimide composite and proposed a new non-crimp hybrid structure for better mechanical properties and erosion resistance. The above hybridization is classified into interlaminar, laminate, which involves depositing layers composed of different fibres, and intralaminar, where different types of fibres are entangled within a single layer.

In our previous study, a vine-like structure fibre hybridization was proposed. Inspiration and sketches are shown in figure 1. Wrapping reinforced fibre bundle for high unidirectional compressive performance [10], polybenzoxazole (PBO) fibers was used as the covered filament, which consists of rigid rod chain molecules, it has high tensile strength and a high modulus, the reinforced fibre bundle was ultra-high molecular weight polyethylene fibre. The vine-tree structure is widely observed in nature when the plant has a growth habit of trailing or climbing stems. The vines use trees for growth rather than devoting energy to development of supportive tissue, enabling the vine to reach sunlight with a minimum investment of energy. The trees may also facilitate the transportation of nutrient substances. Such hierarchical vine-tree structures offer synergy between the vines and trees as well as the maximum utilization of sunshine and limited soil and space, which could also be a promising universal architecture in both macro- and micro-worlds. The experimental results showed that the wrap structure affects the compressive failure pattern, and then improve the compression strength and modulus of unidirectional composites.

In this paper, the effect of wrapping filament diameter on the compression, tension and impact properties of composite was investigated. Five types of polyester monofilament was used to wrap the carbon fibre bundle. Finally, the PET/CFRP wrapped hybrid composite was made by VARTM(vacuum assisted resin transfer moulding) with epoxy resin. The mechanic behaviour and failure mechanism of the material were analysed.



Fig. 1. Vine-like structure

EXPERIMENTAL

Materials

Carbon fibre was employed as reinforcing the material, which was purchased from Toray Co. Ltd. (Tokyo, Japan) with a tensile strength of 3530 MPa and a tensile modulus of 230 GPa. There is 3000 single fibres in a bundle of carbon fibre (3K). The polyester filament was used as the wrapping fibres, it was offered by Bosidi new material Co., Ltd. (Dongguan, China). Polyester filaments was a kind of mono-filament, the shape of those sections was round, their diameter was 0.1 mm, 0.2 mm, 0.4 mm and 0.6 mm. A thermosetting epoxy compound system was obtained from Jiafa Chem Co., Ltd. (Changshu, China). The mixture ration of epoxy resin(1.12–1.16 g/cm³ in density, 0.54–0.57 eq/100 g in Epoxy value, 175–185 in Epoxy equivalent, 2500 MPa/s in viscosity) and curing agent (0.92–0.96 g/cm³ in density, 450–510 mg KOH/g in amine value, 55–60 g/eq in active hydrogen equivalent, 40–80 MPa/s in Viscosity) was 100:27 at ambient temperature.

Preparation of WHC

The Wrapped carbon fibre bundles with mono-filament Hybrid Composite (WHC) were prepared using a custom winding machine and VARTM method. Firstly, the PET filament was wrapped on a spool rather than having a sleeve on the hollow shaft. With the carbon bundle throughout the centre of the shaft, the PET filament wrapped the carbon fibre upon spool rotation. Then, a unidirectional fabric was prepared by a rotary arrangement method. Four layers were paved for a composite laminate, and composed with the epoxy resin used the VARTM process. A schematic diagram is shown in figure 2.

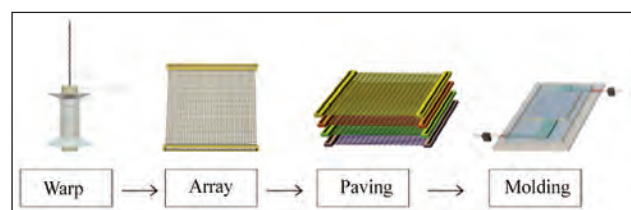


Fig. 2. Schematic of the preparation process for WHC

Samples

Five groups of samples were prepared, four kinds of PET mono-filaments with different diameters (0.1 mm,

Table 1

DETAILS OF THE SPECIMENS		
Sample	Diameter of PET (mm)	Thickness (mm)
CFRP	-	1.38
0.1P/CFRP	0.1	1.65
0.2P/CFRP	0.2	1.97
0.4P/CFRP	0.4	3.68
0.6P/CFRP	0.6	4.69

0.2 mm, 0.4 mm and 0.6 mm) were used in wrap hybrid fibre, a group of no hybrid sample was prepared for comparison. All samples were prepared with the same effective fibre volume content (refers to carbon fibre volume content). The sample names and thickness listed in table 1.

Measurement and characterization

Impact test was performed by the Charpy impact test machine (XJJ-50S, HengSi Instruments Co., Ltd. China). Flat composite samples were placed in the middle of the test machine. Impactor had a smooth hemispherical striker with a diameter of 2 mm. The falling height of the impactor was adjusted to the energy requested to the values of 7.5 J. The energy absorbed and impact strength of the specimen was collected.

Compressive and tensile testing was carried out by a universal testing machine (WDW-20, 20 kN load cell, made by Tianchen testing machine manufacturing Co., Ltd. China). Compression specimens were loaded until failure using a constant crosshead speed of 0.5 mm in -1 . In addition to compressive stress, strain data was also collected for each composite configuration with strain gauges (8 mm gauge length) being carefully installed at the mid-span of the test gauge lengths.

A crosshead speed of 2 mm/min was used for the tensile test. Also, a single strain gauge was attached to the centre of the specimen in the longitudinal direction to measure the tensile strain.

RESULTS AND DISCUSSION

Figure 3 shows the effect of fibre diameter on the impact strength of the material. As can be seen from the figure 3, fibre wrapping improves the impact resistance of the composite material. Impact strength decreases as diameter increases and is highest for a diameter of 0.4 mm.

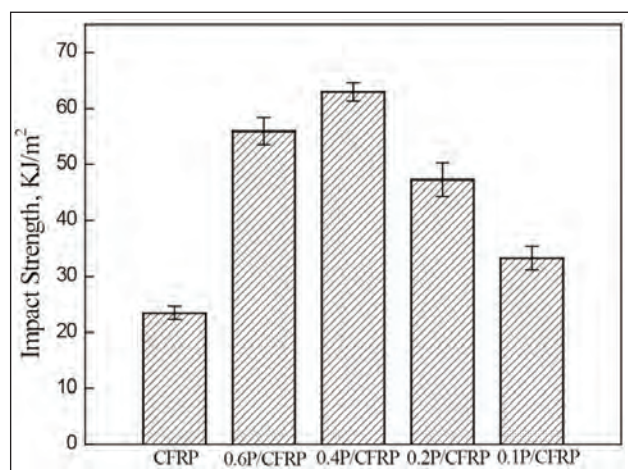


Fig. 3. Effect of diameter on the impact strength

As for the failure mechanism and energy absorption characteristics of the cantilever beam impact test, the failure of the laminate occurs in two steps during

impact. First, deformation takes place due to compressive force and shear. This is followed by the formation of interlayer fractures and the eventual failure of the material. Compared with its tensile properties, carbon fibre has relatively poor compression and shear properties, which is also the reason for the low impact resistance and toughness of reinforced carbon fibre composites. In this study, part of the impact energy due to compression and shear of the carbon fibre is transformed into the tensile strain energy of the PET fibre. Therefore, the impact strength of the fibre-wrapped reinforced composites is higher than that of the pure carbon fibre composites. Impact resistance also increases with increasing fibre diameter.

On the other hand, the lower surface energy of the PET fibre results in its relatively poor interfacial adhesion with epoxy resin. As the diameter of the PET fibre increases, its contact area with the resin increases, thus lowering its interlayer or inter-bundle fracture energy. Therefore, the impact strength for a fibre diameter of 0.6 mm is lower than that for a diameter of 0.4 mm. In summary, a PET fibre with a diameter of 0.4 mm gives the composite material the best overall impact strength, which represents a 147% increase compared with unwrapped carbon fibre composites.

Figure 4 shows the effects of fibre diameter on the tensile strength of the material. As can be seen from the figure, wrapping with polyester fibre contributes little to the tensile strength of the composites. Moreover, the performance of the composites decreases with increasing polyester fibre diameter. There are two reasons for this, the poor interfacial bonding between the PET fibre and the epoxy resin, and the buckling of the carbon fibre as PET wraps around and coats it.

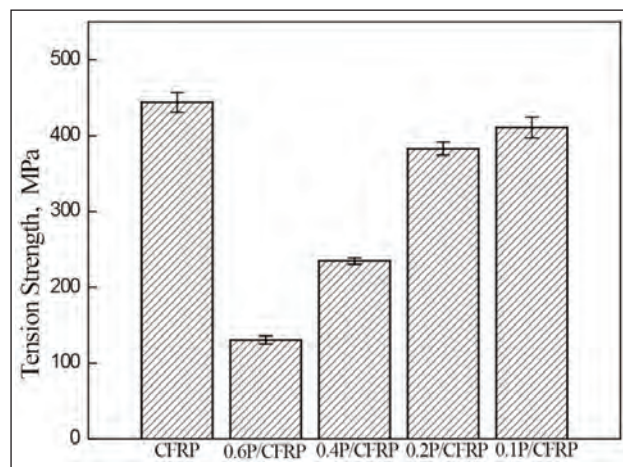


Fig. 4. Effect of diameter on the tensile strength

The hardness of the polyester fibre also increases with increasing diameter, making it less deformable during wrapping. The carbon fibre is thus more prone to buckling, the degree of which has a great influence on the tensile strength of this composite material. The phenomenon was depicted in figure 5. From our

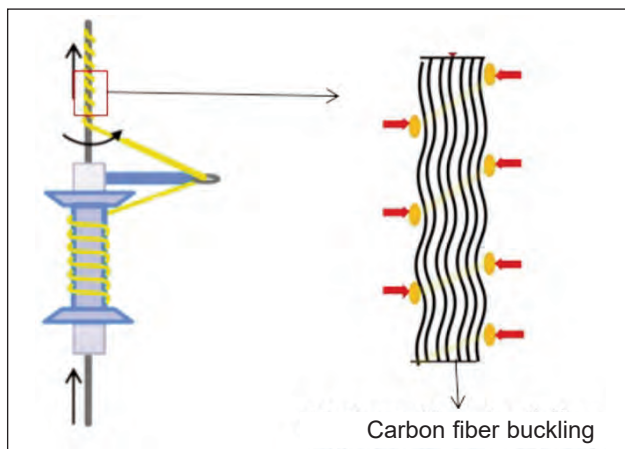


Fig. 5. Schematic diagram of carbon fibres buckling in the wrap process

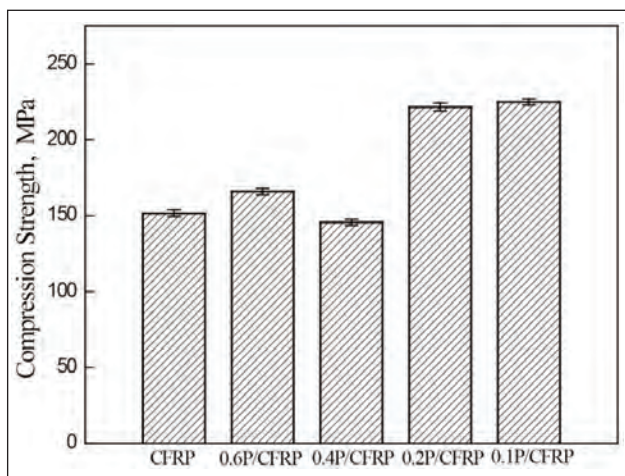


Fig. 6. Effect of diameter on the compressive strength

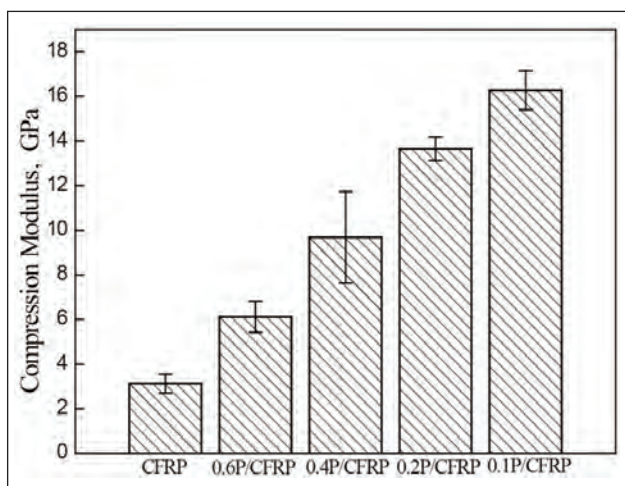


Fig. 7. Effect of diameter on the composite modulus

experimental results, we determined that the buckling of the carbon fibre bundle becomes more severe when wrapped with polyester fibre with a larger diameter. It is, therefore, necessary to optimize the diameter of the wrapping fibre for the wrapping process. Figures 6 and 7 show the compressive strength and modulus of the composite material. From these data,

we concluded that fibre wrapping improves the compressive strength and modulus of the composite material. Reducing the fibre diameter results in a gradual increase in the performance of the composite material during compression because the fibre wrapping functions differently than during stretching. Part of the compressive and shear energy on the carbon fibre is converted into the tensile strain energy of the PET fibre, as in the case of impact, thus increasing the compressive strength of the carbon fibre. As shown in the SEM image of figure 8, the compression failure of the wrapped composite material adopts the form of a torsional failure, which is similar to a shear failure, rather than the buckling failure of the fibre, such that brittle fracture is observed during the failure of the carbon fibre within the resin wrapping. The PET wrapping, therefore, alters the compression failure mode of the composite material and improves its performance during compression. Using a thinner PET fibre is more effective for enhancing this property of the composite material.

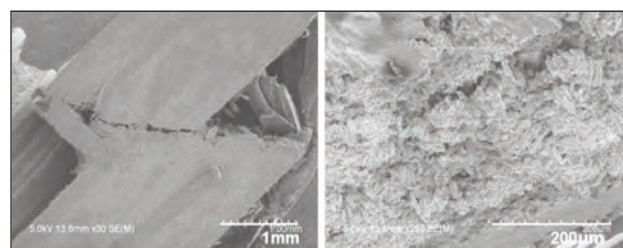


Fig. 8. Morphologies of the fracture surface of 0.2P/CFRP

CONCLUSIONS

With the data analysis in the above sections, the effects of diameter on the impact behaviour of WHC composites can be summarized as follows:

Polyester fibre wrapping improves the impact strength of the composites, which increases and then decreases as the diameter of the polyester fibre increases. The maximum impact strength of 62 KJ/m² was reached when the polyester fibre diameter was 0.4 mm, representing a 147% enhancement compared with the unwrapped material.

Wrapping with polyester harms the tensile properties of the composites because buckling of the carbon fibre can happen during wrapping, the degree of which has a great influence on the tensile strength of the composites. Moreover, the polyester fibre does not play a significant role in preventing tensile failure, and thus the tensile strength of the material drops.

Though the polyester fibre wrapping causes different degrees of buckling on the carbon fibre bundles, overall it improves the performance of the composite material during compression. Thinner wrapping fibres are more effective for enhancing the compression property of the composites. The fracture mode of the material during compression failure is also changed by wrapping with fibre. The failure of the carbon fibre adopts the form of a torsional failure, similar to shear failure.

The diameter of the polyester fibre used for wrapping should be optimized as per the application of the composite material.

Fibres with higher tensile strengths provide better impact resistance, while thinner wrapping fibres enhance the compression properties of the composite material more effectively.

ACKNOWLEDGEMENTS

This work has been financially supported by the Open Project Program of Anhui Province College Key Laboratory of Textile Fabrics, Anhui Engineering and Technology Research Center of Textile (2018AKLTF05), Anhui Province International Science and Technology Cooperation Program (1804b06020360), as well as Science and Technology Planning Project of Wuhu City (No. 2018yf47).

REFERENCES

- [1] Li, W., Guo, Q.F., *Application of carbon fiber composites to cosmonautic fields*, In: Chinese Journal of Optics, 2011, 4, 3, 201–212
- [2] Qian, D., Bao, L., Takatera, M., et al., *Fiber-reinforced polymer composite materials with high specific strength and excellent solid particle erosion resistance*, In: Wear, 2010, 268, 3, 637–642
- [3] Bunsell, A.R., Renard, J., *Fundamentals of Fibre Reinforced Composite Materials*, In: B. Cantor, M. J. Goringe (Eds), Institute of Physics Publishing: Bristol and Philadelphia, 2005, Ch.1., 1–17
- [4] Gillespie, J.W., DeVault, J.B., *High-Performance Structural Fibers for Advanced Polymer Matrix Composites*, In: A. Mozhi (Eds), The National Academies Press: Washington, DC, 2005, 18–26
- [5] Nur, S., Safri, A., Thariq, M., et al., *Impact Behaviour of Hybrid Composites for Structural Applications: A Review*, In: Compo Part B, 2018, 112–121
- [6] Senthilkumaar, S., Varadarajan, P.R., Porkodi, K., Subbhuraam, C.V., *Adsorption of methylene blue onto jute fiber carbon: kinetics and equilibrium studies*, In: Journal of colloid and interface science, 2005, 284, 1, 78–82
- [7] Hung, P.Y, Lau, K.T, Cheng, L.K, et al., *Impact response of hybrid carbon/glass fiber reinforced polymer composites designed for engineering applications*. In: Compo Part B, 2018, 86–96
- [8] Zheng, Y., Sun, Y., Li, J., et al., *Tensile response of carbon-aramid hybrid 3D braided composites*, In: Mater Design, 2017, 246–252
- [9] Liu, B., Xu, A., Bao, L., *Erosion characteristics and mechanical behavior of new structural hybrid fabric reinforced polyetherimide composites*, In: Wear, 2016, 368, 335–343
- [10] Ruan, F, Bao, L., *Improved longitudinal compression performance of a unidirectional fiber reinforced composite with a filament covering*, In: Polym Compo, 2016, 37, 11, 3127–3133

Authors:

FANGTAO RUAN^{1,2}, CHENGLONG XIA¹, LI YANG^{1,2}, ZHENZHEN XU^{1,2},
FEIYAN TAO¹

¹Anhui Polytechnic University, School of Textile and Garment, 241000, Wuhu, China

²International Cooperation Research Center of Textile Structure Composite Materials,
241000, An Hui Province, China

Corresponding author:

FANGTAO RUAN
e-mail: ruanfangtao@ahpu.edu.cn

Statistical analysis of the 3D electroconductive composites based on copper and graphene

DOI: 10.35530/IT.072.02.20207

RALUCA MARIA AILENI
LAURA CHIRIAC

DOINA TOMA

ABSTRACT – REZUMAT

Statistical analysis of the 3D electroconductive composites based on copper and graphene

This paper presents several aspects of the multivariate analysis of electroconductive composite based on Copper (Cu) and Graphene. The analysis was developed by using the parameters (dependent and independent variables), which characterize the composite materials with electroconductive properties. The experimental samples were obtained by using 100% cotton fabrics with different structures. The goals followed through the variation of the fabric structures (e.g., plain weave, twill, panama, ribs) were to investigate if the fabric structure or ratio has or not influence on electroconductive properties of the textile materials obtained by conductive coating. The samples created were based on standard, and 3D digital printing technologies, more specifically on the textile surface, have deposited conductive paste containing copper microparticles and graphene filaments. The initial coating with conductive polymeric paste based Cu was developed by scraping of the paste on the fabric. Previously the 3D printing advanced technology by fused deposition modeling (FDM) of the Conductive Graphene filaments was used.

Keywords: composites, textile, electroconductive, resistance, conductive, copper, microparticles, sensors, 3D, Graphene

Analiza statistică a compozitelor 3D electroconductive pe bază de cupru și grafen

Această lucrare prezintă câteva aspecte privind analiza multivariată a compozitelor electroconductive pe bază de cupru (Cu) și grafen. Analiza a fost dezvoltată pe baza parametrilor (variabile dependente și independente), care caracterizează materialele compozite cu proprietăți electroconductive. Probele experimentale au fost obținute din materiale textile din 100% bumbac, având diferite structuri. Variația structurii țesăturii (de exemplu: pânză, diagonal, panama, ribs) a avut ca scop investigarea influenței structurii și a raportului de legătură asupra proprietăților electroconductive ale materialelor textile cu acoperiri conductive. Probele au fost realizate utilizând tehnologiile clasice și tehnologia imprimării digitale 3D, mai precis pe suprafața textilă au fost depuse paste conductive cu conținut de microparticule de cupru și filamente de grafen. Depunerea inițială a pastei polimerice conductive pe bază de Cu a fost realizată prin metoda raclării. Ulterior, a fost utilizată tehnologia avansată de imprimare 3D prin depunerea pe suprafața textilă a filamentelor topite de grafen conductiv.

Cuvinte-cheie: compozite, textil, electroconductiv, rezistența, conductiv, cupru, microparticule, senzori, 3D, grafen

INTRODUCTION

The conductive textile materials development is based on advanced manufacturing such as 3D printing, or advanced materials development such as ESD (electrostatic discharge) or conductive filaments graphene-based PLA (polylactic acid) matrix, and is of real interest in current research. However, the new technologies and techniques have several new parameters, and the multivariate analysis of the coated materials must analyse complex data sets. In scientific literature similar approaches can be observed in using multivariate analysis for developing fibres, yarns, or fabric models [1–4]. However, this technique is used to explain the feasibility of two-way prediction by developing models for fibre and yarn and reverse models relating yarn to fibre using multivariate. In this paper, the multivariate analysis [4–7] used to investigate the influence of the independent and dependent variables in the electroconductive textile development. In general conductive fabrics are

achieved by conductive polymers (polyaniline, polypyrrole, polythiophene, poly(3,4-ethylene dioxythiophene) polystyrene sulfonate (PEDOT: PSS), or graphene [7–11]) or by distributing conductive metal micro/nanoparticles in the polymeric matrix [12–14] (e.g. PVA (polyvinyl alcohol)). Numerous scientific researches present the manufacturing of conductive materials based on graphene oxide [15–17]. The improvement of the electrical conductivity is the main subject in researches that describe the method for obtaining the conductive yarns based on carbon black nanoparticles (CB) and PVA, and the method to improve the surface conductivity by plasma-assisted attachment of functionalized carbon nanotubes on PET (poly(ethylene terephthalate)) [18, 19], by printing method. However, special attention was paid to the investigation of the physical properties of conductive materials such as metal composite, or electromagnetic shielding performance achieved through textiles with conductive and magnetic properties [20].

EXPERIMENTAL PART

In the experimental part, we developed 20 experimental samples using cotton fabric (BBC) 100% with different structures (e.g. plain weave, twill, weft rib, warp rib, panama) with electroconductive properties based on traditional technologies for thin-film deposition by scraping/printing and 3D digital printing. To achieve the experimental samples functionalized by submission of copper (Cu) or nickel (Ni) microparticles have been used, the classic technology printing (conductive polymeric paste with Cu microparticles), scraping, and advanced technology for submission by the 3D digital printing based on the conductive graphene filaments.

To obtain electroconductive properties for direct printing/scraping, the polyvinyl alcohol (PVA), and metallic microparticles (Cu I, Cu II, Cu III, and Ni) were used.

The experimental part consists of two parts:

1. Development of the fabrics (20) with electroconductive properties by scraping of the conductive paste based on water, a binder (PVA) and microparticles of Cu (Cu I microparticles with size less than 45 μm ; Cu III microparticles with size less than 75 μm ; Cu II microparticles with size in the range 14–25 μm), and Ni (Ni microparticles with size less than 50 μm), followed by drying at a temperature of 23–24°C for 20 hours and the crosslinking for 3 minutes at 160°C for functionalization by increasing the electroconductive character (conductive, semiconductive or dissipative).

2. Deposition of the thermoplastic material (Conductive Graphene PLA) in the form of fused filaments by FDM 3D printing extruder at 200–240°C.

Table 1 presents the surface resistance (R_s [Ω]) and conductance G (S) for samples 1–20. For samples 1–7 it was used the same type of conductive paste based on PVA, H_2O and Cu II microparticles, for samples 8–14 a conductive paste based on Cu I microparticles, PVA and H_2O has been used, for samples 15–19 a conductive paste based on Cu III microparticles has been used, while for sample no. 20 a conductive paste based on PVA, H_2O , and Ni microparticles has been used (table 1). These 20 samples have been developed based on seven weaved structures from 100% cotton yarns (plain weave 1/1 (with cotton yarns Nm 20/2 on weft), plain weave 1/1 (with cotton yarns Nm 20/3 on weft), twill 2/2, twill 3/1, panama, weft rib weave, warp rib weave).

In the case of samples 1–7, 8–14, and 15–19 changing the structure of textile support has not influenced

Table 1

EXPERIMENTAL PLAN-SAMPLES FUNCTIONALIZED BY COATING WITH A CONDUCTIVE PASTE BASED ON MICROPARTICLES								
Sample no.	Ni	Cu I	Cu II	Cu III	PVA	H_2O	R_s (Ω)	G (S)
1			x		x	x	10^{11}	10^{-11}
2			x		x	x	10^{11}	10^{-11}
3			x		x	x	10^{12}	10^{-12}
4			x		x	x	10^9	10^{-9}
5			x		x	x	10^8	10^8
6			x		x	x	10^9	10^9
7			x		x	x	10^9	10^9
8		x			x	x	10^3	10^{-3}
9		x			x	x	10^3	10^{-3}
10		x			x	x	10^3	10^{-3}
11		x			x	x	10^3	10^{-3}
12		x			x	x	10^3	10^{-3}
13		x			x	x	10^3	10^{-3}
14		x			x	x	10^3	10^{-3}
15				x	x	x	10^{10}	10^{-10}
16				x	x	x	10^{12}	10^{-12}
17				x	x	x	10^{10}	10^{-10}
18				x	x	x	10^{11}	10^{-11}
19				x	x	x	10^{10}	10^{-10}
20	x				x	x	10^4	10^{-4}

the electrical conductivity or surface resistance. Moreover, the changing of the conductive paste composition for sample groups 1–7, 8–14, and 15–19 has been generated an increasing or reducing the surface resistance (R_s) of the textile materials coated and in consequence and decreasing or increasing the electrical conductance (G) values are presented in table 1.

For all experimental samples the physico-mechanical parameters such as thickness δ [mm], the mass M [g/m^2], the permeability to air Pa [$\text{l}/\text{m}^2/\text{s}$], the surface resistance R_s [Ω] have been investigated in the laboratory and these are listed in table 2.

Figure 1 presents the topographic analysis of the surface of the textiles on the basis of the optical microscopy with the digital camera, magnification (4 \times), the surface of the initial fabric 0.1 (without metallic microparticles) (figure 1, a) and the surface of the fabrics microparticle of Cu II, Cu I, Cu III and Ni (figures 1, b and 1, e).

From samples 8–15 that present a lower surface resistance the sample no. 10 was selected, that presents a proper distribution of the conductivity on the entire surface, to test the electrical conductivity using a 9V battery and a 3 mm led and has proved that the textile surface coated by using our conductive paste developed it allows electrical the current flow.

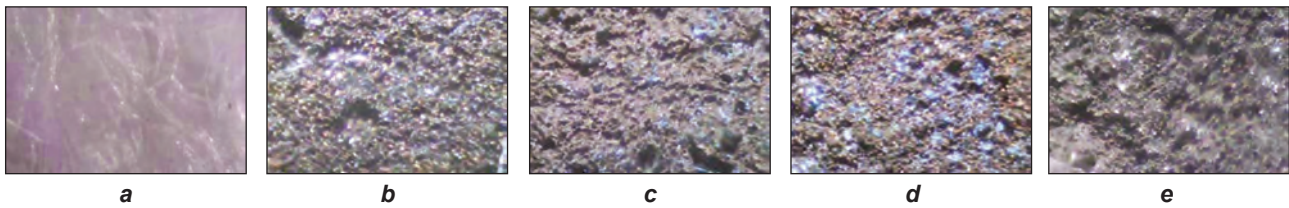


Fig. 1. Topographic analysis of the fabric surface based on optical microscopy with the digital camera: a – fabric without microparticles submitted; b – sample no. 3 with Cu II; c – sample no. 10 with Cu II; d – sample no. 17 with Cu III; e – sample no. 20 with Ni

Table 2

PHYSICAL-MECHANICAL AND ELECTRICAL PARAMETERS FOR SAMPLES 1–20				
Sample no.	M (g/m ²)	δ (mm)	Pa (l/m ² /s)	Rs (Ω)
1	863	2.28	7.55	10 ¹¹
2	858	2.07	12.2	10 ¹¹
3	897	2.13	27.83	10 ¹²
4	720	2.75	9.03	10 ⁹
5	816	3.25	19.15	10 ⁸
6	824	3.05	25.94	10 ⁹
7	995	5.82	256.4	10 ⁹
8	760	2.25	9.52	10 ³
9	776	1.77	33.16	10 ³
10	670	2.19	11.10	10 ³
11	761	3.22	14.35	10 ³
12	721	3.42	24.54	10 ³
13	702	3.52	31.92	10 ³
14	780	5.38	264.8	10 ³
15	1276	2.68	101.99	10 ¹⁰
16	925	2.96	31.22	10 ¹²
17	1020	2.93	9.83	10 ¹⁰
18	841	2.01	15.07	10 ¹¹
19	1033	3.34	24.74	10 ¹⁰
20	828	4.42	109.1	10 ⁴



Fig. 2. Electrical conductivity test for sample 10



Fig. 3. 3D printing on the surface coated with paste based Cu microparticles

After depositing the conductive paste based copper, on sample no. 10 the 3D conductive graphene filaments by 3D printing (figure 3) have been deposited using conductive filaments based Graphene. The surface obtained has been tested to investigate the

surface resistance, and we obtained a surface resistance of 10³ Ω, and that indicates the 3D textile composite based on conductive Cu paste and graphene filaments (figure 4) has a pronounced surface conductivity. It can be used for technical purposes to develop flexible sensors or electrodes.

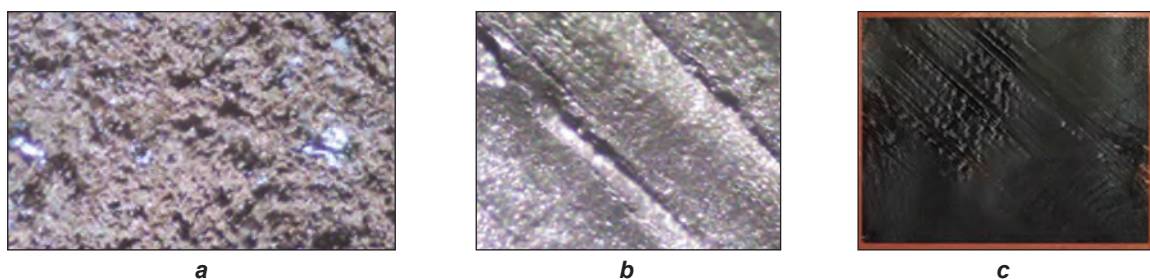


Fig. 4. 3D textile composite based on Cu microparticles and graphene filaments: a – Surface coated with paste based Cu microparticles (optic microscopy view using a digital camera); b – Graphene filaments deposited (optic microscopy view using a digital camera); c – 3D textile composite based Cu microparticles and Graphene (digital camera view)

RESULTS AND DISCUSSIONS

For parameters such as electrical surface resistance, the thickness (δ), air permeability (Pa), conductance (G) and mass (M) have been developed a multivariate analysis. In figures 5–9 are presented the 3D representations of the electrical resistance (Rs) in the function of the thickness (δ), mass (M), air permeability (Pa), and conductance (G) using MATLAB software. For experimental parameters (Rs, M, δ , Pa, G) it was performed an analysis of the correlation coefficient Pearson (1) between Rs and Pa, δ , M, G:

$$r_{xy} = \frac{\frac{1}{n} \sum (x - \bar{x})(y - \bar{y})}{s_x s_y} \quad (1)$$

where x, y represent the individual values of the variables x and y ; \bar{x}, \bar{y} represent the arithmetic mean of all the values of x, y ; s_x, s_y represents the standard deviation of all values x and y .

$$r_{RsPa} = \begin{vmatrix} 1.0000 & -0.1290 \\ -0.1290 & 1.0000 \end{vmatrix} \Leftrightarrow \\ \Leftrightarrow r_{12_{RsPa}} = r_{21_{RsPa}} = -0.1290 \quad (2)$$

$$r_{Rs\delta} = \begin{vmatrix} 1.0000 & -0.2143 \\ -0.2143 & 1.0000 \end{vmatrix} \Leftrightarrow \\ \Leftrightarrow r_{12_{Rs\delta}} = r_{21_{Rs\delta}} = -0.2143 \quad (3)$$

$$r_{RsM} = \begin{vmatrix} 1.0000 & 0.1490 \\ 0.1490 & 1.0000 \end{vmatrix} \Leftrightarrow \\ \Leftrightarrow r_{12_{RsM}} = r_{21_{RsM}} = 0.1490 \quad (4)$$

$$r_{RsG} = \begin{vmatrix} 1.0000 & -0.2948 \\ -0.2948 & 1.0000 \end{vmatrix} \Leftrightarrow \\ \Leftrightarrow r_{12_{RsG}} = r_{21_{RsG}} = -0.2948 \quad (5)$$

Analysing the values of the correlation coefficients r_{RsPa} (2), $r_{Rs\delta}$ (3), r_{RsM} (4), and r_{RsG} (5), it can be

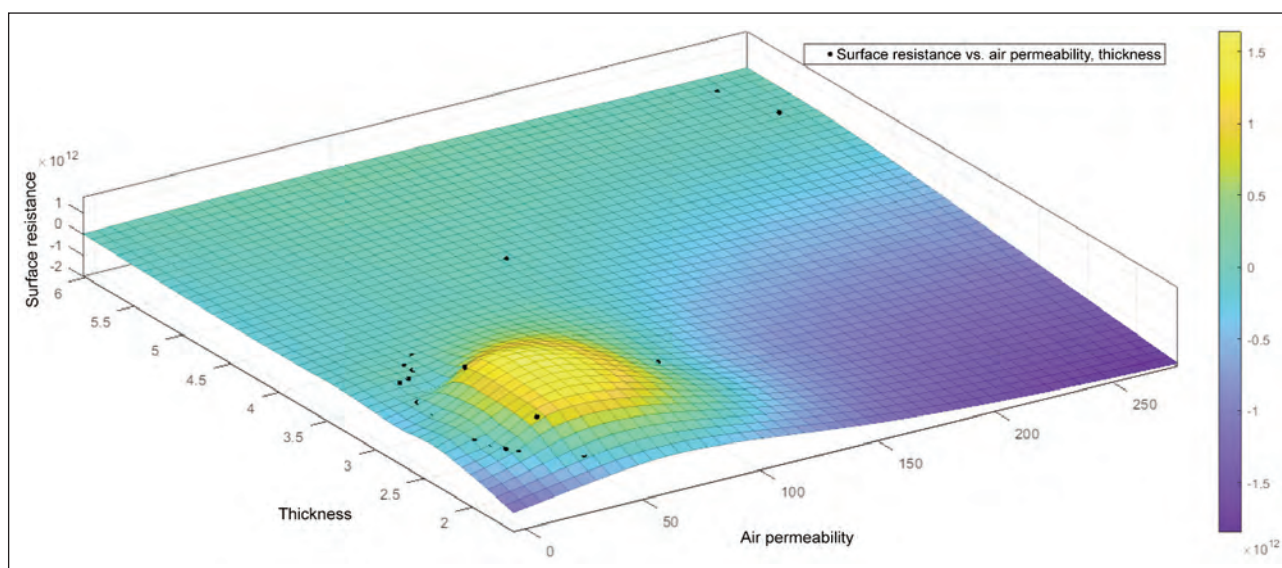


Fig. 5. 3D representation of the surface resistance according to the air permeability (Pa) and thickness (δ) ($R_s = f(\text{Pa}, \delta)$)

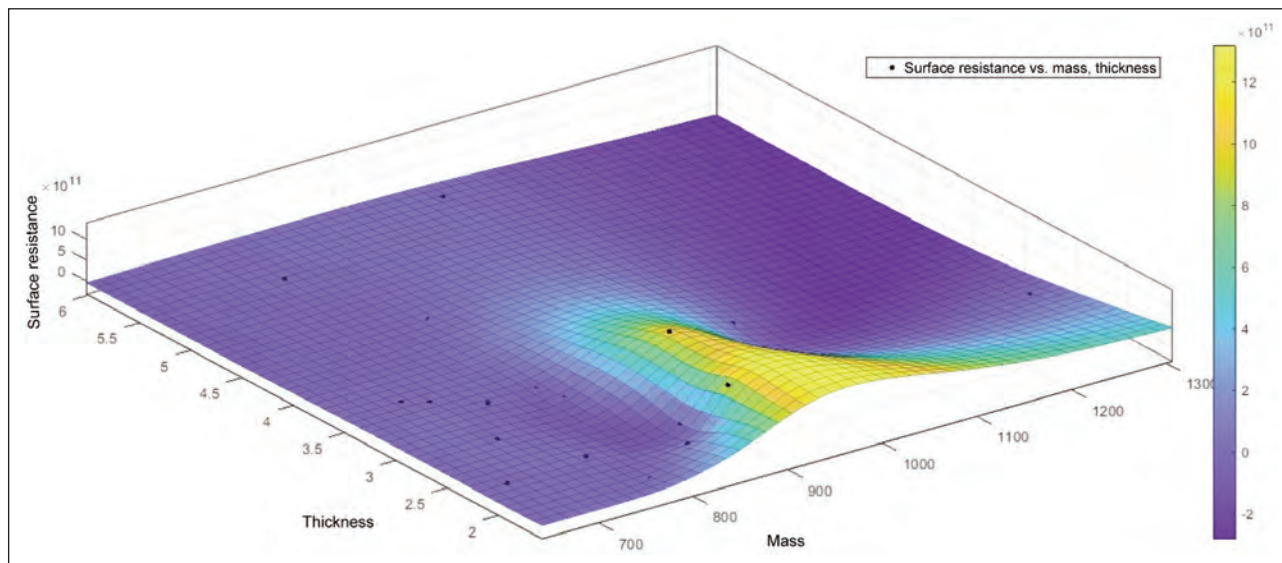


Fig. 6. 3D representation of the surface resistance (R_s) according to the mass (M) and thickness (δ) ($R_s = f(M, \delta)$)

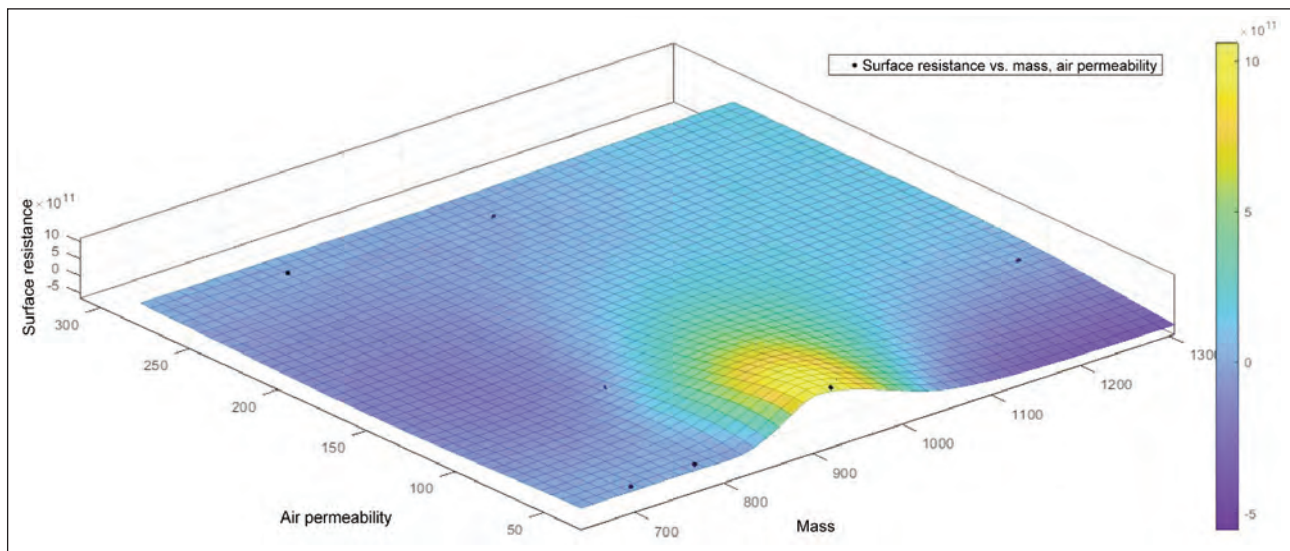


Fig. 7. 3D representation of the surface resistance (R_s) according to the air permeability (P_a) and mass (M) ($R_s = f(P_a, M)$)

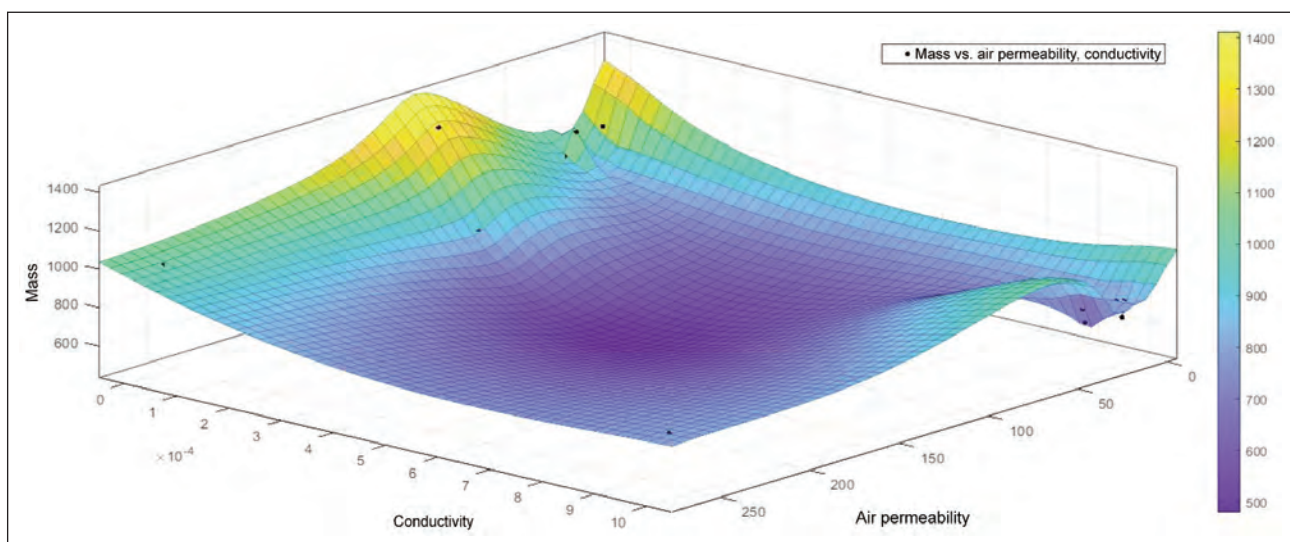


Fig. 8. 3D representation of the surface resistance (R_s) according to the thickness (δ) and conductance (G) ($R_s = f(\delta, G)$)

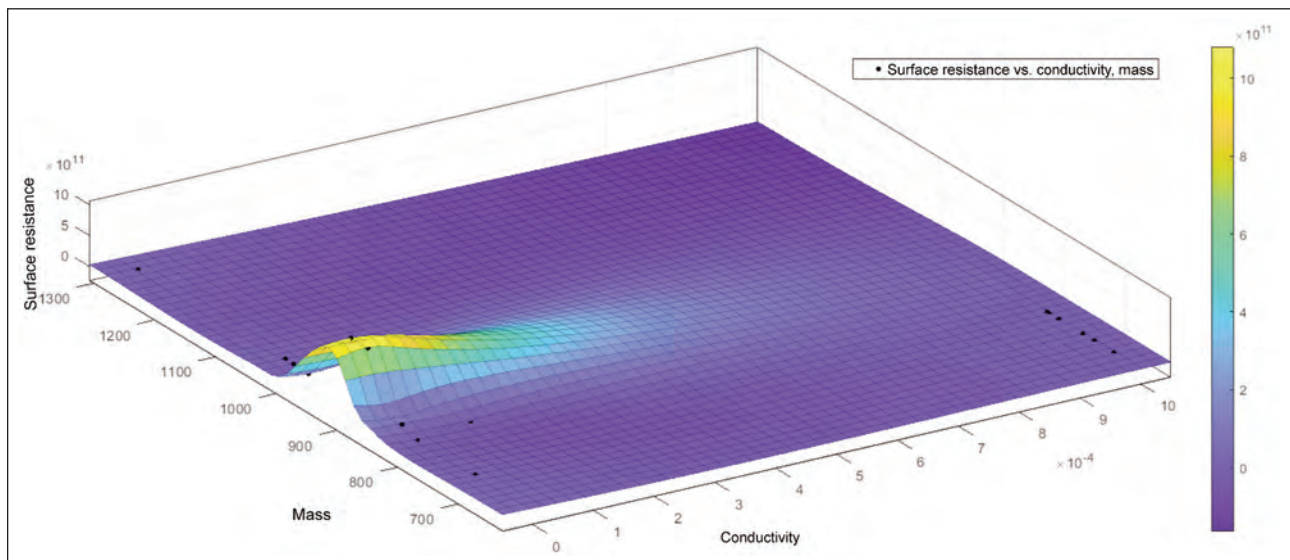


Fig. 9. 3D representation of the surface resistance (R_s) according to the mass (M) and conductivity (G) ($R_s = f(M, G)$)

observed that between the surface resistance (R_s) and air permeability (Pa), conductance (G), thickness (δ) of the samples treated with a conductive paste based on Cu I, Cu II, Cu III, and Ni, it is a lower negative inverse proportionality relationship, and this indicates that the reduction of the surface resistance value was generated through increasing the thickness. Thickness increasing can be achieved through an additional continuous layer of conductive paste deposited, increasing the conductivity (by using conductive paste). Air permeability does not influence considerably surface resistance and conductivity because the correlation coefficient between air permeability and surface resistance is negative (-0.1290), but it is very close to zero. Because the electrical resistance is inversely proportional with the electrical conductance (5), and the mass has a lower positive direct relationship with the surface resistance, this means that an increasing in the values of the mass cannot have a substantial impact on decreasing the conductivity.

Increasing of mass (due to the conductive paste) can generate the air permeability reduction, but cannot affect very strongly the surface resistance and conductivity because depending on paste composition that can generate conductive or antistatic conductivity, a supplementary continuous layer of paste, with conductive/dissipative effect, deposited on a textile previously treated with the same paste does not affect the surface resistance or conductivity, but can generate the reduction of the air permeability and the increasing of mass and thickness values.

CONCLUSIONS

For samples 8–15 and 20 it is evident that the surface resistance values are specific to the conductive materials (10^1 – $10^5 \Omega$) and in case of the samples 1–7, and 15–19 the surface resistance has the values in the range 10^8 – $10^{12} \Omega$ that is specific to static dissipative materials (10^6 – $10^{12} \Omega$).

Based on the analysis of the Pearson correlation coefficient, it can be concluded that mass, the thickness can increase by an additional continuous layer of conductive paste deposited on the textile material. In the meantime, a continuous layer of paste with conductive/dissipative properties will affect the air permeability generating the reduction of the air permeability values. Taking into account that all positive or negative correlation coefficients are very close to zero we can conclude that the inverse or direct proportionality ratio between parameters can affect to a very small extent the values of the surface resistance or conductivity and the critical aspect that should be considered is the composition of the conductive paste that can generate the antistatic or conductive surface effect and this does not depend on textile structure.

ACKNOWLEDGMENTS

The research presented in this paper was prepared in the INCDTP laboratories. Funds support this work from MEC, National Project "Composite materials with electroconductive properties, based on 3D polymeric array for sensorial monitoring system and electromagnetic waves attenuation (3D ELECTROTEX)", Contract PN 19 17 01 01.

REFERENCES

- [1] Manzoor, S., Shah, M.H., Shaheen, N., Khaliq, A., Jaffar, M., *Multivariate analysis of trace metals in textile effluents in relation to soil and groundwater*, In: Journal of Hazardous Materials, 2006, 137, 1, 31–37
- [2] Chatfield, C., *Introduction to multivariate analysis*, Routledge, 2018
- [3] Bing, X., Wegkamp, M.H., *Adaptive estimation of the rank of the coefficient matrix in high-dimensional multivariate response regression models*, In: The Annals of Statistics, 2019, 47, 6, 3157–3184
- [4] Fu, K.K., Padbury, R., Toprakci, O., Dirican, M., Zhang, X., *Conductive textiles*, In: Engineering of High-Performance Textiles, 2017, 305
- [5] Zulan, L., Zhi, L., Lan, C., Sihao, C., Dayang, W., Fangyin, D., *Reduced Graphene Oxide Coated Silk Fabrics with Conductive Property for Wearable Electronic Textiles Application*, In: Advanced Electronic Materials, 2019, 5, 4, 1800648
- [6] Trovato, V., Teblum, E., Kostikov, Y., Pedrana, A., Re, V., Nessim, G., Rosace, G., *Designing of carbon nanotubes/cotton fabric composite for e-textiles: effect of carbon nanotubes length on electroconductive properties*, In: Autex 2019: Textiles at the crossroads, 2019, 1–6
- [7] Method for preparing graphene-polyester nanocomposite fiber, WO2017066937A1, 2015
- [8] Lee, J.H., Lee, C.S., Kim, Y.S., Song, H.J., U.S. Patent No. 9,214,559. Washington, DC: U.S. Patent and Trademark Office, US20140299475A1, 2015
- [9] Graphene-based sensor, WO2017220979A1, 2016
- [10] Graphene/cotton cloth flexible conducting fabric and preparing a method of graphene/cotton cloth flexible conducting fabric, CN105088749A, 2015
- [11] Electrically conductive textile materials and methods for making the same, US4803096A, 1987
- [12] Metallization of textile structures, EP2397577B1, 2010
- [13] Method for forming interconnections between electronic devices embedded in textile fibers, Howland, C.A., U.S. Patent No. 10,448,680, Washington, DC: U.S. Patent and Trademark Office, 2019
- [14] Electrically conductive textile materials and methods for making the same, US4803096A, 1987
- [15] Wang, F., Xu, Z. *Graphene and graphene oxide-reinforced 3D and 4D printable composites*, In 3D and 4D Printing of Polymer Nanocomposite Materials, Elsevier, 2020, 259–296
- [16] Weis, J.E., Charpentier, S., Kempinska, A., *Graphene Research and Advances Report*, December 2019

- [17] Shathi, M.A., Minzhi, C., Khoso, N.A., Rahman, T., Bidhan, B., *Graphene coated textile-based, highly flexible, and a washable sports bra for human health monitoring*, In: Materials & Design, 2020, 108792
- [18] Haji, A., Rahbar, R.S., Shoushtari, A.M., *Plasma assisted attachment of functionalized carbon nanotubes on poly(ethylene terephthalate) fabric to improve the electrical conductivity*, In: Polimery, 2015, 60, 5, 337–342
- [19] Haji, A., Rahbar, R.S., Shoushtari, A.M., *Improved microwave shielding behavior of carbon nanotube-coated PET fabric using plasma technology*, In: Applied surface science, 2014, 311, 593–601
- [20] Wang, Y., Song, Y., Qi, Q., Wang, W., Yu, D., *Robustly Magnetic and Conductive Textile with High Electromagnetic Shielding Performance prepared by Synchronous Thiol-ene Click Chemistry*, In: Industrial & Engineering Chemistry Research, 2019
-

Authors:

RALUCA MARIA AILENI, LAURA CHIRIAC, DOINA TOMA

The National Research & Development Institute for Textiles and Leather,
16 Lucretiu Patrascanu, 030508, Bucharest, Romania

Corresponding author:

RALUCA MARIA AILENI
e-mail: raluca.aileni@incdtp.ro

Permeability properties of woven fabrics containing two-ply fancy yarns

DOI: 10.35530/IT.072.02.1712

MIHA POZDEREC

DUNJA ŠAJN GORJANC

ABSTRACT – REZUMAT

Permeability properties of woven fabrics containing two-ply fancy yarns

The basic intention of the presented research is to analyse the permeability properties of woven fabrics containing two-ply fancy yarns in the weft direction. Within the framework of presented research, two-ply fancy yarns were analysed. Because of their structure, they are classified as fancy yarns with structural effects. The first analysed two-ply fancy yarn is made of the mixture of 81% cotton and 19% viscose. The second is made of the mixture of 67% viscose and 33% flax. For the purpose of the presented research, woven fabrics containing two-ply fancy yarn were made in three different densities in weft (10 threads per cm, 13 threads per cm, and 16 threads per cm) in the twill weave T 1/3 Z. The theoretical part includes the historical development of the production of the fancy yarns, a detailed discussion of the ring production processes, the types and the structure of the fancy yarns, their use, and the global and European market of the fancy yarns. The experimental part consists of three parts. In the first part, the structural properties of the analysed fancy yarns were researched (the fineness of the fancy yarn, the frequency of repeating the effects per one meter of the yarn, the direction of twisting the fancy yarn, the number of the twists of the basic and the effective part, the diameter of the fibers, the diameter of the basic and the effective part, the fineness of individual components, the direction of the twist of individual components, and the percentage of the inside twist of individual components). In the second part, constructional properties of the analysed woven fabrics with the fancy yarn in the weft were researched (mass, thickness, the density of the warp and weft threads, and openness of the surface). In the third part, permeability properties of the analysed woven fabrics with the fancy yarn in the weft were researched where greater attention was paid to air permeability and water vapour permeability. The results of the research showed that the samples with the first two-ply fancy yarn in the weft (81% cotton and 19% viscose) have greater air permeability and water vapour permeability. Meanwhile, the samples with the second two-ply fancy yarn in the weft (67% viscose and 33% flax) have lesser abrasion resistance and poorer dimensional stability while being washed.

Keywords: two-ply fancy yarn, air permeability, water vapour permeability

Permeabilitatea țesăturilor ce conțin fire fantezie dublu răsucite

Obiectivul studiului este de a analiza permeabilitatea țesăturilor ce conțin fire fantezie dublu răsucite în direcția bătăturii. În cadrul acestui studiu, au fost analizate firele fantezie dublu răsucite. Datorită structurii lor, acestea sunt clasificate ca fire fantezie cu efecte structurale. Primul fir fantezie dublu răsucit analizat este fabricat din amestec de 81% bumbac și 19% viscoză. Al doilea este compus din amestec de 67% viscoză și 33% in. În scopul studiului prezentat, țesăturile ce conțin fire fantezie dublu răsucite au fost realizate în trei desimi diferite în bătătură (10 fire per cm, 13 fire per cm și 16 fire per cm) cu legătură diagonal T 1/3 Z. Partea teoretică include istoria producției de fire fantezie, o discuție detaliată a proceselor de producție, tipurile și structura firelor fantezie, utilizarea acestora și piața globală și europeană a firelor fantezie. Partea experimentală este formată din trei părți. În prima parte, au fost analizate caracteristicile structurale ale firelor fantezie (finețea firului fantezie, frecvența de repetare a efectelor per metru de fir, direcția de răsucire a firului fantezie, numărul de răsuciri ale părții de bază și ale celei efective, diametrul fibrelor, diametrul părții de bază și a celei efective, finețea componentelor individuale, direcția răsucirii componentelor individuale și procentul răsucirii în interiorul componentelor individuale). În a doua parte, au fost analizate caracteristicile țesăturilor cu firul fantezie în bătătură (masă, grosime, desimea în urzeală și în bătătură). În a treia parte, a fost analizată permeabilitatea țesăturilor cu firele fantezie în bătătură, unde s-a acordat o mai mare atenție permeabilității la aer și permeabilității la vapori de apă. Rezultatele studiului au arătat că probele cu primele fire fantezie dublu răsucite în bătătură (81% bumbac și 19% viscoză) au o permeabilitate mai mare la aer și la vapori de apă. Pe de altă parte, probele cu al doilea fir fantezie dublu răsucit în bătătură (67% viscoză și 33% in) au avut o rezistență mai mică la abraziune și o stabilitate dimensională mai slabă la spălare.

Cuvinte-cheie: fir fantezie dublu răsucit, permeabilitate la aer, permeabilitate la vapori de apă

INTRODUCTION

The term “fancy yarn” refers to yarns containing deliberately planned irregularities, which make them distinct from classical yarns or multifilament ones. Fancy yarns represent only a few percent of the total world production earlier, their process is longer and

slower, which is why they are considered special products and their price is much higher [1–5]. Fancy yarns, especially two-ply, on the other hand, are increasingly relevant in the fashion industry. This is also the main reason why our research focuses on two-ply fancy yarn which is produced with ring

process and is most commonly used for high-quality garments. Some authors in the literature are also concentrated on the quality of fancy yarns in the last five years [6, 7]. Few papers also mention the evaluation of air permeability of fabrics woven with slub yarns [8] and also the performance of knitted fabrics produced from fancy yarns [9]. Some authors are also concentrated on efforts to methodise, problems and new suggestions of fancy yarns production [10] and also on comparison between ring spun and also fancy yarns [11].

The purpose of the presented research was to investigate the influence of two-ply fancy yarn on the permeability properties of woven fabrics with fancy yarn in the weft direction. Two different two-ply fancy yarns were analysed, both of which consist of a basic and effective component, which, due to the structure with the thickened places, belonged to fancy yarns with structural effects. Within the framework of the research, six fabrics were made from fancy yarns in the weft direction. The warp was in all samples from the classical ring spun yarn (100% cotton), and the weft in the first three samples from a two-ply fancy yarn, where one component is made of ring spun yarn, while the second one consists from multifilament yarn (81% cotton and 19% viscose), and in the other three samples from the two-ply fancy yarn, more precisely two single ring spun yarns (67% viscose and 33% flax). Woven fabrics were woven at three different densities in the weft (10 threads/cm, 13 threads/cm and 16 threads/cm) and the same densities in the warp direction (20 threads/cm) in the twill weave T 1/3 Z. More attention was paid to air permeability and water vapour permeability. Abrasion resistance and dimensional stability in the washing of analysed fabrics with fancy yarn were also investigated. The results of the presented research will show the effect of two-ply fancy yarn in the weft direction on the permeability properties of analysed woven fabrics.

THEORETICAL PART

Historical development of the production of fancy yarns

It is not known exactly when we first encountered fancy yarns, since there is not much tangible evidence of their emergence. The claims argue that this is primarily a conclusion based on archaeological finds in the old graves, that they had effective beginnings early in the early weavers, which should be used during the weaving in various ways to achieve a wide spectrum of color and structural effects. The mentioned weavers are also supposed to be able to anticipate texture changes that would result from differences in yarn thickness. Thus, the yarn produced would correspond to a pre-planned sample and structure [1, 2].

Unlike other fancy yarns, it is easier to find evidence of metal yarns confirming that Egyptians and Babylonians used them in ritual and ritual clothing materials. The yarn from that time was not permanent

and thoughtful, but they were a cheap way to achieve the effects. Throughout history, metallic yarns have been used in different periods, including Elizabeth and their contemporaries all over Europe for embroidering and making lace. Findings prove that metal yarns used for decorating in the sixteenth and seventeenth centuries consist of thin metal strips wrapped around a silk or flax core [1, 2].

One important statement claims that in the eighteenth century, yarns made from a bundle of silk filaments tied around the silk core were often used. The resulting effect was referring to the chenille yarn, which made it possible to conclude that this was perhaps the first real two-ply fancy yarn that was developed. There are conclusions based on the records that in the aforementioned century there were four basic types: the so-called classic yarn consisting of fine stripes wrapped around the core; a spiral yarn containing two yarns wrap around the core; flattened yarn, composed of a straightened metal wire and a metal effective double yarn, consisting of a flat yarn wrapped around the spiral thread [1, 2].

It has been proven that at the end of the nineteenth century, the development of fancy two-ply yarns, as we know it today, has begun, and with it an increase in the volume of devices intended to produce special effects. With the prevalence of an improved electronically controlled process in the late twentieth and early twenties, it was easier to produce diverse effects while maintaining a uniform level of quality [1, 2].

Production process of fancy yarns

Over the years, many different methods have been developed to produce fancy yarns. Among the main four today are the ring process, a hollow spindle process, a combined process, and a process for the manufacture of chenille yarn. Unlike the first three mentioned processes that produce several visually similar types earlier, the process for production chenille yarns is considered to be less versatile since it produces only one type of yarn. In addition to the four main procedures, there is also a dual process, a condenser process, a rotor process, a friction process, and air-jet process [2]. Most of the fancy yarns are made by the ring process. Thus, more attention in the paper is given to the fancy yarns which are produced using ring process. [2, 3]

Production of fancy yarns using the ring process

In spite of the modern spinning processes used in the past twenty years to produce the fancy yarns, the ring process remains the leader in the spinning field, as it is still produced approximately eighty percent earlier [2]. In the case of a ring process, the proposed roving is supplied through a three roller and two aprons draw frame. The first pair of rollers that feeds the roving are called the feed or back rollers and the last pair, which separates the thinned formation - yarn, are called the front rollers. Between feeding and front rollers are the so-called apron rollers, with upper and lower apron, which allow for controlled control of

fibers in drawing zone of the draw frame. After drawing, it is followed by reinforcement with a twisting at the same time winding the yarn onto the cops [2].

The yarn that leaves the spinning roller and passes through the thread guide, which is located exactly above the ring spindle, is provided with the help of the ring-traveller-spindle mechanism. Produced yarn is wound on the cops after transmitting the vitle in the same place. Cops is mounted on the spindle and spins with it. During its rotation, the tension is drawn by a runner circling the circumference of the ring, and in this way it transmits the real twist to yarn. The height of the yarn winding is regulated by the train on which the spindle is installed. The train rises and descends all the time to wind down the so-called filling and separation layers, then rises gradually to a higher level, until the entire layer is wound up on the cops [2].

The ring process is regarded as the most flexible, as it is possible on the ring tower to retrofit a mechanical or electronic control device that allows programmed effects to be produced, such as thickened, thinned effects and different turns per yarn length.

The thickness of the yarn length is achieved by the programmed and controlled steering of the stepping motor, which drives the feeding and pulley roller in a simple binary expansion. The effect of the thickened place is achieved by briefly accelerating the rotation of the feed roller at the unchanged rotational speed of the discharge cylinder in the extender. The length, intensity and repetition of the effects are controlled by the settings of the control unit. A variety of turns per length of fancy yarn is achieved by changing the rotational speed of the spindle during the transmission of the real twist to produced yarn [1–4].

The main disadvantage of producing fancy yarns after the ring process is in long-lasting and costly manufacturing processes. Fancy yarns composed of one or more basic, one or more effective and, in most cases, binding yarns, are made in two or more separate transitions of the ring spinning machine in the ring process to produce fancy yarns [1, 2].

The production of loops and lace yarns, consisting of two basic components, supplied over a pair of feed rollers and a fancy yarn, supplied with a pair of rollers. Since they are supplied at different speeds, the base yarns are able to pass through groove slits on the upper separating cylinder, allowing the base and effective grooves to merge when leaving the separating rollers. The resulting triangle represents an area where the excessive effect produces loops or laces. The size of the effects is regulated by changing the size of the spin triangle while it is regulated by changing the tension during spinning, the twist degree and the groove of the upper roller [1, 2].

When the fancy yarn is much thicker than the base, the roller is replaced by a smooth top roller so that it is raised and the pressure can be applied to the base yarn. This feeder system also applies to fancy yarns that contain only one basic component [1, 2].

The global and European marketplace of fancy yarns

Over the last decade, there has been a noticeable increase in the worldwide interest in the production of fancy yarns worldwide, which is expected to grow steeply in the next decade following the latest market research. The reason for the interest is most likely due to the liberalization of the international market of fancy yarns between Asia and Europe, which are the largest exporters and dominate the field of production. In addition to the Asian countries, including China, Japan, Korea and India, and Europe, which is in favor of Germany, France, Great Britain, Russia and Italy, the production of effects has already taken place in North America, South America and Africa. In recent years, lower production has been observed. The most demand and consequently the production is intended for chenille, ondé, gimp and loop, lace and flame fancy yarns. When it comes to the effect of the market of fancy yarns earlier, it should be noted that their use is not so common, and that their market value will continue to be unparalleled in comparison with the rest of the textile market [4, 5].

The latest trends in the yarns production field foresee a bright future for fancy yarns, as they will continue to be present in knitted clothes, which will be radiant appearance, due to the influence of various metallic colors, loose vitters, small knots and various large flames [10–12]. The worldwide market for fancy yarn is expected to grow at a CAGR of roughly 5.6% over the next five years, according to a new Global Info Research study. This information focuses on the fancy yarn in global market, especially in North America, Europe and Asia-Pacific, South America, Middle East and Africa [13].

EXPERIMENTAL PART

Presentation of analysed fancy yarns and fabrics with fancy yarns

In the experimental part, two-ply fancy yarns were analysed, both of which consist of a basic and effective component that produces effects at intervals. The first analysed fancy yarn labeled FY1 is a two-ply fancy yarn, made of cotton ring spun yarn which is plied with viscous multifilament yarn. The ratio of the both components in the mixture presents 81% cotton and 19% viscose, while the second analysed two-ply fancy yarn, labeled FY2, from two single ring spun yarns from a mixture of 67% viscose and 33% flax. Because of their recognizable effects, which are visible as bold spots with fewer turns, they belong to the fancy yarns with structural effects. They are made by ring process, on the bobbin twist of the Alma Saurer machine. Table 1 presents the structural properties of the analysed two-ply fancy yarns.

In table 2, the structural properties of the individual components of the analysed two-ply fancy yarns are presented earlier.

Table 1

STRUCTURAL PROPERTIES OF ANALYSED FANCY YARNS			
Sample	Yarn structure	Fineness (tex)	Frequency of repetition of effects on meter of yarn (%)
FY1	Two-ply fancy yarn	180	23
FY2	Two-ply fancy yarn	230	17
Sample	Twist direction (S/Z)	Number of twist of basic part (T/20 cm)	Number of twist of effective part (T/10 cm)
FY1	S	88	40
FY2	S	52	10

Table 2

STRUCTURAL PROPERTIES OF THE INDIVIDUAL COMPONENTS OF THE ANALYSED TWO-PLY FANCY YARNS						
Sample	Diameter of fibres d_v (μm)		Diameter of basic part of fancy yarn d_t (μm)		Diameter of effective part of fancy yarn d_e (μm)	
	Component1	Component2	Component1	Component2	Component1	Component2
FY1	Component1	Component2	Component1	Component2	Component1	Component2
	21.7	33.3	757	343	1995	351
FY2	Component1	Component2	Component1	Component2	Component1	Component2
	17.5	12.7	622	614	625	1415
Sample	Fineness T_t (tex)		Twist direction (S/Z)		Percent of twist P_v (%)	
FY1	Component1	Component2	Component1	Component2	Component1	Component2
	146	34	S	S	4	0.8
FY2	Component1	Component2	Component1	Component2	Component1	Component2
	117	113	Z	Z	0.8	0.8

Note: FY1 – Component1 (cotton ring spun yarn), Component2 (viscose multifilament yarn); FY2 – Component1, Component2 (single ring spun yarn from the mixture of viscose and linen).

Table 3

STRUCTURAL PROPERTIES OF FABRICS WITH TWO-PLY FANCY YARN IN WEFT				
Sample	Density on the weaving machine (threads/cm)		Mass M (g/m^2)	Thickness d (mm)
	Warp	Weft		
FY1_10	Warp	Weft	231.8	1.120
	20	10		
FY1_13	Warp	Weft	303.9	1.157
	20	13		
FY1_16	Warp	Weft	351.9	1.174
	20	16		
FY2_10	Warp	Weft	286.7	0.980
	20	10		
FY2_13	Warp	Weft	339.4	0.984
	20	13		
FY2_16	Warp	Weft	369.9	0.992
	20	16		
Sample	Warp density (threads/cm)		Weft density (threads/cm)	Openess of area (%)
FY1_10	24		13	8.74
FY1_13	26		15	3.96
FY1_16	28		18	3.19
FY2_10	25		14	4.58
FY2_13	27		16	3.54
FY2_16	29		19	2.35

Presentation of analysed fabrics with two-ply fancy

In the framework of the research, the woven fabrics in the twill weave T 1/3 Z were analysed with the two-ply fancy yarns in the weft direction which are marked with FY1 and FY2. The classical ring spun cotton yarn was used in the warp direction. Woven fabrics were made at three different densities in the weft, namely 10 threads/cm, 13 threads/cm and 16 threads/cm, with a density of 20 threads/cm in the warp direction, on the weaving machine Minifaber with TIS electronic jacquard mechanism. The designation of the samples consists of a series of analysed effects of the earlier and number of weft threads per centimeter. Table 3 presents the structural properties of fabrics with two-ply fancy yarn in weft.

Table 4 shows the properties of the ring spun cotton yarn in the warp direction.

Table 4

PROPERTIES OF THE RING SPUN COTTON YARN IN THE WARP DIRECTION			
Sample	Yarn	Fineness (tex)	Number of twist (T/m)
Warp	Ring spun	16 (2·8 tex)	542 Z

Presentation of the methods used

The fineness of fancy yarn

Fineness or linear density is a physical quantity that is defined as mass per unit length. It provides the most useful way of expressing fineness that affects the properties of yarn. The length of the mass is determined indirectly, by compression, capacitive methods or direct, gravimetric determination [12, 14, 15].

Method of work:

The linear density of fancy yarns has been measured in accordance with ISO 2060 Textiles – Yarn from packages – Determination of linear density (mass per unit length) by the skein method [16]. A gravimetric method was performed whereby the measured length of two-ply fancy yarn which amounts 1 m was weighed. Twenty measurements were made for each sample of the analysed fancy yarn and individual components. From the readings of the measured mass of the fancy yarn sample and the individual components, the average value of the linear density was calculated according to the equation:

$$T_t = \frac{m \cdot 10^3}{l} \quad (1)$$

where T_t is linear density (tex), m – mass of yarn (g), l – length of yarn (m).

The twist direction of two-ply fancy yarn

During the spinning process, a yarn is formed by the inserting twist, which is defined by the twist direction (left or right) and the number of turns. The direction of the twist is indicated by the capital letters S or Z. When the turns of the yarn are in the left direction, the yarn has so-called S-twist, when they are in the right

direction, the yarns has so-called Z-twist. The direction of the coil is determined optically or on a device for measuring the number of turns called the Torsiometer [12, 14, 15].

Method of work: the twist direction of the two-ply fancy yarn was previously determined in accordance with the ISO 2 standard, Textiles – Designation of the direction of twist in yarns and related products [17]. Optical determination of the winding direction and determination of the torsiometer for each sample of the analysed two-ply fancy yarn and its individual components were carried out. The direction of the twist was indicated by a capital letter, where the mark S represents the left twist and the mark Z indicates the right twist of the yarn.

The number of twist of two-ply fancy yarn

The number of twist is very important for mechanical properties of yarn, which include breaking strength, elongation, and elasticity. The number of twist also influences on appearance of the yarn. The number of twist of single yarn is determined indirectly by measuring the number of turns required to completely unroll the yarn and then twisting in the opposite direction to the original number of turns, while the number of turns of ply yarn is determined directly, at thus measuring the number of turns required to completely unroll the yarn [12, 14, 15].

Method of work: the number of twist was previously determined in accordance with ISO 2061, Textiles – determination of twist in yarns – Direct counting method [18]. A direct determination of the number of turns of two-ply fancy yarn was carried out on a Torsiometer device. First, the aforementioned determination of the pattern direction of the sample was carried out. A preparatory needle was used to help separate the individual components. When these two were completely unwound, the number of turns from the differential counter was read. Twenty-five measurements were made for each sample of the analysed fancy yarn. Due to the presence of effects occurring at intervals, the turns were measured to be 20 cm at the base part and at 10 cm at the effect part. From the readings of the measurements of the fancy yarn sample, the average value of the number of turns was calculated.

Percent of twist of two-ply yarn components

The percent of twist is defined as a change in the length of the plies, which is seen as an extension of the component when unwinding the yarn twisted. It is dependent on the different characteristics of yarn, which include the composition, the length and direction of the twist. The percent of twist is determined by measuring the initial length of plied yarn and the final, unwinding length, after untwisting [14].

Method of work: measurement of the percent of twist of each component was carried out in such a way that the individual components of the sample of two-ply fancy yarn of an initial length of 10 cm were untwisted. After untwisting, the length of each component was re-measured. Ten measurements were made for each sample of the analysed fancy yarn.

From the value of the final length of the individual components of the fancy yarn, the mean value of the percent of the twist was calculated according to the equation:

$$P_v = \frac{l_k - l_z}{l_z} \cdot 100 \quad (2)$$

where P_v is percent of twist (%), l_k – final length after untwisting (cm), l_z – initial length of two-ply yarn (cm).

Mass of fabrics with fancy yarn

The surface mass is defined as the mass per unit area in g/m^2 . The mass of a square meter of textile material is determined by accurately measuring the cut-out sample of a given size, usually 10×10 cm while the mass of the running meter is determined by accurately measuring the mass of the entire width of the sample at one-meter length [12, 14].

Method of work: the surface mass of fabrics with fancy yarn was measured in accordance with SIST EN 12127, Textiles – Fabrics – Determination of mass per unit area using small samples [19]. The measurement of the square mass of the square meter was carried out in such a way that the fabric sample with dimension 10×10 cm was weighed. Five measurements were made for each fabric sample with the fancy yarn. From the readings of the measured mass of the fabric sample, the average value of the surface mass was calculated according to equation:

$$M = \frac{m \cdot 10^4}{S} \quad (3)$$

where M is fabric surface mass (g/m^2), m – fabric weight (g), S – fabric surface (cm^2).

Thickness of fabrics with fancy yarn

Thickness is defined as the measurement of height between two parallel surfaces separated by a textile material at a specified pressure. When measuring thickness, the shape and size of the pressure leg, measurement time, and pressure should be taken into account. The thickness affects the insulation and permeability properties of the textile material [12, 14]. Method of work: the thickness of fabrics with fancy yarn has been measured in accordance with ISO 5084, Textiles – Determination of thickness of textiles and textile products [20]. The thickness measurement was performed on a device called Micrometer at a pressure of 20 cN/cm^2 . Five measurements were made at five different locations for each fabric pattern. From the average measurements of the fabric sample, the average thickness value was calculated and expressed in mm.

Density of fabrics with fancy yarn

The density of the weave is defined by the number of warp and weft threads per unit length. The air permeability and thermal conductivity of the textile material depend to a large extent on the density of the warp and the weft. It is determined by counting and given by the number of threads/cm [12, 14].

Method of work: the density of fancy yarn fabrics has been measured in accordance with SIST EN 1049-2,

Textiles – Woven fabrics – Construction – Methods of analysis – Part 2: Determination of number of threads per unit length [21]. The warp and weft density of the fabric was measured using a thread counter (frame magnifier with surface of 1 cm^2) by counting the warp threads at five different locations along the entire width of the fabric, while the weft threads were counted at five places the length of the fabric, as far apart as possible. From the values of the warp and weft threads of each fabric sample with fancy yarn, the average density value was calculated.

Openness of the area of fabric with fancy yarn

The surface openness is defined as the empty spaces between the warp and weft threads in the fabric and the empty spaces between the fibers in non-woven fabrics. It is determined by image analysis using ImageJ (free program by Wayne Rashband, National Institute of Health, United States of America) and reported in percentages [14].

Method of work: the measurement of the surface area of the fancy yarn fabrics was carried out by image analysis, using a shot of the analysed sample of the yarn fabric, using ImageJ [23]. The image was previously recorded on a Leica stereomicroscope at $10 \times$ magnification. Three measurements were made for each fabric sample. From the measured values of the fabric sample measurements, the average value of the openness of area was calculated.

Air permeability of fabrics with fancy yarn

Air permeability is defined as the airflow velocity that passes perpendicularly through the textile material on a given surface, pressure and time. It is measured as the amount of air passing through 1 m^2 of textile material within 1 minute at the selected pressure. Air permeability is one of the most important properties that affect porosity, insulating properties, rain and wind protection, and filtering ability. To a large extent, it depends on the structural properties of textile material, which include yarn properties, weave and density of the thread [12, 14].

Method of work: the air permeability of fabrics with fancy yarn was measured according to SIST EN ISO 9237; Textiles – Determination of the air permeability of textiles [23]. Measurement was carried out on the air-permeability measuring device, called AirTronic 3240A, with a measuring surface of 50 cm^2 and a selected pressure of 100 Pa . Through the sample, the air was passed, which passed through the measuring system, which showed the quantity of air in $[l/h]$. Ten measurements were made at different places of each fabric sample with fancy yarn. The average value of the air permeability was calculated from the readings of the measurements of the sample of the fabric with fancy yarn.

Water vapour permeability of woven fabrics with fancy yarn

The water vapour permeability is defined as the amount of water vapour that passes through 1 m^2 textile material in a given area within 24 hours. The

water vapour permeability is influenced by the structural properties of textile material, which include the construction properties of fabric, chemical composition of yarn and the density of the thread. It can be determined by the method with water or by the method using a drying agent [12, 14].

Method of work: the permeability of water vapour of woven fabrics with fancy yarn was measured according to ASTM E96/E96M; Textile – Determination of water vapour permeability [24]. The measurement was carried out using the water method, where the sample was embedded in a glass container with a metal cover, 3 cm in diameter, containing 7 ml of distilled water. A glass container with a sample was inserted into the desiccator. After 1 hour of standstill at room temperature, the prepared sample container was weighed on an electronic weigh and then after 24 hours of rest in the desiccator, thus eliminating the influence of moisture. Two measurements of each sample of the fabric with fancy yarn were made. From the measured mass of the sample of the fabric with fancy yarn, both the mass at room temperature and the mass in the desiccator, the mean water vapour permeability value was calculated according to the equation:

$$WVT = \frac{m_r}{S \cdot t} \quad (4)$$

where WVT is water vapour permeability ($\text{g}/\text{m}^2\text{h}$), m_r – mass difference (g), S – area of the metal cover opening (m^2), t – time (h).

Abrasion resistance of fabrics with fancy yarn

Abrasion resistance is defined as the resistance of textile material to loss of weight due to a certain load on abrasion. It is a relative criterion for the wearability of textile products in their use. It measures as an assessment of damage to the appearance of worn textile material compared to the original one. Abrasion resistance is influenced by the load of textile material, the time, the number of turns and the method of abrasion resistance, which can be one-way, circular or multi-directional [12, 14].

Method of work: abrasion resistance of fabrics with fancy yarn was measured according to SS-EN ISO 12947-2; Textiles – Determination of the abrasion resistance of fabrics by the Martindale method – Part 2: Determination of specimen breakdown [25]. Measurement was performed on a device called Martindale at 1000, 3000, 5000, 7000, 10000 and 12000 cycles. A round sample with a diameter of 2.9 cm was inserted into the cradle at a load of 12 kPa where it was circularly rubbed along a standard wool fabric installed on the device. Two samples of each yarn fabric with fancy yarn were made. The appearance of the analysed wear sample of the fancy yarn fabric was compared with standard photographs and estimated with the degree of peeling 5 to 1 (grade 5 means that peeling is not noticeable, while grade 1 means a strong peeling).

Dimensional stability in the washing of fabrics with fancy yarn

Dimensional stability in washing is defined as a dimensional change, which is expressed in the form of shrinkage or stretching during washing. During the washing process, the textile material is exposed to mechanical stress. It is measured as a change in the dimensions that occurs during the washing process. The dimensional stability of washing is influenced by the structural properties of textile material, which include the fabric construction, the yarn characteristics and the density of the thread. The type of washing program selected, the washing temperature, the time, the number of centrifuge plants and detergent [12] have an important influence on the dimensional change in washing.

Method of work: the dimensional stability of washing fabrics with fancy yarns was measured according to EN ISO 5077; Textiles – Determination of dimensional change in washing and drying [26]. The measurement was carried out in a classic household washing machine Gorenje WA 64153, a wash program with a temperature of 40°C , a centrifuge with 1300 rpm and the use of a liquid detergent. A square of 10×10 cm square was drawn inside a sample of 20×20 cm. After the wash, the size of the square was re-measured, and the dimensional change was determined in the warp and weft direction. Two measurements of each sample of the fabric with fancy yarn were made. From the measured values (final length B in cm) of the sample of the fabric with fancy yarn, the mean value of the dimensional change in washing, according to the equation, was calculated:

$$D_s = \frac{A - B}{A} \cdot 100 \quad (5)$$

where D_s is dimensional stability (%), A – initial length (cm), B – final length (cm).

RESULTS WITH DISCUSSION

Permeability properties of fabrics with fancy yarn

Air permeability results of fabrics with fancy yarn

Figure 1 shows the results of air permeability of fabrics with fancy yarn.

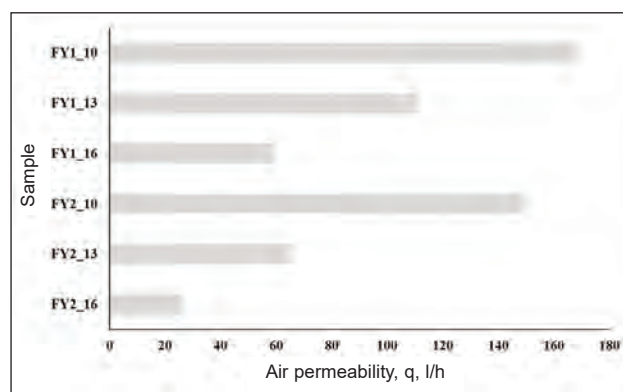


Fig. 1. The results of air permeability of analysed fabrics with fancy yarn

From the measured results of the air permeability of woven fabrics with fancy yarn, it is evident that the samples with the first analysed fancy yarn, labeled FY1_10, FY1_13 and FY1_16, made from 81% cotton and 19% viscose, express the highest air permeability. The reason is most likely to have a higher frequency of repetition of effects per meter of yarn (23%), namely a larger total diameter at the effective part (component1 – 1995 μm , component2 – 351 μm), but a smaller overall diameter on the base part (component1 – 757 μm , component2 – 343 μm). The FY2_10 sample has a lower air permeability (149.42 l/h) compared to the FY1_10 sample (168.16 l/h), the FY2_13 sample has a lower air permeability (65.07 l/h) compared to the FY1_13 sample (111.38 l/h) and the FY2_16 sample has a lower air permeability (25.7 l/h) than the FY1_16 (59.06 l/h) sample. The reason lies in the higher masses per unit area of the samples FY2_10, FY2_13 and FY2_16. The highest air permeability has the FY1_10 sample – 168.16 l/h, which has the smallest density (231.84 g/m^2) compared to other samples, the lowest density of the thread (warp – 24 threads/cm, weft – 13 threads/cm), maximal surface opening (8.74%) and minimal thickness (1.120 mm) between samples with yarn FY1 in weft. The smallest air permeability has a sample labeled FY2_16, which is only 25.7 l/h. The reasons are the highest mass (369.93 g/m^2), the maximal density of the thread (warp – 29 threads/cm, weft – 19 threads/cm) and the smallest openness of the surface (2.35%) among all samples.

Based on the measured results shown, it can be concluded that the structure of fancy yarn labeled FY1 with a smaller total diameter of the base part having a higher frequency of repetition is influenced by higher air permeability, a greater difference between the diameter of the components, both the base and the effective part and the higher frequency of repetition of the effects per meter of yarn, which consequently affect the greater openness of the surface. The samples with the first analysed fancy yarn in the weft, labeled FY1, made from 81% cotton and 19% viscose, express increased air permeability. The reason is most likely to have a higher frequency of repetition of effects per meter of yarn (23%). Higher openness of the surface influences higher air permeability or a greater number of empty interstices between the threads of the fabric. It is confirmed that the structural properties of textile material are affected by air permeability. Particularly important is the density of the threads of the fabric, since due to the increase, the air passage through the textile material is reduced. The reasons for the lowest air permeability of the sample labeled FY2 are the highest mass, the maximal density of the thread (warp – 29 threads/cm, weft – 19 threads/cm) and the smallest openness of the surface (2.35%) among all samples.

The results of water vapour permeability of woven fabrics with fancy yarn

Figure 2 shows the results of water vapour permeability of woven fabrics with fancy yarn.

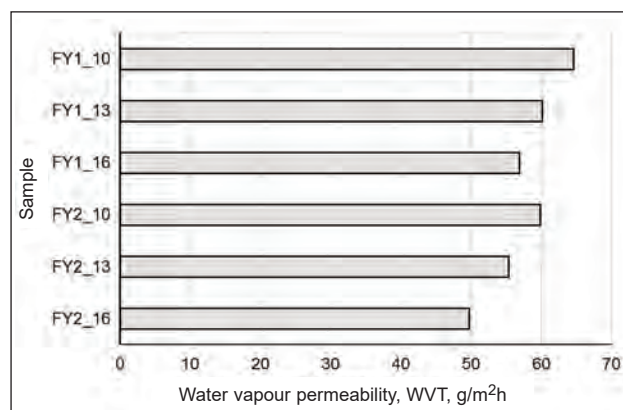


Fig. 2. Results of water vapour permeability of analysed fabrics with fancy yarn

From the calculated results of the water vapour permeability of woven fabrics with fancy yarn it is evident that in all three adjusted densities on the weaving machine (10 threads/cm, 13 threads/cm and 16 threads/cm) samples with the second analysed two-ply fancy yarn with the label FY2, made from a mixture of 67% viscose and 33% flax, express less water vapour permeability. The reason is probably the lower frequency of repetition of effects per meter of yarn (17%), namely a larger total diameter of the base part (component1 – 622 μm , component2 – 614 μm), but a smaller overall diameter of the effective part (component1 – 625 μm , component2 – 1415 μm). The FY1_10 sample has a higher water vapour permeability (64.58 $\text{g}/\text{m}^2\text{h}$), compared to the FY2_10 sample (59.82 $\text{g}/\text{m}^2\text{h}$), the FY1_13 sample has a higher water vapour permeability (60.12 $\text{g}/\text{m}^2\text{h}$) in comparison with the FY2_13 sample (55.36 $\text{g}/\text{m}^2\text{h}$) and the FY1_16 sample has a higher water vapour permeability (56.85 $\text{g}/\text{m}^2\text{h}$) compared to the FY2_16 sample (49.7 $\text{g}/\text{m}^2\text{h}$). The minimal water vapour permeability expresses the FY2_16 sample, which has mass 369.9 $\text{g}/\text{m}^2\text{h}$, and a maximal thickness (0.992 mm) and a maximal thread density (warp – 29 threads/cm) in comparison with other samples with yarn FY2 in weft – 19 threads/cm) and minimal surface opening (2.35%) among all samples. The highest permeability of the water has a sample labeled FY1_10, which has mass 231.8 $\text{g}/\text{m}^2\text{h}$. The reasons for this are the fiber composition (81% cotton and 19% viscose), the smallest thickness (1.120 mm) between the samples with yarn FY1 in weft and the minimal density of threads (warp – 24 threads/cm, weft 13 – threads/cm) and openness of the surface (8.74%) among all samples.

Based on the calculated results shown, it can be concluded that the lower water vapour permeability is influenced by the structure of the fancy yarn labeled FY2 with a lower frequency of repetition of the effects per meter, having a smaller overall diameter and a smaller difference between the diameter of the components, both on the base and the effective part of the yarn, which influences on the openness of the surface increase. That results in a minor passage of

water vapour through the textile material. It is confirmed that the water vapour permeability is influenced by the structural properties. In particular, the material composition of the textile material is important. It is known that viscose fibers have a higher hydrophilicity (12 to 14%) compared to cotton (7 to 11%), which makes them more absorbing, retaining and preventing its transition to the environment.

Abrasion resistance of fabrics with fancy yarn

Table 5 presents the results of the abrasion resistance of fabrics with fancy yarn.

From the results of the abrasion resistance of woven fabrics with fancy yarn, it is evident that the samples with the first analysed fancy yarn with the mark FY1,

which is made from 81% cotton and 19% viscose, are more resistant to rubbing. The reason is most likely a larger number of turns, both on the base (88 T/20 cm) and the effective part (40 T/10 cm). In the case of FY1_10, FY 1_13, FY 1_16 and FY 2_16 with 12000 turns or rubbs did not break the thread, while in the case of the FY 2_10 and FY 2_13 samples, the basic threads in the effective part were completely broken. There was no breakage in the sample FY 2_16, most likely due to the maximal density of the thread (warp – 29 threads/cm, weft – 19 threads/cm). The highest abrasion resistance was measured with the FY 1_16 sample, which has an fancy yarn in a weft with a larger number of turns (basic part 88 T/20 cm, effective

Table 5

ABRASION RESISTANCE OF ANALYSED FABRICS WITH FANCY YARN			
Sample	Comparable and estimated appearance of the sample at a given number of turns		
	1000	3000	5000
FY1_10	There is no difference in the appearance of the sample (peeling grade 5)	There is no difference in the appearance of the sample (peeling grade 5)	Light peeling, partially pulled fibers (peeling grade 4)
FY1_13	There is no difference in the appearance of the sample (peeling grade 5)	There is no difference in the appearance of the sample (peeling grade 5)	There is no difference in the appearance of the sample (peeling grade 5)
FY1_16	There is no difference in the appearance of the sample (peeling grade 5)	There is no difference in the appearance of the sample (peeling grade 5)	There is no difference in the appearance of the sample (peeling grade 5)
FY2_10	Light peeling, partially pulled fibers (peeling grade 4)	Moderately increased peeling and extracting fibers (peeling grade 3)	Moderately increased peeling and extracting fibers (peeling grade 3)
FY2_13	There is no difference in the appearance of the sample (peeling grade 5)	Light peeling, partially pulled fibers (peeling grade 4)	Light peeling, partially pulled fibers (peeling grade 4)
FY2_16	There is no difference in the appearance of the sample (peeling grade 5)	There is no difference in the appearance of the sample (peeling grade 5)	Light peeling, partially pulled fibers (peeling grade 4)
Sample	Comparable and estimated appearance of the sample at a given number of turns		
	7000	10000	12000
FY1_10	Light peeling, partially pulled fibers (peeling grade 4)	Moderately increased peeling and extracting fibers (peeling grade 3)	Very high peeling without brake (peeling grade 2)
FY1_13	Light peeling, partially pulled fibers (peeling grade 4)	Light peeling, partially pulled fibers (peeling grade 4)	Moderately increased peeling and extracting fibers (peeling grade 3)
FY1_16	There is no difference in the appearance of the sample (peeling grade 5)	Light peeling, partially pulled fibers (peeling grade 4)	Light peeling, partially pulled fibers (peeling grade 4)
FY2_10	Very high peeling without brake (peeling grade 2)	Very high peeling without brake (peeling grade 2)	Increased peeling. perfect deformation and thread breakage (peeling grade 1)
FY2_13	Moderately increased peeling and extracting fibers (peeling grade 3)	Moderately increased peeling and extracting fibers (peeling grade 3)	Very high peeling without brake (peeling grade 2)
FY2_16	Moderately increased peeling and extracting fibers (peeling grade 3)	Very high peeling without brake (peeling grade 2)	Very high peeling without brake (peeling grade 2)

Note: Peel grades: 5 – No difference; 4 – Slight difference and/or slight peeling; 3 – Moderate difference. Peeling of different size and density moderately the surface of the sample; 2 – Significant difference and/or pronounced peeling; 1 – Great difference and strong peeling.

part 40 T/10 cm), maximal thickness (1.174 mm) between all samples and maximal density yarn (warp – 28 threads/cm, weft – 18 threads/cm) between samples with yarn FY1 in the weft. The smallest abrasion resistance has a sample labeled FY 2_10. The reasons for this are the fiber composition (67% viscose and 33% flax), fancy yarn in a weft with a smaller number of turns (basic part 52 T/20 cm, effective part 10 T/10 cm) and minimal thickness (0.980 mm) of the sample.

On the basis of the comparable results shown, it can be concluded that the structure of the fancy yarn with a greater number of turns is affected by the greater resistance of the textile material, both on the base and the effective part, which influence the better twisting of the fibers into the core of the yarn. It is confirmed that the structural properties of textile material are affected by the abrasion resistance. In particular, the raw material composition is important. It is known that cotton fibers are well resistant to rubbing, compared to flax and viscose, which are less resistant.

Results of dimensional stability in the washing of fabrics with fancy yarn

Figure 3 shows the results of dimensional stability in the washing of fabrics with fancy yarn.

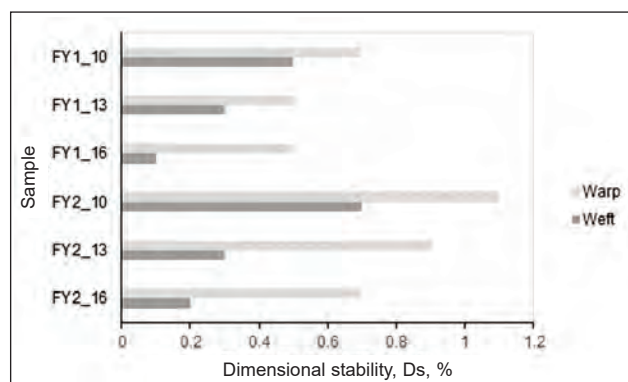


Fig. 3. Results of dimensional stability in the washing of analysed fabrics with fancy yarn

From the calculated results of dimensional stability in the washing of woven fabrics with fancy yarn, it is evident that the samples with the second analysed two-ply fancy with a mark FY2, made from 67% viscose and 19% flax, express increased shrinkage. The reason is probably in the smaller number of turns, both on the base (52 T/20 cm) and the effective part (10 T/10 cm) and the smaller percentage of the shrinkage (component 1: 0.8%, component2: 0.8%). The FY1_10 sample has a lower percentage of shrinkage (warp: 0.7%, weft: 0.5%) compared to the FY2_10 sample (warp: 1.1%, weft – 0.7%), the FY1_13 sample has a smaller percentage of shrinkage, warp: 0.5%, weft: 0.3%) compared to the FY2_13 sample (warp: 0.9%, weft: 0.3%) and the FY1_16 sample has a smaller percentage of shrinkage (warp: 0.5%, weft: 0.1) compared to the FY2_16 sample (warp: 0.7%, weft: 0.2%). There was no stretch for any sample of

the analysed fabrics. All samples have a greater shrinkage in the warp direction (from 0.5% to 1.1%) than in the weft direction (from 0.1% to 0.7%). The worst dimensional stability in the washing has the FY2_10 sample, which shrunk by as much as 1.1% in the warp direction and by 0.7% in the weft direction, which has in comparison with other samples with yarn FY2 in the weft, the smallest mass (286.67 g/m²), minimal thread density (warp – 25 threads/cm, weft – 14 threads/cm) and minimal thickness (0.980 mm) between all samples. The best dimensional stability with the washing has a sample labeled FY1_16, which shrunk by 0.5% in the warp direction and by 0.1% in the weft direction. The reasons are the raw material composition (81% cotton and 19% viscose), the highest mass (351.92 g/m²), maximal density of the thread (warp – 28 threads/cm, weft – 18 threads/cm) of the samples FY1 in weft and maximal thickness (1.174 mm) between all samples.

On the basis of the calculated results, it can be concluded that the structure of the fancy yarn with a smaller percentage of the twist and a smaller number of turns, both the basic and the effective part, is influenced by the poorer dimensional stability in washing and consequently, larger shrinkage. It is confirmed that the dimensional stability of washing is influenced by the structural properties of the textile material. In particular, the raw material composition is important, as natural fibers, including cotton, linen and viscous, are shrunk in the washing process. For this reason, samples of an appropriately larger size were analysed. Smaller shrinkage in washing is also influenced by higher density of threads of fabric and thickness, despite the smaller fineness of the analysed fancy yarn.

CONCLUSIONS

Based on a study of the permeability properties, abrasion resistance and dimensional stability of fabrics with two-ply fancy yarn, it can be concluded that:

- Samples with the first analysed two-ply fancy yarn FY1, which is made from 81% cotton and 19% viscose, have higher air permeability than the samples with the second two-ply fancy yarn FY2, which is made from 67% viscose and 33% flax. It can be concluded that the structure of fancy yarn express important influence on increased air permeability. The most important parameters that have an important influence on air permeability increase are: a smaller total diameter of the base part, which is more often repeated, a higher frequency of repetition of the effects per meter of a yarn and a greater difference between the diameter of the components, both the basic and the effective part, creating more empty places between threads, affecting the increased passage of air through the textile material. It is confirmed that the greater air permeability of the textile material is also influenced by the lower density of the fabric and the consequent greater openness of the surface;

- Samples with a second analysed two-ply fancy yarn FY2, made from 67% viscose and 33% flax have lower water vapour permeability than the samples with the first two-ply fancy yarn FY1. It can be concluded that the lower vapour permeability is influenced by the structure of the fancy yarn with a lower frequency of repetition of the effects per meter of yarn having a smaller overall diameter and a smaller difference between the diameter of the components, both on the base and the effective part of the yarn, which reduces the openness of the surface, causes a slight passage of water vapour through the textile material. It has been confirmed that the higher permeability of the water vapour of the textile material is influenced by the fiber composition and the lower density of the threads of the fabric;
 - Samples with the first analysed two-ply fancy yarn FY1, which is made from 81% cotton and 19% viscose, have higher abrasion resistance. It can be concluded that the structure of fancy yarn with a greater number of turns affects the greater abrasion resistance, both on the base and the effective part, which influence the better twisting of the fibers into the yarn, which makes the yarn harder to unfold. It has been confirmed that the strength of the textile material, the greater the thickness and the higher the density of the fabric are affected by the greater abrasion resistance;
 - Samples with a second analysed two-ply fancy yarn FY2, which is made from 67% viscose and 33% flax have a worse dimensional stability when washing. It can be concluded that the structure of the fancy yarn with a smaller number of turns, both on the base and the effective part and the smaller percentages of the twist, is affected by the worse dimensional stability in washing or the greater shrinkage of the textile material. It is confirmed that the minor dimensional change in washing is influenced by the raw material composition of the textile material, the greater the thickness and the higher the density of the threads of the fabric.
- Fancy yarns have become increasingly popular in the fashion industry lately. Due to the better mechanical properties and larger effects (higher difference between the base and effective part of the two-ply yarn), two-ply fancy yarn are mostly used, among other types of fancy yarns. New insights into the permeability properties of two-ply fancy yarns produced from the mixture cotton/viscose and viscose/flax blends thus make a new contribution to the development, production and responsiveness of fancy yarns in fabric during wearing the clothes from them.

REFERENCES

- [1] Gong. R.H., Chapter 4: *Developments in fancy yarns. Specialist Yarn and Fabric Structures: Developments and Applications*, Edited by R. H. GONG. Cambridge, Philadelphia, New Delhi: Woodhead Publishing Limited, 2011, 75–106
- [2] Gong, R.H., Wright. R.M., *Fancy yarns – Their Manufacture and Application*, 1st edition, New York: Woodhead Publishing Limited, 2002, 31–83
- [3] Tasnim, N.S., *Technology, structure and applications of fancy yarns*, V International Journal of Engineering Research and Applications, 2012, 2, 3, 3109–3150
- [4] Lawrence, C.A., *Fundamentals of spun yarn technology*, CRC Press, London, 2002, 481–499
- [5] Kovačević, S., Schwarz, I.G., Skenderi, Z., *Diversity of spun yarn properties sized with and without prewetting*, In: *Industria Textila*, 2016, 67, 2, 91–99
- [6] AlShukur, M., *The quality of fancy yarn: Part i: Methods and concepts*, In: *International Journal of Textile and Fashion Technology*, 2013, 3, 1, 11–24
- [7] Grabowska, K.E., Ciesielska, I.L., Vasile, S., *Fancy yarns – An appraisal*, In: *Autex Research Journal*, 2009, 9, 3, 74–81
- [8] Özgen, B., Altaş, S., *Evaluation of air permeability of fabrics woven with slub yarns*, In: *Tekstil Ve Konfeksiyon*, 2017, 27, 2, 126–130
- [9] Atef, R., Elbealy, R., Badr, A.A., Abd Elkhalek, R., *Performance of Knitted Fabrics Produced from Fancy Yarns with Different Slub/Meter and Blend Ratio*, In: *Journal of Textile Science Engineering*, 2018, 8, 5, 2–7
- [10] Petrulytė, S., *Fancy Yarns: Efforts to Methodise, Problems, and New Suggestions*, In: *Materials Science*, 2004, 10, 1, 85–88
- [11] Soud, H., Babay, A., Sahnoun, M., Cheikrouhou, M., *A comparative quality optimisation between ring spun and slub yarns by using desirability function*, In: *Autex Research Journal*, 2008, 8, 3, 72–76
- [12] Jinlian, Hu., *Fabric testing*, Boston: Woodhead Publishing Limited, 2008, 90-224
- [13] *Fancy Yarn Market 2019 Global Industry Size, Revenue Growth Development, Business Opportunities, Future Trends, Top Key Players, Market Share and Global Analysis by Forecast to 2024*, 2019, Available at: <https://www.marketwatch.com/press-release/fancy-yarn-market-2019-global-industry-size-revenue-growth-development-business-opportunities-future-trends-top-key-players-market-share-and-global-analysis-by-forecast-to-2024-2019-04-26> [Accessed May 2019]
- [14] Saville, B.P., *Physical testing of textiles*, Boston: Woodhead Publishing Limited, 2002, 77–242
- [15] Subhash, B., Barrie Fraser, W., *Engineering Fundamentals of Ring Spinning/Twisting, Over-end Unwinding and two-for-one twisting in textile process*, Sydney: DEStech Publications, 2015, 21–31

- [16] ISO 2060 Textiles – Yarn From Packages – Determination Of Linear Density (Mass Per Unit Length) By The Skein Method, 1994
- [17] ISO 2 Textiles – Designation Of The Direction Of Twist In Yarns And Related Products, 1973
- [18] ISO 2061 Textiles – Determination Of Twist In Yarns – Direct Counting Method, 2015
- [19] SIST EN 12127 Textiles – Fabrics – Determination of mass per unit area using small samples, 1999
- [20] ISO 5084 Textiles – Determination of thickness of textiles and textile products, 1996
- [21] SIST EN 1049-2 Textiles – Woven fabrics – Construction – Methods of analysis – Part 2: Determination of number of threads per unit length, 1999
- [22] Welcome. ImageJ: An open platform for scientific image analysis, Available at: <https://imagej.net/Welcome> [Accessed May 2019]
- [23] ISO 9237 Textiles – Determination of permeability of fabrics to air, 2002
- [24] ASTM E96/E96M Textiles – Standard Test Methods for Water Vapor Transmission of Materials, 2014
- [25] ISO 12947-2 Textiles – Determination of the abrasion resistance of fabrics by the Martindale method – Part 2: Determination of specimen breakdown, 2016
- [26] ISO 5077 Textiles – Determination of dimensional change in washing and drying, 2009

Authors:

MIHA POZDEREC, DUNJA ŠAJN GORJANC

University of Ljubljana, Faculty of Natural Sciences and Engineering, Department of Textiles,
Graphic Arts and Design, 1000, Ljubljana, Slovenia
e-mail: pozderecmiha@gmail.com

Corresponding author:

DUNJA ŠAJN GORJANC
e-mail: dunja.sajn@ntf.uni-lj.si

Thermal and evaporative resistance measured in a vertically and a horizontally oriented air gap by Permetest skin model

DOI: 10.35530/IT.072.02.202038

FREDERICK FUNG
LUBOS HES

ROSHAN UNMAR
VLADIMIR BAJZIK

ABSTRACT – REZUMAT

Thermal and evaporative resistance measured in a vertically and a horizontally oriented air gap by Permetest skin model

This paper is a study of the correlation of the thermal resistance (R_{ct}) and the evaporative resistance (R_{et}) in vertically and horizontally oriented air gaps by using the portable Permetest skin model. Experiments were done in a climatic chamber; an isothermal condition for R_{et} tests and non-isothermal condition for R_{ct} tests. Foamed polyethylene air gap distance rings were prepared with a thickness of 2, 4 and 5 mm and their combinations to simulate the air gap distance from 0 to 16 mm which is more than the expected average gap in clothing systems. Test samples were woven fabric of 100 percent cotton, 100 percent polyester and their blends plus 100 percent of polypropylene, all have similar weight and structure. Results showed that with the increasing thickness of the air gap, R_{ct} increased in a polynomial trend and R_{et} in a linear proportional rate up to 12 mm then started to change due to the effect of free convection and the different properties of materials. The surprising positive observation is that results from the horizontally and vertically oriented air gaps are very similar, and most of the results from the vertical air gap are slightly lower than the results from the horizontal air gap in all materials.

Keywords: evaporative resistance, thermal resistance, Permetest skin model, vertical orientation, horizontal orientation, woven materials

Rezistența termică și rezistența la vapori de apă măsurate în straturi de aer orientate vertical și orizontal utilizând modelul de piele Permetest

Această lucrare este un studiu al corelației rezistenței termice (R_{ct}) și rezistenței la vapori de apă (R_{et}) în straturi de aer orientate vertical și orizontal, utilizând modelul portabil de piele Permetest. Experimentele au fost realizate într-o cameră climatică; în condiții izoterme pentru testele R_{et} și în condiții neizoterme pentru testele R_{ct} . Au fost pregătite inelele de distanță a stratului de aer din spuma de polietilenă cu o grosime de 2, 4 și 5 mm și combinațiile lor, pentru a simula grosimea stratului de aer de la 0 la 16 mm, care reprezintă mai mult decât grosimea medie în sistemele de îmbrăcăminte. Probele de testare au fost țesături din 100% bumbac, din 100% poliester și amestecurile lor plus din 100% polipropilenă, cu masă și structură similare. Rezultatele au arătat că, odată cu creșterea grosimii stratului de aer, R_{ct} a crescut într-o tendință polinomială, iar R_{et} într-o rată proporțională liniară de până la 12 mm, apoi a început să se modifice datorită influenței convecției libere și a diferitelor proprietăți ale materialelor textile. Observația pozitivă surprinzătoare este că rezultatele straturilor de aer orientate orizontal și vertical sunt foarte similare, iar rezultatele obținute în stratul de aer vertical sunt ușor mai scăzute decât cele obținute în stratul de aer orizontal pentru toate materialele textile.

Cuvinte-cheie: rezistență la vapori de apă, rezistență termică, model de piele Permetest, orientare verticală, orientare orizontală, țesături

INTRODUCTION

The air gap in clothing patternmaking is the wearing ease for ergonomic movement. It is everywhere around the wearer's body when he put on clothes to give him the freedom of movement and the thermal protection from the cold. Depending on the posture and ergonomic movement, the orientation of the air gap can be vertical, horizontal or at an angle.

Researches on the air gap related to clothing comfort in articles are either using thermal manikin (vertical air gap) or sweating guarded hot plate (horizontal air gap) so called skin model for tests; for examples, using skin model and thermal manikin for determination

of thermophysiological properties of different garments and materials like protective clothing, multi-layered garments, fabrics in the dry and wet state, footwear materials and for testing of clothing and fabric parameters [1–6] by using both apparatuses separately but not the comparison between them. Articles on vertical air gap related to clothing comfort are just a few; like Satusumoto et al. [7] compared quasi-clothing heat transfer between a vertical hot plate and the thermal manikin and concluded that “the vertical hot plate was more accurate than the thermal manikin because of the manikin could not reproduce the same setup of construction factors like precise air

space sizes". The research is interesting to use the vertical hot plate skin model for the test but only the schematic is shown in the article which is not clarified enough to understand how this apparatus operates in the experiment, and there is no mention of any recognized procedure standard is applied to the vertical skin model test. More, using space bars to keep the air gap distance even is not realistic since in real life clothing hanging on the body will be naturally influenced by the gravity, mechanical properties of the fabric, posture of the body, environmental conditions and other factors, which will influence the evenness of the air gap. Udayraj et al. [8] concluded that vertical air gap orientation has a higher protective value than horizontally oriented air gap in firefighter protective clothing. To understand more about the difference between the orientations of the air gap, an experiment was set up based on seven samples of woven materials, five air gap distances, vertical (V)/horizontal (H) orientation and R_{ct}/R_{ef} two types of test. However, when using a standard skin model in the vertical or horizontal orientation, serious problems arise because the testing surface area is usually large and the test involving the air gap is practically impossible. The textile material will drape (deform) around the centre area, the effective air gap gets reduced and the measurement suffers from a big error. Moreover, standard skin models as their large size in the vertical direction will cause an uneven distribution of water within the porous measuring plate of the device. Foreseeing these issues of standard skin models, a non-destructive Permetest skin model is chosen [9] which has a small diameter (8 cm) testing plate and a slightly curved surface to allow a very secure and close contact with materials even with air gap distance up to 16 mm and still keeps the material flat for testing. The portable size of Permetest also gives it the advantage of turning a horizontally oriented test into a vertically oriented test in a second. In real life, most of the clothing systems' air gaps are

vertically oriented, for example; sleeves, trousers, torso and so on that understanding the relationship of horizontal and vertical air gaps is crucial. More, the Permetest skin model enables the measurement of thermophysiological parameters of fabric systems consisting of multi-layered fabrics with air gaps between these fabrics. This solution can serve for experimental determination of thermal and evaporative resistance of real garment systems which involve gaps extending from 2 to 16 millimetres.

EXPERIMENT

Materials and methods

Seven samples of material were 100 percent cotton, 100 percent polyester and their blends plus 100 percent polypropylene as the counter sample. All samples were purchased from the same textile manufactory except 20% and 65% polyester/cotton blends were from one local retail store. Tested samples were woven material and had a similar square mass; their structures and their properties were tested by Fx3300; Moisture Management Tester; Planimeter to obtain the mean values which are shown in table 1. Air gap distance rings were used to create the preferred air gap sizes for the experiment and were made of 100 percent foamed polyethylene (with very low thermal conductivity reaching 0,035 W/m/K), relatively good conditions for the possible development of free convection between the sample and the simulated human skin (perforated hotplate) are maintained. The distant rings were prepared with a thickness of 2, 4 and 5 mm and their combinations to simulate the air gaps from 2 to 16 mm, which is more than for the expected average gap in clothing systems [10, 11]; details and usage are presented in table 2. To balance the thickness of the air gap distance created by the stack of rings and to maintain the smooth air current flew inside the wind channel, two types of air gap distance ring were cut: outer rings were put around the base of the hotplate for

Table 1

SEVEN TESTED MATERIALS AND THEIR PROPERTIES							
Tested materials	100% Cotton	80/20% Cotton/Polyester	70/30% Cotton/Polyester	50/50% Cotton/Polyester	35/65% Cotton/Polyester	100% Polyester	100% Polypropylene
Structure	Plain Weave	2/2 Basket Weave	Plain Weave	Plain Weave	Plain Weave	Plain Weave	2/2 Right Twill
Thickness (mm)	0.37	0.55	0.58	0.33	0.23	0.43	0.63
Square mass (g/m ²) non-compressed	154	225	226	159	102	156	252
Density warp/weft (per cm)	26/22	24/14	16/14	26/24	24/28	16/22	32/34
Air permeability (l/m ² /s)	277	234	241	272	523	564	74
Absorption rate top/bottom (%/s)	13/36	21/34	24/43	12/39	8/19	8/20	61/10
Porosity (%)	70	70	60	70	70	70	70
Drapability (%)	34	30	32	39	43	43	10

Table 2

DIMENSION OF AIR GAP DISTANCE RINGS FOR THE HOTPLATE AND THE LIFTING MECHANISM			
Air gap Distance Ring in 100% foamed polyethylene			
Thickness	2 mm	4 mm	5 mm
Number of ring on the hotplate	1	2	2
Diameter of outer circumference	8 cm	-	-
Diameter of inner circumference	6 cm	-	-
Number of ring for the hotplate lifting mechanism	1	1	2
Diameter of outer circumference	12 cm	-	-

counter thickness; inner rings were placed inside the wind tunnel on the hotplate to create the air gap distance. The outer ring was 12 cm in diameter on the outer circle and 8 cm on the inner circle, ring width is 2 cm for supporting the wider base of the measuring head. The inner ring for the hotplate was 8 cm in diameter on the outer circle and 6 cm on the inner circle, ring width is 1 cm. Each sample material was tested five times under 0, 4, 8, 12, 16 mm air gap distance and because of the compact size of the Permetest that allows the possibility to carry out the measurements of thermal and water vapor resistance both in horizontal and vertical positions of the simulated gaps, thus respecting the real conditions of wearing the clothing (figure 1).

Permetest skin model was chosen to use for the experiment for its portable size (540 × 230 × 130 mm, net weight 7 kg), versatility to change from a vertical to horizontal orientation in a second and the relatively short measuring time for the test. Permetest skin model is a commercial computer-controlled instrument respecting the modified ISO 11092 Standard. It consists of a box of electronics (with digital indicators and operating knobs), and on the right side of the box attached to an outstanding air tunnel. To the bottom of the tunnel, a measuring head is installed which contains a circular porous hotplate with an 8 cm diameter measuring area. The measuring head is connected to a lifting mechanism that allows the hotplate to move up and down when putting the sample onto the measuring hotplate. A small square heat power sensor is installed beneath the centre of the hotplate (figure 2).

Experiment

Air temperature in the climatic chamber was always $23 \pm 0.5^\circ\text{C}$ at 40–50% of relative humidity and the wind speed was set to 1.0 m/s. Evaporation resistance R_{et} was measured at these isothermal conditions and the driving force was only the difference between the saturated water vapour pressure in the measuring head of the instrument and the water vapour pressure in the instrument channel. Thermal resistance R_{ct} of the tested fabrics was measured at the same temperature and relative humidity of the air in the channel, but the temperature of the measuring head was increased to $33 \pm 0.1^\circ\text{C}$, thus providing the driving force of 10°C . It is important to mention that

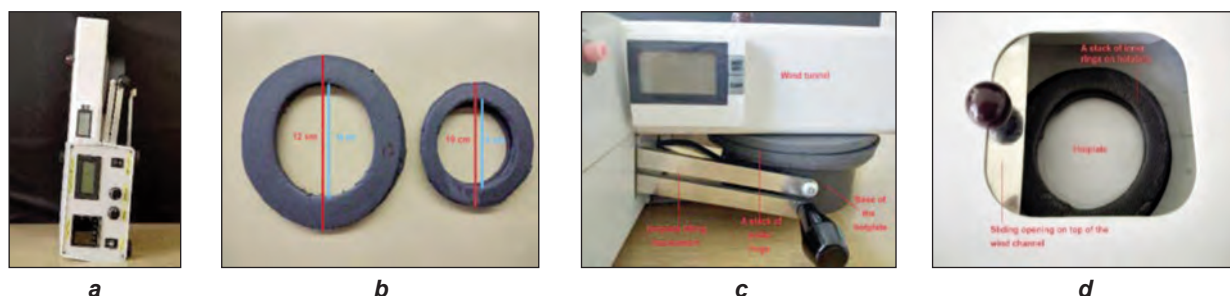


Fig. 1. a – Permetest skin model in the vertical orientation; b – sizes of outer and inner rings; c – placement of outer rings between the wind tunnel and the base of the hotplate; d – top view on inner rings placed inside the wind tunnel on the hotplate

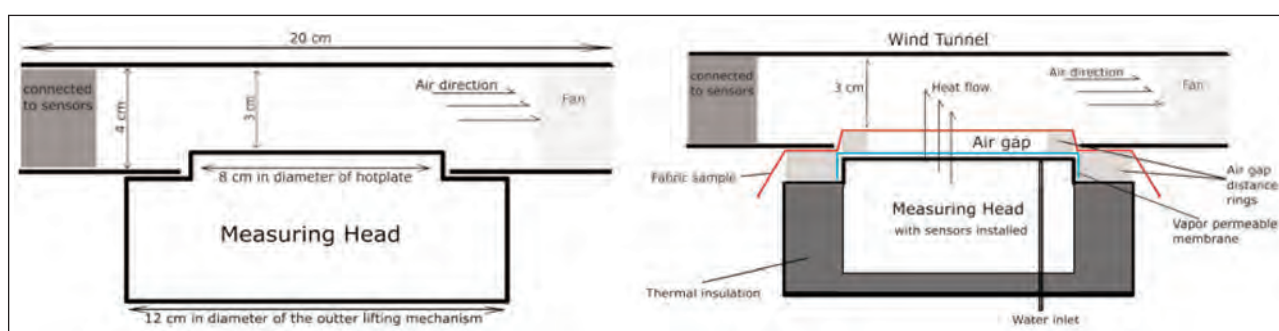


Fig. 2. Cross-section of Permetest showing the dimensions of the instrument and the assemble of the tested sample and the air gap distance rings on the hotplate

the special program of the instrument compensates all deviations of the air temperature and humidity against the conditions used in the determination of the R_{et} and R_{ct} parameters of a special hydrophobic calibration fabric in a standard skin model [12]. That is why in several European and African countries the Permetest instrument was accredited as satisfying the ISO 11092 standard.

In real life clothing systems, total thermal resistance (R_{ct}) unit in $mK \cdot m^2/W$ and total evaporative resistance (R_{et}) unit in $Pa \cdot m^2/W$, consist of resistances of the boundary layer ($(R_{ct})_{BL}$ or $(R_{et})_{BL}$), resistances of air gaps ($(R_{ct})_{AG}$ or $(R_{et})_{AG}$) and resistances of fabrics ($(R_{ct})_F$ or $(R_{et})_F$) and are expressed by the equations 1 and 2.

$$(R_{ct})_{Total} = (R_{ct})_{BL} + (R_{ct})_{AG} + (R_{ct})_F \quad (1)$$

$$(R_{et})_{Total} = (R_{et})_{BL} + (R_{et})_{AG} + (R_{et})_F \quad (2)$$

The air gaps are important because sometimes air gaps ($(R_{ct})_{AG}$ or $(R_{et})_{AG}$) may present more than half of the total thermal resistance (R_{ct}) or evaporative resistance (R_{et}) in a clothing system. When using the Permetest skin model, each measurement consists of two tests. The first test without the sample serves for the determination of thermal or evaporative resistance of the boundary layer, the result is hidden and will not be shown on the digital screen. The second test determines the resistance of the tested sample with the air gap, plus the boundary layer. Then from the second value, the instrument program will automatically deduce the value of the boundary layer and gives out the effective value of R_{ct} or R_{et} which is only including the values of air gap and fabric as expressed in equations 3 and 4.

$$(R_{ct})_{Total} - (R_{ct})_{BL} = (R_{ct})_{AG} + (R_{ct})_F \quad (3)$$

$$(R_{et})_{Total} - (R_{et})_{BL} = (R_{et})_{AG} + (R_{et})_F \quad (4)$$

When all the measurements of R_{ct} and R_{et} on air gaps covered by different fabrics are executed; then from the achieved experimental effective values ($(R_{ct})_{Eff}$ or $(R_{et})_{Eff}$) deduced the R_{ct} or R_{et} values of these fabrics ($(R_{ct})_F$ or $(R_{et})_F$), achieved for the air gap with the zero thickness, to get the $(R_{ct})_{AG}$ or $(R_{et})_{AG}$ parameters as in the equations 5 and 6.

$$(R_{ct})_{AG} = (R_{ct})_{Eff} - (R_{ct})_F \quad (5)$$

$$(R_{et})_{AG} = (R_{et})_{Eff} - (R_{et})_F \quad (6)$$

As follows from the common principles of heat and mass transfer, the R_{ctAG} and R_{etAG} resistances are proportional to the air gap thickness (h) and indirectly to the effective levels of air thermal conductivity (λ) in the unit of $W/mK \cdot m$ in equation 7 and diffusion coefficient (D_p) of water vapour in the air in the unit of $kg/Pa \cdot s \cdot m$ and equation 8. However, a detailed analysis of these effects would exceed the scope of this study.

$$R_{ctAG} = h / \lambda \quad (7)$$

$$R_{etAG} = h / D_p \quad (8)$$

RESULTS

Results are effective data (fabric and air gap only) which are divided into two groups: Thermal resistance group (R_{ct}) and Evaporative resistance group (R_{et}). Each group was analyzed by three statistic methods which were correlation coefficient (r), linear regression (R^2) and two-way ANOVA with replication.

The correlation coefficient of R_{ct} and R_{et} in vertical and horizontal orientations of seven materials

Results showed in table 3, the correlation coefficient r between the horizontal and vertical orientation of air gaps in R_{ct}/R_{et} tests of seven materials are very strong and positive: the lowest values ($r = 0.94$) are 80/20% and 70/30% cotton and polyester blend in R_{ct} tests, and other results from R_{ct}/R_{et} of all materials are close to 1.

R^2 – Regression between the vertically and the horizontally oriented Permetest results from seven materials

The R^2 of R_{ct} and R_{et} from all seven materials in table 4 are demonstrating the strong relationship between the vertical and horizontal air gap orientations that, when any changes in R_{ct} , it will be highly reflected by the changes in R_{et} or vice versa.

Two-way ANOVA with five repetitions results from vertically and horizontally oriented permetest from seven materials

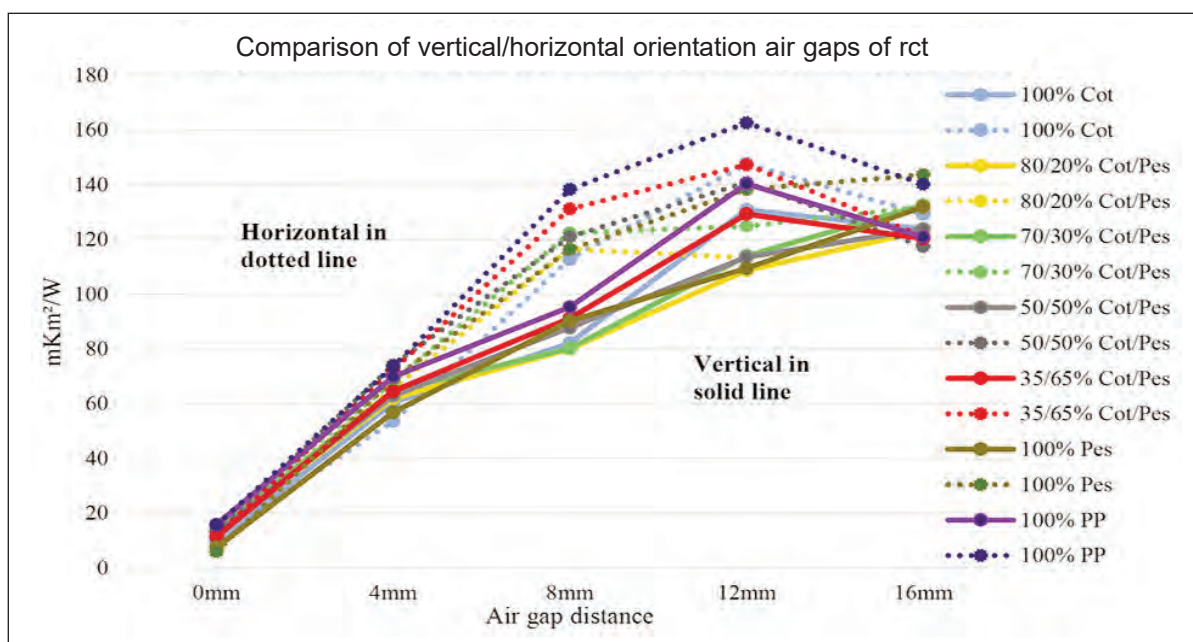
Results from R_{ct} and R_{et} of all seven materials show that the p-value < 0.01 which means there is a significant difference between the vertically and the horizontally oriented air gaps from the Permetest skin model. The reason is that even the experiments were done by using the same Permetest skin model, however; the vertical and horizontal orientation of the instrument was causing some difference in the resulting values. R_{ct} experiments were done under non-isothermal conditions, the driving force was the temperature difference. Hot air rises and cool air falls that happen naturally in the vertical air gap, but in the horizontal air gap; the air has to travel through a distance inside the wind channel before exiting. R_{et} experiments were done under isothermal condition, saturated vapour pressure is the driving force. In the horizontal air gap, water vapour molecules are concentrated at the bottom and rising to the top inside the wind channel. However, when it is in the vertical orientation, the rising water vapour molecules may escape through the fan that will cause the lower values of R_{et} and it also leads to the R_{ct}/R_{et} results that the vertically oriented resulting values seem always lower than the horizontally oriented values from the air gap distance 0–16 mm (figures 3, 4 and 5).

Table 3

CORRELATION COEFFICIENT RESULTS OF R _{ct} /R _{et} AND THE COMBINATIONS OF VERTICAL/HORIZONTAL ORIENTAL AIR GAP DISTANCES FROM 7 MATERIALS									
100% Cotton					80/20% Cotton/Polyester				
R _{ct}		R _{et}			R _{ct}		R _{et}		
H	V	H	V	H	V	H	V	H	V
H	1	H	1	H	1	H	1	H	1
V	0.97	V	0.96	V	1	V	0.94	V	0.98
70/30% Cotton/Polyester					50/50% Cotton/Polyester				
R _{ct}		R _{et}			R _{ct}		R _{et}		
H	V	H	V	H	V	H	V	H	V
H	1	H	1	H	1	H	1	H	1
V	0.94	V	0.98	V	1	V	0.95	V	0.97
35/65% Cotton/Polyester					100% Polyester				
R _{ct}		R _{et}			R _{ct}		R _{et}		
H	V	H	V	H	V	H	V	H	V
H	1	H	1	H	1	H	1	H	1
V	0.96	V	0.99	V	1	V	0.99	V	1.00
100% Polypropylene									
R _{ct}					R _{et}				
H		V			H		V		
H	1	V			H	1	V		
V	0.97	1			V	0.98	1		

Table 4

R ² RESULTS OF R _{ct} /R _{et} BETWEEN VERTICAL AND HORIZONTAL AIR GAPS OF SEVEN MATERIALS							
Vertical Vs Horizontal R ²	100% Cotton	80/20% Cotton/Polyester	70/30% Cotton/Polyester	50/50% Cotton/Polyester	35/65% Cotton/Polyester	100% Polyester	100% Polypropylene
R _{ct}	0.94	0.89	0.88	0.89	0.92	0.98	0.95
R _{et}	0.92	0.97	0.95	0.93	0.99	1	0.96

Fig. 3. Visual comparison of vertical and horizontal orientations of the air gap of R_{ct}

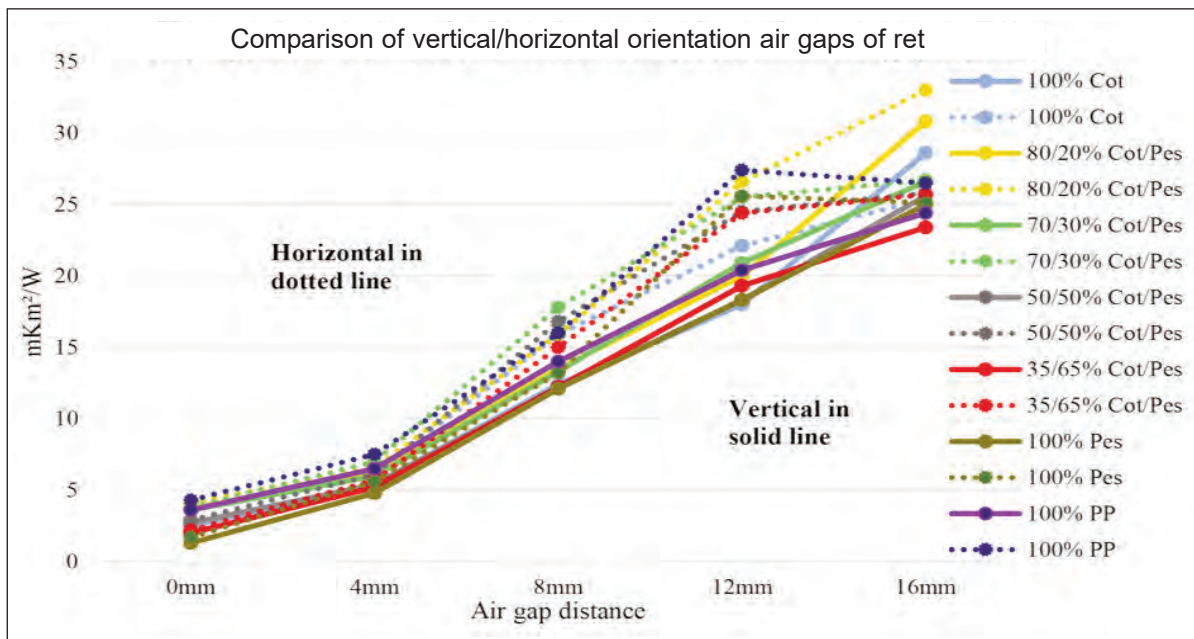


Fig. 4. Visual comparison of vertical and horizontal orientations of the air gap of R_{et}

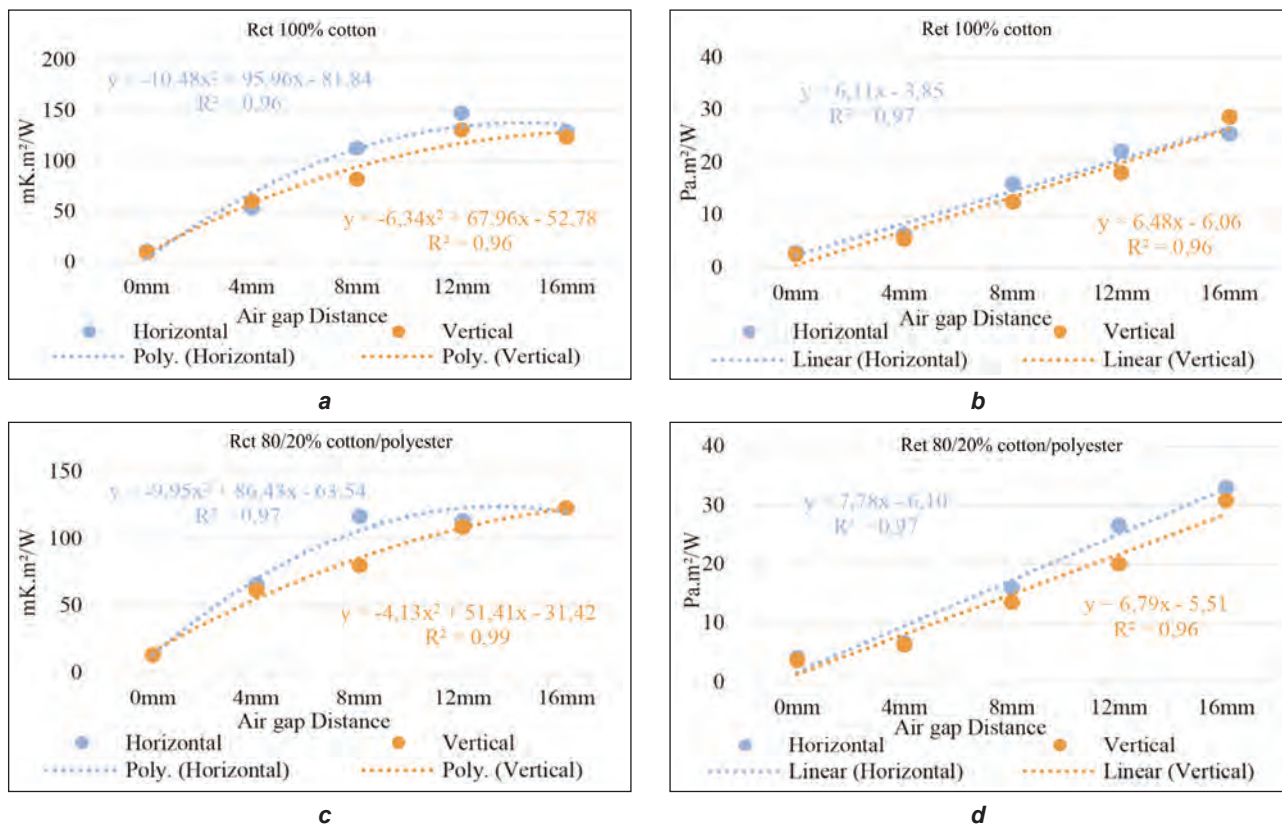


Fig. 5. Samples of the best-fit equation for R_{ct} and R_{et} for the vertical and horizontal air gap orientation of seven materials: a – R_{ct} 100% Cotton; b – R_{et} 100% Cotton; c – R_{ct} 80/20% Cotton/Polyester; d – R_{et} 80/20% Cotton/Polyester

CONCLUSIONS

Based on the results of thermal resistance (R_{ct}) and the evaporative resistance (R_{et}) of seven materials: 100% cotton, 100% polyester and their blends plus 100% polypropylene; that were tested in vertically and horizontally oriented air gaps of 0, 4, 8, 12, 16 mm combinations concluded that (based on the best fitting line, figure 5) increases in the air gap,

influences R_{ct} increasing in a polynomial proportional rate and R_{et} increases in a linear proportional rate. Both rise up to around 12 mm then the R_{ct} increases slower while R_{et} is still increasing at a linear rate with the air gap distance increases. Also, from the results of the correlation coefficient showed that all seven materials have a very strong and positive relationship between the horizontally and the vertically oriented

air gaps from 0 to 16 mm, and each of their values is almost 1 and their R^2 also close to 1 which indicates that for every unit increases in the vertical air gap, almost the same amount of unit will increase in the horizontal air gap. More, the two-way ANOVA showed that in the thermal and the evaporative resistance, both p-values of all seven materials $p < 0.01$ which means that there is a significant difference between the vertical and the horizontal orientations.

This is because when hot and less dense air rises in the vertically oriented air tunnel, it escapes faster than in the horizontal air tunnel where the air has to travel a small distance to the opening of fans, through it to escape. This may also cause the resulting values from the horizontally oriented air gap are a bit higher than the vertically oriented results in general of a single layer of fabric sample tests.

REFERENCES

- [1] Fukazawa, T., Lee, G., Matsuoka, T., Kano, K., Tochihara, Y., *Heat and Water Vapour Transfer of Protective Clothing Systems in a Cold Environment, Measured with a Newly Developed Sweating Thermal Manikin*, In: Eur. J. Appl. Physiol., 2004, 92, 645–648, <https://doi.org/10.1007/s00421-004-1124-3>
- [2] Reiners, P., Kyosev, Y., *About the Thermal Conductivity of Multi-layer Clothing*, Hochschule Niederrhein, University of Applied Sciences Faculty of Textile and Clothing Technology Mönchengladbach, Germany
- [3] Stoffberg, M.A., Hunter, L., Botha, A., *The Effect of Fabric Structural Parameters and Fiber Type on the Comfort-Related Properties of Commercial Apparel Fabrics*, In: Journal of Natural Fibers, 2015, 12, 6, 505-517, <https://doi.org/10.1080/15440478.2014.967370>
- [4] Bogusławska-Bączek, M., Hes, L., *Effective Water Vapour Permeability of Wet Wool Fabric and Blended Fabrics*, In: Fibres & Textiles in Eastern Europe, 2013, 21, 1, 97
- [5] Akalović, J., Skenderi, Z., Rogale, S.F., Zdraveva, E., *Water Vapor Permeability of Bovine Leather for Making Professional Footwear*, In: Leather & Footwear, 2018, 67, Original Scientific Paper UDC: 675.14.031.1.017.6:685.345
- [6] Gericke, A., Pol, J., *A Comparative Study of Regenerated Bamboo, Cotton and Viscose Rayon Fabrics, Part 1: Selected Comfort Properties*, In: Journal of Family Ecology and Consumer Science, 2010, 38
- [7] Satsumoto, Y., Ishikawa, K., Takeuchi, M., *Evaluating Quasi-Clothing Heat Transfer: A Comparison of the Vertical Hot Plate and the Thermal Manikin*, In: Textile Research Journal, 1997, 67, 7, 503–510, <https://doi.org/10.1177/004051759706700705>
- [8] Udayraj, Talukdar, P., Das, A., Alagirusamy, R., *Numerical Modeling of Heat Transfer and Fluid Motion in Air Gap between Clothing and Human Body: Effect of Air Gap Orientation and Body Movement*, In: International Journal of Heat and Mass Transfer, 2017, 108, 271–291, <https://doi.org/10.1016/j.ijheatmasstransfer.2016.12.016>
- [9] Hes, L., Araujo, M., *Simulation of the Effect of Air Gaps between the Skin and a Wet Fabric on Resulting Cooling Flow*, In: Textile Res. Journal, 2010, 80, 14, 1488–1497
- [10] Joseph, H., *Patternmaking for Fashion Design – Armstrong*, 2013, ISBN 9781292024813
- [11] Cole, J., *Patternmaking with Stretch Knit Fabrics*, 2016, ISBN 9781501305047
- [12] Per Me Test Manual 09 | Measuring Instrument | Calibration, Available at: <https://www.scribd.com/document/60715185/Per-Me-Test-Manual-09> [Accessed on November 24, 2020]
- [13] Richter, J., Staněk, K., *Measurements of Water Vapour Permeability – Tightness of Fibreglass Cups and Different Sealants and Comparison of μ -value of Gypsum Plaster Boards*, In: Procedia Engineering, 2016, 151, 277–283

Authors:

FREDERICK FUNG¹, LUBOS HES¹, ROSHAN UNMAR², VLADIMIR BAJZIK¹

¹Technical University of Liberec, Faculty of Textile Engineering, Evaluation Department, Liberec Czech Republic

²University of Mauritius, Reduit 80837, Mauritius

Corresponding author:

FREDERICK FUNG
e-mail: tassfashion@gmail.com

Measuring the effectiveness of signals approach in an early warning system for crises and its impact on textile industry: a case study for South-East Asia

DOI: 10.35530/IT.072.02.1780

MUHAMMAD ZAHID NAEEM
CRISTI SPULBAR
ABDULLAH EJAZ

RAMONA BIRAU
TIBERIU HORAȚIU GORUN
CRISTIAN REBEGEA

ABSTRACT – REZUMAT

Measuring the effectiveness of signals approach in an early warning system for crises and its impact on textile industry: a case study for South-East Asia

Following the work of Kaminsky, Lizondo, and Reinhart (1997), Signals Extraction Approach has been adopted with some extensions for South-East Asian (SEA) region to investigate the performance of the technique as an Early Warning System (EWS) during Asian Financial Crisis (AFC) and Global Financial Crisis (GFC). This approach is very original in the context of investigating the impact on the dynamics of the textile industry in South-East Asia. Two additional approaches namely Signal to Noise Balance (STNB) and Kuipers Score (KS) have also been utilised. Outcome suggested that variables performed well both during AFC and GFC. However, predictive ability of variables was less during GFC compared to the AFC indicating that there may exist some complex phenomenon which requires composite statistical methods.

Keywords: early warning system, financial crises, signals, signals to noise balance, Kuipers score, South-East Asia, textile industry

Măsurarea eficacității semnalelor într-un sistem de avertizare timpurie pentru crize financiare și impactul asupra industriei textile: studiu de caz pentru Asia de Sud-Est

În urma lucrărilor științifice publicate de către Kaminsky, Lizondo și Reinhart (1997), abordarea privind extragerea semnalelor a fost adoptată cu unele extensii pentru regiunea Asiei de Sud-Est. Scopul principal al acestui studiu empiric este acela de a investiga performanța tehnicii menționate anterior ca Sistem de avertizare timpurie (EWS) în timpul perioadei crizei financiare asiatice, precum și în timpul și crizei financiare globale. Această abordare este originală în contextul analizei impactului asupra dinamicii industriei textile din Asia de Sud-Est. Au fost, de asemenea, utilizate două metodologii econometrice suplimentare, și anume Raportul Semnal-Zgomot (STNB) și Scorul Kuipers (KS). Rezultatul a sugerat că variabilele au avut rezultate bune atât în timpul crizei financiare asiatice, cât și în perioada crizei financiare globale. Cu toate acestea, capacitatea predictivă a variabilelor a fost mai mică în timpul crizei financiare globale comparativ cu criza financiară asiatică, indicând că poate exista un fenomen complex care necesită metode statistice compozite.

Cuvinte cheie: Sistem de avertizare timpurie, crize financiare, semnale, Raportul Semnal-Zgomot, Scorul Kuipers, Asia de Sud-Est, industria textilă

INTRODUCTION

Financial crises have become relatively frequent events since the beginning of the 1980s [1] and are observed in three primary forms which are: debt crises, currency crises and banking crises (both latter crises are collectively called as twin crises). These events have contributed to an increased interest in the matters of the financial market's problems and its instability. Financial crises in general are not singular events and have been occurring from time to time and actually are the product of the errors committed in the financial sector. They are disconcerting events which at first seem impenetrable, but soon their damage undeniably grows and becomes more and more widespread. Moreover, there often lie obscure and complicated financial institutions and instruments, e.g. program trading during the 1987 stock market

crash, junk corporate bonds in the savings and loan debacle in the early 1990, the technology stock blast, and many more are examples of it. Realising the nature and severity of crises is really important because of the huge costs attached to them and therefore such issues are required to be forestalled. Early Warning Systems (EWS) offer a secure platform to study and anticipating such events with the aid of models/techniques to assist policy makers in determining how to react to the upcoming heat and as a solution, either crises can be prevented or at least their impact can be softened. Yildiz [2] suggested that nowadays to establish an effective chain of supply has become one of the prerequisites for the survival of the companies in an environment of increasing competition with the effect of the globalization. There are few techniques available to be

utilised as an EWS and from time to time there have been an increase in them because of the nature of crises and with the invention of new techniques and approximations. However, a technique which has been vastly used as an EWS: Signals extraction approach has its own significance when it comes to crisis assessment.

Sugihara [3] discussed important issues regarding the so-called “Asian textile complex” in the 1970s, in which Japan produced rayon yarn, Taiwan wove rayon cloth, and Hong Kong made the cloth into an apparel and exported the apparel to the US. Verret [4] highlighted relevant aspects regarding textile industries of lower-wage countries of South-East Asia. Frynas [5] suggested that in certain developing countries in Asia such as China, the Philippines and Indonesia, human rights standards are lower, and garment firms violate some of the key internationally accepted human rights.

As an initial step towards investigating the conduct of financial crises, this paper has applied signals approach to the selected region in order to investigate that how efficient and helpful is this approach in capturing the crises episodes during the Asian financial crisis and can global financial crisis also be captured? For this purpose, few additional steps have also been taken to make the study more concrete and reliable. This can assist in building consensus onto which tools should be utilised and what characteristics they should bear in order to better capture such disturbances. In the following section, some of the literature is reviewed based on crises and the tools which have been used frequently in the past. As a succeeding step, details are provided on methodology directing how to work on an early warning system which include; defining of objectives, country coverage, time period, the method used, the variables selected. The details about the main technique applied, which is signals approach, are discussed separately. Consequently, results, discussion and analysis section is provided, followed by the conclusion of the study.

LITERATURE REVIEW

Financial markets have always taken on new strategies to cope with the ambiguities and learnt many lessons from the history of crises. Although, the response of such markets was largely reactive instead of being proactive, but still markets learnt enough to avoid past mistakes to be replicated in the future. The learning procedure is rather complex, but nevertheless it can be resumed based on the model studies which are recognized to be generation models that capture the symptoms of distress ranging from recessions to exaggerated cycles in credit markets. Three of such major categories which have been talked about previously are reviewed here to some extent. Krugman’ model of currency crises which is well known to be as a first generation model of currency crises developed in the light of Latin American crises of the 1960s and 1970s suggested

that, under a specified exchange rate, domestic credit expansion in excess of money demand growth leads to gradual and persistent loss of reserve levels and which in fact can create a speculative attack on the currency [6]. If attacks occur, can immediately deplete the reserves and authorities can be forced to abandon the parity. This process usually ends with the attack because economic agents understand that fixed exchange rate will collapse ultimately and in case of attack, they can suffer a capital loss on their holdings of domestic money. Krugman’ work has been extensively expanded and these extensions have shown that speculative attacks would generally come before with a substantial currency appreciation and trade-balance deterioration [7]. Krugman’s idea gave a bunch of thought processes and understanding, however, it was not in accordance with the occurrence of later crises therefore it was declined because many of such crises happened without that explained phenomenon. As a consequence, some other explanation was taken of what was left unexplained in first generation models.

Currency crises in the European Monetary System (EMS) 1992–1993 and Mexican crisis of 1994–1995 gave rise to second generation models of crises. These models indicated that the decision to give up the parity may stem from the authorities’ concern about the development of other key economic variables. Ozkan and Sutherland [8] suggested a model which explained the aim of the authorities to maintain the exchange rate specified on the basis of certain values. It is founded on the benefits gained from maintaining the exchange rate fixed and deviations of output going beyond certain levels. Later models also suggested that crises may arise without any detectable change in the economic fundamentals as the contingent nature of economic policies can give rise to multiple equilibria and generate self-fulfilling crises; an idea very similar to Obstfeld work [9]. The Models also indicated that the market can achieve equilibrium with favourable as well as adverse economic fundamentals depending on the expectations of investors and their respective activities. The unexplained reasons for expectations shift required another model which could explain such reasons. The next generation of models for crises were developed after the 1994–1995 Tequila crises and the Asian financial crisis in 1997–1998. Aside from the recognition that the behaviour of market participants influences also the decisions of policymakers, the chief features of those mannequins are the integration of moral hazard, information asymmetries, herding and contagion effects [10]. These models were better as they could explain whatever the previous generation models were unable to explain, especially anything which was not based on fundamentals. Convincingly, these generation models describe the build-up of crises and the reasons for them on a timeline which gives a thorough understanding about the occurrences of crises with the passage of time.

With regards to crises and its estimation, it is always advantageous to have a common set of constituents,

which might cause those disruptions. Recent empirical research showed that although the causes of crises are not equal, however, they are connected to each other on a bigger chassis. Kaminsky [11] showed that most of the past crises were characterized by a large number of weak economic fundamentals, suggesting that it would be hard to characterise them as self-fulfilling crises. Thus, any new attempt is always an advantage in order to get early warning models to detect such weaknesses in advance to allow policymakers to consider appropriate steps well ahead to at least minimise the effects of such turbulences. There are a few techniques which have been applied in the past as early warning systems in crises and such techniques have been very helpful in anticipating crises. These applications in early warning systems follow some major methodological model approaches: i) the leading indicator approach, ii) the linear-dependent variable approach, iii) the discrete-dependent variable approach, iv) other approaches apart from the three aforementioned ones, such as artificial neural networks, latent variable threshold models, autoregressive conditional hazard models and Markov regime switching models [12]. The linear dependent variable approach has been used in many fields. In the field of financial economics, consider for example, Sachs, Tornell and Velasco [13] in which the survey analysed the Mexican crisis in 1994–95 and its aftermaths. The model used three explanatory variables using linear regression to determine whether a country is vulnerable to a crisis and applied a crisis index, which was a weighted average of the devaluation of the exchange rate against the USD and the percentage change in foreign exchange reserves. Explanatory variables included the percentage changes in i) the real depreciation of the exchange rate ii) the ratio of the size of the claims of the banking sector to the private sector to GDP which captures the resilience and weakness of the banking sector, and iii) the reserve adequacy measured as M2 to the stock of foreign exchange reserves. The linear regression captured even small alterations in the explanatory variables because of the steady dependent variable. Nevertheless, non-linearities were not captured. After analysing, the survey concluded that the combination of overvalued exchange rates, recent lending booms and low reserves relative to short-term commitments of the central bank are contributors to the crises and the current account data, capital flows and fiscal policies do not provide further explanatory power. A cornerstone study in the early warning framework of leading indicators approach was carried by Kaminsky, Lizondo and Reinhart [14]. In this approach, signals are extracted from a set of indicators and these signals are then channelled to generate information for crisis occurrence or non-occurrence. Although traditionally, this approach has been used to predict business cycle turning points, however, because of its easy to use features, this approach has been extensively applied in the EWS literature and is considered among the best EWS approaches

available. An overview of the performance of various crises models, which were tracked by the international monetary fund, provides some information regarding EWS and their probability of predicting the crises. For example, Berg, Borensztein and Pattillo [15] compared the models from the IMF's Developing Country Studies Division (DCSD) and Kaminsky, Lizondo and Reinhart [16], with three private sector models from Goldman Sachs, Credit Suisse, First Boston and Deutsche Bank, which have short signalling windows. Out of the five models, KLR [16] model performed best in the relevant out-of-sample test. The private sector models performed poor out-of sample, although, the in-sample performance of all the models was satisfactory.

OBJECTIVES OF THE CURRENT STUDY

The current study is dedicated to developing an early warning system with the help of existing signals approach along with some modifications in order to analyse the crises and also to test the model' performance based on the selected variables for the region under consideration. Although there have been criticism on signals approach, its advantages and easy to use features cannot be ignored given its ability to perform very well in situations where complex modelling is not preferred. The analysis of the study helps to determine the crisis probability and hence the predictive ability of the model.

RESEARCH METHODOLOGY

In order to carry out EWS, some basic steps need to be followed. These steps assist in investigating the crisis with convenience. Each step is therefore explained separately to provide better understanding about application of the EWS.

Defining the crisis

The first and most important step is to define the crisis as crisis can have many diverse definitions depending upon the way the research is being conducted. The current study has followed the definition of KLR [16] and a crisis is defined as a situation in which the Exchange Market Pressure Index (EMPI) is above its mean position by more than 1.5 standard deviation i.e.

$$Crisis = \begin{cases} 1 & \text{if } EMPI_t > \mu_{EMPI} + 1.5\sigma_{EMPI} \\ 0 & \text{otherwise} \end{cases} \quad (1)$$

Exchange market pressure index is calculated based on the changes in exchange rate, interest rates, and the level of reserves as defined by Kaminsky and Reinhart [16]. This index includes nominal exchange rate, interest rate and change in reserves. Negative changes in reserves and positive changes in exchange rate and high interest rate indicate that the pressure on the market is increasing [17]. In theory, the calculation of the index is done by focusing on each of the variable and observing their behaviour. EMPI can be generated using the following formula:

$$EMPI_t = \frac{\left(\frac{NER_t}{RES_t}\right) - \mu_{NER}}{\sigma_{NER}} \quad (2)$$

$$J_t = \left(\frac{dINT_t - dINT_{t-12}}{dINT_{t-12}}\right) \quad (3)$$

$$NER_t = \left(\frac{dNER_t - dNER_{t-12}}{dNER_{t-12}}\right) \quad (4)$$

$$RES_t = \left(\frac{dRES_t - dRES_{t-12}}{dRES_{t-12}}\right) \quad (5)$$

where d in the $dINT_t$, $dNER_t$ and $dRES_t$ represents the 12 months percentage change of the variables. In the above equations, J_t , NER_t and RES_t represents the nominal exchange rate, interest rate, and reserves respectively, whereas, μ and σ represents the respective mean and the standard deviation of the variables respectively. This unusual behaviour is identified for each indicator and a signal is issued when it reaches certain extreme levels, called threshold point, and cross that threshold. *EMPI* will generate a crisis signal when it surpasses the threshold point.

Choice of variables

A number of 26 variables in total were chosen in the study to cover different sectors. The variables are subject to the availability of data from the selected six countries, i.e. Indonesia, Malaysia, Philippines, Singapore, South-Korea, and Thailand. For all the variables (except variables based on rates and the ratio based variables), the indicator on a specific month is defined as a percentage change in the level of the variable with respect to its level 12 months ago. This transformation of data based on 12-months adjustment ensures that the data is comparable across countries and the variables are free from seasonal effects, stationary, and with well-defined moments.

Countries coverage

This study focused on selected ASEAN+ economies which covers Indonesia, Malaysia, Philippines, Singapore, South-Korea, and Thailand, with developed economies (Singapore and South-Korea) and Emerging Market Economies (EME) (Indonesia, Malaysia, Philippines, and Thailand). This combination of countries provides opportunity to examine the behaviour of crises for different economies. KLR [14] suggested that, in order to select a country for the analysis, it should have encountered at least one crisis in the past. All the selected countries fulfil this requirement.

Time period covered

The study used 222 observations from January 1993 to June 2012 from ASEAN countries. In the case of unavailability of monthly data, interpolated data from quarterly observations were taken. However, if no

observations were available for any variable, then these variables are not included in the calculations of signals as otherwise that variable will get penalized and it will affect the probability of overall results. Moreover, the data was divided into two different sample periods which are in-sample and out of sample. Data on which the model has been applied and results have been generated primarily is called in-sample data and it includes the time period from January-1993 to December-2003 which covers the Asian financial crisis. The remaining data has been used to test the performance of the model and is called out-of-sample data which includes the time period from January-2004 to June-2012 which covers the global financial crisis. In the study, there is a signalling horizon which is the time prior to the onset of a financial crisis, within which variables are supposed to give warnings for a possible occurrence of the crisis. The current study used a priori 15-months crisis window to generate and issue signals before the crisis could erupt so that policy makers and authorities have reasonable time to deal with the situations.

SIGNALLING EXTRACTION METHOD

Signal extraction method is a technique which captures the behaviour of the variable(s) on a certain scale and then each indicator is analysed separately within this univariate approach to observe a crisis. Therefore, the behaviour of each indicator is monitored to identify its deviation from its normal behaviour beyond a certain threshold. If an indicator crosses that threshold level, it is said to issue a signal. For better explanation, a signal can be defined and captured on a binary scale variable. Let "X" denotes a vector of the "n" indicators and " $X_{t,j}$ " denotes the value of indicator "j" in time period "t", then the signal " $S_{t,j}$ " of indicator "j" in time period "t" on a binary scale is defined as:

$$S_{t,j} = \begin{cases} 1 & \text{if } |X_{t,j}| > |X_t^j| \\ 0 & \text{otherwise} \end{cases} \quad (6)$$

where $|X_t^j|$ is the threshold value for that particular variable. If any variable crosses that threshold, it will provide a signal for a crisis.

Performance of indicators

To determine the performance of the indicators, the signalling window is defined as a time period within which each variable is expected to show its sensitivity for anticipating crisis. In this study, the period of 15 months is selected to capture the signalling prior to and after the known date of the crisis; a collective period of 30 months. The reason to keep a window of 15 months on both sides is to provide enough time for variables to respond because in some situations, certain variables are more affected later on or immediately after the crisis but not before. So, this period of 30 months, captures the behaviour of variables under all the possible circumstances. The behaviour of each variable can be explained properly with the help

of a crisis matrix to aid in understanding the terminologies applied in the approach. Table 1 represents the matrix in which, if an indicator issues a signal within the provided window preceding a crisis, this signal is considered as a good signal. However, if a signal is not followed by a crisis within a given time period, it is called a bad signal or noise. The ratio of false signals to good signals is called noise-to-signal ratio and it plays a vital role in calculating the goodness of fit of the model. However, if the variable does not signal any crisis followed by a crisis within the time period, it is taken as a missed signal and if no signal was issued followed by no crisis then it is taken as a good silence.

Table 1

CRISIS MATRIX		
	Crisis within 30-months	No Crisis within 30-months
Signal Issued	A	B
No Signal Issued	C	D

Note: A – Good Signal: Period in which an indicator issued a signal followed by the crisis within given time period; B – Bad Signal: Period in which an indicator issued a signal followed by no-crisis within a given time period; C – Missed Signal: Period in which an indicator issued no signal and crisis occurred within a given time period; D – Good Silence: Period in which no signal was issued, followed by no crisis.

Noise to signal ratio is defined as follows:

$$\text{Noise-signalratio}(\omega) = \text{NTSR} = \frac{B/B+D}{A/A+C} = \frac{\beta}{1-\alpha} \quad (7)$$

It is the ratio of bad signals to the months in which bad signals could have been issued to the good signals over the months in which good signals could have been issued. α and β are type-I and type-II errors respectively. The lower the NTSR is, the better is the performance of the variable as less and less false signals will be issued. However, in reality, NTSR is adjusted in a way where a low combination between type-I and type-II errors can be found.

$$\text{Type I error } (\alpha) = C / A+C \quad (8)$$

$$\text{Type II error } (\beta) = B / B+D \quad (9)$$

Where type-I error is the chance of missing a crisis when actually there is a crisis and type-II error is the chance of alarming false crisis when there is no crisis in reality. The variables with least value in terms of noise to signal ratio are considered as best and more accurate. Based on the information from NTSR, a decision criteria can be formulated on to which variables to keep and which ones to eliminate from the set of possible variables as noisy variables that are not preferable. In order to generate the optimal set of threshold for each indicator, KLR [14] method was followed and the thresholds were defined in relation to the percentiles of the distribution of observation of the indicators. Percentiles were chosen and an optimal level of percentile was selected according to one that minimizes the noise-to-signal ratio. Percentile

level chosen for each indicator is uniform across countries, but its corresponding country specific threshold values would most probably differ.

Signal to Noise Balance and Kuipers Score

In order to compare the performance of the variables, two additional comparative measures have also been considered which can suggest the goodness of fit for the approach. These measures are Signal to Noise Balance (STNB) firstly implemented by Rocha, Perrelli and Mulder [18] and Kuipers Score (KS) as applied in Berg, Candelon and Urbain [19]. Signal to noise balance is the difference between the percentage of pre-crisis periods called correctly and the percentage of false alarms.

$$\text{STNB} = (A - B) / (A + C) \quad (10)$$

The advantage of using this approach is that the relative number of classified incidents (crisis alarms “C”, tranquil periods “D”) does not affect the ratio as explained by Oka [20]. This ratio is easily interpretable in a sense that it can reach a maximum value of 100 when all pre-crisis periods are called correctly and no false alarms are issued. The difference is negative when model issues more false alarms than good alarms per pre-observed crisis periods. On the other hand, Kuipers Score is a difference between no. of good signals to the total good signals during crisis period and no. of bad signals to the total bad signals during that period respectively.

$$\text{KS} = A / (A + C) - B / (B + D) \quad (11)$$

KS is used as a goodness of fit for indicators as the indicators are considered to be performing better if their KS is towards positive side and a score of 1 will show that a variable indicator correctly called 100% of the crisis. These scores are meant to give an indication of the average closeness of the predicted probabilities and the observed realizations.

Composite indices

In order to collect all the compulsory information from the signalling extraction and other applied methods, the formulation of the composite index is required as with the help of it, time-varying probability of a crisis can be mapped. Not only this, but it can also combine the information obtained from the individual indicators in a meaningful way. It can be realized that the greater number of signals coming from different sectors of the economy, the higher the chances are there of financial collapse.

First index combines all the signals of a variable on a time scale, let “X” with the vector of “n” indicators. In any given period, there may be zero or “n” signals. Thus, the first composite indicator I_t^1 is defined as:

$$I_t^1 = \sum_{j=1}^n S_t^j \quad (12)$$

where, S_t^j is equal to one if $j(X_t^j)$ crosses the threshold in equation 6 during period “t” and zero otherwise. The number of signals, however, may not be a good composite leading indicator for crises as sometimes

the signals issued can be of very extreme level but it will still be taken as a normal signal. In other words, this statistic will not discriminate between the signals provided by a mild and an extreme unnatural behaviour of a variable. To stretch an example, consider an economic situation where an extreme real appreciation of the domestic currency may signal a future crisis with more accuracy than just a mild appreciation of it. To account for this information, two different thresholds for each variable are defined, X_m^j the mild threshold and X_e^j the extreme threshold. X_m^j will issue a mild signal in period t , $SM_t^j = 1$, when $|X_m^j| < |X_t^j| < |X_e^j|$ where m and e denotes mild and extreme time periods respectively, and extreme signal will be issued and $SE_t^j = 1$ when $|X_e^j| < |X_t^j|$. Thus the second composite indicator, I_t^2 accounts for the intensity of the signal for each univariate indicator. This indicator is defined as:

$$I_t^2 = \sum_{j=1}^n (SM_t^j + 2SE_t^j) \quad (13)$$

Indicator I_t^2 will have twice the weight of mild signal and hence this index can take the value between 0 and $2n$. It is noted in the literature [21] that the above two indicators cannot capture certain situations in the economy. For example, if output collapses in one month following instability, the stock market may sharply decline the following month, and foreign exchange reserves can be depleted within two months' time. Subsequently, exports may decline substantially within three months' time and so on. As a result, it cannot be asserted at the end of last month that the only sign of distress in the economy is the loss of export markets. Instead the overall problems are multiple. To capture the on-going deterioration in fundamentals, the index can be formulated as:

$$I_t^3 = \sum_{j=1}^n S_{t-s,t}^j \quad (14)$$

where $S_{t-s,t}^j$ is equal to one if the variable "j" signals at least once in period "t" or in the previous "s" periods and zero otherwise. In this model "s" is equal to eight as suggested in KLR [16].

In addition to the above three indices, the final composite index is defined as the weighted average of the signals of each indicator, where the inverse of noise-to-signal ratio has been applied as weights. Let ω_j denotes the noise-to-signal ratio of indicator "j", and then the composite index of "n" indicators is defined as:

$$I_t^4 = \sum_{j=1}^n \frac{1}{\omega_j} S_{t,j} \quad (15)$$

Development of all the indices is very crucial in order to generate all the possible information coming from the variables as these indices play a decisive role in realizing the performance of the variables.

EMPIRICAL RESULTS, DISCUSSION AND ANALYSIS

After transforming the data according to the chosen criteria mentioned earlier, the specific thresholds for variables have been generated based on the percentiles of the distribution of variables. After attempting some of the thresholds and observing their performance, 85th percentile is selected as the upper bound to signal distress and 15th percentile as the lower bound to signal a disruption. When it comes to index building and counting for extreme signals, 90th and 10th percentiles are taken as thresholds for respective variables. From these thresholds, the signals have been generated based on the signal extraction matrix given in table 1. From these signals, the good and bad signals have been calculated and noise-to-signal ratio is generated for each variable. Variables with NTSR more than 1 are of no significance and therefore dropped from the study in calculating the probability because variables with NTSR of more than 1 indicates that for a particular variable, there are more bad signals than good signals which is not preferable.

As the study has been carried out in two parts, one being in-sample and another as out-of-sample, the results are also discussed separately for each variable across the country. The performance of the indicators is observed in two parts. Firstly, the performance of the variables in each country is observed and spotted that which variables were significant for a particular country. Subsequently, each variable and its performance in the sample countries is realized which provides the information about the overall performance of a particular variable in the region. In this way, not only overall factors which affected the region can be realized, but country specific reasons can also be captured. Figure 1 highlights the in-sample performance of variables for the Malaysian economy as an example.

As can be seen in figure 1, almost all the variables signalled crisis during the crisis window as all the variables crossed the threshold levels and this performance is satisfactory. Complete details of the behaviour of the variables both in in-sample and out-of-sample is also observed and can be provided upon request as it is not added here due to space limitation. For the variables and their performance from the country' perspective in the in-sample study is provided as follows: for Indonesia; the variables which performed well with low NTSR are, stock price, M2/reserves, interest rate, reserves, non-bank liabilities, M2 multiplier, M2, and exports respectively. Variables which have low NTSR also performed well on the NTSB and Kuipers Score which is positive observation.

In case of Malaysia, the variables which performed well based on low NTSR are: Interest rate, inflation rate, exports, stock price, M2, output, reserves, and bank securities respectively. The variables which scored below one on NTSR, also scored better on

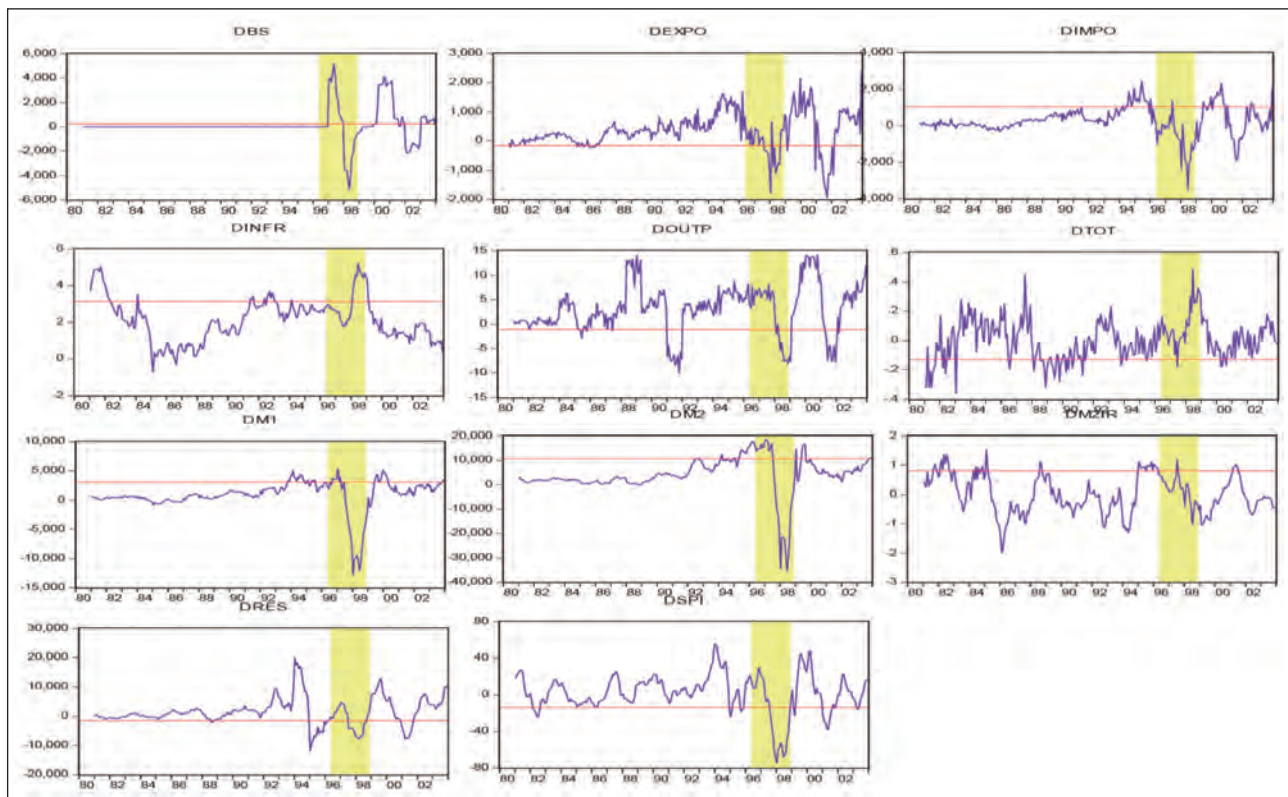


Fig. 1. Variables behaviour (Malaysia)

Kuipers Score. However, the STNB score of these variables is negative except interest rate and inflation rate, which indicates that other variables, generated on average, the more percentage of false alarms as compared to crisis periods correctly called. For the Philippines, the variables which were significant on low NTSR include: Inflation rate, DC/GDP, reserves, M2, M1, and budget deficit/surplus. Inflation rate performed well on both KS and STNB and it correctly called 38% of the crisis. Other variables have negative observation for STNB indicating that these variables generated more false alarms than good signals during crisis period. As of Singapore, indicators performed well during the crisis and variables which were positive during crisis based on low NTSR are: Exports, M2/reserves, exchange rate, reserves, M2 multiplier, Budget deficit/surplus, and terms of trade respectively. All these variables hint to the monetary issues which was the actual problem during that time period. The variable which showed highest significance is exports which correctly called (59%) of the crisis. Variables performance for South-Korea is best in the sample. Variables of significance include: Reserves, interest rate, CA/GDP, inflation rate, M2M, No. of Bankruptcies, output, DC/GDP, M2/reserves, non-Bank liabilities, exports, bank reserves/bank assets, and fiscal balance/GDP. Almost all the significant variables performed well both on STNB and KS with M2M correctly calling 70% and DC/GDP calling (57%) of the crisis. Results for Thailand indicated that variables which proved to be significant on low NTSR are reserves, exchange rate, stock price, inflation rate, exports, and fiscal balance/GDP respectively,

with stock price and international reserves performing very well on KS and STNB and correctly calling (84%) and (65%) of the crisis respectively. As Thailand was the major country to be hit by the crisis during AFC and the significance of exchange rate, reserves, and stock prices clearly explain the troubles for this country. Based on the NTSR across the region, i.e. South-East Asia (SEA), the variables which performed better and were highly significant include: reserves, exports, and inflation rate. Most of the variables showed partial significance, i.e. these variables were significant in some countries, but did not show signs of significance in other countries that include: Interest rate, exchange rate, M2/Reserves, M2 multiplier, DC/GDP, fiscal balance/GDP, stock prices, the level of output, and budget deficit/surplus. Remaining other variables proved to be insignificant for the sample countries which indicate that those variables either have nothing to specify during the crisis or had negligible effects (table 2).

The overall analysis of crisis indicators is significant based on all the applied approaches as can be seen from tables 3 and 4 as these variables were successful in highlighting the main symptoms of crisis during the AFC because most of the variables related to AFC were highly significant in the region (e.g. Reserves, exports). Therefore, the satisfactory performance of these variables during the AFC ensures that these variables can perform well within this approach and crises can be detected.

The sample countries were also affected during the GFC, hence, the testing sample (out-of-sample) results can be interesting in a way that whether the

Table 2

SIGNIFICANCE OF VARIABLES ON THE BASIS OF NTSR, NTSB, AND KS FOR THE WHOLE SAMPLE PERIOD												
Indicator	Indonesia		Malaysia		Philippines		Singapore		South Korea		Thailand	
	I.S	O.S	I.S	O.S	I.S	O.S	I.S	O.S	I.S	O.S	I.S	O.S
International reserves	XZ	XYZ	XZ	XYZ	XZ	XZ	XZ	XYZ	XYZ		XYZ	
Interest rate	XYZ		XYZ			XZ			XYZ	XYZ		
Exports	XZ	XYZ	XZ	XYZ		XYZ	XZ	XYZ	XZ	XYZ	XZ	XYZ
Imports		XYZ		XYZ				XYZ		XYZ		XYZ
Terms of trade		XYZ		XYZ		XYZ	XZ	XYZ				XYZ
Current account of GPD									XYZ			
M1				XYZ	XZ							XYZ
M2	XZ		XZ	XYZ	XZ							
M2/International reserves	XYZ			XYZ			XYZ		XYZ	XZ		
M2 multiplier	XYZ	XYZ					XZ		XYZ	XYZ		
Domestic credit/GDP		XYZ		XYZ	XZ			XYZ	XYZ			XYZ
Domestic real interest rate										XYZ		
Bank deposit				XYZ						XYZ		XYZ
Bank reserves/Bank assets		XYZ		XYZ				XZ	XZ			XYZ
Fiscal balance/GDP				XYZ					XZ	XYZ	XZ	
Output			XZ	XYZ					XYZ	XYZ		
Stock Price	XYZ	XYZ	XZ	XYZ							XYZ	
Oil Price		XZ										
Gold Price												
Inflation rate			XYZ	XYZ	XYZ	XYZ		XYZ	XYZ	XYZ	XYZ	XYZ
Budget deficit-surplus					XZ	XYZ	XZ	XYZ		XYZ		
Non-bank liabilities	XYZ	XZ				XYZ		XZ	XYZ			XYZ
Bank Securities			XZ	XYZ								
No. of bankruptcies												
Lending to Deposit Rate				XYZ		XYZ		XYZ		XYZ		XYZ
Fiscal balance/GDP												

Note: I.S. stands for in-sample and O.S. stands for out-sample data; X, Y, and Z represents the significance of the variables on the bases of NTSR, STNB, and KS.

Table 3

RESULTS OF SIGNALS APPROACH IN-SAMPLE						
Indicator	Threshold Value	Noise to Signal Ratio $[B/(B+D)]/[A/(A+C)]$	Signal to Noise Balance $[A/(A+C) - B/(A+C)]$	Kuipers Score $[A/(A+C) - B/(B+D)]$	Conditional Crisis Probability $A/(A+B)$	Percentage pre-crisis periods correctly identified $A/(A+C)$
INDONESIA						
International reserves	-708.270	0.306	-	0.1789	0.5	25.806
Interest rate	24.9	0.153	0.2581	0.4369	0.666	51.612
Exports	-352.5	0.982	-0.3548	0.0029	0.238	19.23
Imports	619.82	1.166	-0.5455	-0.0354	0.218	21.212
Terms of trade	-0.291	2.45	-0.2258	-0.0469	0.111	3.225
M1	3525.15	1.17	-0.7097	-0.0390	0.210	25.806
M2	16007.16	0.532	-0.3548	0.2264	0.365	48.387
M2/International reserves	4827.114	0.13	0.2581	0.3087	0.785	35.483
M2 multiplier	30193200	0.357	0.0645	0.1658	0.571	25.806
Fiscal balance/GDP	-	-	-0.5161	-0.1584	-	-
Stock Price	-17.35	0.092	0.2258	0.2929	0.769	32.258

Table 3 (continuation)

Indicator	Threshold Value	Noise to Signal Ratio [B/(B+D)]/[A/(A+C)]	Signal to Noise Balance [A/(A+C) - B/(A+C)]	Kuipers Score [A/(A+C) - B/(B+D)]	Conditional Crisis Probability A/(A+B)	Percentage pre-crisis periods correctly identified A/(A+C)
Inflation rate	5.977	1.091	-0.7419	-0.0265	0.219	29.032
Non-bank liabilities	389.7	0.306	0.0000	0.4471	0.5	64.516
Bank Securities	3300	11.66	-1.1935	-0.3440	0.025	3.225
MALAYSIA						
International reserves	-1513.672	0.548	-0.3548	0.2041	0.358	45.161
Interest rate	10.289	0.015	0.6129	0.6354	0.952	64.516
Exports	-165.344	0.330	-0.0323	0.2807	0.481	41.935
Imports	1042.636	12.277	-1.2581	-0.3638	0.024	3.225
Terms of trade	-0.13	2.14	-0.1935	-0.0370	0.071	3.225
M1	3006.84	1.091	-0.7419	-0.0265	0.219	29.032
M2	10688.45	0.4412	-0.2258	0.2884	0.410	51.612
M2/International reserves	0.798647	2.915	-0.5484	-0.1236	0.095	6.451
Fiscal balance/GDP	-0.022	3.069	-0.5806	-0.1335	0.05	6.451
Output	-1.017	0.450	-0.2308	0.1691	0.363	30.769
Stock Price	-13.906	0.429	-0.1935	0.2760	0.416	48.387
Inflation rate	3.129	0.1705	0.1290	0.2408	0.642	29.032
Bank securities	226.400	0.857	-0.7727	0.0777	0.292	54.545
PHILIPPINES						
International reserves	-789.012	0.345	-0.0323	0.1690	0.470	25.806
Exports	-51.642	6.75	-0.6774	-0.1856	0.043	3.225
Imports	418.969	1.168	-0.5405	-0.0455	0.25	27.027
Terms of trade	-0.13	6.138	-0.6129	-0.1658	0.047	3.225
M1	1067.901	0.908	-0.4324	0.0296	0.3	32.432
M2	4244.656	0.497	-0.1351	0.2444	0.439	48.648
M2 multiplier	0.730	1.402	-0.3514	-0.0543	0.217	13.513
Domestic credit/GDP	0.311	0.323	-0.0323	0.3925	0.486	58.064
Bank reserves/						
Bank assets	0.063	9.2	-0.9355	-0.2648	0.032	3.225
Fiscal balance/GDP	-0.015	4.143	-0.8065	-0.2028	0.068	6.451
Inflation rate	5.7	0.083	0.2973	0.3468	0.823	37.837
Budget deficit-surplus	-167.910	0.92	-0.4516	0.0179	0.25	22.580
Lending to Deposit Rate	1.726	11.68	-0.7838	-0.2888	0.032	2.702
SINGAPORE						
Nominal exchange rate	1.575	0.426	-0.2258	0.3331	0.418	58.064
International reserves	573.492	0.46	-0.1935	0.2089	0.4	38.709
Exports	-209.206	0.326	-0.0323	0.3478	0.484	51.612
Imports	-	-	-1.0270	-0.4000	-	-
Terms of trade	-0.06	0.997	-0.2903	0.0003	0.235	12.903
M1	1924.487	12.852	-0.8649	-0.3203	0.029	2.702
M2	8156.652	1.081	-0.4324	-0.0199	0.264	24.324
M2/International reserves	0.091	0.389	0.0000	0.0990	0.5	16.216
M2 multiplier	0.48	0.486	-0.0811	0.1664	0.444	32.432
Bank Deposits	-	-	-0.5806	-0.1782	-	-
Bank reserves/Bank assets	0.015464953	4.092	-1.1935	-0.2993	0.0698	9.677

Table 3 (continuation)

Indicator	Threshold Value	Noise to Signal Ratio [B/(B+D)]/ [A/(A+C)]	Signal to Noise Balance [A/(A+C) – B/(A+C)]	Kuipers Score [A/(A+C) – B/(B+D)]	Conditional Crisis Probability A/(A+B)	Percentage pre-crisis periods correctly identified A/(A+C)
Inflation Rate		-	-0.2162	-0.0842	-	-
Budget deficit-surplus	-494934.947	0.708	-0.5484	0.1223	0.302	41.935
Non-bank liabilities	2.921	3.7	-0.4595	-0.1459	0.095	5.405
Lending to Deposit Rate	3.411	3.738	-1.1622	-0.3701	0.094	13.513
SOUTH-KOREA						
International reserves	-505.4051163	0.021	0.4194	0.4417	0.933	45.161
Interest rate	11.5	0.024	0.4054	0.4219	0.941	43.243
Exports	-92.2	0.460	-0.1935	0.2089	0.4	38.709
Imports	-	-	-1.1081	-0.4316	-	-
Terms of trade	-0.13	2.608	-0.4839	-0.1038	0.105263158	6.451
Current account to GDP	-0.011	0.027	0.3226	0.3449	0.916	35.483
M1	6378.252	6.42	-0.8378	-0.2933	0.057	5.405
M2	39226.666	2.804	-0.8378	-0.2438	0.121	13.513
M2/International reserves	3.004	0.389	0.0000	0.0165	0.5	2.702
M2 multiplier	1.558	0.104	0.5135	0.6290	0.787	70.270
Domestic credit/GDP	0.240	0.333	0.0811	0.3781	0.538	56.756
Bank reserves/Bank assets	0.021	0.552	-0.2581	0.1444	0.357	32.258
Fiscal balance/GDP	-0.023	0.726	-0.0968	0.0529	0.4	19.354
Output	0.66	0.276	0.0323	0.2335	0.526	32.258
Inflation rate	4.422	0.064	0.2703	0.3033	0.857	32.432
Non-bank liabilities	680	0.389	0.0000	0.2145	0.5	35.135
Bank securities	26470	2.077	-0.7027	-0.1747	0.157	16.216
No. of bankruptcies	1202.4	0.122	0.3514	0.4504	0.76	51.351
Lending to Deposit Rate	1.305	4.414	-0.8378	-0.2768	0.081	8.108
THAILAND						
International reserves	-158.594	0.076	0.4839	0.5957	0.8	64.516
Exports	-51.885	0.3273	-0.0323	0.3255	0.483	48.387
Imports	844.256	13.631	-0.9189	-0.3414	0.027	2.702
Terms of Trade	-	-	-0.1935	-0.0594	-	-
Fiscal balance/GDP	-0.01	0.562	-0.1613	0.0846	0.352	19.354
Stock Price	-170.009	0.106	0.5484	0.7496	0.742	83.870
Inflation rate	3.852	0.1557	0.3243	0.4563	0.714285714	54.05405405
Budget deficit-surplus	-577.071	1.074	-0.4839	-0.0144	0.222	19.354
Lending to Deposit Rate	-	-	-1.1351	-0.4421	-	-

Table 4

RESULTS OF SIGNALS APPROACH OUT-SAMPLE						
Indicator	Threshold Value	Noise to Signal Ratio [B/(B+D)]/ [A/(A+C)]	Signal to Noise Balance [A/(A+C) – B/(A+C)]	Kuipers Score [A/(A+C) – B/(B+D)]	Conditional Crisis Probability A/(A+B)	Percentage pre-crisis periods correctly identified A/(A+C)
INDONESIA						
Nominal exchange rate	-	-	0.0968	0.1041	-	-
International reserves	-2618.57	0.45	0.0323	0.1241	0.538	22.580
Interest rate	15.188	2.838	-0.3548	-0.1186	0.133	6.451

Table 4 (continuation)

Indicator	Threshold Value	Noise to Signal Ratio [B/(B+D)]/[A/(A+C)]	Signal to Noise Balance [A/(A+C) – B/(A+C)]	Kuipers Score [A/(A+C) – B/(B+D)]	Conditional Crisis Probability A/(A+B)	Percentage pre-crisis periods correctly identified A/(A+C)
Exports	-2118.37	0.084	0.2581	0.2659	0.9	29.032
Imports	2736.565	0.147	0.2903	0.2750	0.909	32.258
Terms of trade	-0.21	0.354	0.0968	0.1041	0.714	16.129
M1	13069.22	3.1	-0.2581	-0.1355	0.166	6.451
M2	49858.53	3.1	-0.2581	-0.1355	0.166	6.451
M2/International reserves	7837.612	3.1	-0.2581	-0.1355	0.166	6.451
M2 multiplier	75568750	0.118	0.2581	0.2558	0.9	29.032
Domestic credit/GDP	-0.025289	0.1208	0.2414	0.2425	0.888	27.586
Domestic real interest rate	-	-	0.2903	0.2750	-	-
Bank reserves/Bank assets	0.041	0.267	0.1667	0.1952	0.727	26.666
Fiscal balance/GDP	-0.011	1.765	-0.1429	-0.0820	0.3	10.714
Stock Price	21.6288	0.0449	0.3871	0.4005	0.928	41.935
Oil Price	109.256	0.611	-0.0645	0.0627	0.416	16.129
Gold Price	-	-	0.2903	0.2750	-	-
Inflation rate	-	-	-0.0476	-0.0476	-	-
Non-bank liabilities	199	0.977	-0.0323	0.0044	0.4615	19.3548
Bank securities	7200	4.189	-0.2581	-0.2058	0.166	6.451
Lending to Deposit Rate	-	-	-0.0323	0.0044	-	-
MALAYSIA						
Nominal exchange rate	-	-	0.3871	0.4024	-	-
International reserves	-455.641	0.040	0.3871	0.4024	0.909	32.258
Interest rate	6.364	6.112	-0.4194	-0.1649	0.909	32.258
Exports	-2118.37	0.075	0.2903	0.2982	0.909	32.258
Imports	1904.575	0.375	0.1000	0.1250	0.909	32.258
Terms of trade	-0.05	0.62	0.0667	0.0632	0.909	32.258
M1	9856.47	0.1293	0.2333	0.2322	0.909	32.258
M2	44073.97	0.5172	0.1000	0.0966	0.909	32.258
M2/International reserves	0.490	0.555	0.0333	0.0296	0.909	32.258
M2 multiplier	1.551	1.586	-0.1304	-0.0765	0.909	32.258
Domestic credit/GDP	0.017	0.113	0.2609	0.2699	0.909	32.258
Bank deposits	44.489	0.107	0.2800	0.2855	0.888	32
Bank reserves/Bank assets	0.014	0.076	0.2800	0.2956	0.888	32
Fiscal balance/GDP	-0.015	0.517	0.1000	0.0966	0.909	32.258
Output	-8.854	0.115	0.2759	0.2746	0.909	32.25
Stock Price	-26.89	0.098	0.2581	0.2618	0.909	32.258
Inflation rate	4.401	0.295	0.1667	0.1644	0.909	32.258
Non-bank liabilities	-461.932	3.039	-0.2258	-0.1973	0.230	9.677
Bank securities	2058.104	0.273	0.2258	0.2343	0.769	32.258
No. of bankruptcies	-	-	0.2333	0.2322	-	-
Lending to Deposit Rate	2.271	0.189	0.0968	0.1046	0.909	32.258
PHILIPPINES						
Nominal exchange rate	43.151	0.654	-0.0968	0.0668	0.4	19.354
International reserves	2523.143	0.612	-0.0323	0.0749	0.9	31.034

Table 4 (continuation)

Indicator	Threshold Value	Noise to Signal Ratio [B/(B+D)]/[A/(A+C)]	Signal to Noise Balance [A/(A+C) - B/(A+C)]	Kuipers Score [A/(A+C) - B/(B+D)]	Conditional Crisis Probability A/(A+B)	Percentage pre-crisis periods correctly identified A/(A+C)
Interest rate	10.1366	6.112	-0.4194	-0.1649	0.066	3.225
Exports	-884.952	0.111	0.2759	0.2759	0.9	31.034
Imports	806.861	1.206	-0.0357	-0.0296	0.444	14.285
Terms of trade	-0.099	0.772	0.0357	0.0406	0.555	17.857
Current account to GDP	0.001	1.631	-0.1935	-0.0611	0.25	9.677
Domestic real interest rate	-	-	-0.3448	-0.2439	-	-
Bank reserves/Bank assets	-	-	-0.8889	-0.1951	-	-
Fiscal balance/GDP	-0.011	1.206	-0.0357	-0.0296	0.444	14.285
Inflation rate	8.794	0.111	0.2759	0.2759	0.9	31.034
Budget deficit-surplus	-404.679	0.125	0.2581	0.2826	0.833	32.258
Non-bank liabilities	15.530	0.452	0.1429	0.2085	0.615	38.095
Lending to Deposit Rate	2.683	0.070	0.3103	0.3204	0.909	34.482
SINGAPORE						
Nominal exchange rate	-	-	-0.4839	-0.2113	-	-
International reserves	4965	0.328	0.0968	0.1733	0.615	25.806
Exports	-5331.318	0.229	0.2258	0.2237	0.818	29.032
Imports	5574.6545	0.1149	0.2667	0.2655	0.9	30
Terms of trade	-0.09	0.258	0.2000	0.1977	0.8	26.666
M1	17484.858	6.557	-0.3226	-0.1793	0.083	3.225
M2	44440.492	6.557	-0.3226	-0.1793	0.083	3.225
M2/International reserves	0.111	2.068	-0.1000	-0.1069	0.333	10
M2 multiplier	0.932	2.068	-0.1000	-0.1069	0.333	10
Domestic credit/GDP	0.470	0.114	0.2667	0.2655	0.9	30
Domestic real interest rate	-	-	-0.3667	-0.2683	-	-
Bank deposits	78.895	1.293	-0.0333	-0.0391	0.444	13.333
Bank reserves/Bank assets	0.014	0.878	-0.0333	0.0203	0.454	16.666
Fiscal balance/GDP	-0.01	1.06	-0.0690	-0.0084	0.4	13.793
Inflation rate	6.676	0.114	0.2667	0.2655	0.9	30
Budget deficit-surplus	-1150643.906	0.198	0.1935	0.2326	0.75	29.032
Non-bank liabilities	3.419	0.840	-0.0968	0.0257	0.384	16.129
Lending to Deposit Rate	14.425	0.068	0.3226	0.3304	0.916	35.483
SOUTH-KOREA						
Nominal exchange rate	942.2	0.382	0.0323	0.1595	0.533333333	25.80645161
International reserves	2262	0.040	0.3871	0.4024	0.928	41.935
Interest rate	6.718	0.058	0.4194	0.4557	0.882	48.387
Exports	-5428.3	0.111	0.2581	0.2581	0.9	29.032
Imports	7291	0.1336	0.2258	0.2236	0.888888889	25.806
Terms of trade	-0.08	1.068	0.0000	-0.0089	0.5	12.903
M1	13814.407	7.724	-0.2500	-0.2401	0.111111111	3.571428571
M2	54319.986	7.724	-0.2500	-0.2401	0.111	3.571

Table 4 (continuation)

Indicator	Threshold Value	Noise to Signal Ratio [B/(B+D)]/[A/(A+C)]	Signal to Noise Balance [A/(A+C) – B/(A+C)]	Kuipers Score [A/(A+C) – B/(B+D)]	Conditional Crisis Probability A/(A+B)	Percentage pre-crisis periods correctly identified A/(A+C)
M2/International reserves	0.303	0.919	-0.0500	0.0121	0.428	15
M2 multiplier	0.487	0.772	0.0357	0.0406	0.555	17.857
Domestic credit/GDP	-	-	-0.3214	-0.3103	-	-
Domestic real interest rate	0.051	0.064	0.3448	0.3549	0.916	37.931
Bank deposits	-655.885	0.104	0.2581	0.2600	0.9	29.032
Bank reserves/Bank assets	0.022	6.146	-0.2857	-0.1838	0.1	3.571
Fiscal balance/GDP	-0.009	0.855	0.0323	0.0234	0.555	16.129
Output	-3.365	0.1293	0.2333	0.2322	0.888888889	26.666
Inflation rate	4.35	0.2152	0.2258	0.2278	0.818181818	29.032
Budget deficit-surplus	-23287.008	0.050	0.3548	0.3675	0.923	38.709
Bank securities	64000	6.305	-0.3548	-0.1711	0.076923077	3.225806452
No. of bankruptcies	318	2.906	-0.3226	-0.1230	0.142857143	6.451612903
Lending to Deposit Rate	1.572	0.265	0.1724	0.2027	0.727	27.586
THAILAND						
Nominal exchange rate	-	-	-0.4839	-0.2113	-	-
International reserves	-	-	-0.4516	-0.2373	-	-
Interest rate	-	-	-0.3871	-0.1690	-	-
Exports	-2252.676	0.104	0.2581	0.2600	0.9	29.032
Imports	2775.414	0.129	0.2333	0.2322	0.888	26.666
Terms of trade	-0.019	0.129	0.2333	0.2322	0.888	26.666
M1	4054.611	0.1111	0.2667	0.2667	0.9	30
M2	32112.103	8.275	-0.2333	-0.2425	0.111	3.333
M2/International reserves	-	-	-0.2667	-0.2759	-	-
M2 multiplier	-	-	-0.2667	-0.2759	-	-
Domestic credit/GDP	0.313	0.208	0.2258	0.2297	0.818	29.032
Domestic real interest rate	-	-	-0.1333	-0.0976	-	-
Bank deposits	-80.238	0.295	0.1667	0.1644	0.777	23.333
Bank reserves/Bank assets	0.039	0.589	0.0345	0.0849	0.545	20.689
Fiscal balance/GDP	-0.025	1.295	-0.0333	-0.0391	0.444	13.333
Inflation rate	5.961	0.5172	0.1000	0.0966	0.666666667	20
Non-bank liabilities	4500	0.1751	0.1935	0.2395	0.75	29.03225806
Bank securities	5127.976	6.83	-0.3871	-0.1881	0.071	3.225
Lending to Deposit Rate	5.5	0.068	0.2903	0.3004	0.909	32.258

same set of variables can be able to pick the turbulence during GFC or not? If the results are satisfactory, then it can be concluded that these indicators can perform well and be able to highlight the main causes of crisis and can show the transformation of the crises through their signalling performance under the signal extraction approach.

For out of sample studies, the variables' response has also been observed individually for all sample countries. For Indonesia, significant variables include stock price, exports, M2M, DC/GDP, imports, bank reserves/bank assets, terms of trade, reserves, oil prices, and non-bank liabilities respectively based on their low NTSR. These variables showed a positive

inverse relationship for STNB and KS to NTSR of variables. Maximum percentage of crisis called in the group is by stock price which is (40%). Indicators for Malaysia which have NTSR lower than one, include: Reserves, exports, bank reserves/bank assets, stock price, bank deposits, DC/GDP, output, M1, lending to deposit ratio, bank securities, inflation rate, imports, M2, fiscal balance/GDP, M2/reserves, and terms of trade respectively. Almost all the variables are positive on KS and STNB and maximum no. of crisis called correctly for a variable is (33%) which is on a lower side.

In case of the Philippines, lending/deposit ratio, exports, inflation rate, budget deficit/surplus, non-bank liabilities, reserves, exchange rate, and terms of trade are significant on lower NTSR respectively with lending to deposit ratio correctly calling (35%) of the crisis. Almost all significant variables performed well based on KS and STNB. For Singapore, the variables with significant low NTSR are: Lending/deposit ratio, imports, DC/GDP, inflation rate, budget deficit/surplus, exports, and terms of trade, reserves, non-bank liabilities, and bank reserves/bank assets respectively. Lending to deposit ratio scored maximum and correctly called (36%) of the crisis. All significant variables also performed considerably well on KS and STNB. Indicators for South-Korea, which are significant on the basis of low NTSR are reserves, budget deficit/surplus, interest rate, bank deposits, exports, output, imports, and inflation rate, lending to deposit ratio, exchange rate, M2M, fiscal balance/GDP, and M2/reserves respectively. Interest rate scored better in all areas including STNB and KS and called (49%) of the crisis correctly. In case of Thailand, lending to deposit ratio, exports, M1, imports, terms of trade, non-bank liabilities, DC/GDP, bank deposits, inflation rate, and bank reserves/bank assets are significant with low NTSR respectively. The variable which performed best is lending/deposit ratio and it correctly called (33%) of the crisis. Variables performance on STNB and KS is supportive as almost all significant variables scored positively on both KS and STNB.

Further, when the variables are analysed on the regional basis, the indicators which are significant include: reserves, exports, imports, DC/GDP, bank deposits, bank reserves/bank assets, inflation rate, budget deficit/surplus, non-bank liabilities, lending/deposit rate. Among the variables which were significant for some countries but did not provide significant information for other countries include: Exchange rate, terms of trade, M2/reserves, M2 multiplier, fiscal balance/GDP, output levels, and stock prices. All other variables were mostly insignificant in providing any information with regards to the crisis. In the analysis, variables which are of more significant to notice include DC/GDP, bank deposits, bank reserves/bank assets, and lending to deposit rate ratios. All these variables clearly indicate the banking sector problems which relate to the GFC crisis.

The overall test analysis indicated that variables performance remained significant in out-of-sample study as can be realized from tables 3 and 4. However, the crisis probability to correctly call them was on the lower side which suggested that although this approach can be helpful in understanding and analysing the market situations, it cannot be taken as a sole method to indicate a crisis as asserted by Berg et al. [15]. Another interesting observation to notice is that both KS and STNB proved to be complementary approaches because almost all the variables which were significant based on NTSR also scored positive in both KS and STNB as highlighted in tables 3 and 4.

CONCLUSIONS

As previously asserted, the purpose of the current study is to contribute to the existing literature on financial crises EWS in a way to improve the methods of mapping the turmoil in the financial markets using already existing signals approach with some extension which include, use of broad definition of crisis, different signalling window, additional complementary approaches alongside NTSR and extended dataset. Current study developed an early warning system to identify that which variables tend to indicate that a country might be vulnerable to a financial crisis. In particular, it extended a developed model of KLR [16] and evaluated it based on in-sample performance of the indicators and also the test sample probabilities of crisis. The model proved to be helpful in identifying the turmoil, and this assessment of vulnerabilities can be applied to any individual country or a group of countries over the time.

The performance was mixed for the early warning system as the model generated many false alarms and various indicators did not provide the synthetic vulnerability of a country. However, the model was able to correctly point out the vulnerabilities during crisis periods for different countries such as South-Korea, Malaysia and Thailand. Selected threshold level seems to be playing a major role in signalling false alarms as the number of false alarms were mostly dependent on the threshold used. The lower the threshold chosen, the more signals the model will produce and can generate more noise. However, surging the threshold level reduces the number of wrong signals, but at the expense of missing crises signals. Therefore, it is always very critical to find and apply threshold where the model can produce the least amount of false alarms with optimum crisis signals. The threshold is also very sensitive, as crises are very devastating to the economy and if the model missed the crisis, it can directly cost the economy. However, on the other hand, if the model produced false alarms and indicates an upcoming crisis whereby policy makers take an action based on the model, then it can also cost the economy indirectly as the measures taken by policy makers can be self-destroyer in the absence of a crisis. Moreover, policy makers always have to keep in mind the accuracy of such a system as it is highly likely to be imperfect.

Instead, the goal should be to improve the market performance and the model should be able to address as many shortcomings as possible to help policy-makers in their decision making.

We investigated the effectiveness of signals approach in an early warning system for crises and its impact on textile industry in South-East Asia. Moreover, the dynamics of the textile industry has a significant contribution in achieving a sustainable level of economic growth. Nevertheless, many general conclusions can be drawn from the study: Crises by their nature are uncertain and therefore their exact timing cannot be predicted. Most variables provided early indications but there were many false alarms as well. Among the variables which performed very well during crises include: Reserves, exports, inflation rate, DC/GDP, exchange rate, stock prices, and the level of output. Many of the other variables were significant during one crisis, but did not show any significance during another crisis, which can be explained on the basis that both crises were different in their happenings as AFC was more of currency related crisis, however, GFC was related to banking sector problems and some of the variables which directly relates to banking sector were highly significant during latter crisis that include lending/deposit ratio and bank reserves/bank assets.

For the ability to show the disruptions, the model performance was satisfactory and it did identify the vulnerabilities present within the countries. However, it performed poorly at predicting the crises which is a weak point in the study and suggests refining further the early warning system which might be useful to incorporate additional explanatory variables or to find alternative statistical methods. As a consequence of this a future study can be conducted which include statistical approach as a complementary to this non-parametric approach to be employed as an early warning system to improve the scheme in general even if both approaches can be utilized in tandem to obtain robust solutions with more satisfaction, reliability, and accuracy.

On the other hand, Batool et al. [22] suggested that COVID-19 pandemic outbreak affected the entire economic system. Implicitly, a future direction of research could follow the impact of the Covid-19 crisis on the textile industry in the case of emerging countries. Mehdiabadi et al. [23] highlighted a relevant aspect such as the fact that global economy is constantly changing, which is the main reason for innovation and technological development to contribute in order to achieve sustainable development.

REFERENCES

- [1] Tomczyńska, M., *Early Indicators of Currency Crises*, In: Review of. Center for Social and Economic Research-Case, 2000, 208
- [2] Yildiz, A., *Interval type 2-fuzzy TOPSIS and fuzzy TOPSIS method in supplier selection in garment industry*, In: *Industria Textila*, 2016, 67, 5, 322–332
- [3] Sugihara, K., *Multiple Paths to Industrialization: A Global Context of the Rise of Emerging States*, In: Otsuka K., Sugihara K. (eds) *Paths to the Emerging State in Asia and Africa. Emerging-Economy State and International Policy Studies*. Springer, Singapore, 2019
- [4] Verret, R., *Technological Developments in the Textile Industry*, In: *The Journal of The Textile Institute*, 1991, 82, 2, 129–136, <https://doi.org/10.1080/00405009508658752>
- [5] Frynas, J.G., *The Transnational Garment Industry in South and South-East Asia: a Focus on Labor Rights*, In: Frynas J.G., Pegg S. (eds) *Transnational Corporations and Human Rights*, Palgrave Macmillan, London, 2003
- [6] Krugman, P., *Vehicle Currencies and the Structure of International Exchange*, In: *Journal of Money Credit and Banking*, 1980, 513–526
- [7] Agenor, P.R., Bhandari, J.S., Flood, R.P., *Speculative Attacks and Models of Balance of Payments Crises*, In: Working Paper – International Monetary Fund, 1992, 357–394
- [8] Ozkan, F.G., Sutherland, A., *Policy Measures to Avoid a Currency Crisis*, In: *Economic Journal*, Royal Economic Society, 1995, 510–519
- [9] Obstfeld, M., *Rational and Self-Fulfilling Balance of Payments Crises*, In: *The American Economic Review*, 1986, 72–81
- [10] McKinnon, R., Pill, I., *Credible Economic Liberalizations and Overborrowing*, In: *American Economic Review*, 1997, 1, 89–193
- [11] Kaminsky, G. L., *Varieties of Currency Crises*, In: Working Paper – NBER, 2003, 1–31
- [12] Percic, S., Apostoaie, C., Cocriș, V., *Early Warning System for Financial Crisis – A Critical Approach*, In: Working Paper CES, 2013, 77–88
- [13] Sachs, J., Tornell, A., Velasco, A., *Financial Crises in Emerging Markets: The Lessons from 1995*, In: Working paper – NBER, 1996, 1–65
- [14] Kaminsky, G., Lizondo, S., Reinhart, C., *Leading Indicators of Currency Crises*, In: Staff Papers – International Monetary Fund, 1997, 48–64
- [15] Berg, A., Borensztein, E., Pattillo, C., *Assessing Early Warning Systems: How have they Worked in Practice?*, In: Working Paper – International Monetary Fund, 2004, 1–45
- [16] Kaminsky, G., Lizondo, S., Reinhart, C., *The Twin Crises: The Causes of Banking and Balance-of-Payments Problems*, In: *American Economic Review*, 1999, 473–500

- [17] Berg, A., Pattillo, C., *Are Currency Crises Predictable? A test*, In: Staff Papers: International Monetary Fund, 1999, 1–32
- [18] Rocha, M.D., Perrelli, R., Mulder, C.B., *The Role of Corporate, Legal and Macroeconomic Balance Sheet Indicators in Crisis Detection and Prevention*, In: Working Paper – International Monetary Fund, 2002, 1–27
- [19] Berg, J.V., Candelon, B., Urbain, J., *A cautious note on the use of panel models to predict financial crises*, In: Economic Letters, 2008, 80–83
- [20] Oka, C., *Anticipating Arrears to the IMF: Early Warning Systems*, In: Working Paper – International Monetary Fund, 2003, 1–34
- [21] Reinhart, C., Kaminsky, G., *The Twin Crises: The Causes of Banking and Balance of Payment Problems*, In: The American Economic Review, 1999, 473–500
- [22] Batool, M., Ghulam, H., Hayat, M.A., Naeem, M.Z., Ejaz, A., Imran, Z.A., Spulbar, C., Birau, R., Gorun, T.H., *How COVID-19 has shaken the sharing economy? An analysis using Google trends data*, In: Economic Research-Ekonomska Istraživanja, 2020, <https://doi.org/10.1080/1331677X.2020.1863830>
- [23] Mehdiabadi, A., Tabatabeinasab, M., Spulbar, C., Karbassi Yazdi, A., Birau, R., *Are We Ready for the Challenge of Banks 4.0? Designing a Roadmap for Banking Systems in Industry 4.0.*, In: International Journal of Financial Studies, Special Issue “The Financial Industry 4.0”, 2020, 8, 2, 32

Authors:

MUHAMMAD ZAHID NAEEM¹, CRISTI SPULBAR², ABDULLAH EJAZ³,
RAMONA BIRAU⁴, TIBERIU HORAȚIU GORUN⁵, CRISTIAN REBEGEA⁶

¹School of Business and Economics, University of Brunei Darussalam, Darussalam, Brunei
e-mail: drmznaeem@gmail.com

²University of Craiova, Faculty of Economics and Business Administration, Craiova, Romania
e-mail: cristi_spulbar@yahoo.com

³Bredin College of Business and Health Care, Edmonton, AB, Canada
e-mail: ejazabdullah03@gmail.com

⁴Faculty of Education Science, Law and Public Administration, Constantin Brancusi University of Targu Jiu, Romania

⁵Constantin Brancusi University of Targu Jiu, Faculty of Education Science, Law and Public Administration, Romania
e-mail: gorunhoratiu@yahoo.com

⁶University of Craiova, Faculty of Economics and Business Administration, Craiova, Romania
e-mail: cristian.rebegea@brd.ro

Corresponding author:

RAMONA BIRAU
e-mail: ramona.f.birau@gmail.com

Analysis and forecast of textile industry technology innovation capability in China

DOI: 10.35530/IT.072.02.1759

QIAN XU
HUA CHENG

YABIN YU

ABSTRACT – REZUMAT

Analysis and forecast of textile industry technology innovation capability in China

The textile industry of China has been facing with fierce competition and transformational pressures. It is of great significance to study the evolution of textile industry's technological progress and to predict the trends. The study analyses the technological innovation ability of China's textile industry based on the data of 270,145 patent applications from 1987 to 2016. At the same time, the Logistic model is used to forecast the technology innovation capability of China's textile industry. The study found out: the number of Chinese textile patent applications is on a upward trend; enterprises and universities are the most important patentee; the regional distribution of textile technology innovation is uneven; the number of patent applications in the southeast coastal areas is the largest; the distribution of the IPC is also uneven, D06 (fabric treatment) having the largest number of patent applications and the fastest growth rate; China's textile industry technology innovation has entered a maturity stage in 2018, and will enter the recession stage after 2027 based on the Logistic model.

Keywords: *textile industry, patent analysis, technology life cycle, S-shaped Growth Curvetrend forecast*

Analiza și prognoza capacității de inovare tehnologică a industriei textile din China

Industria textilă din China s-a confruntat cu o concurență acerbă și cu presiuni de transformare. Studiarea evoluției progresului tehnologic al industriei textile și prognoza tendințelor au o mare semnificație. Studiul analizează capacitatea de inovare tehnologică a industriei textile din China pe baza datelor a 270.145 de cereri de brevet din perioada 1987–2016. În același timp, modelul logistic este utilizat pentru a prognoza capacitatea de inovare tehnologică a industriei textile din China. Studiul a concluzionat următoarele: numărul cererilor de brevet din industria textilă din China înregistrează o tendință ascendentă; întreprinderile și universitățile dețin cele mai multe brevete; distribuția regională a inovației tehnologice textile este inegală; numărul cererilor de brevet în zonele de coastă sud-estice este cel mai mare; distribuția IPC este, de asemenea, inegală, D06 (tratarea țesăturii) având cel mai mare număr de cereri de brevet și cea mai rapidă rată de creștere; inovația tehnologică în industria textilă din Chinei a intrat într-o etapă de maturitate în 2018 și va intra în etapa de recesiune după 2027 pe baza modelului logistic.

Cuvinte-cheie: *industria textilă, analiza brevetelor, ciclul de viață al tehnologiei, prognoza Curvetrend de creștere în formă de S*

INTRODUCTION

The textile industry of China has made great achievements since the late 1970s. From 2006 to 2016, the annual growth rate of industrial added value of industrial enterprises above designated size was 9.48%, and the average annual compound growth rate of total profit was 15.15%. According to the “13th Five-Year Plan for Textile Industry” issued by the Ministry of Industry and Information Technology in September 2016, the proportion of China's total textile exports to the world has increased from 10.42% in 2000 to 38.60% in 2015. At present, as China's economy shifts from a high-speed growth stage to a high-quality development stage, the textile industry has entered a new stage of comprehensively promoting high-quality development, and technological innovation is undoubtedly an important guarantee for high-quality development.

Technological innovations are critical to the development of technology strategies and policies, tracking the historical process of technological innovation and predicting future trends [1]. Patents are an effective indicator to measure technological innovation. The amount of patent applications can directly reflect the R&D strength and output level of the innovative subject [2]. Patent analysis is the most accurate method to predict short- and medium-term technological developments [3]. Analysis of patent-related historical information such as regional distribution and field distribution can accurately predict the main competitors, as well as the development of core technologies at various stages [4]. More and more industrial technology researches are based on patents [5, 6]. Nicolas Grandjean believes that patent information analysis can provide information on industrial technology activities, research and development trends, emerging fields, and cooperation [7]. Alan Porter and

Nils Newman mined patent texts to study industrial technology innovation models [8]. Luan analysed global electric vehicle patents and found that electric vehicle patent high-yield institutions and hot technology fields [9].

The development of industrial technology is similar to the evolution process of life from birth, growth, maturity, decline, and death. It will experience different characteristics in different stage [10]. An analysis of the stage of the technology life cycle (TLC) can accelerate the forward-looking layout of industrial technology R&D and can also promote the sustainable development of the textile industry. A commonly used method to evaluate the TLC is the S-shaped growth curve [11]. Huang [1] used the S-curve method to analyse the development trajectory of 3D printing technology. It believed that 3D printing technology began to sprout in 1985–2004, and began to enter the growth stage in 2005, and predicted to enter maturity in 2016. Boretos [12] uses the S-curve to predict mobile phone trends. Chen et al. [13] compared the life cycle and development potential of the two technical fields of hydrogen energy and fuel cell, and predicted its development prospects. Daim et al. [14] also used S-curve to predict the development of three emerging technologies in fuel cell, food safety and optical storage. Liu and Wang [15] used S-curve and Logistic models to predict the trend of Japanese biped robot walking technology, and believed that the technology will continue to develop in Japan for decades.

In summary, the current researches on technical capabilities and technology trends are mostly focused on the micro-level technical field, while there are fewer studies on patent analysis and prediction on the industrial level. Besides, the technology innovation research based on patent analysis of textile industry is relatively lacking. With the new round of textile technology revolution, more precise research is needed on textile technology capabilities and technological innovation trends. The study analyses the patents to measures the trend, the regional distribution of applications and the technical fields. At the same time we use the method of S-Shaped Growth Curve to predict the trend of China's textile industry.

DATA SOURCE

The data comes from the textile industry patent information service platform (<http://chinaip.sipo.gov.cn>). According to the International Patent Classification, the technical fields related to patents are divided into eight parts: A, B, C, D, E, F, G, and H. Textile technology, together with papermaking technology, is in the Part D, including D01-D07, D21 (paper and other small categories). D01-D06 represents the aspects of raw materials, spinning, weaving, knitting, sewing and fabric treatment; D07 is the rope technology. Compared with the patent application, the information of patents grants may be delayed due to the time. In different years, there is a deficiency for patent grants to reflect the trend of technological innovation

[13]. Therefore, the research selects the data of patent application. D01-D06 was selected to retrieve the invention patents and utility model patents applied between 1987 and 2016. The search term used is: IPC=D01 or D02 or D03 or D04 or D05 or D06 (table 1).

Table 1

IPC DISTRIBUTION OF TEXTILE PATENT	
IPC Class	Name
D01	Natural or chemical thread or fibre; spinning
D02	Mechanical finishing, warping or mechanization of yarns, yarns or ropes
D03	Weaving
D04	Weaving, lace making, knitting, sash, non-woven fabric
D05	Sewing, embroidering, tufting
D06	Fabric processing, washing, flexible materials not included in other types

METHODS

Patent analysis

The number of patents, types of patents, and categories of patents reflects the trend of technological innovation in the industry. Through the analysis of these information, we can understand the technological innovation capabilities of industries and formulate corresponding countermeasures [16]. The patent measurement method can be used to grasp the spatial and temporal distribution of countries and regions, enterprises and inventors distributed in a certain technical field to analyse the transfer of technology centres and the rise and fall of enterprises and industries. Enterprises can grasp the competitive situation, formulate corresponding countermeasures, and predict development trends by measuring their own patents and competitors' patents. The study reveals the layout and competition of textile industry technology innovation from the perspective of patent application trend, applicant distribution, and technical field distribution to reflect China's textile technology innovation capability and development trend.

Technology life cycle theory and logistic model

The technology life cycle theory believes that the development of technology can be divided into four stages: (1) at the germination stage, there are few technological innovations, mostly basic innovations, and the technical direction is uncertain; (2) during the growth phase, new technologies continue to extend into the entire field. Technology becomes more attractive and more innovative entities are involved in R&D. Innovation subjects and outputs are proliferating; (3) at the maturity stage, the R&D technology is mature. But due to the market restriction, the number of patent applicants is basically unchanged. The growth rate of technological innovation is also slowing down; (4) during the recession period, the technology is aging. The company gets lower profits and

withdraws from the market, resulting in a decrease in the number of technological innovations. The entire industry needs new and alternative technologies to emerge, which will trigger a new round of technological changes. Kim [17] proposes the use of patent data for technical life cycle judgment. With time as the horizontal axis and patent application for the vertical axis to create visual graphics, the shape of the technology trend seems like the English letter "S". The curve changes correspond to different stages of the technology life cycle, as shown in figure 1. This method has been widely recognized.

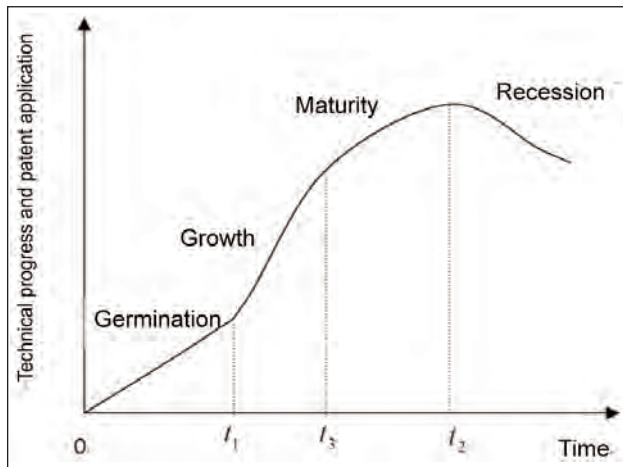


Fig. 1. S-shaped Growth Curve of the technology life cycle

The study uses the Logistic model to measure the technology life cycle. Assume that the abscissa is time t , the ordinate is the cumulative amount of patent $f(t)$. The Logistic curve formula is $y = \frac{k}{1 + ae^{-kbt}}$ (k for the maximum amount of accumulation, a , b are constants, t for time). The first derivative is:

$$\frac{dy}{dt} = \frac{-k * (-kb) * ae^{-kbt}}{(1 + ae^{-kbt})^2} = \frac{bk^2 \left(\frac{k}{y} - 1\right)}{\frac{k^2}{y^2}} = by(k - y) \quad (1)$$

If $\frac{dy}{dt} = 0$, then $y = 0$ or $y = k$. This equation shows that there is no maximum or minimum between these two limits and is therefore monotonic.

The second derivative is:

$$\frac{d^2y}{dt^2} = bk * \frac{dy}{dt} - 2by * \frac{dy}{dt} = b * \frac{dy}{dt} (k - 2y) = b^2y(k - y) (k - 2y) \quad (2)$$

If $\frac{d^2y}{dt^2} = 0$, then $y = 0$, $y = k$, $y = \frac{k}{2}$, there is a unique inflection point $y = \frac{k}{2}$, substitute $y = \frac{k}{1 + ae^{-kbt}}$, get $y = \frac{\ln a}{bk}$, that is, the inflection point coordinates are $\left(\frac{\ln a}{bk}, \frac{k}{2}\right)$. Below the inflection point, the curve is convex downward; above the inflection point, the curve is convex. The cumulative amount changes from rapid growth to slow growth, so this point can be

regarded as the cut-off point between growth and maturity, which is recorded as $t_0 = \frac{\ln a}{bk}$.

In general, when the cumulative amount reaches 10%, the curve enters the growth phase from the introduction period, and the time boundary point is recorded as t_1 . When the cumulative amount reaches 90, the curve enters the recession period from the maturity period, and the time boundary point is recorded as t_2 . The time of growing is the time interval between the growth period and the maturity period, recorded as t_3 , as is in figure 1.

Since the Logistic curve is a symmetric S-curve, the boundary point coordinates of each period can be derived using its image properties.

The logic curve is symmetric about the centre of the inflection point $\left(\frac{\ln a}{kb}, \frac{k}{2}\right)$. Therefore, the curve of the cumulative amount from 10% to 90% is also symmetric about the centre of the point $\left(\frac{\ln a}{kb}, \frac{k}{2}\right)$. Then the growth period is the same as the maturity time, that is $\frac{t_3}{2}$. And the time boundary between the introduction period and the growth period is $t_1 = t_0 - \frac{t_3}{2}$. The time demarcation point between maturity and recession is $t_2 = t_0 + \frac{t_3}{2}$. The dividing point between growth and maturity is $t_0 = \frac{\ln a}{bk}$.

The study uses Loglet-Lab2 software for life cycle estimation. The results of the Loglet Lab software include three parameters: Saturation, Growth Time, and Midpoint [18]. Saturation is the maximum utility value generated by using a certain technology; Growth Time is 10%–90% of the maximum utility value generated by a certain technology; Midpoint is the inflection point of the S curve, the technical utility growth rate reaches a maximum at this point.

ANALYSIS AND DISCUSSION

Trends of textile technology innovation

The number of patent applications reflects the innovation ability in the industrial or technical field to a certain extent. From 1987 to 2016, the number of textile industry patents in China is 270,145 totally, including 148,489 invention patents and 121,656 utility models. The number of patent applications and the trend are shown in figure 2. It can be seen from figure 2 that the invention patents and utility model patents of textile industry in China are generally on the rise. From the perspective of patent application trend, the number of applications for invention patents and utility model patents before 2000 was small and the growth was slow, in its infancy stage. Accelerated from 2001 to 2008, invention patents and utility model patents had grown faster than the previous stage. After 2008, with the promulgation and implementation of the National Medium- and Long-Term Science and Technology Development Plan (2000–2020) and the promotion of national science and technology policies, textile patents entered a

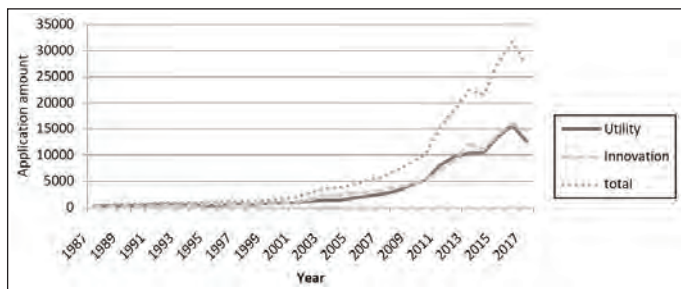


Fig. 2. Annual trends of Chinese textile patent applications from 1987 to 2016

stage of rapid growth. As seen from figure 2, the development curve of invention patents and utility model patents crossed in 2009. In 2010 and 2011, the invention patents were close to utility model patents, and their amount was basically the same.

Regional distribution of textile technology innovation

The regional distribution of textile patents covers 31 provinces and cities nationwide, and statistics on the total number of patent applications (including invention patents and utility model patents) in the textile sector of each province. Currently, the top ten provinces with most patent applications are Jiangsu, Zhejiang, and Guangdong, Shandong, Shanghai, Anhui, Fujian, Tianjin, Beijing, Hubei (table 2).

Table 2

TOP 10 PROVINCES OF THE TEXTILE INDUSTRY	
Applicant provinces and cities	Number of patents
Jiangsu	80110
Zhejiang	58831
Guangdong	20271
Shandong	19602
Shanghai	15878
Anhui	11724
Fujian	10446
Tianjin	6768
Beijing	6730
Hubei	5257

An analysis of the number of patents in the region finds that the regional distribution of patent applications of textile industry in China was uneven. The patent applications in the eastern coastal areas (including Shanghai, Jiangsu, and Zhejiang) accounted for almost two-thirds of the total applications in the field. It can be seen that the eastern coastal areas have obvious advantages in technological innovation in the textile field, because Jiangsu, Zhejiang and Shanghai are the centre of China's textile industry. In the core area, a large number of textile enterprises have gathered, and they have accumulated a solid technical foundation. At the same time, they have

gathered textile universities such as Donghua University, Jiangnan University and Suzhou University. The development of the northern coast (including Beijing, Tianjin, Hebei, and Shandong) is relatively stable. The southern coastal areas (including Fujian, Guangdong, and Hainan) and the middle reaches of the Yangtze River (including Hubei, Hunan, Jiangxi, and Anhui) have developed rapidly in recent years and have become an important role in the technological innovation of the domestic textile industry. The middle reaches of the Yangtze

River have a good development momentum and great potential. In the north-eastern region, south-western regions (Yunnan, Guizhou, Sichuan, Chongqing, Guangxi) and the north-western regions (Gansu, Qinghai, Ningxia), the number of textile patent applications is small, indicating that their textile industry technological innovation is still in a relatively weak state. While undertaking the transfer of the eastern textile industry, the weak region must pay attention to the improvement of independent innovation capability.

Distribution of textile technology innovation fields

A statistical analysis of the top 20 for patent applications in the textile field finds that companies and universities were important forces (table 3). Donghua University has 2,423 textile licensing patents, ranking first, followed by Jiangnan University, Zhejiang University of Technology, Tianjin Polytechnic University, Suzhou University and Wuhan Textile University. There are 14 companies in the top 20 patent applications, including 6 foreign companies, from Korea, Japan, and Switzerland.

Distribution of technological innovation in the textile industry

The ranking of each textile industry branch technical field according to invention patent applications statistics is the same as that according to total patent applications statistics, and the order from high to low is D06, D01, D03, D04, D05, and D02, as shown in table 4. Except D05, the proportion of invention patents is 49% and above. The number of invention patents applied in the field of D06 (treatment of fabrics, etc.; washing; flexible materials not included in other categories) and D01 (natural or artificial wire or fibre; spinning) are located in the first and second place respectively, the focus research field of textile technology in China. Then followed by D04 (tape; lace; knitting; finishing). Although the total number of D05 (sewing; embroidery; tufting) is similar to D03, most of D05 are utility model patents, invention patents accounting for a relatively small proportion. The number of patent applications and invention patent applications in the field of D02 (yarn; mechanical finishing of yarn or rope; warping or warping) is the least.

Table 3

TOP 20 INSTITUTIONS OF CHINESE TEXTILE INDUSTRY PATENT APPLICANTS					
Serial number	Applicant	No. of patents	Serial number	Applicant	No. of patents
1	Donghua University	3128	11	Matsushita Electric Industrial Co., Ltd.	797
2	Wuxi Little Swan Co., Ltd.	3113	12	Samsung Electronics Co., Ltd.	733
3	Qingdao Haier Washing Machine Co., Ltd.	1779	13	Ritter Machinery	702
4	Jiangnan University	1610	14	Toray Fiber Research Institute (China) Co., Ltd.	683
5	Haier Group	1593	15	Ningbo Cixing Co., Ltd.	680
6	LG Electronics Co., Ltd.	1355	16	Tianjin Polytechnic University	673
7	Lejin Electronics (Tianjin) Electric Co., Ltd.	1201	17	Suzhou University	661
8	Zhejiang Sci-Tech University	1041	18	Natur DuPont	650
9	Guangdong Esque Textile Co., Ltd.	967	19	Wuhan Textile University	639
10	Nanjing Lejin Panda Electric Co., Ltd.	951	20	Qingdao Haier Drum Washing Machine Co., Ltd.	559

Table 4

FIELD DISTRIBUTION OF TEXTILE PATENT APPLICATIONS						
Field	D01	D02	D03	D04	D05	D06
Utility model	22829	4524	11834	13306	15447	43713
Invention patent	26156	6076	11442	12912	8447	54550
Total	48985	10600	23276	26218	23894	98263
Proportion of invention	0.53	0.57	0.49	0.49	0.35	0.55

Technology life cycle prediction

The study analyses the patent data of textile industry in China from 1987 to 2016, and uses the Logistic model to calculate the technical life cycle of the textile industry. Based on the S curve, the technical trend is predicted to determine the stage characteristics of s textile industry in China. Based on the theory of Logistic Growth, the cumulative product of the patent is the vertical axis, and the patent application year is the horizontal axis. The trend of the textile technology is shown in figure 3 using Loglet Lab software. The dots in the figure indicate the actual number of accumulated patents, and the solid line indicates the estimated accumulative number of patents. The saturation point, growth time and turning point were calculated. As shown in table 5, the cumulative number of patents for the saturation point was 628,841.54, and the growth time was 19.24 years. The inflection point of the s curve occurred in 2017. The application began in 1987. The system has estimated its growth time to be 19 years, that is, the patent application continues to grow until 2006, which is the budding period. Then the patent application entered the growth period. This period has shown an accelerated growth trend. It is expected that the textile industry patents will show a decelerating trend from 2018 to 2028, but the total amount is still increasing, and this stage is a mature period. It is expected that the patent saturation value will be 628,841.54 pieces.

After that, the patent growth will enter a recession period, the space for technology development is small, and the application volume is gradually reduced.

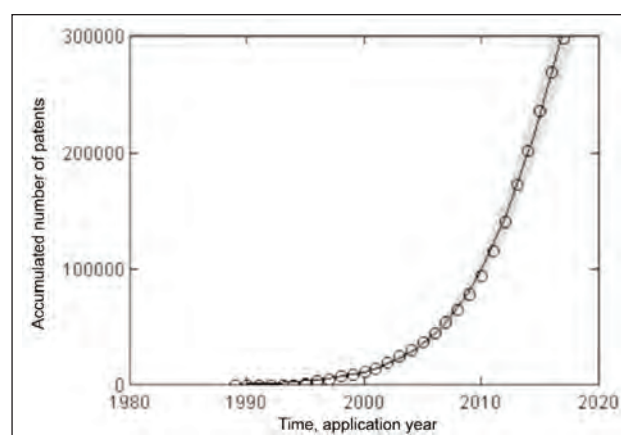


Fig. 3. S-shaped Growth Curve of China's textile industry technology innovation

Table 5

THE RESULT OF S-SHAPED CURVE FITTING	
Variable	Value
Saturation	628,841.54
Midpoint	2,017.322
Growth time	19.24

The figure 3 indicates that the technical life cycle of the textile industry has entered a mature stage. As shown in table 6, textile industry technology has entered a mature stage in 2018, and the total number of patents is still growing, but the speed is reduced slowly. Innovation of textile industry in China is shifting from pursuing quantity to pursuing quality. The result is consistent with the overall situation of the textile industry. At the mature stage, the industry has strong R&D capabilities and mature technology. It is the best time for the synergetic development between innovation quantity and innovation quality, most likely to produce key technologies.

Table 6

FORECAST OF TECHNOLOGY GROWTH STAGE OF TEXTILE INDUSTRY			
Budding stage	Growing phase	Maturity stage	Recession phase
1987–2006	2007–2017	2018–2027	After 2027

CONCLUSIONS

Based on the data of textile industry patent application in China from 1987 to 2016, the study uses the patent measurement method to analyse the technological innovation capability, including the distribution of innovation regions and subjects, as well as the distribution and structure of major technical fields. And based on the number of patent applications per year, the Logistic model is used to measure the life cycle stage of textile industry in China.

First of all, the number of technological innovations in the Chinese textile industry has shown a rapid upward trend. However, the growth rate of utility model patent is fast, and its proportion is close to invention patent's proportion. Secondly, the regional distribution of invention patent applications, patentees, and technical fields of the Chinese textile industry from 1987 to 2016 were analysed. It was found that the areas of technological innovation in the Chinese

textile industry were mainly distributed on the south-east coast. Enterprises and universities were the important R&D subjects. The study also found the development was uneven among the six major technical fields of the textile industry, in which D06 (fabric treatment) had the largest number of patent applications and the fastest development rate, while D02 (spinning) had the slowest development rate. Thirdly, using the Logistic model to measure the technology life cycle stage, China's textile industry technology entered a growth stage in 2007 and entered a mature stage in 2018.

Based on the above analysis, first of all, the quality of innovation in China's textile industry needs to be further improved. This requires the competent authorities of the textile industry to play the role of government's macro-control and coordination, to guide and support the technological investment and research of textile enterprises, especially small and medium-sized textile enterprises. The government should provide diverse financing channels, building a good independent innovation platform combining technology and finance, promoting high-quality development of the textile industry. Secondly, the Chinese government should strengthen research and development investment in the textile industry in less developed regions, and guide the textile industry in less developed regions to shift from labour-intensive to innovation-driven. In addition, textile enterprises should choose the direction and field of technological innovation according to their own conditions. Enterprises with strong R&D capabilities should strive in cutting-edge fields and develop basic patent technologies; those with weaker strengths should avoid fields where patent applications are relatively concentrated and break through weak areas. Finally, the technological research in each sub-sector of the textile industry has entered a mature stage. It is necessary to strengthen the Industry-University-Research cooperation and multidisciplinary integration, starting from new energy, new materials, new technologies and other aspects to promote a new round of technological change.

REFERENCES

- [1] Huang, Y., Zhu, D., Qian, Y., *A hybrid method to trace technology evolution pathways: a case study of 3D printing*, In: *Scientometrics*, 2017, 111, 1, 185–204
- [2] Griliches, Z., *Patent Statistics as Economic Indicators: a survey*, In: *Journal of Economic Literature*, 1990, 28, 4, 1661–1707
- [3] Campbell, R.S., *Patent Trends as a Technological Forecasting Tool*, In: *World Patent Information*, 1983, 5, 3, 137–143
- [4] Fleisher, C.S., Bensoussan, B.E., *Strategic and Competitive Analysis*, In: Englewood Cliffs: Prentice-Hall, 2003, 347–363
- [5] Choi, C., Park, Y., *Monitoring the organic structure of technology based on the patent development paths*, In: *Technological Forecasting and Social Change*, 2009, 76, 6, 754–768
- [6] Lee, S., Yoon, B., Park, Y., *An approach to discovering new technology opportunities: Keyword-based patent map approach*, In: *Technovation*, 2009, 29, 6–7, 1–497
- [7] Grandjean, N., Charpiot, B., Pena, C.A., *Competitive intelligence and patent analysis in drug discovery: Mining the competitive knowledge bases and patents*, In: *J. Drug Discovery Today Technologies*, 2005, 2, 3, 211–215
- [8] Porter, A.L., Newman, N.C., *Patent Profiling for Competitive Advantage*, 2004
- [9] Chunjuan, L., *Quantitative analysis of patents in the global electric vehicle industry*, In: *Technology and Innovation Management*, 2011, 32, 2, 114–116

- [10] Bengisu, M., Nekhili, R., *Forecasting emerging technologies with the aid of science and technology databases*, In: Technological Forecast & Social Change, 2006, 73, 7, 835–844
- [11] Meyer, P.S., Yung, J.W., Ausebel, J.H., *A primer on logistic growth and substitution the mathematics of the Loglet Lab software*, In: Technological Forecast & Social Change, 1999, 6, 1, 247–271
- [12] Boretos, G.P., *The future of the mobile phone business*, In: Technological Forecast & Social Change, 2007, 74, 3, 331–340
- [13] Yu, H.C., Chia, Y.C., Shun, C.L., *Technology forecasting and patent strategy of hydrogen energy and fuel cell technologies*, In: International Journal of Hydrogen Energy, 2011, 36, 12, 6957–6969
- [14] Tugrul, U.D., Guillermo, R., Hilary, M., Pisek, G., *Forecasting emerging technologies: use of bibliometrics and patent analysis*, In: Technological Forecasting and Social Change, 2006, 73, 8, 981–1012
- [15] Liu, C.Y., Wang, J.C., *Forecasting the development of the biped robot walking technique in Japan through S-curve model analysis*, In: Scientometrics, 2010, 82, 1, 21–36
- [16] Rajeswari, A.R., *Forecasting of science & technology expenditure of India by simulation method*, In: Scientometrics, 1989, 17, 3, 227–251
- [17] Kim, B., *Managing the transition of technology life cycle*. In: Technovation, 2003, 23, 5, 371–381
- [18] Cioffi, D.F., *A tool for managing projects: An analytic parameterization of the S-curve*, In: International Journal of Project Management, 2005, 23, 215–222
-

Authors:

QIAN XU^{1,2}, HUA CHENG¹, YABIN YU^{1,2}

¹School of Economics and Management, Zhejiang Sci-Tech University, Hangzhou, 310018, 5 Second Avenue, Xiasha Higher Education Zone, Hangzhou, Zhejiang, China
e-mail: xuqian@cjlu.edu.cn

²School of Economics and Management, China Jiliang University, Hangzhou 310018, 258 Xueyuan Street, Xiasha Higher Education Zone, Hangzhou, Zhejiang, China

Corresponding author:

HUA CHENG
e-mail: chenghua@zstu.edu.cn

Optimisation of accounting model of inventory management in the textile industry

DOI: 10.35530/IT.072.02.1769

IVAN MILOJEVIĆ
SNEŽANA KRSTIĆ

MIHAILO ĆURČIĆ

ABSTRACT – REZUMAT

Optimisation of accounting model of inventory management in the textile industry

The supply system consists of several elements, which in their characteristics are distinguished in the overall structure of the supply system. They are defined uniquely in accordance with the function they perform, and in reality they appear at all levels of the budget system organization. Functioning of the supply system is possible only with the existence of certain inventories or reserves of material assets. The stocks represent the prescribed and determined quantities of material assets stored in the warehouses in order to ensure the normal functioning of the institutions.

Using the supplies management accounting model in textile industry is providing a continuous provision of equipment. This is essential to reach the adequate level of competence, which is in line with autonomous budget financing companies. Taking into account the specificity of the institutions, with an emphasis on the quality of the equipment, there is also the possibility for savings in maintaining them.

The aim of this paper is to present how the inventory management accounting system can optimize costs in the textile industry due to the full satisfaction of the optimal supply criterion.

Keywords: *textile, management, accounting, model, supplies, efficiency*

Optimizarea modelului contabil de gestionare a stocurilor în industria textilă

Sistemul de aprovizionare este format din mai multe elemente care, prin caracteristicile lor, se disting în structura generală a sistemului. Ele sunt definite în mod unic în conformitate cu funcția pe care o îndeplinesc și, în realitate, ele apar la toate nivelurile organizării sistemului bugetar. Funcționarea sistemului de aprovizionare este posibilă numai cu existența anumitor stocuri sau rezerve de active materiale. Stocurile reprezintă cantitățile prescrise și determinate de active materiale existente în depozite, pentru a asigura funcționarea normală a instituțiilor. Utilizarea modelului contabil de gestionare a consumabilelor în industria textilă oferă o furnizare continuă de echipamente. Acest lucru este esențial pentru a atinge nivelul adecvat de competență, în conformitate cu organizațiile autonome de finanțare bugetară. Ținând seama de specificul instituțiilor, cu accent pe calitatea echipamentelor, există și posibilitatea de a economisi în scopul întreținerii acestora. Scopul acestei lucrări este de a prezenta modul în care sistemul contabil de gestionare a stocurilor poate optimiza costurile în industria textilă datorită satisfacției depline a criteriului optim de aprovizionare.

Cuvinte-cheie: *textil, management, contabilitate, model, consumabile, eficiență*

INTRODUCTION

The stock of supplies is carried out periodically according to the plan of supply or demand as needed, as well as direct purchase, where it is necessary to keep a record of the level of inventory level. When completing the supply [1] with the purchase from the market, it is particularly important to pay attention to the choice of the supplier, i.e. to the ability of the supplier to deliver the goods and services of the required quality in accordance with the agreed deadlines. In the textile industry [2], this is particularly important for the successful performance of work and the performance of other tasks, where it is necessary to prepare certain quantities and a range of material resources that will be spent [3].

A particularly important source of funds is material reserves that are provided and are limited by the material possibilities of the textile industry [4, 5], so that the level of reserves changes according to the

material possibilities, the state policy, and the degree of social and economic development of the state. Material reserves are planned and maintained at certain levels of organization of the state in accordance with the economic possibilities and needs of the textile market. The material reserves are planned and maintained at the appropriate level in accordance with economic opportunities and needs. There is a possibility of increasing them by intensive industrial production and imports. At certain levels of organization [6] of the state, the amount and structure of material reserves are determined in accordance with the law and according to special plans.

This paper is contained in four different parts. After "Methods of Modeling" where are defined the exact ways of upcoming research, we presented the "Modeling Results" of it. Once we had had the data, we have discussed them, at the "Discussion" part of the paper. At the very end, we drew a conclusion, and bulleted all the used references in this research.

METHODS OF MODELING

The costs that are the subject of our research [7] are related to the total costs of securing supplies [8] of spare materials. In order to solve such a problem, the minimization of these costs [9] requires prior formation of the appropriate mathematical model of inventories, and then by solving it, the minimum total cost of inventory is determined. In order to create such a methodical stock model it is necessary to fulfil certain conditions and assumptions [10]. In the given planning period T , the demand, which will be denoted by x , is a stochastic variable with the known law of probability $p(x)$. Costs per unit of supply, if they are purchased on a regular basis, are C_1 . Costs per unit of stock, if purchased through the occurrence of defects, are C_2 . Costs can also be included in these costs due to lack of supplies. In practice, it is usual that C_2 costs are significantly higher than the cost of C_1 ; Initial supplies are equal to zero.

If x is marked with demand, and y with the level of inventory, then: if it is $x \leq y$, that is, if the level of inventory is higher than demand, then the costs of inventories will be paid $C_1(y-x)$; if $y > x$, that is, if the demand is higher than the available stocks, then the costs of extraordinary or urgent purchases which are $C_2(x-y)$. Taking into consideration that the demand x is stochastic, and that the probability of a failure on the $p(x)$ agent is known, which means that the expected total costs will be obtained by adding the individual costs, for each x , multiplied by the corresponding probability $p(x)$ that the total cost function, denoted by $F(y)$, is reduced to the expected value, can be written in the following form:

$$F(y) = C_1 \sum_{x=0}^y (y-x)p(x) + C_2 \sum_{x=y+1}^{\infty} (x-y)p(x) \quad (1)$$

In order to determine the minimum expected total cost for this stock problem, it is necessary to determine the minimum of this function. Starting from the fact that this model refers to the provision of spare parts of assets, the minimization of this function will be assumed if the variables can be taken only by discrete and integer non-negative values. In this case, if there is some value in y^* , where the previously mentioned function takes its minimum value, the following condition must be fulfilled:

$$F(y^*-1) > F(y^*) < F(y^*+1) \quad (2)$$

If the functions $F(y-1)$ and $F(y+1)$ are formed, then the conditions under which $y=y^*$ will be determined. Starting from the function 1 in which the variable is replaced by $y-1$, it gets:

$$F(y-1) = C_1 \sum_{x=0}^{y-1} (y-1-x)p(x) + C_2 \sum_{x=y}^{\infty} (x-y+1)p(x) \quad (3)$$

$$F(y-1) = C_1 \sum_{x=0}^{y-1} (y-x)p(x) + C_2 \sum_{x=y}^{\infty} (x-y)p(x) - C_1 \sum_{x=0}^{y-1} p(x) + C_2 \sum_{x=y}^{\infty} p(x) \quad (4)$$

Based on the relationship of function $F(y)$ and $F(y-1)$, a connection can be established between functions which can be written in the form of the following double inequality:

$$p(x \leq y^* - 1) < \frac{C_2}{C_1 + C_2} < p(x \leq y^*) \quad (5)$$

This means that if there is some value in y^* that minimizes the function of the expected total cost, then in y^* it must fulfil the conditions by the given equation 5. The equation 5 is important not only because it determines the optimal conditions that the variable must fulfil, but also because it can also determine the optimal value of the stock in y^* which minimizes the expected cost of the stock. This is achieved by first forming a table in which one line, or one column, represents the probability cumulative $p(x=y)$, and then, based on the known values for C_1 and C_2 , the quotient is calculated:

$$k = \frac{C_2}{C_1 + C_2} \quad (6)$$

After that in a row or column, the probability cumulative is determined by the values of the coefficient k . Each of these cumulative probabilities $p(x=y)$ corresponds to one value in y . This value for y , which corresponds to a higher value of cumulative probabilities, represents the required optimal solution in y^* . Using the equation 5, an optimal solution can also be performed, that is, the limits within which the costs of C_1 and C_2 can be determined without the change of the optimum solution:

$$C_1 < \frac{p(x \geq y^*)}{p(x \leq y^* - 1)} \quad (7)$$

$$C_1 > \frac{p(x \geq y^* + 1)}{p(x \leq y^*)} \quad (8)$$

because

$$p(x \leq y^*) = 1 - p(x > y^*) = 1 - p(x \geq y^* + 1) \quad (9)$$

The inequalities 7 and 8 can be combined into one double inequality of the form

$$\frac{p(x \leq y^* + 1)}{p(x \leq y^*)} C_2 < C_1 < \frac{p(x \geq y^*)}{p(x \leq y^* - 1)} C_2 \quad (10)$$

which set the upper and lower limits within which the costs of C_1 can be moved, without changing the optimal solution. The lower and upper limits within which the costs of C_2 may be changed without affecting the change in the optimal solution are:

$$\frac{p(x \leq y^* + 1)}{1 - p(x \leq y^* - 1)} C_1 < C_2 < \frac{p(x \leq y^*)}{1 - p(x \leq y^*)} C_1 \quad (11)$$

or otherwise written:

$$\frac{p(x \leq y^* + 1)}{p(x \geq y^*)} C_1 < C_2 < \frac{p(x \leq y^*)}{p(x \geq y^* + 1)} C_1 \quad (12)$$

MODELING RESULTS

We determined by means of a weighted arithmetic mean method that the average cost of purchasing and storing spare materials [11] of technical means

Table 1

THE PROBABILITY OF REPLACEMENT OF SPARE MATERIALS								
Number of spare materials replaced x	0	1	2	3	4	5	6	7
The probability of replacement $p(x)$	0	0.25	0.30	0.20	0.10	0.10	0.05	0

during the purchase of the funds itself, when the supplier timely performed the service of delivery of the spare materials, amounted to $C_1 = 1,500$ € for one spare material. In the period when the supplier did not deliver spare materials when purchasing the asset, the occurrence of the defect, the period of placing the asset out of use using the weighted arithmetic mean method, it was two months in length and the costs of emergency supplies [12] amounted to an average $C_2 = 6,000$ €. Through a population survey using the Poisson's Distribution [13], the probability of replacing spare materials during the exploitation period of the observed assets has been obtained. These probabilities are shown in table 1.

Using a stochastic inventory model throughout the research population, we have set a relationship for solving the problem of determining the optimal size of the order of the spare material in y^* , in a regular way, for which the total cost of providing the stock will be minimal [14], and then determine the amount of these minimum costs and limits within which change the costs of C_1 and C_2 , with the optimal solution remaining unchanged.

Starting from the initial quantities that we carried out in the research process based on the primary data $C_1 = 1,500$ € and $C_2 = 6,000$ € we get the value of the parameter k , which shows the share of the price of the spare material, that spare material was not delivered when buying the asset in the total price.

$$k = \frac{6,000}{1,500 + 6,000} = 0.8 \quad (13)$$

Starting from the assumption that Poisson's probability distribution, the sample share of the entire population is obtained as a cumulative probability parameter; we performed the calculation in the table 2.

Based on the data from the cumulative probability table $p(x \leq y)$, we obtained

$$0.75 < k < 0.85 \quad (14)$$

which means it is:

$$y^* = 4 \quad (15)$$

because this value for y corresponds to a higher cumulative probability.

DISCUSSION

By obtaining the result, we confirmed the assumption that regular supply [15] was supposed

to provide $y^* = 4$ spare materials [16], and with a 85% probability, we can claim that the amount of 4 units of spare materials that is obtained is sufficient to eliminate all defects on the asset being monitored, while it is assumed the risk of 15% that one or two spare materials will be procured by emergency supplies in the event of a lack of supplies [17], which in any case in an emergency situation represents an insufficient level of probability of reliability of the purchase of spare materials [18]. In that case, the minimum costs would be

$$F(y^* = 4) = 1,500 \sum_{x=0}^4 (4 - x)p(x) + 6,000 \sum_{x=5}^{\infty} (4 - x)p(x) \quad (16)$$

$$F(y^* = 4) = 1,500(3 \cdot 0.25 + 2 \cdot 0.30 + 1 \cdot 0.20) + 6,000(1 \cdot 0.10 + 2 \cdot 0.05) = 3,525 \text{ €} \quad (17)$$

A mathematical check of the minimum costs of purchasing a spare material is carried out so that the optimal result is reduced by 1, i.e. the magnification by 1, $F(y^* - 1 = 3)$ and $F(y^* + 1 = 5)$:

$$F(3) = 1,500(2 \cdot 0.25 + 2 \cdot 0.30) + 6,000(1 \cdot 0.10 + 2 \cdot 0.10 + 3 \cdot 0.05) = 3,900 \text{ €} \quad (18)$$

and

$$F(5) = 1,500(4 \cdot 0.25 + 3 \cdot 0.30 + 2 \cdot 0.20 + 1 \cdot 0.10) + 6,000(1 \cdot 0.05) = 3,900 \text{ €} \quad (19)$$

How it was checked that it was:

$$F(3) > F(4) < F(5) \quad (20)$$

these are, indeed, for $y^* = 4$, the minimum costs, and therefore the boundary of the cost changes C_1 and C_2 , for which there will be no change in the optimal solution. These boundaries are determined by equations 8 and 12, which means that the boundary of the cost change C_1 is valid

$$\frac{p(x \geq 5)}{p(x \leq 4)} \cdot 6,000 < C_1 < \frac{p(x \geq 4)}{p(x \leq 3)} \cdot 6,000 \quad (21)$$

Table 2

PROBABILITY AND CUMULATIVE PROBABILITY OF REPLACEMENT OF SPARE PARTS								
y	0	1	2	3	4	5	6	7
x	0	1	2	3	4	5	6	7
$p(x)$	0	0.25	0.30	0.20	0.10	0.10	0.05	0
$p(x \leq y)$	0	0.25	0.55	0.75	0.85	0.95	1.00	1.00

$$\frac{0.15}{0.85} \cdot 6,000 < C_1 < \frac{0.25}{0.75} \cdot 6,000 \quad (22)$$

from where the required limits for changing the cost of C_1 are ultimately determined:

$$1,058.82 < C_1 < 2,000.00 \quad (23)$$

The same as in the previous case, the limits in which the costs of C_2 can be moved without changing the optimal solution $y^*=4$, are:

$$\frac{0.75}{0.25} \cdot 1,500 < C_2 < \frac{0.85}{0.15} \cdot 1,500 \quad (24)$$

from where it gets:

$$4,500.00 < C_2 < 8,500.00 \quad (25)$$

The verification of the obtained solutions is carried out by assuming that the first is that $C_1 = 1200$, and then that $C_1 = 1,890$. In the first case it is:

$$k = \frac{6,000}{1,200 + 6,000} = 0.8333 \quad (26)$$

in the other:

$$k = \frac{6,000}{1,890 + 6,000} = 0.7604 \quad (27)$$

So, in both cases it is

$$0.75 < k < 0,85 \quad (28)$$

which means that the mentioned changes in the cost of C_1 do not affect the change of the optimal solution. A similar check can also be done for the costs of C_2 ,

which means that the changes and costs of C_2 will not lead to the change of the optimal solution $y^*=4$.

CONCLUSION

In the conducted research, we have shown that savings could be achieved by timely procurement and delivery of an optimal quantity of spare parts $y^*=4$ by suppliers, over €12,000 in the probability of a failure in the observed assets of 85%. In this case, there was a risk with a 15% probability of failure and there is no pre-supplied spare part. On the other hand, the existence of inventories would speed up the correction of the asset as soon as possible, which would reduce the time of the inaccuracy of the observed asset and further influence the adequate equipment of the institution with equipment, which is a very important element for the textile industry. Using this model, it would be possible to continuously provide the equipment for textile industry, which is crucial for the successful achievement of the appropriate level of competence, and of particular importance for textile companies that work on the principle of autonomous budget financing.

ACKNOWLEDGEMENTS

This research is a part of the project no. VA-DH5/17-19 – Development of the financial service of the Army of Serbia from 1985 to 2015, financed by the Ministry of Defense of the Republic of Serbia. Project period: 2016-2020.

REFERENCES

- [1] Rao, C.M., Rao, K.P., Muniswamy, V.V., *Delivery Performance Measurement in an Integrated Supply Chain Management: Case Study in Batteries Manufacturing Firm*, In: Serbian Journal of Management, 2011, 6, 2, 205–220
- [2] Bruce, M., Daly, L., Towers, N., *Lean or agile: A solution for supply chain management in the textiles and clothing industry*, In: International Journal of Operations & Production Management, 2004, 24, 2, 15–170
- [3] Aureo, B., *Razvoj računovodstva*, In: Oditor – časopis za Menadžment, finansije i pravo, 2016, 2, 3, 39–48
- [4] Koyuncu, I., Kural, E., Topacik, D., *Pilot scale nanofiltration membrane separation for waste management in textile industry*, In: Water & Science Technology, 2001, 43, 10, 233–240
- [5] Chen, L., Yan, X., Yu, H., *Developing a modular apparel safety architecture for supply chain management: the apparel recycle perspective*, In: Industria Textila, 2018, 69, 1, 24–30, <http://doi.org/10.35530/IT.069.01.1380>
- [6] Zhao, M., Nichols, T., *Management Control of Labour in State-Owned Enterprises: Cases From the Textile Industry*, In: The China Journal, 1996, 36, 1–21
- [7] Lambert, D.M., Cooper, M.C., Pagh, J.D., *Supply Chain Management: Implementation Issues and Research Opportunities*, In: The International Journal of Logistics Management, 1998, 9, 2, 1–20
- [8] Cooper, M.C., Lambert, D.M., Pagh, J.D., *Supply Chain Management: More Than a New Name for Logistics*, In: The International Journal of Logistics Management, 1997, 8, 1, 1–14
- [9] Prdić, N., *Konkurentska prednost preduzeća na osnovu benčmarking analize poslovanja*, In: Oditor – časopis za Menadžment, finansije i pravo, 2017, 3, 3, 107–117
- [10] Backović, M., Vuleta, J., Popović, Z., *Ekonomsko-matematički metodi i modeli*, Centar za izdavačku delatnost: Ekonomski fakultet, Beograd, 2014
- [11] Thomas, D.J., Griffin, P.M., *Coordinated supply chain management*, In: European Journal of Operational Research, 1996, 94, 1, 1–15
- [12] Mentzer, J.T., DeWitt, W., Keebler, J.S., Min, S., Nix, N.W., Smith, C.D., Zacharia, Z.G., *Defining supply chain management*, In: Journal of Business Logistics, 2001, 22, 2, 1–25
- [13] Žižić, M., Lovrić, M., Pavličić, D., *Metodi statističke analize*, Centar za izdavačku delatnost: Ekonomski fakultet, Beograd, 2003
- [14] Nuševa, D., Marić, R., *Quick Response Logistics in Retailing as an Information Technology Based Concept*, In: Strategic Management, 2017, 22, 4, 32–38
- [15] Olateju, O.E., Fabson, T.V.O., *A Comparative Study of Simulation and Time Series Model in Quantifying Bullwhip Effect in Supply Chain*, In: Serbian Journal of Management, 2011, 6, 2, 145–154

- [16] Hilletoft, P., Hilmola, O-P., *Supply chain management in fashion and textile industry*, In: International Journal of Services Sciences, 2008, 1, 2, 127–147
- [17] Koprulu, A., Albayrakoglu, M.M., *Supply chain management in the textile industry: A supplier selection model with the analytical hierarchy process*, In: ISAHP, 2007
- [18] Lambert, D.M., Cooper, M.C., *Issues in Supply Chain Management*, In: Industrial Marketing Management, 2000, 29, 1, 65–83
-

Authors:

IVAN MILOJEVIĆ, SNEŽANA KRSTIĆ, MIHAILO ĆURČIĆ

University of Defence, Military Academy, Public Finance Department,
Pavla Jurišića Šturma 33, 11000, Belgrade, Serbia
e-mail: drimilojevic@gmail.com, snezanakrstic17@gmail.com

Corresponding author:

MIHAILO ĆURČIĆ, Ph.D.
e-mail: curcicmihailo@gmail.com

Effect of silk sericin pre-treatment on dyeability of woollen fabric

DOI: 10.35530/IT.072.02.1771

CENGIZ ONUR ESER

ARZU YAVAS

ABSTRACT – REZUMAT

Effect of silk sericin pre-treatment on dyeability of woollen fabric

Silk fibres consist of sericin and fibroin. 20–25% of silk fibre is sericin. Sericin is biodegradable, antibacterial, and UV resistant. In this study, silk sericin protein was applied to wool fabric as a pre-treatment. Wool fabrics pre-treated with silk sericin were dyed with Eriofast Red B and Eriofast Blue 3R dyestuffs. Colour and reflectance measurements of the dyed wool samples were carried out. Washing, rubbing, light fastness properties were explored. Moreover, hydrophilicity, nitrogen content (Kjeldahl Method), FTIR and ESCA analysis were performed on the sericin applied wool fabric samples. Pre-treatment with sericin was found to increase the hydrophilicity level of wool fibres. Pre-treatment with silk sericin also increased the colour yield of wool fibre dyed with Eriofast Red B and Eriofast Blue 3R. It was determined that the wool fibre fabrics pre-treated with sericin displayed sufficient colour and colour fastness values even after dyeing at lower dyeing temperatures.

Keywords: silk sericin, wool, dyeing, fastness, *Bombyx mori*, biopolymer

Influența pretratării cu sericină din mătase asupra capacității de vopsire a țesăturilor din lână

Fibrele de mătase sunt formate din sericină și fibroină. Aproximativ 20–25% din fibra de mătase este sericină. Sericina este biodegradabilă, antibacteriană și rezistentă la radiații UV. În acest studiu, proteina sericinei din mătase a fost aplicată pe țesătura din lână ca pretratament. Țesăturile din lână pretratate cu sericină din mătase au fost vopsite cu coloranți Eriofast Red B și Eriofast Blue 3R. S-au efectuat măsurători ale rezistenței culorii și reflectanței pentru probele de lână vopsite. S-au analizat proprietățile de rezistență la spălare, la frecare și la lumină. Mai mult, hidrofilia, conținutul de azot (metoda Kjeldahl), analiza FTIR și ESCA au fost efectuate pe probele de țesătură din lână, pe care a fost aplicată sericina. S-a constatat că pretratamentul cu sericină a crescut nivelul de hidrofilie a fibrelor de lână. Tratamentul prealabil cu sericină din mătase a crescut, de asemenea, randamentul tinctorial al fibrelor de lână vopsite cu Eriofast Red B și Eriofast Blue 3R. S-a stabilit că țesăturile din fibră de lână pretratate cu sericină au indicat valori suficiente ale rezistenței culorii, chiar și după vopsire la temperaturi de vopsire mai scăzute.

Cuvinte-cheie: sericină din mătase, lână, vopsire, rezistența culorii, *Bombyx mori*, biopolimer

INTRODUCTION

Raw silk consists of 20–25% sericin and 70–75% fibroin [1]. These ratios vary according to the type of silkworm, care and feeding conditions, country and region where it grows. The formula of the sericin is $C_{15}H_{25}N_5O_8$ [2]. There are significant differences between sericin and fibroin. For instance, sericin contains more hydroxyl and carboxyl groups than fibroin and the amorphous structure is much higher in the case of sericin when compared with fibroin [2]. As a result of both its amorphous structure and the hydroxyl and carboxyl groups contents, sericin dissolves in hot water, especially slightly alkaline hot water [3]. Since sericin is a layer that covers the fibroin protein and covers the bright, beautiful appearance of fibroin, sericin is usually removed before dyeing [4, 5]. It is really significant to degum silk yarns completely (to remove sericin efficiently) when silk will be dyed to dark shades. Since, the traces of sericin could result in unlevelled dyeing. It is

known that the degummed silk fiber displays higher luster and softer hand when compared with raw silk fiber [6]. In the removal of the sericin; different methods such as enzymatic, conventional soap and soap-soda methods can be applicable. Enzymatic, classical soap and soap-soda methods were compared and it was found that enzymatic processes led to better results than others [4, 7]. In another study, it was reported that Savinase® was the most suitable enzyme for sericin removal [8]. From the industrial point of view, sericin removal from the silk fibre can result in severe environmental pollution because of their rich organic contents [9, 10].

In the recent years, there is a tendency towards ecological processes and biochemicals instead of toxic chemicals in textile finishing processes. One of the largest candidates in the textile sector is the sericin [11]. The sericin displays high moisture absorption, antimicrobial and UV protection properties [12, 13]. There are studies in the literature that sericin protein

is applied to textile materials. Babu and Ravindra reported that the hygroscopic properties of polyester coated with sericin protein increased 5 times compared to untreated sample [14]. In the study of Haggag et al., in order to increase the printability of woollen fabric with acid, reactive and basic dyes, hydrogen peroxide-sodium sulfite and sericin was applied to wool fabrics [15]. Jassim et al. investigated the antimicrobial properties of the sericin obtained from Bombyx Mori silkworm silk. When treated with 2% sericin, there was a decrease in the proportion of bacteria [16]. In 2011, Khalifa et al. applied the extracted sericin to woollen fabric. As a result of the applications, water absorption showed a high value at 5% sericin concentration. Optimum antibacterial properties were determined at pH 3.8 [17]. In the study conducted by Das et. al., sericin treated jute fibres were dyed with reactive dyes without salt [18]. In this research study, silk sericin protein was applied to wool fabric as a pre-treatment. Sericin pre-treated wool fabrics were dyed with Eriofast Red B and Eriofast Blue 3R dyestuffs. In here, it was investigated whether wool fibres pre-treated with sericin can be dyed at lower temperatures without the loss of colour yield.

MATERIALS AND METHODS

Materials

In this study, a plain bleached woven 100% wool fibre fabric with the weight of 150 g/m² (with 53.35 Stensby whiteness value) was utilized.

Application (pre-treatment) of silk sericin and subsequent dyeing process

Sericin pre-treatment was carried out in an Atac Lab-Dye HT machine with 5% Sericin (obtained from Bombyx mori silkworm, Sigma-Aldrich) and 25 g/l Na₂SO₄ at a liquor ratio of 20:1 [17]. After pre-treatment with sericin, Atac Lab-Dye HT laboratory type dyeing machine was used for wool fabric dyeing operations. Exhaustion dyeing method for wool was carried out at 95°C for 60 minutes (figure 1).

Two different dyestuffs in red (Eriofast Red B reactive dye, Huntsman) and blue (Eriofast Blue 3R reactive dye, Huntsman) color and silk sericin (Bombyx mori (silkworm) Sigma-Aldrich) were used in this study. Apart from dyeing at 95°C, Eriofast Red B dyestuff was also applied to pre-treated wool fabrics accord-

ing to the same dyeing recipe at 75°C, 80°C, 85°C. The dyed wool samples were firstly rinsed in cold water and then washed off at 45–50°C and 60°C for 10 minutes, respectively.

Analysis and testing

Colorimetric measurement

Stensby whiteness and yellowness values (E313 YI) of the sericin-pretreated wool fabric samples were determined. The average of the measurements was calculated from four different points from fabric samples. The CIE L*, a*, b*, C*, and h° coordinates were measured from the reflectance values at the appropriate wavelength of maximum absorbance for each dyed wool fabric sample with the utilization of a DataColor SpectraFlash 600 (Datacolor International, Lawrenceville, NJ, USA), spectrophotometer under illuminant D65, using a 10° standard observer.

Fourier transform infrared spectroscopy (FTIR)

IR spectra were taken to investigate the changes in the surface structure and chemical structure of the treated wool fibres. Perkin Elmer Spectrum Two™ ATR/FTIR instrument was used for FTIR analysis. From the obtained spectra, characteristic bands were examined and sericin treated and sericin untreated wool samples were compared.

Nitrogen determination by Kjeldahl method

The Kjeldahl method is generally utilized to determine the nitrogen content in organic and inorganic samples. Kjeldahl method was used to determine the nitrogen content of the sericin applied and non-applied wool fabric samples. Nitrogen was determined by Gerhardt Kjeldahlterm Vaposdest. In this method, the nitrogen content of the organic materials containing nitrogen is converted to ammonia to determine the nitrogen content of the sample.

ESCA Test Analysis

ESCA (Electron Spectroscopy for Chemical Analysis), also known as XPS (X-ray Photoelectron Spectroscopy), is the energy analysis of photoelectrons constituted at the surface of the fabric sample by X-Ray irradiation.

Hydrophilicity determination

Hydrophilicity property (water absorption property) of the treated and untreated wool fabric samples was determined according to TS 866 standard. This test is based on measuring the absorption time of the water droplets dropped onto the textile material. Moreover,

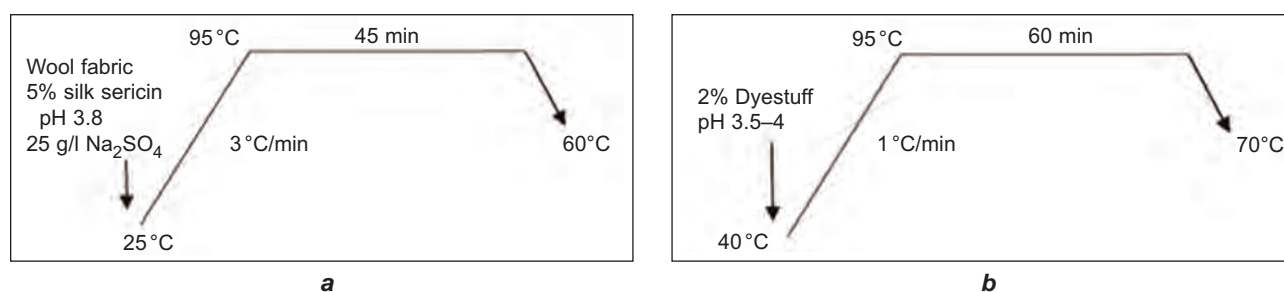


Fig. 1. Silk sericin pre-treatment process and following wool dyeing process:
a – sericin pre-treatment profile; b – dyeing profile

sinking test was also applied to the treated and untreated wool fabric samples according to TS 629 BS EN 14697 standard. The essence of this method is based on the determination of the immersion time of the sample deposited on the water by completely absorbing the water.

Dyeing uptake analysis

The absorbance values of the dye solutions (before and after dyeing process) were measured by utilizing a Perkin Elmer UV-Visible spectroscopy instrument. λ_{max} values of the dyebath containing Eriofast Red B reactive dye and Eriofast Blue 3R reactive dye were 515 nm and 590 nm, respectively. The absorbance values of the studied reactive dyes at their λ_{max} points were considered for dye-uptake calculations. The percentage reactive dye uptake by the wool fabrics was calculated using below equation:

$$Dye\ Uptake\ (\%) = \frac{(A_b - A_a)}{A_b} \times 100 \quad (1)$$

where A_b is the absorbance of the dye bath before dyeing process, A_a – the absorbance of dye bath after dyeing process.

Colour fastness determination

Wash, rub and light fastness properties were investigated. Wash fastness to domestic laundering (C06) was determined according to ISO 105:C06 A2S test in a M228 Rotawash machine (SDL ATLAS, UK). The wash fastness test was performed at 40°C. Both dry and wet rub fastness tests were performed according to the ISO 105: X12 protocol. Colour fastness of the dyed wool fabrics to washing and to dry & wet rubbing was determined via using ISO grey scales.

RESULTS AND DISCUSSIONS

Effects of silk sericin pre-treatment on wool fabric

The whiteness values of the sericin applied wool fabrics decreased by about 2 points compared to the untreated wool fabric. In parallel with the decrease in whiteness degree, the yellowness values of the sericin applied wool fabrics increased (table 1).

Table 1

WHITENESS AND YELLOWNESS INDEX LEVELS OF UNTREATED AND SERICIN PRE-TREATED WOOL FABRICS		
Fabric samples	Whiteness value (Stensby)	Yellowness index (E313)
Control (untreated wool)	53.35	21.93
Sericin treated wool	51.61	22.09

In the literature, the nitrogen content of wool fibre is given as in the range of 16%–17% [19, 20]. The nitrogen content of the sericin applied wool fibre was measured as 18% (table 2). Therefore, the nitrogen content of the wool fibres pre-treated with sericin protein via exhaustion method increased (table 2). The increase in nitrogen content of the wool fibre fabric indicates that the application of sericin protein to wool fibres was successful.

Table 2

NITROGEN DETERMINATION BY KJELDAHL METHOD	
Fabric samples	Amount of Nitrogen (%)
Control (untreated wool)	16
Sericin treated wool	18

ESCA analyses were performed to determine the changes in surface characteristics of wool fibres before and after sericin pre-treatment. The results of this analysis are shown in figure 2.

The N content (%) increased in the structure of wool fibres when treated with sericin (figure 2). The nitrogen content of sericin-treated wool fibres increased from 6.5% to 6.6%.

Both hydrophilicity test methods showed that the hydrophilicity property of sericin treated wool fabrics improved when compared to untreated wool fabric (table 3).

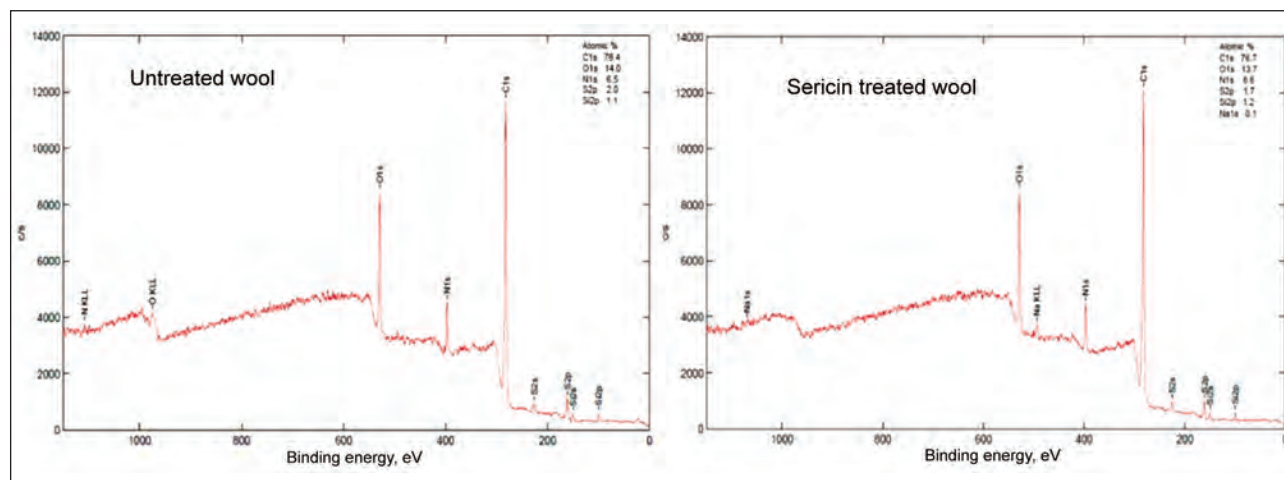


Fig. 2. ESCA analysis graphs of sericin pre-treated and un-treated wool fabrics

Table 3

HYDROPHILICITY PROPERTIES OF UNTREATED AND SERICIN TREATED WOOL FABRICS		
Hydrophilicity test methods	Control (untreated wool)	Sericin treated wool
Sinking test method (sinking time in seconds)	245	90
Drop test method (wetting time in seconds)	337	115

According to the FTIR spectrum of the sericin pre-treated wool fibre; the number of H and OH groups increased at 3000 cm^{-1} wavelength with pre-treatment of sericin (figure 3).

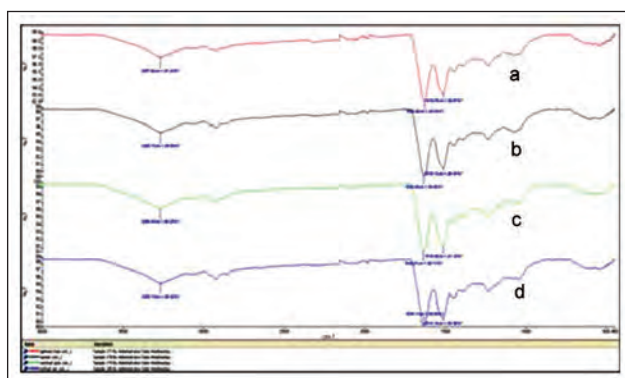


Fig. 3. FTIR graph of: a – untreated wool fabric (as control); b – sericin pre-treated wool fabric, c – untreated dyed wool fabric; d – sericin pre-treated and dyed wool fabric

Effects of silk sericin treatment on colour strength and fastness properties

Dye-uptake results

In order to determine the effect of sericin pre-treatment on reactive dye uptake, pre-dyeing and post-dyeing

samples were taken from dye baths and dye-uptake (%) values were calculated and shown in table 4. Table 4 shows that pre-treatment with sericin increases the amount of dyestuff absorbed by wool fibres.

In earlier study, it was reported that the functional groups present in sericin i.e. $-\text{NH}_2$, $-\text{COOH}$, and $-\text{OH}$ increased the reactivity of cotton fibre fabric towards natural dye that subsequently improved the dye-uptake results [21]. It is known that the more amine groups results in more positive places on the fibre material as a place to bind the available reactive dyes [22]. By applying the sericin containing NH_2 , $-\text{COOH}$, and $-\text{OH}$ groups [20] as pre-treatment to wool fibre, the number of functional groups that will make covalent bonds with reactive dyestuffs in wool fibre increased [22] and consequently dye-uptake increased. The K/S and L^* , a^* , b^* , h° and C^* values of the sericin pre-treated and untreated dyed wool fabrics are given in table 5.

The L^* (Lightness / Darkness; Black = 0 and White = 100) value of the woollen sample dyed with Eriofast Red B after pre-treatment with sericin protein was lower than the untreated sample (table 5). The colour is darker in the case of sericin pre-treated wool fabric than the untreated sample. The colour strength of the sericin pre-treated wool fabric (K/S value of 14.15) increased by 57% compared to the colour strength of the sericin-pre-treated wool sample (K/S value of 9.03) (table 5). The sericin pre-treated wool fabric is more red (a^* ; Red = Positive Value ($+a^*$) and Green = Negative Value ($-a^*$) and more yellow (b^* ; Yellow = Positive Value ($+b^*$) and Blue = Negative Value ($-b^*$)) than the sericin untreated wool fabric. Chroma (C^*) and hue angle (h°) values of sericin treated wool fabric were higher than those of untreated wool fabric counterparts (table 5).

In the case of wool fibres pre-treated with sericin and dyed; L^* (lightness-darkness) value decreased, and therefore leading to higher colour strength. The colour strength value (K/S value of 9.37) of the pre-treated

Table 4

DYE-UP TAKE RESULTS OF SERICIN PRE-TREATED AND UNTREATED WOOL FABRICS				
Dye Type	Eriofast Red B Reactive Dye		Eriofast Blue 3R Reactive Dye	
Fabric Type	control (untreated wool)	sericin treated wool	control (untreated wool)	sericin treated wool
λ_{max} (nm)	515		590	
Dye uptake (%)	62	99	66	91

Table 5

COLORIMETRIC PROPERTIES OF SERICIN PRE-TREATED WOOL FABRICS DYED AT 95°C							
Dye type	Fabric type	Colour strength (K/S)	L^*	a^*	b^*	h°	C^*
Eriofast Red B	control untreated wool)	9.03	46.53	52.65	4.53	52.85	4.92
	sericin treated wool	14.15	41.03	55.47	10.5	56.45	10.72
Eriofast Blue 3R	control (untreated wool)	6.81	41.30	2.28	-36.64	273.45	36.66
	sericin treated wool	9.37	36.92	4.63	-37.53	277.14	37.57

with sericin and dyed wool fabric with Eriofast Blue 3R is higher than the colour yield value of the non-pre-treated and dyed wool fabric (6.81). Sericin pre-treated wool fibres; L^* (lightness-darkness) value decreased, ie darkened colour. a^* increased; The sericin pre-treated sample is redder than the sericin untreated sample. b^* value of the series of pre-treated wool fabric decreased; The series has shifted to more blue than the sample without pre-treatment. The C^* value of the sericin-treated wool fabric (Chroma, Saturation) and h° (hue angle) increased compared to the untreated fabric (table 5). Sericin pre-treated samples were redder (with higher a^* values) than sericine untreated samples. The b^* value of the pre-treated woollen fabric of the series decreased. Therefore, the colour of the sericin pre-treated wool fabric shifted to a more blue colour than the sericin-untreated sample (table 5).

The dyeing was also carried out at 75°C, 80°C and 85°C (apart from 95°C) with the idea that wool fibre could be dyed at lower temperatures without damaging the fibres and as a result, energy and time savings could be achieved. The colour characteristics of the dyed samples are given in table 6. The colour strength of the untreated wool sample and dyed with Eriofast Red B at 95°C was 9.03 and the colour strength of the sericin pre-treated and dyed wool sample was measured as 14.05. The colour strength value of pre-treated and dyed wool fabric at 85°C

(K/S value of 12.78) was higher than the colour strength of untreated and dyed sample at 95°C (K/S value of 9,03) (table 6). When pre-treated with sericin, it is also possible to dye wool fabric at 85°C with high colour yields (table 6 and figure 4).

The sericin pre-treated wool fibre dyed at 80°C (K/S value of 9.24) displayed approximately similar colour strength value with the un-pre-treated wool fabric dyed at 95°C (K/S value of 9.03) (table 6 and figure 4). When the dyeing temperature is lowered to 75°C; the colour strength of sericin treated wool fabric was measured as K/S of 8.50. This value is less than the colour strength value of the sericin un-treated reference wool fabric dyed at 95°C (K/S value of 9.03).

According to the results obtained; with the application of sericin protein as a pre-treatment, it is possible to dye wool fibres at lower temperatures, i.e. at 85°C or at 80°C instead of 95°C. However, in determining the optimum dyeing temperature, fastness properties as well as colour yield should be taken into consideration.

Colour fastness performance of dyed woollen fabrics

The rubbing fastness results of the woollen fabric samples dyed at different temperatures (95°C, 85°C, 80°C, 75°C) are the same for sericin pre-treated and un-pre-treated samples (table 7). Although the colour yields of sericin pre-treated wool fibres are higher than the colour yields of sericin untreated wool fibres,

it is noteworthy that the rubbing fastness properties of the sericin pre-treated wool fibres were at same level with the rubbing fastness properties of the untreated wool fibres (table 7).

Washing fastness values for cotton fibre staining of wool fabrics dyed at 80°C and 75°C were lower than those of wool fabrics dyed at 85°C and 95°C (table 8). Wool fabrics dyed with Eriofast Red B at 80°C and 75°C started to contaminate cotton fibre with 4/5 and 4 grey scale rating, respectively (table 8).

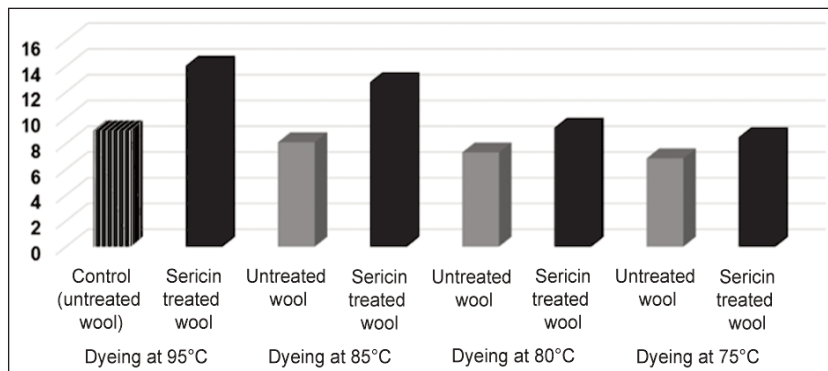


Fig. 4. Colour strength (K/S) of pre-treated or untreated and dyed (at different dyeing temperatures) wool fabrics

Table 6

COLORIMETRIC PROPERTIES OF PRETREATED (WITH SERICIN) AND DYED WOOL FABRICS AT DIFFERENT TEMPERATURES							
Dyeing temperature (Dyed with Eriofast Red B)	Fabric type	Colour strength (K/S)	L^*	a^*	b^*	h°	C^*
95°C	Control (untreated wool)	9.03	46.53	52.65	4.53	52.85	4.92
	Sericin treated wool	14.15	41.03	55.47	10.50	56.45	10.72
85°C	Untreated wool	8.11	45.99	54.44	6.04	54.78	6.33
	Sericin treated wool	12.78	42.37	56.07	10.07	56.99	10.19
80°C	Untreated wool	7.32	48.70	60.30	10.83	61.04	10.88
	Sericin treated wool	9.24	47.43	61.55	11.30	62.02	10.39
75°C	Untreated wool	6.86	52.10	58.90	8.82	60.01	8.06
	Sericin treated wool	8.50	49.49	61.16	10.24	62.10	10.02

Table 7

RUB FASTNESS PROPERTIES OF PRETREATED AND DYED WOOL FABRICS							
Dyestuff	Dyeing temperature	K/S (untreated wool)	K/S (sericin pretreated wool)	Rub fastness (X12) (cotton staining)			
				Wet*		Dry*	
				untreated wool	sericin pretreated wool	untreated wool	sericin pretreated wool
Eriofast Red B	95°C	9.03	14.15	3	3	4	4
Eriofast Red B	85°C	8.11	12.78	3/4	3/4	4/5	4/5
Eriofast Red B	80°C	7.32	9.24	3/4	3/4	4/5	4/5
Eriofast Red B	75°C	6.86	8.50	3/4	3/4	4/5	4/5
Eriofast Blue 3R	95°C	6.81	9.37	3/4	3/4	5	5

* Intermediate rating with underlined numbers indicates that the specimen's staining tended to be towards the underlined end of the range, and an underlined figure indicates that the grading was probably within a 0.25 point of that value.

Table 8

WASH FASTNESS PROPERTIES OF PRETREATED AND DYED WOOL FABRICS								
Dye Type	Dyeing temperature	Treatment*	Wash fastness staining (C06-A2S)					
			Wool	Polyacrylic	Polyester	Nylon	Cotton	Acetate
Eriofast Red B	95°C	-	5	5	5	5	5	5
		+	5	5	5	5	5	5
Eriofast Red B	85°C	-	5	5	5	5	5	5
		+	5	5	5	5	5	5
Eriofast Red B	80°C	-	5	5	5	5	4/5	5
		+	5	5	5	5	4/5	5
Eriofast Red B	75°C	-	5	5	5	5	4	5
		+	5	5	5	5	4	5
Eriofast Blue 3R	95°C	-	5	5	5	5	5	5
		+	5	5	5	5	5	5

* – untreated wool; + sericin treated wool

Thanks to the application of the sericin protein as a pre-treatment, the wool fibre can be dyed at lower dyeing temperatures (for instance: 10°C lower; 85°C versus 95°C) with good level of colour fastness.

CONCLUSIONS

Sericin is an amorphous and globular protein and constitutes 25 to 30% of the silk proteins. In this study, the effects of biodegradable, antibacterial, UV resistant silk sericin protein on the dyeing of wool fabrics were investigated. It was determined that the whiteness of the sericin pre-treated wool fabrics decreased by 2 points but the hydrophilicity values improved. Eriofast Red B and Eriofast Blue 3R reactive dyes were applied on sericin pre-treated and non-pre-treated wool fabrics. It was determined that the colour strengths of wool fabrics pre-treated with sericin increased in the case of both reactive dyes.

The rub fastness results of the wool fabric samples dyed at different temperatures (95°C, 85°C, 80°C, 75°C) are the same for sericin pre-treated and unpre-treated samples. Washing fastness decreased for wool fabrics dyed at 80°C and 75°C. With the application of the sericin protein as a pre-treatment, it was determined that the wool fabric could be dyed with Eriofast Red B reactive dye at 10°C lower dyeing temperature (85°C) leading to high colour strength and good colour fastness levels. Overall, sericin pre-treated and dyed wool fibre fabrics displayed sufficient colour and colour fastness values even after dyeing at lower dyeing temperatures.

ACKNOWLEDGEMENT

Authors thank to Pamukkale University for their support. This paper was supported by Pamukkale University BAP (Scientific research project) Project No: 2015FBE017.

REFERENCES

- [1] Karmakar, S.R., *Chemical Technology in The Pre-Treatment Process Of Textiles*, In: Elsevier Science B.V., 1999
- [2] Yazıcıoğlu, G., Gülümser, G., *İpek ve Diğer Salgı Lifleri*, In: E.Ü. Mühendislik Fakültesi Ders Kitapları Yayın, 1993, 27
- [3] Anış, P., *Tekstil Ön Terbiyesi*, In: Alfa Akademi Basım Dağıtım, Bursa, 2005

- [4] Duran, K., Özdemir, D., ve Namlıgöz, E.S., *İpek Liflerindeki Serisinin Enzimatik Olarak Uzaklaştırılması*, In: Tekstil ve Konfeksiyon, 2007, 3, 182–186
- [5] Tarakçıoğlu, I., *Tekstil Terbiyesi ve Makineleri*, Cilt, 1979, 2
- [6] Ahsen, K.M., *Dyeing of Wool and Silk Fibres with a Conductive Polyelectrolyte and Comparing Their Conductance*, Report no. 2011.7.10, In: Masters in Textile Technology University of Boras, 2011, Available at: <http://www.diva-portal.org/smash/get/diva2:1308230/FULLTEXT01.pdf> [Accessed on November 2019]
- [7] Nargunamani, M., Selvakumar, N., *Degumming of Silk*, In: Colourage, 2002, 43–47
- [8] Atav, R., Ekinci, S., Namırtı, O., *İpekteki Serisin Artıklarının Giderilmesinde En Uygun Aktif Merkeze Sahip Proteaz Enziminin Belirlenmesi*, In: XIII. Uluslararası İzmir Tekstil ve Hazır Giyim Sempozyumu, İzmir, 2014
- [9] Capar, G., Aygun, S.S., Gecit, M.R., *Treatment Of Silk Production Wastewaters By Membrane Processes For Sericin Recover*, In: J Memb Sci., 2008, 325, 2, 20–931
- [10] Mowafi, S., El-Kheir, A.A., Taleb, M.A., El-Sayed, H., *Keratin and Sericin: State of the Art and Future Outlook*, In: Der Pharma Chemica, 2016, 8, 21, 22–30, <http://www.derpharmachemica.com/archive.htm>
- [11] Rajendran, R., Balakumar, C., Sivakumar, R.T., Amruta, N., *Extraction and application of natural silk protein sericin from Bombyx mori as antimicrobial finish for cotton fabrics*, In: The Journal of The Textile Institute, 2011, 103, 4, 458–462
- [12] Gupta, D., Chaudhary, H., Gupta, C., *Sericin-based polyester textile for medical applications*, In: The journal of The Textile Institute, 2015, 106, 4, 366–376
- [13] Saha, J., Mondal, M.I.H., Sheikh, M.R.K., Habib, M.A., *Extraction, Structural and Functional Properties of Silk Sericin Biopolymer from Bombyx mori Silk Cocoon Waste*, In: J Textile Sci Eng, 2019, 9, 1, <https://doi.org/10.4172/2165-8064.1000390>
- [14] Babu, K.M., Ravindra, K.B., *Bioactive Antimicrobial Agents For Finishing of Textiles for Health Care Products*, In: The Journal of The Textile Institute, 2015, 106,7, 706–717
- [15] Haggag, K., Kantouch, F., Allam, O.G., El-Sayed, H., *Improving Printability of Wool Fabrics Using Sericin*, In: Journal of Natural Fibers, 200, 6, 3, 236–247
- [16] Jassim, K., Al-Saree, O., *Study of the Antimicrobial Activity of Silk Sericin From Silkworm Bombyx Mori*, In: Dept. of Basic Science, 2010, 23, 2
- [17] Khalifa, I.B., Ladhari, B., Touay, M., *Application of sericin to modify textile supports*, In: The Journal of The Textile Institute, 2011, 103, 4, 370–377
- [18] Das, D., Bakshi, S., Bhattacharya, P., *Modification of Jute With Sericin For Improvement In Dyeing*, In: International Journal of Latest Trends in Engineering and Technology, <http://dx.doi.org/10.21172/1.122.02>
- [19] Akcalı, K., Blut, M.O., *Plazma Teknolojilerinin Yün Elyafı Üzerindeki Etkileri Üzerine Bir İnceleme*, In: Mühendislik Bilimleri ve Tasarım Dergisi, 2012, 2, 1, 65–72
- [20] Simpson, W., Crawshaw, G.H., *Wool: Science and Technology*, In: The Textile Institute, 2008
- [21] Bhandari, B., Saroj, S., Singh, J., Neelam, M.R., *Effect of sericin treatment conditions on dye ability of cotton fabric*, In: Journal of Applied and Natural Science, 2018, 10, 1, 102–106
- [22] Umam, K., Fitria, N., *Surface Modification of Polyester Fiber With Sericin for Cold Reactive Dyeing*, In: AIP Conference Proceedings, 2018, <https://doi.org/10.1063/1.5082406>

Authors:

CENGİZ ONUR ESER, ARZU YAVAS

Pamukkale University, Engineering Faculty, Textile Engineering Department,
20160, Denizli, Turkey

Corresponding author:

ARZU YAVAS
e-mail: aocerdem@pau.edu.tr

The impact of online marketing on the use of textile packaging: an approach to consumer behaviour

DOI: 10.35530/IT.072.02.202019

STEFAN-CLAUDIU CAESCU
FLORINA BOTEZATU
RALUCA-GIORGIANA CHIVU

IONUT-CLAUDIU POPA
MARGARETA STELA FLORESCU

ABSTRACT – REZUMAT

The impact of online marketing on the use of textile packaging: an approach to consumer behaviour

Online marketing is the act of utilizing online channels and tools to spread a message or idea about an organization's image, items, or administrations to its potential clients. The strategies and methods used for Internet showcasing incorporate email, online networking, show promoting, website streamlining, Google AdWords, and that's just the beginning.

Online marketing has become more and more used in recent years, whether it is about promoting products or services, or it is about ideas, concepts, and beliefs. Considering this aspect, this article aims to identify the influence of online communications on the adoption or acceptance by consumers of products packaged in textiles. In recent years there has been a significant discussion in the literature on the role and purpose of packaging (promotion, product protection, advertising), but they have not highlighted consumer preferences for packaging and the impact of online marketing on them.

Keywords: attributes of packaging, behaviour influences, marketing concept, online marketing, textile packaging

Impactul marketingului online asupra utilizării ambalajelor textile: o abordare a comportamentului consumatorului

Marketingul online este actul de a utiliza canale și instrumente online pentru a distribui un mesaj sau o idee despre imaginea, articolele sau informațiile administrative ale unei organizații către clienții potențiali ai acesteia. Strategiile și metodele utilizate pentru prezentarea pe internet includ e-mail marketing, rețele online, promovarea prin evenimente, eficientizarea site-ului web, Google AdWords și multe altele.

Marketingul online a devenit din ce în ce mai utilizat în ultimii ani, fie că este vorba despre promovarea produselor sau serviciilor, fie despre idei, concepte, credințe. Având în vedere acest aspect, prezentul articol își propune să identifice influența comunicărilor online asupra adoptării sau acceptării de către consumatori a produselor ambalate în materiale textile. În ultimii ani, a existat un interes semnificativ în literatura de specialitate cu privire la rolul și scopul ambalajului (promovare, protecția produselor, publicitate), dar nu a evidențiat preferințele consumatorilor pentru ambalaje și impactul marketingului online asupra acestora.

Cuvinte-cheie: attribute ale ambalajului, influențe ale comportamentului, concept de marketing, marketing online, ambalaje textile

INTRODUCTION

In a world where consumers are increasingly adopting online shopping habits, marketing strategies are consequently adapting to this trend, with online marketing increasing its versatility as well. Considering this, the present research aims to address the impact of online marketing on the acceptance of textile packaging, by identifying the factors playing a role in the changes in consumer's behaviour and establishing the determinants.

Marketing is an essential part of any business or idea, and without solid marketing goals and the right strategy for achieving them, a company cannot grow and will not be resilient in the market in the long run. With the advances of our society, especially the Internet, many online promotion tools and techniques are now available to any organization and have often

proven to be more profitable than the traditional marketing tools used for decades. As a result, according to Kotler & Keller [1], online marketing channels are increasingly important not only in building and consolidating brands, but in increasing sales as well and as Popescu [2] asserts, "in the face of a dynamic, ever-changing environment, the modern organization must seek to adapt to its evolution".

Thus, according to Negricea [3], online communication has advantages for consumers and marketers, the Internet enabling direct interaction between consumers with common interests not only between producer and consumer. Furthermore, Negricea [3] observed that the marketing specialist benefits from the emergence of new sales channels, targeted messaging, measurability, continuous availability of messages, interactive dialogue with the consumer, personalization of the offer, loyalty, while the consumer

enjoys advantages such as ease of online activity, continuous availability of the offer, a wide range of information sources, access to other customer reviews, fundamental decisions, quick and even real-time response, information available on request, as well as a high degree of satisfaction.

The most important online marketing tools are online advertising, email marketing, search marketing, newsgroups (social media), website and blog marketing. In addition, "on a variety of digital platforms, a wide range of consumer engagement practices have evolved, including, for example, advertising games, reading (and writing) customer reviews, and watching, appreciating, and distributing consumer videos, brand, blogs" [4].

"Online advertising is any form of impersonal communication, paid or compensated by barter, through which information about products, services, ideas or values are transmitted by an identifiable organization or person, through the website or by email [3]. Thus, "the Internet has become a media vehicle for sponsored communications" [5], which are now almost daily or even daily in the life of an Internet user.

Email marketing summarizes all communications, commercial or not, initiated by a company with the help of email and aim to strengthen and maintain the relationship with the consumer, developing and managing the database [3]. Data on current and potential customers enables an increase in the conversion rate and in reach via promotional messages or public information about the company. Newsletters fulfil several tasks such as: remembering the company's presence, providing information to the consumers, increasing brand credibility, facilitating online ordering for the organization's products or services, and obtaining customer feedback [6].

A website is an online marketing tool without which the virtual presence of the company would be severely affected and is "the basis of internet marketing" [7]. The website must be designed in a way that facilitates its navigation and provides an effortless experience for the visitor. A well-structured website influences users to take as many actions as possible. The site informs and promotes the company's products or services.

GENERAL INFORMATION ABOUT CONSUMER BEHAVIOUR AND ONLINE MARKETING INFLUENCES

Since the end of the year, the term online marketing and social media have developed significantly [8]. There is another type of promotion that focuses on offering new potential advertisements to advertisers to provide information regarding a good or service. This contrasts with the usual average impact across other communication channels, mainly due to the possibility of feedback from other buyers through reviews [8]. Buyer behaviour is a significant part of advertising, as it helps advertisers safely design promotional campaigns for the target group.

Millions of dollars are spent on marketing trying to study consumers' behaviour and to influence what, when and how they consume. This kind of knowledge enables a versatile marketing research. A TV commercial can be annoying when it interrupts a favourite show, but it can also be an excellent source of information on the target audience and on the underlying behavioural assumptions. Indeed, given the pervasive nature of advertisements, understanding how they try to influence consumers is essential in understanding our environment [9].

Consumer behaviour is a form of manifestation and of the decision process of the human behaviour in general. As a result of this marketing component, the action of explain consumer behaviour was defined by specialists in several ways, none of which enjoyed universal significance. In a narrow sense, consumer behaviour reflects people's preference in buying, consuming material goods and services as well as their stance on certain social aspects. It encompasses the entire conduct of the end-user of tangible and intangible assets [10].

The theory of the psychological and social network offers a considerable promise for improving our understanding of internet marketing in several dimensions.

First, the Internet is an environment through which consumers interact, communicate and respond. The theory of the psychological and social network thus provides an essential framework for correlating internal and social decision-making processes.

Second, the Internet is complex and requires an understanding of consumers' existing attitudes, beliefs, and social interactions that manifest and then transfer from the store to their online experiences.

Third, because many shopping experiences are based on impact, the Internet is a composite of visual, individual, and interpersonal stimuli. Eventually, the Internet is increasingly becoming a social environment through which consumers seek and share information with others.

In general, information processing has been and should continue to be a key topic in Internet marketing. The way consumers process, evaluate and respond to the stimuli of the information they are exposed to is an essential source of theoretical and applied materials for web designers and users.

Research examining information processing, learning and attitude formation in the context of mobile communications, multiple marketing communications, integrated communication channels, social content and user-generated content is particularly justified [11].

Consumers may prefer information through experience, rather than search, even when the experience is expensive. Searching can sometimes be even more expensive. For example, in purchasing most appliances, consumers face this problem.

Determining by inspection the time flow of services from alternative brands of a device is extremely difficult. Therefore, the experience could be used as a cheaper information procedure.

We assume that, although we have experienced in brands of the same product, the consumer can certainly determine the preferred brand among them. Moreover, the favourite brand will remain so over time. This is also true for adopting changes to already known products and ideas. We still believe that the only way to experience the difference is to buy it. As in the case of search, the consumer should obtain information through experience until the marginal cost of the data becomes more significant than his marginal profitability.

Online marketing has led to significant changes in consumer behaviour in terms of access to information and news, changes caused mainly by changes in factors that contribute to shaping online consumer behaviour such as increasing knowledge about a particular product or service or identifying a new need. This is due to the relevance of marketing research that shows that web experience generates changes in mental processes that trigger the decision to adopt ideas much faster. Therefore, marketers should recognize the importance of studying the factors that influence online consumer behaviour and their growing power in the digital world.

Various types of factors influence consumer behaviour. For the most part, traders cannot control these factors, but they must take them into account. Traders need to understand both the theory and the reality of consumer behaviour.

Web experience includes elements such as researching, browsing, finding, selecting, comparing and evaluating alternatives, as well as interacting and trading with that particular company influenced by web page design. The purpose of these elements is to attract consumers and change the outcome of online interaction.

The most representative psychological factor that influences consumers' online behaviour is online perception. Perception is the process of interpretation by which consumers understand their environment. Many people believe that attitude is passive; that is, you can see and hear what is there objectively. However, people actively perceive stimuli and objects in the environment, including the online world. At the same time, perception is an approximation of reality. The brain tries to make sense of the stimuli to which it is exposed.

Personality greatly influences online consumer behaviour. In the online environment, consumers may have different characters compared to everyday life; they can use their ego to communicate in different personalities or mixed identities. Social networks are full of ideas designed by people to increase their chances of socializing with another virtual environment, and marketers focus on the visual and auditory characteristics of a product or service to connect with the inner part of the consumer and identity/virtual identities. [12]

Online strategies should first focus on the market segment with a high degree of involvement in Internet marketing, such as students or business professionals with a high level of education and income.

By providing more information about products, customer service and convenient payment methods, internet marketing can help increase the frequency of online shopping and money spent. The online purchase rate is limited by low revenue. To reach these consumers, the online marketing manager should emphasize the promotion of the company and the promotion of products through advertising. As increased trust and, ultimately, use, the implementation of more information and development can stimulate the use and rates of online shopping [13].

TEXTILE PACKAGING – NEW MARKETING CONCEPT

The package represents the science, quality and innovation of framing or securing items for circulation, storage, trading and use. The package contains, insures, blocks, ships, lights and sells. Customers consider the quality of the item and its ease of use; however, they also appreciate the package plan of an item when purchasing a particular product.

The package of an item is more than a way of assurance and capacity, assuming the first impact for a buyer when buying an item (packaging design, handling), thus fulfilling one of the main purposes when purchasing a good (content protection, ease The packaging and its characteristics are an essential factor because package components, such as package shading, foundation image, package material, text style, cover structure, printed data and development, are considered important factors in selling an item. Packaging plays a crucial role in the visual presentation of the product, especially in the retail sector (where packaging is visible and accessible for analysis by shopping) and could be treated as one of the most significant elements to have an impact on the buyer's choice.

As Rundh [14] points out, the package stands out for the consumer of a specific brand, contributing to the improvement of the image and the recognition of an item by the comparator. In this way, the package plays an important place in the presentation of correspondence and could be treated as one of the most significant variables that affect the buyer's choice. Packaging encourages buyers to choose the item from the full range of comparable items, practically contributing to the formation of the decision to purchase a particular good or brand. According to Kotler [1], there are six components that must be evaluated when using package options: size, structure, material, shading, content and brand.

Renaud [15] analysed the elements of brand and product legitimacy, as well as purchasing behaviour. Packaging/labelling has a relative significance when contrasted with other properties of the item, such as rating systems used in consumer buying behaviour (e.g., if a consumer is familiar with a particular product, it will not change preferences depending on the packaging of other similar products).

According to Prathiraja [16], when a buyer ponders purchasing options, their choice often gravitates

towards the marking on the items, especially if they recognize it. Many buyers are willing to pay extra if the information on the package is trustworthy. Nutrition labelling can be considered a method of promotion used to provide customers with relevant data on the nutritional values of the product. There are consumers who do not appreciate a substance added to a product (for obtaining functional foods), because in general, buyers are convinced of the content of the supplement, depending on the promotion, the general messages of well-being and their knowledge in food sciences. As Jeddi pointed out [17], packaging made of cheap materials such as polyolefin filaments, have modified the standard materials used for packaging, generating the creation of advanced strategies and applications for packaging and labelling. The high quality and consistency of the designed materials, combined with modern materials that contribute to the promotion strategies have allowed the adaptation of packaging used in mass production, for protection, efficient handling and increasingly efficient circulation capacity in the case of powdered contents and granules, raw materials, composts, sand concrete, sugar, flour and dyes. Lighter clothing, including nonwovens, such as wet, glued fabrics, is used as packaging in the food industry, in the transportation of medicines and the protection of electronic parts. Leather belts and materials are generally used for bonding and include high thickness polyethylene, low thickness polyethylene, polypropylene, biaxially located polypropylene, polystyrene, polycarbonate, polyester, nylon and fluoropolymers. Depending on the idea of the item to be incorporated and the type of material used, the grouping may be called dynamic incorporation, aseptic package, which maintains the food grouping, clinical/pharmaceutical package, a grouping of hazardous substances and new package (sales label) [18].

MODELLING THE CONSUMER'S BEHAVIOR REGARDING THE ACCEPTANCE OF TEXTILE PACKAGING

Modelling of the consumer's behaviour regarding the acceptance of packaging made of textile materials represents the analysis of the factors that contribute to the formation of the preference and the adoption of the new proposed packaging. The research methodology consisted on one hand (if later "on the other hand" is used), in conducting quantitative research among consumers to identify issues such as time spent online, the attention they pay to online advertising, the perceived impact that online marketing has on purchasing and consumption decisions, and on the adoption of textile packaging. On the other hand, quantitative research also identified the aspects that consumers consider useful and necessary in packaging and the conditions under which they might adopt or create a preference for packaging made of textiles.

The tool used in quantitative research was a questionnaire consisting of 25 questions, six of which were related to identification and classification. For modelling by structural equations, the least-squares technique and the WarpPIs program were used (modelling by structural equations was performed using the least-square technique and the WarpPis program). Modeling by structural equations is a multivariable measurable examination method that is used to dissect and analyze primary connections. This involves investigating the links between the factors involved and generating sustained links. From a mathematical point of view through the auxiliary association between the estimated factors and the inactive development. Researchers favor this strategy because it assesses dependence and dependent relationships in an individual survey.

The impact of online marketing on consumers' decisions to accept packaging from textiles is achieved by testing each link proposed in the conceptual model (figure 1). For each arrow marked with an Hx,

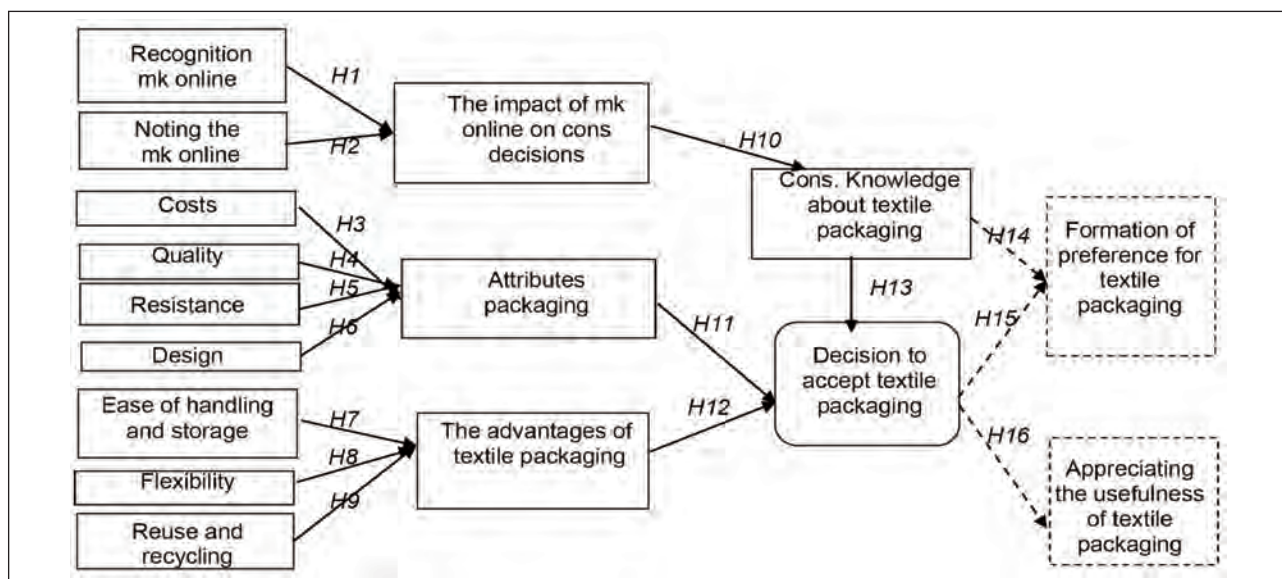


Fig. 1. A conceptual model for Consumer's behaviour regarding the acceptance of textile packaging

VALIDATION OF THE MAIN HYPOTHESES OF THE PROPOSED CONCEPTUAL MODEL				
Hypotheses	Main hypothesis	β	p	Validation
H1	Recognition marketing online → The impact of marketing online on cons. decisions	0.67	<0.01	Yes
H2	Noting the marketing online → The impact of marketing online on cons. decisions	0.42	<0.01	Yes
H3	Costs → Attributes packaging	0.66	<0.01	Yes
H4	Quality → Attributes packaging	0.51	<0.01	Yes
H5	Resistance → Attributes packaging	0.28	=0.04	Yes
H6	Design → Attributes packaging	1.08	<0.01	Yes
H7	<i>Ease of handling and storage → The advantages of textile packaging</i>	0.13	=0.08	No
H8	<i>Flexibility → The advantages of textile packaging</i>	0.01	=0.46	No
H9	Reuse and recycling → The advantages of textile packaging	0.32	<0.01	Yes
H10	The impact of marketing online on cons decisions → Cons. Knowledge about textile packaging	0.85	<0.01	Yes
H11	Attributes packaging → Decision to accept textile packaging	0.23	<0.01	Yes
H12	The advantages of textile packaging → Decision to accept textile packaging	0.54	<0.01	Yes
H13	Cons. Knowledge about textile packaging → Decision to accept textile packaging	0.35	<0.01	Yes
H14	Cons. Knowledge about textile packaging → Formation of preference for textile packaging	0.90	<0.01	Yes
H15	<i>Decision to accept textile packaging → Formation of preference for textile packaging</i>	0.08	=0.18	No
H16	Decision to accept textile packaging → Appreciating the usefulness of textile packaging	0.31	<0.01	Yes

there is an objective and a related hypothesis according to which there is a direct link between the two connected aspects.

The main hypotheses of the research correspond to the descriptions of the relationships between the latent components of the proposed model (table 1). These are tested by calculating the binding coefficients (Beta-standardized coefficients) corresponding to each causal relationship in the model. The value of the Beta coefficients indicates the strength and the direction of the correlation between the variables (specify which variables) while the validation of the hypotheses are materialized when the value of the related Beta coefficient is higher than 0.1 at a significance threshold $p < 0.05$ [19].

From the results, we can see that most of the proposed hypotheses have been validated efficiently, there are direct and positive links between two variables related to the proposed conceptual model. The invalidated hypotheses support the idea that consumers do not consider the “*possibility of handling and storage*” and “*flexibility of use*” as significant advantages of products packaged in textiles, but also that decision or preference for products packaged in dexterous materials are not necessarily formed.

Below you can see the diagram of the conceptual model generated by the analysis program by WarpPLS structural equations (figure 2).

CONCLUSIONS

The Internet and its ever-evolving technologies have influenced the way customers and vendors interact in the marketplace. Technology has been and will continue to be an engine of Internet marketing. Although several articles have studied the involvement of consumers in the decision to advertise products and purchase, little research has involved internet marketing. The theory of consumer behaviour has become in the last quarter of a century, especially after the emergence of the modern concept of marketing, a distinct and essential area of marketing. The evolution of the ways of approaching consumer behaviour is marked by the achievements obtained over time in terms of human knowledge in general, the explanatory answer on consumer reactions in certain situations and their decision-making processes, being treated from a sociological point of view, psychological or economic, which reflects an abundance of concepts and interpretations. Hence the numerous classifications and influencing factors determined in the research of consumer behaviour.

Such concepts have been successfully applied in the present research with the objective to analyse the impact of online marketing on acceptance of textile packaging. As a conclusion, we can consider that online marketing has a significant impact on consumer decisions in general, and on decisions to

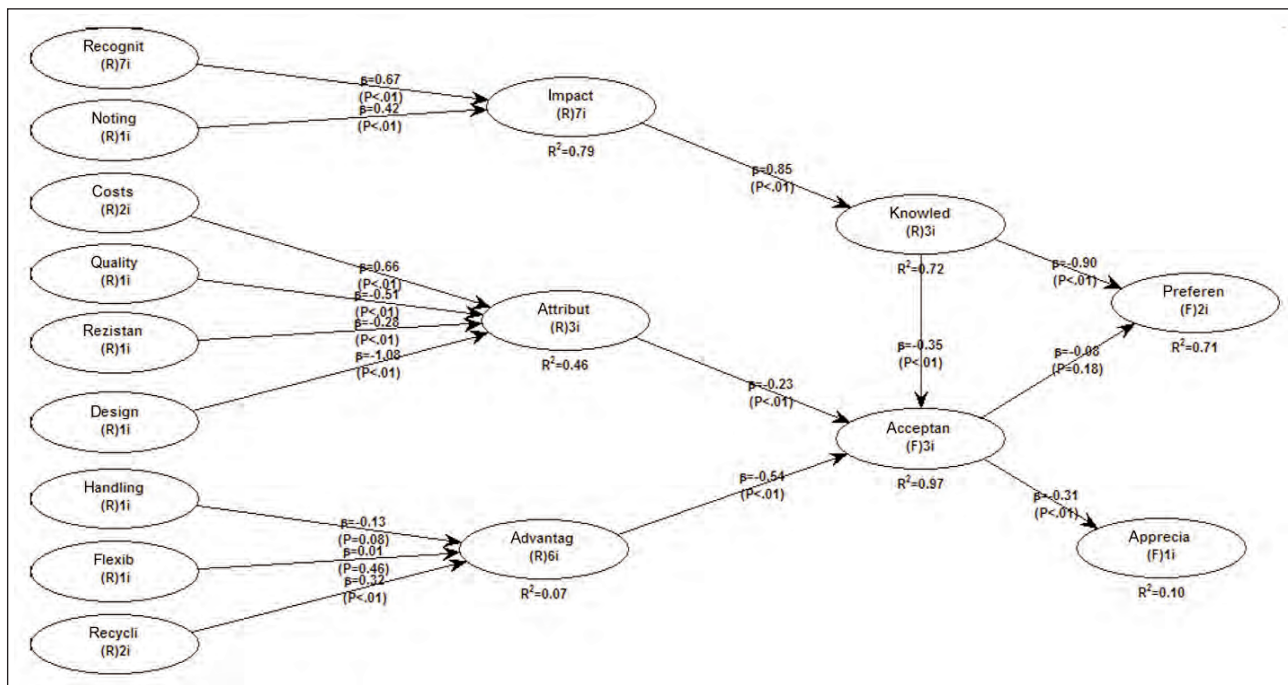


Fig. 2. Validated model for Consumer's behaviour regarding the acceptance of textile packaging (WarpPLS)

adopt and use products packaged in textiles in particular, highlighting again the role that online communications and information have on consumer behaviour. Online marketing, as we have seen in the research, is easily noticed by consumers, and they feel they have a significant level of influence on future

decisions. In the same way, the information from the online environment regarding the packaging made of textile materials contributes directly to the acquisition of knowledge, to the decision to accept them and to the development of preferences for this type of packaging and their advantages.

REFERENCES

- [1] Kotler, P., Keller, K.L., *Marketing Management*, 14th Edition, New Jersey: Prentice-Hall Publishing House, 2012
- [2] Popescu, I.C., *Communication in marketing – concepts, techniques, strategies*, Second Edition revised and added, Bucharest: Uranus Publishing House, 2003
- [3] Negricea, I.C., *Online Marketing Strategies: successful solutions for the development and implementation of online marketing applications in the organization's activity*, Bucharest: University Publishing House, 2010
- [4] Eigenraam, A.W., Eelen, J., Van Lin, A., Verlegh, P.W.J., *A Consumer-based Taxonomy of Digital Customer Engagement Practices*, In: Journal of Interactive Marketing, 2018, 44, 102–121, Available at: <https://www.sciencedirect.com/science/article/pii/S1094996818300495> [Accessed on May 2020]
- [5] Sharma, R., Alavi, S., Ahuja, V., *Generating trust using Facebook – A study of 5 online apparel brands*, In: Procedia Computer Science, 2017, 122, 42–49, Available at: <https://www.sciencedirect.com/science/article/pii/S1877050917325681> [Accessed on May 2020]
- [6] Hudak, M., Kianickova, E., Madlenak, R., *The importance of email marketing in e-commerce*, In: Procedia Engineering, 2017, 192, 342–347, Available at: <http://www.sciencedirect.com/science/article/pii/S18770581732605X> [Accessed on May 2020]
- [7] Madlenak, R., Madleeakova, L., Svadlenkab, L., Salava, D., *Analysis of Website Traffic Dependence on Use of Selected Internet Marketing Tools*, In: Procedia Economics and Finance, 2015, 23, 123–128, Available at: <https://www.sciencedirect.com/science/article/pii/S221256711500355X> [Accessed on May 2020]
- [8] Zarrella, D., *The Social Media Marketing Book*, O'Reilly Media, 2009
- [9] Hawkins, D.I., Mothersbaugh, D.L., *Customer behavior. Building marketing strategy*, 11th edition, United States: Library of Congress Cataloging, 2010
- [10] Balaure, V. (coordinator), Adăscăliței, V., Bălan, C., Boboc, Ș., Cătoi, I., Olteanu, V., Pop, N.A., Teodorescu, N., *Marketing*, 2nd Edition, Bucharest: Uranus Publishing House, 2002
- [11] Cummins, S., Peltier, J.W., Schibrowsky, J.A., Nill, A., *Consumer behavior in the online context*, In: Journal of Research in Interactive Marketing, 2014, 8, 3, 169–202, Available at: <https://www.emeraldinsight.com/doi/pdfplus/10.1108/JRIM-04-2013-0019> [Accessed on May 2020]
- [12] Cetină, I., Munthiu, M.C., Rădulescu, V., *Psychological and social factors that influence online consumer behavior*, In: Procedia – Social and Behavioral Sciences, 2012, 62, 184–188, Available at: <https://www.sciencedirect.com/science/article/pii/S1877042812034702> [Accessed on May 2020]

- [13] Wu, I., *Internet marketing involvement and consumer behavior*, In: Asia Pacific Journal of Marketing and Logistics, 2002, 14, 4, 36–53, Available at: <https://www.emeraldinsight.com/doi/pdfplus/10.1108/13555850210764945> [Accessed on May 2020]
- [14] Rundh, B., *The multi-faceted dimension of packaging*, In: British food journal, 2005
- [15] Renaud, I., *The influence of label on wine consumption: its effects on young consumers' perception of authenticity and purchasing behavior*, Bologna, Italy, 2007
- [16] Prathiraja, P.H.K., Ariyawardana, A., *Impact of nutritional labelling on consumer buying behavior*, In: Sri Lankan Journal of Agricultural Economics, 2003, 5 (1381-2016-115752), 35–46
- [17] Jeddi, N., *The Impact of Label Perception on the Consumers' Purchase Intention: An application on food products*, In: IBIMA business review, 2010
- [18] Dhandapani, Sharma, D.C., *Textiles for packaging*, 2005, 14, 31–34
- [19] Orzan, G., Platon, O.E., Ștefănescu, C.D., Orzan, M., *Conceptual Model Regarding the Influence of Social Media Marketing Communication on Brand Trust, Brand Affect and Brand Loyalty*, In: Economic Computation & Economic Cybernetics Studies & Research, 2016, 50, 1

Authors:

STEFAN-CLAUDIU CAESCU¹, FLORINA BOTEZATU¹, RALUCA-GIORGIANA CHIVU¹,
IONUT-CLAUDIU POPA¹, MARGARETA STELA FLORESCU²

¹Bucharest University of Economic Studies, Faculty of Marketing,
Bvd. Dacia no. 41, 010374, Bucharest, Romania

e-mail: stefan.caescu@mk.ase.ro, botezatufloor@gmail.com, popa.claudiu3@yahoo.com

²Bucharest University of Economic Studies, Faculty of Public Administration and Management,
Piata Romana, no. 6, 010374, Bucharest, Romania
e-mail: margareta.florescu@ari.ase.ro

Corresponding author:

RALUCA-GIORGIANA CHIVU
e-mail: raluca.chivu0126@gmail.com

Thermal comfort properties of cool-touch nylon and common nylon knitted fabrics with different fibre fineness and cross-section

DOI: 10.35530/IT.072.02.20209

YANG YANG
YU XIN
WANG XUNGA

LIU XIN
ZHANG PEIHUA

ABSTRACT – REZUMAT

Thermal comfort properties of cool-touch nylon and common nylon knitted fabrics with different fibre fineness and cross-section

Cool-touch nylon multi-filament yarns with good heat transfer performance are widely used in the development of knitted fabrics for summer and sports clothing. However, the physical properties of cool-touch nylon fibres, and the effect of fineness and cross-section on comfort-related properties of their knitted fabrics are still not well understood. In this study, the physical properties of cool-touch nylon fibres and common nylon fibres, and comfort properties of knitted fabrics from both fibre types were measured and compared. It was found that cool-touch nylon fibres have better moisture absorption, but slightly lower crystallinity than common nylon fibres. Regarding the fibre fineness and cross-section of cool-touch nylon and common nylon, knitted fabrics showed a similar dependence on thermal comfort properties. Cool-touch nylon fabrics had increased wicking capacity, thermal transfer, and cooling properties, but poorer drying performance and moisture permeability compared to common nylon fabrics. It was concluded that using nylon multi-filament yarns made up of finer filaments and cool touch filaments is an effective way to develop thermal-wet comfort knitted fabrics for summer and sports clothing applications.

Keywords: cool-touch nylon, physical performance, cross-section, fibre diameter, thermal comfort

Proprietățile de confort termic ale tricotelurilor din nailon cool-touch și din nailon comun, cu finețe și secțiuni transversale diferite ale fibrelor

Firele multifilamentare din nailon cool-touch, cu performanțe ridicate de transfer de căldură, sunt utilizate pe scară largă în dezvoltarea tricotelurilor pentru îmbrăcămintea pentru sezonul cald și îmbrăcămintea sport. Cu toate acestea, proprietățile fizice ale fibrelor de nailon cool-touch și influența fineții și a secțiunii transversale a acestor fibre asupra proprietăților de confort ale tricotelurilor nu sunt încă bine înțelese. În acest studiu, au fost măsurate și comparate proprietățile fizice ale fibrelor de nailon cool-touch și ale fibrelor din nailon comun, precum și proprietățile de confort ale tricotelurilor din ambele tipuri de fibre. S-a constatat că fibrele de nailon cool-touch au o absorbție a umidității mai ridicată, dar cristalinitate ușor mai scăzută decât fibrele din nailon comun. Din punct de vedere al fineții și secțiunii transversale a fibrelor de nailon cool-touch și nailon comun, tricotelurile prezintă o dependență similară de proprietățile de confort termic. Tricotelurile din nailon cool-touch au o capacitate ridicată de absorbție, transfer termic și proprietăți de răcire, dar performanțe mai scăzute de uscare și permeabilitate la umiditate comparativ cu tricotelurile din nailon comun. S-a ajuns la concluzia că utilizarea firelor multifilamentare din nailon formate din filamente mai fine și filamente cool-touch este o modalitate eficientă de a dezvolta tricoteluri cu proprietăți de confort termic pentru îmbrăcămintea pentru sezonul cald și îmbrăcămintea sport.

Cuvinte-cheie: nailon cool-touch, performanță fizică, secțiune transversală, diametrul fibrei, confort termic

INTRODUCTION

Nylons are high-performance materials with attractive physical and mechanical properties. They have moisture sensitive performance (official regain, 4.5%) [1], and their knitted fabrics offer good thermo-physiological comfort as well as high elasticity [2]. Thus, nylon knitted fabrics are widely used in the development of summer and sports clothing.

Thermal comfort plays an important role in determining clothing comfort and affects human physical and psychological well-being [3]. Cool-touch feeling has received much attention for summer clothing as well as sports and outdoor apparel for healthy living [4]. To improve the cool-touch feeling of nylon fabrics, many

effective methods have been reported, such as metal sputtering [5], nano-coating [6] on nylon fabrics, and producing cool-touch nylon fibres by adding nanoparticles to nylon matrix [7]. Jade-containing cool-touch nylon fibres [8] that were prepared by mixing jade nanoparticles into thermoplastic melt and extruding the melt to produce filaments, have attracted increasing attention in the development of knitted fabrics for sports clothing. Thermal comfort is mainly determined by air permeability, moisture management properties, and heat transfer performance. In a warm and humid environment, high air permeability increases comfort, and high thermal conduction of fabric is beneficial for cooling body when excessive

heat is produced [9]. Excellent moisture absorption and transfer by a fabric have the benefit of maintaining a dry and comfortable microclimate near skin after excessive sweating. A large amount of heat also could be absorbed and diffused during the moisture transfer process, which promotes the cooling function of clothing [10].

Factors that affect the thermal comfort properties of fabrics can be basically categorized into fibre, yarn, and fabric properties [11]. In terms of fibre properties, hydrophilicity, thermal conductivity, and the cross-section of a fibre influence heat and moisture transfer capacity [4, 12]. The hydrophilicity of fibre greatly influences its wicking behaviour [13], and the moisture sorption of fibre material in a fabric is associated with cool-touch feeling when skin contacts the fabric [14]. The fineness of fibres greatly affects the thermal comfort property of fabrics [15], and thermal comfort is enhanced with the decrease of fibre diameter. The composition and fibre cross-section affected the cooling efficiency of fabrics, especially, knitted fabric containing polyester yarns with grooved surface showed good cooling capacity [16]. Furthermore, the thickness and porosity of fabric [17] affect the thermal comfort properties of fabrics, as increasing the fabric thickness improves thermal insulation and higher porosity benefits breathability.

However, few studies have been reported on the properties of cool-touch nylon fibres containing jade nanoparticles and their fabrics. This work aims to extend the scope of thermal comfort research on cool-touch nylon fibres and their knitted fabrics by conducting a comparative study between cool-touch

nylon and common nylon. In this work, physical properties of cool-touch nylon and common nylon fibres, breathability, moisture transfer, thermo-physiological and cooling characteristics of their knitted fabrics, were investigated and compared. Meanwhile, the effects of fibre fineness and cross-section on the thermal comfort properties of knitted fabrics were analysed.

MATERIALS AND METHODS

Materials

We selected four cool-touch nylon filaments with varied fibre fineness and cross-section but same denier (D) (70D), and four common nylon filaments with same specifications. All filaments were produced by Taihua New Material Co., China. Information on these filaments is shown in table 1. The surface morphology and cross-section profile of cool-touch nylon fibres and common nylon fibres are shown in figure 1. With increasing filament numbers (F) within the multifilament yarns, the average fibre diameter (d) of cool-touch nylon filament and common filament is reduced.

Knitted fabric samples made from these nylon filament yarns were produced on a Double rib circular knitting machine (E22). During production, all machine parameters for these samples were kept the same, and each fabric had an identical 1×1 interlock structure. Because single fine nylon filament is not suitable for this knitting machine, two filament yarns were combined to form a twisted yarn. The specification of eight knitted fabric samples are shown in table 2.

Table 1

THE SPECIFICATION OF COOL-TOUCH NYLON FILAMENT (CPA) AND COMMON NYLON FILAMENT (PA)								
Characteristics	CPA				PA			
Cross-section	Crisscross(+)		Circle(O)		Crisscross(+)		Circle(O)	
Number of filaments in yarn	34	68	48	68	34	68	48	68

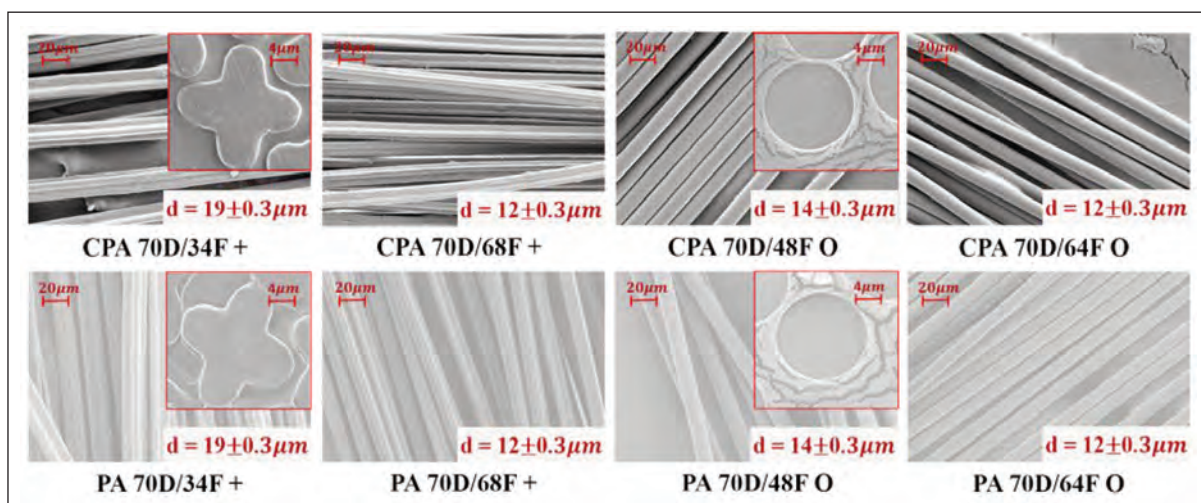


Fig. 1. Fiber surface and cross-section morphology of nylon filaments

THE SPECIFICATION OF FABRIC SAMPLES PREPARED BY NYLON TWISTED YARNS								
Characteristics	70D/34F +		70D/68F +		70D/48F O		70D/68F O	
	CPA	PA	CPA	PA	CPA	PA	CPA	PA
Weight (g/m ²)	221	218	221	225	218	220	221	223
Wale density (/5 cm)	68	68	70	68	70	70	68	68
Course density (/5 cm)	70	72	72	74	72	72	72	72
Thickness (mm)	0.900	0.883	0.813	0.826	0.840	0.840	0.834	0.836

Methods

Thermal performance of both cool-touch nylon and common nylon fibres was measured with a Differential Scanning Calorimeter (TA Q200, TA Instruments, USA). The crystallinity of fibres was calculated by ratio of heat associated with melting (fusion) of fibres against the heat of fusion for a 100% crystalline nylon sample [18].

Moisture regain is defined as the percentage of moisture present in a textile material of oven dry weight. The drying weight was obtained by drying fibre samples for 4 hours at a specific temperature of 105±3°C. The moisture was absorbed by a sample in the standard atmosphere (20±2°C and 65±2% relative humidity) for over 48 hours after drying.

Wicking height of fabric samples was measured through a vertical wicking test method. The fabric strips (2.5 cm × 30 cm) were suspended vertically in such a way that their lower ends were immersed in a reservoir with distilled water. The scale adjacent to the stripes was used to measure the wicking height in six intervals (each of five minutes) for 30 minutes.

Drying rate of fabric samples was tested with a RF4008HP Drying Rate Tester (heated-plate method, REFOND Equipment Co., China) according to AATCC MT 201 standard. The fabric test area was 15 × 15 cm².

Thermal-physiological properties of fabric were evaluated through a Sweat Guarded Hotplate apparatus (YG606, Ningbo Textile Instrument Factory, China), according to ASTM D1776/D1776M-16-2008 standard. The *q-max value* of fabric samples was tested by the KES-F7 (Kato Tech Co., Japan) in the standard environment to evaluate the transient cool-touch performance.

Dynamic cooling property was tested by measuring the thermal properties of wet fabric [19]. The test was performed by YG606 II Thermal Resistance Tester (Ningbo Textile Instrument Factory, China) that was refitted by adding a program to control heating power (22.0 W). This setup contains a testing board with some high precision temperature sensors to record the temperature changes of test board surface. Since the inner surface of fabric contacts the surface of test board, the temperature of fabric inner surface with time was measured in the testing process. The conditioned samples were soaked in water with the set weight of 20 g.

One-way ANOVA analysis (SPSS v.22.0, IBM Corp.) was performed to determine whether the varied fibre diameter and cross-section significantly affect comfort-related properties. The symbols "***" and "**" in the results represent significant differences at 99% and 95% confidence intervals respectively.

RESULTS AND DISCUSSION

Properties of filaments

Thermal properties

Cool-touch nylon fibres show lower melting enthalpy and crystallinity than those of common nylon fibres (table 3), indicating that the introduction of jade nanoparticles inhibited the crystallization of nylon fibres. Coarser cool-touch nylon and common nylon fibres 70D/48FO and 70D/34F+ show lower melting enthalpy and crystallinity than finer fibres 70D/68FO and 70D/68F+ respectively. The melting enthalpy and crystallinity of fibres with crisscross sections are higher than fibres with circular sections. The crystallinity of nylon fibres is also dependent on the conditions during the fibre extrusion process, which affect fibre fineness and cross-section.

Table 3

MELTING ENTHALPY AND CRYSTALLINITY OF COOL-TOUCH AND COMMON NYLON FIBRES				
Specification	Melting enthalpy (J/g)		Crystallinity (%)	
	CPA	PA	CPA	PA
70D/68F O	40.92	42.78	17.79	18.60
70D/48F O	36.34	39.1	15.80	17.00
70D/68F +	45.93	52.21	19.97	22.70
70D/34F +	42.22	47.47	18.36	20.64

Moisture regain is an important parameter to evaluate the moisture absorption capacity of a material. As shown in table 4, cool-touch nylon filaments have higher moisture regain than common nylon filaments with the same specifications, indicating the addition of jade nanoparticles increases the moisture absorption capacity of fibres. This is mainly caused by good moisture absorption of nano-jade [20] and the amorphous region of cool-touch fibres. Furthermore, moisture regain values of 70D/68F + and 70D/68F O filaments are higher than those of 70D/34F + and 70D/48F O filaments respectively, and moisture

THE RATE OF MOISTURE REGAIN OF COOL-TOUCH NYLON AND COMMON NYLON FILAMENTS					
Property	Filaments	70D/34F +	70D/68F +	70D/48F O	70D/68F O
Moisture regain (%)	CPA	5.46 (0.14)	6.00 (0.19)	5.30 (0.25)	5.59 (0.21)
	PA	4.56 (0.31)	4.87 (0.13)	4.33 (0.17)	4.70 (0.22)

Note. Data in brackets is the standard deviation of the mean.

regain of 70D/68F + filaments are also higher than 70D/68F O filaments. These results demonstrate that finer fibres and crisscross fibres are beneficial for moisture absorption due to the increase of fibre surface area.

Properties of knitted fabrics

Wicking height

The wicking heights of cool-touch nylon and common nylon fabric samples along wale and course directions in 30 minutes are shown in figure 2. It shows that wicking height of cool-touch nylon knitted fabrics is higher than common nylon knitted fabrics with the same yarn specifications. This is due to higher moisture and water absorption abilities of cool-touch fibres. Fibre cross-section and fineness have similar effects on wicking height of cool-touch nylon fabrics and common nylon fabrics. Higher wicking height is presented by common and cool-touch knitted fabrics prepared by crisscross section fibres, indicating crisscross section is conducive to improve vertical wicking capacity for fabrics. It is known that imbibition occurs mainly due to capillary forces, and capillary force arises from the geometry of the pores in the textiles [21]. The crisscross section nylon fibres have grooves on their surface, forming more capillaries inside the fabric which improve the wicking ability. For the samples with circular cross-section, wale and course wicking heights of fabrics made of finer fibres are higher than those of the fabrics made of coarser fibre. This is because the capillary force of fabrics made up of circular cross-section filaments is generated by spaces between the fibres. With the increase

of fibre quantity (decrease of fibre diameter) in a fixed space, there is an increase in the capillaries formed by voids between fibres. Therefore, increasing the fibre quantity or decreasing fibre diameter of yarn promotes the wicking ability of the resultant fabric. However, for the samples with crisscross section, fabrics made of finer fibres have lower wicking height. Even though the liquid movement firstly begins in the smaller capillaries under capillary pressure, it then continues to fill the larger capillaries [22]. Overlarge or undersized capillary radius decreases wicking ability of fabrics [23]. The capillary radius of the finer crisscross section fibres is too small to form effective capillaries. Meanwhile, the increased specific surface area benefits the moisture absorption but prohibits the moisture transfer. Whereas, the coarser fibres have relatively large capillary radius, which forms more effective capillaries, and are more conducive to the wicking effect of fabrics.

Drying property

As shown in figure 3, cool-touch nylon fabrics have slightly lower drying rate than common nylon fabrics made up of yarns with same specifications. This is mainly because better moisture absorption of cool-touch nylon fabrics inhibits water evaporation, which leads to poorer drying performance. It is also known that the higher drying speed is exhibited by samples made up of circular cross-section fibres in the group of fabrics made up of 70D/68F filaments over crisscross section fibre groups. The reason may be attributed to the tiny grooves of fibres within the crisscross section leading to more water being adsorbed. As a result, moisture transferring and evaporating

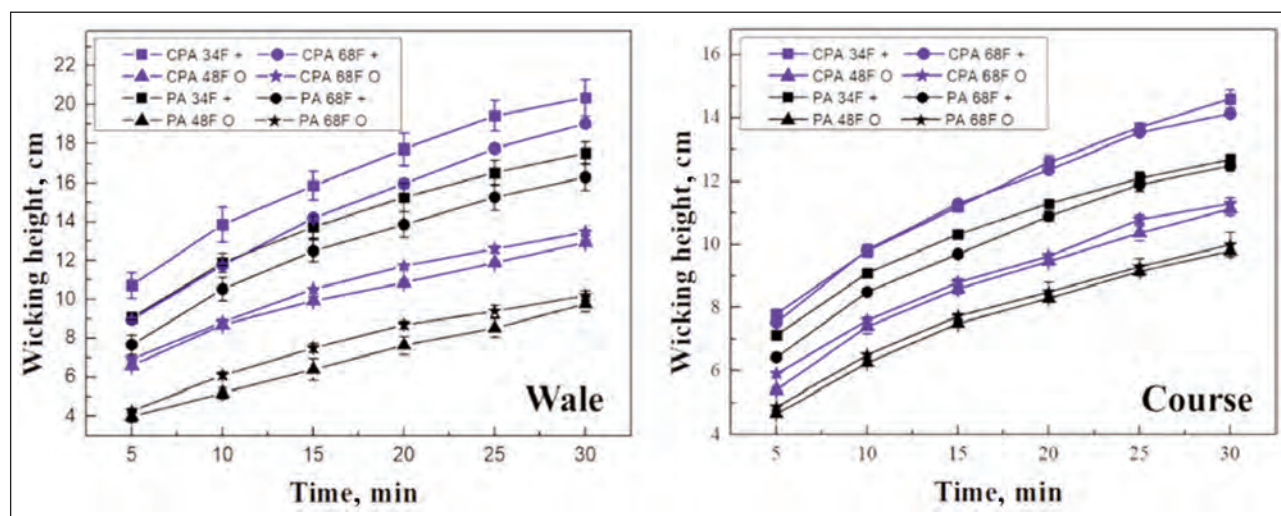


Fig. 2. Wicking height with time of cool-touch nylon and common nylon knitted fabrics

towards outside are confined. Drying speed of cool-touch nylon and common nylon samples with circular cross-section increased successively when fibre diameter decreases, e.g. 70D/48F O and 70D/68F O. This is because more capillaries are formed within the fabric. Thus, there are more channels for water diffusion and evaporation. However, there is no significant difference in drying speed between samples with crisscross section, e.g. 70D/34F + and 70D/68F +. Thus, tiny grooves on finer fibres have a negative effect on drying performance.

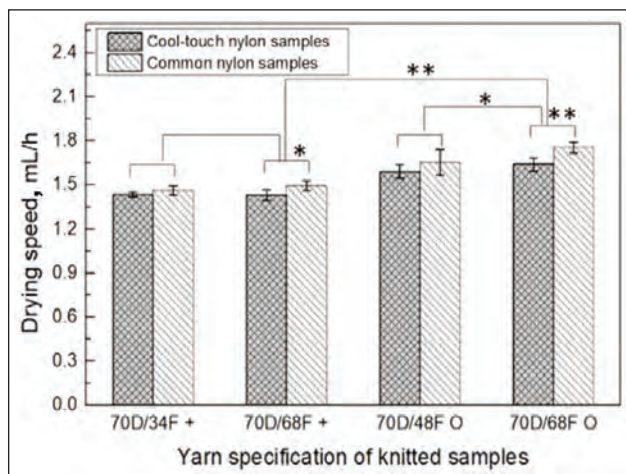


Fig. 3. The drying speed of cool-touch nylon and common nylon knitted samples

Thermal-physiological property

Testing thermal resistance and water vapour resistance can characterize the thermal-physiological properties of fabrics. As shown in figure 4, there are highly significant differences of thermal resistance and water vapour resistance between cool-touch nylon and common nylon fabric samples. The thermal resistance of cool-touch nylon samples is lower than common nylon samples. Conversely, the water vapour resistance of cool-touch nylon samples is

slightly higher than common nylon samples. This illustrates that cool-touch nylon fabrics have better heat transfer performance due to higher thermal conductivity of jade. However, better moisture absorption of cool-touch nylon fibres inhibits moisture transfer, resulting poorer moisture permeability. It also can be found from figure 4 that differences of thermal resistance and water vapour resistance between samples with varied fineness, e.g. 70D/48F O and 70D/68F O, are significant. For samples with similar circular section, thermal resistance of samples made of finer fibres is lower than samples made of coarser fibres, whereas, the water vapour resistance of these samples shows an opposite variation trend. This illustrates that better heat conduction is exhibited by fabrics made of finer fibres. Because thermal conductivity coefficient of fibres is higher than air, the lower fineness of fibres increases the contact area between fibres, which promotes thermal conduction by fibres. However, with the decrease of fineness, the moisture absorption of fibres increases, which has a negative effect on moisture permeability. For samples with similar crisscross section, there is no significant difference in water vapour resistance between fabrics with different fibre fineness. This could be due to the interaction of gaps in fabric and gaps of fibre moisture absorption. However, thermal resistance of samples made up of finer fibres is higher than samples made up of coarser fibres. The opposite trend is shown in samples with circular section. Although decreasing the diameter of crisscross section fibres improves the contact area, more still air remained in finer crisscross section fibres decreases the heat conduction. Fibber cross-section has significant effect on heat transfer performance of fabrics. The thermal resistance of samples made of crisscross section fibres, e.g. 70D/68F +, is higher than samples made of circular cross-section fibres, e.g. 70D/68F O. Irregularity of fibre cross-section hinders heat conduction, because the irregular fibre cross-section

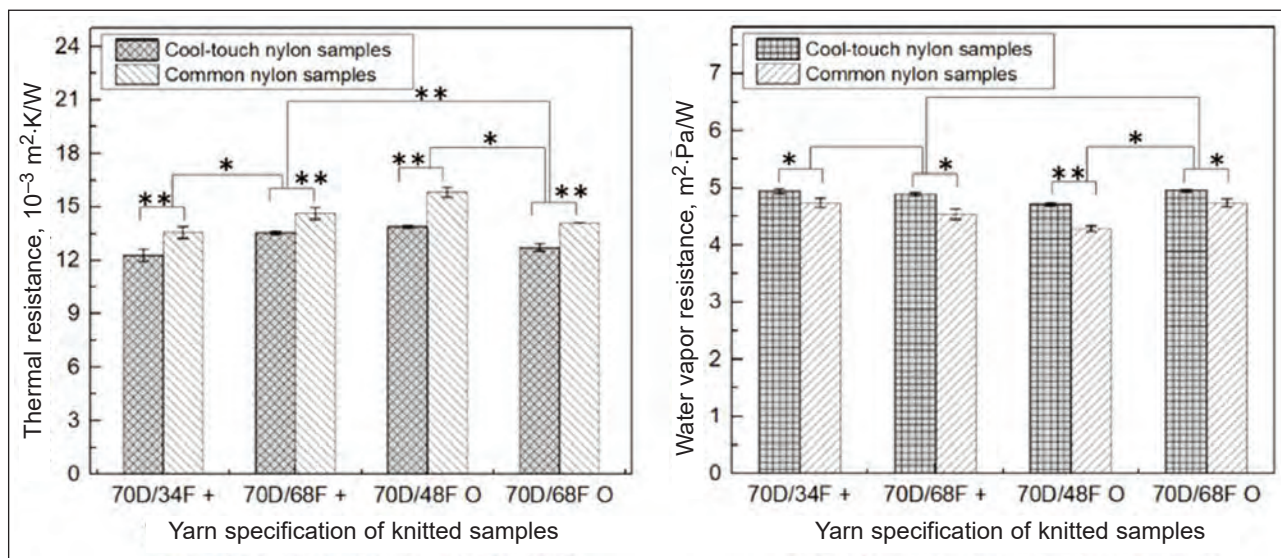


Fig. 4. Thermal resistance and water vapour resistance of cool-touch and common nylon knitted samples

increases the amount of still air contained in fabrics, and reduces the thermal conductivity of the fabric. However, due to the irregularity of fibre cross-section, more water vapour transfer channels are formed, moisture absorption then increases. Thus, there is no significant difference of water vapour resistance between samples 70D/68F + and 70D/68F O.

Transient cool touch performance

With the increase of q-max value, the cool-touch performance is enhanced [24]. The surface morphology and the thermal conductivity of the fabric material are the main factors affecting warm/cool feeling. The q-max values of the cool-touch nylon samples are significantly higher than common nylon samples (figure 5). This suggests that the usage of cool-touch nylon filaments benefits fabrics' transient cool touch performance due to their enhanced thermal conductivity. The q-max values of samples with finer fibres are less than samples with coarser fibres, e.g. samples 70D/34F + and 70D/68F +, samples 70D/48F O and 70D/68F O (figure 5). The main reason is that the q-max value is the maximum heat flux at the moment the body skin contacts fabric, which depends on the thermal transfer capacity of the fabric contacting the skin surface. Coarser fibres are more favourable to

heat transfer through fibres and improve maximum heat flux when body skin contacts fabric.

Dynamic cooling property

The heat and moisture transfer of clothing is a dynamic process after absorbing moisture. The excellent heat conduction and moisture diffusion benefit the improvement of cooling performance. The dynamic cooling function after sweating could be estimated by measuring the heating property of wet fabrics. With the decreasing temperature of samples in a given heating time, the dynamic cooling property is better [19]. As shown in figure 6, a, wet cool-touch nylon samples and common nylon samples have similar heating property, and their heating temperature with time is significantly lower than the test board. This illustrates that wet fabric significantly promotes the cooling function due to moisture transfer and evaporation. It is also shown that there are two stages in the heating process of wet samples. In the first stage, the temperature increases slightly. However, the temperature increases significantly in the second stage. At the beginning, the moisture evaporation takes away much heat and moisture, which improves the heat loss of fabric. More gaps in wet fabric are filled with water rather than still air, which also increases the heat conductivity of fabric. As a result, temperature increases slowly at this stage. Subsequently, the evaporation rate and heat conductivity decrease with decreasing water content, resulting in a rapid increase of temperature.

Figure 6, b shows the temperature difference between wet samples and test board with heating time. It is an important parameter for evaluating the cooling function of fabrics used for summer and sports clothing [19]. The maximum temperature difference is in the range 7°C to 7.88°C. This illustrates that moisture evaporation obviously improves cooling effect.

In order to investigate the cooling efficiency, the average cooling rate was calculated (figure 6, c). With the increasing average cooling rate, the fabric has better cooling performance. The average cooling rates of cool-touch nylon samples are higher than common

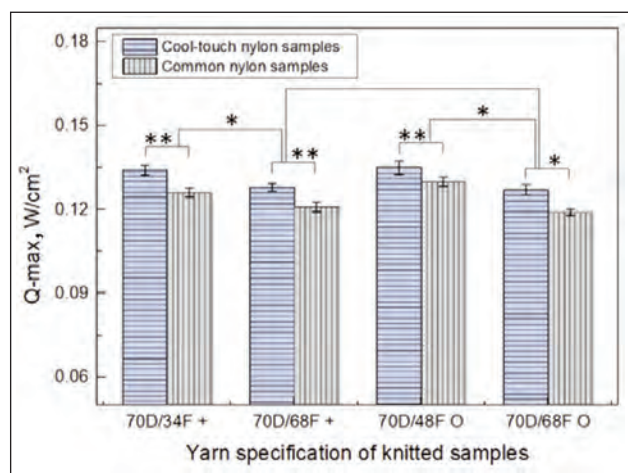


Fig. 5. The q-max values of cool-touch nylon and common nylon knitted samples

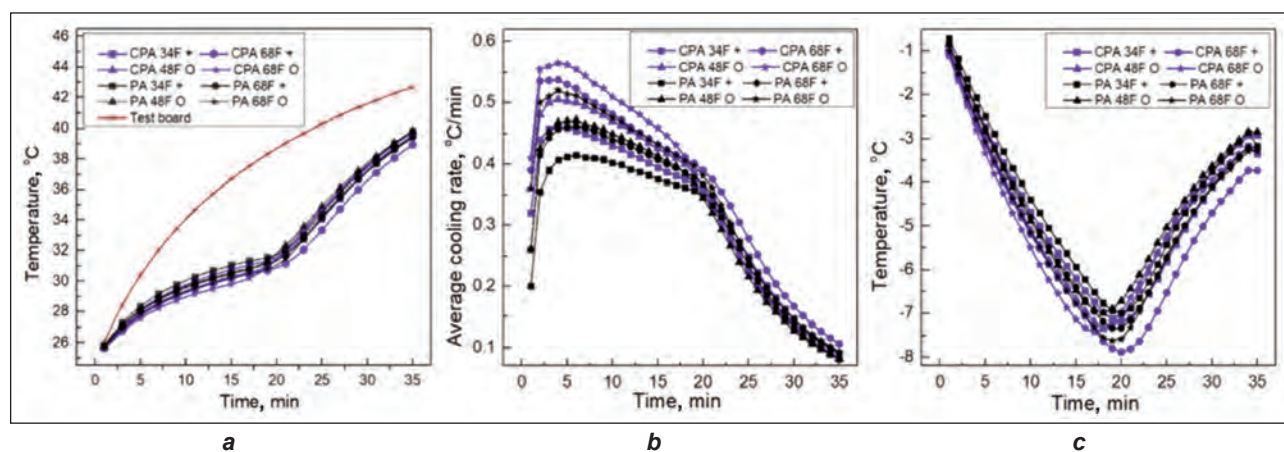


Fig. 6. Dynamic cooling performance of wet samples: a – the temperature variation heating time; b – the temperature difference between wet samples and test board with time; c – the average cooling rate with time

nylon samples with the same specification respectively. It demonstrates that cool-touch nylon knitted fabrics have better cooling performance. This is explained by better heat transfer ability of cool-touch nylon fabrics than common nylon fabrics.

Furthermore, samples made up of finer fibres have better cooling property than samples made up of coarser fibres. Meanwhile, higher cooling rate is exhibited by samples made up of circular cross-section fibres in the group of samples made up of yarns with 68F. Fibbers with crisscross section have no positive effect on the improvement of the dynamic cooling property of knitted fabrics prepared by nylon filaments used in this work. Thus, to improve the dynamic cooling property of nylon knitted fabrics used for summer and sports clothing, using filaments made of finer fibres and cool touch filaments with circular cross-section is an effective way.

CONCLUSION

In this work, the physical properties of cool-touch nylon filaments and common nylon filaments, and thermal comfort properties of their knitted fabrics with 1×1 interlock structure were investigated. Meanwhile, the effects of fineness and fibre cross-section of

common and cool-touch nylon filaments on comfort properties of their knitted fabrics were examined. It was found that cool-touch nylon fibres had better moisture absorption, but slightly lower crystallinity than common nylon fibres. Cool-touch nylon fabrics had better wicking capacity, thermal transfer and cooling properties, but poorer drying performance and moisture permeability than common nylon fabrics. Fibre fineness and cross-section had similar effects on thermal comfort properties of cool-touch nylon and common nylon knitted fabrics. Finer fibres were conducive to improve drying performance, thermal transfer and dynamic cooling properties of their knitted fabrics. Nylon yarns with fine crisscross section filaments had no positive effect on thermal-wet comfort ability of their fabrics. Therefore, using nylon multi-filament yarns with finer filaments and cool touch filaments provides an effective way to develop thermal-wet comfort knitted fabrics used for summer or sports clothing.

ACKNOWLEDGEMENTS

This work was supported by National Key R&D Program of China under Grant 2017YFB0309100, "the Fundamental Research Funds for the Central Universities under Grant CUSF-DH-D-2018024", and China Scholarship Council under Grant 201806630035.

REFERENCES

- [1] Jia, N., Fraenkel, H., Kagan, V., *Effects of moisture conditioning methods on mechanical properties of injection molded nylon 6*, In: Journal of Reinforced Plastics and Composites, 2004, 23, 7, 729–737
- [2] Kumar, B., Kumar, M., Parthiban, M., Ramachandran, T., *Effect of Pique and Honeycomb Structures on Moisture Management Properties of Eri Silk Knitted Fabrics*, In: Journal of Natural Fibers, 2019, 16, 1–10
- [3] Pan, Y., Hsieh, C., Lou, C., Wang, C., Lin, Z., Chen, Y., Lin, J., *Elastic knits with different structures composed by using wrapped yarns: Function and comfort evaluations*, In: Fibers and Polymers, 2017, 18, 9, 1816–1824
- [4] Park, J., Yoo, H., Hong, K., Kim, E., *Knitted fabric properties influencing coolness to the touch and the relationship between subjective and objective coolness measurements*, In: Textile Research Journal, 2018, 88, 17, 1931–1942
- [5] Han, H., Kim, J., *A study on the thermal and physical properties of nylon fabric treated by metal sputtering (Al, Cu, Ni)*, In: Textile Research Journal, 2018, 88, 21, 2397–2414.
- [6] Rezaei, F., Maleknia, L., Valipour, P., Chizari, G., *Improvement properties of nylon fabric by corona pre-treatment and nano coating*, In: The Journal of The Textile Institute, 2016, 107, 10, 1223–1231
- [7] Ahn, K., Kim, K., Kim, M., Kim, J., *Fabrication of silicon carbonitride-covered boron nitride/Nylon 6, 6 composite for enhanced thermal conductivity by melt process*, In: Ceramics International, 2015, 41, 2, 2187–2195
- [8] Liu, Y., Meng, J., Han, Y., Shan, H., *Development of Jade Nylon-Based Fibers and Viscose Blended Yarn*, In: Advanced Materials Research, 2011, 332, 2135–2141
- [9] Guo, S., Yu, D., Liu, Y., Wang, Z., Zhu, C., Zhang, H., *Design and development of cool multifunctional composite high-grade fabrics*, In: Applied Mechanics and Materials, 2014, 633, 476–479
- [10] Zhou, H., Wang, H., Niu, H., Zeng, C., Zhao, Y., Xu, Z., Fu, S., Lin, T., *One-Way Water-Transport Cotton Fabrics with Enhanced Cooling Effect*. In: Advanced Materials Interfaces, 2016, 3, 17, 1–6
- [11] Jhanji, Y., Gupta, D., Kothari, V., *Effect of fibre, yarn and fabric variables on heat and moisture transport properties of plated knit*, In: Indian Journal of Fibre & Textile Research, 2017, 42, 3, 255–263
- [12] Jia, T., Wang, Y., Dou, Y., Li, Y., Andrade, M., Wang, R., Fang, S., Li, J., Yu, Z., Qiao, R., Liu, Z., *Moisture Sensitive Smart Yarns and Textiles from Self-Balanced Silk Fiber Muscles*, In: Advanced Functional Materials, 2019, 29, 18, 1808241
- [13] Kumar, B., Das, A., *Vertical wicking behavior of knitted fabrics*, Fibers and Polymers, 2014, 15, 3, 625–631
- [14] Li, Y., Holcombe, B., Dear, R., *Enhancement of coolness to the touch by hygroscopic fibers: part II: physical mechanisms*, In: Textile Research Journal, 66, 9, 587–594
- [15] Gun, A., *Dimensional, physical and thermal comfort properties of plain knitted fabrics made from modal viscose yarns having microfibers and conventional fibers*, In: Fibers and Polymers, 2011, 12, 2, 258–267
- [16] Hesa L., Ursache M., *Effect of composition of knitted fabrics on their cooling efficiency at simulated sweating*, In: Indian Journal of Fibre & Textile Research, 2011, 36, 281–284.

- [17] Nazir, M., Shaker, K., Nawab, Y., Fazal, M., Khan, M., Umair, M., *Investigating the effect of material and weave design on comfort properties of bilayer-woven fabrics*, In: The Journal of the Textile Institute, 2017, 108, 8, 1319–1326
- [18] Millot, C., Fillot, L., Lame, O., Sotta, P., Seguela, R., *Assessment of polyamide-6 crystallinity by DSC*, In: Journal of Thermal Analysis and Calorimetry, 2015, 122, 1, 307–314
- [19] Yang, Y., Zhang, W., Zhang, P., *Evaluation method for the hygroscopic and cooling function of knitted fabrics*, In: Textiles Research Journal, 2019, 89, 23–24, 5024–5040
- [20] Cui, S., Zhu, J., Li, B., Wang, S., Liu, Y., *Structure and Physical Properties of Jade Fiber*, In: Advanced Materials Research, 2012, 441, 767–771
- [21] Parada, M., Derome, D., Rossi, R., Carmeliet, J., *A review on advanced imaging technologies for the quantification of wicking in textiles*, In: Textile Research Journal, 2017, 87, 1, 110–132
- [22] Saricam, C., Kalaoğlu, F., *Investigation of the wicking and drying behaviour of polyester woven fabrics*, In: Fibres & Textiles in Eastern Europe, 2014, 105, 3, 73–78
- [23] Zhang, Y., Wang, H., Zhang, C., Chen, Y., *Modeling of capillary flow in shaped polymer fiber bundles*, In: Journal of materials science, 2007, 42, 19, 8035–8039
- [24] Inoue, T., Nakayama, A., Niwa, M., *Relationship between the warm/cool feeling of fabric and the subjective evaluation of the quality of ladies' knitted fabrics*, In: International Journal of Clothing Science and Technology, 2010, 22, 1, 7–15

Authors:

YANG YANG¹, YU XIN², WANG XUNGA², LIU XIN², ZHANG PEIHUA¹

¹Donhua University, College of Textiles, 2999 North Renmin Road, Songjiang District, 201620, Shanghai, China

²Deakin University, Institute for Frontier Materials, 75 Pigdons Road, Waurn Ponds, 3216, Geelong, Australia

Corresponding authors:

LIU XIN

e-mail: xin.liu@deakin.edu.au

ZHANG PEIHUA

e-mail: phzh@dhu.edu.cn

Effect of plasma grafting with Hexamethyldisiloxane on comfort and flame resistance of cotton fabric

DOI: 10.35530/IT.072.02.1842

RIADH ZOUARI
SONDES GARGOUBI

EMILIA VISILEANU

ABSTRACT – REZUMAT

Effect of plasma grafting with Hexamethyldisiloxane on comfort and flame resistance of cotton fabric

We investigated the potential of atmospheric plasma technology to enhance the properties of textile material against flame propagation before and after washing. The effects of this treatment on the rigidification of the media were also determined using draping and bending stiffness tests. We showed that depositing Silicone molecules on cotton fabrics leads to flame retardant cotton with a conservation of the whole structure after burning. Moreover, washing of the sample evidenced high permanency of the thin grafted coating against chemical domestic washing detergent. Nevertheless, comfort properties of the textile decrease, which limits the applications of the plasma eco-friendly technology in the clothing industry.

Keywords: *plasma activation, Siloxane, comfort, flame resistance*

Influența grefării cu plasmă de hexametildisiloxan asupra confortului și rezistenței la flacără ale materialelor textile din bumbac

A fost investigat potențialul tehnologiei cu plasmă la presiune atmosferică de a spori proprietățile materialului textil împotriva propagării flăcării înainte și după spălare. Influența acestui tratament asupra rigidizării mediilor a fost determinată prin teste de rigiditate la îndoire și drapaj. S-a demonstrat că depunerea moleculelor de silicon pe materialele textile din bumbac conduce la ignifugare, prin conservarea întregii structuri după ardere. Mai mult, spălarea probei a evidențiat o permanență ridicată a stratului subțire grefat la detergentul chimic de spălat pentru uz casnic. Cu toate acestea, proprietățile de confort ale materialelor textile se diminuează, ceea ce limitează aplicațiile tehnologiei ecologice cu plasmă în industria confecțiilor.

Cuvinte-cheie: *activare cu plasmă, Siloxan, confort, rezistență la flacără*

INTRODUCTION

Worldwide demand for functional fibrous materials has increased significantly in recent years [1]. This increase is evidently accompanied with technical quality and environmental requirements [2]. This is particularly true in the field of protective textile, particularly for those facing the risk of fire since the standards and regulations on the fire resistance of textiles have been extended to a large number of sectors such as building, children's nightwear, transport, house equipment and gas barrier [3, 4]. At present, many chemical treatments make it possible to obtain textiles with flame-retardant properties [5], but these processes present some disadvantages as they are generally not eco-friendly [6]. In fact, the conventional processes either need a great consumption of energy and water or impose the use of chemical toxic compounds. Moreover, the final flame resistant material presents a significant change in its properties like a loss of its flexibility which make it less soft and not comfortable in wearing. Furthermore, the treatments are not resistant to washing and the textile becomes flammable after few domestic washing cycles. For these reasons, industries are continuously looking for

new techniques and chemical products which are respectful of environmental safety guidelines and presents acceptable efficiency of ignition. Processes based on padding techniques with eco-friendly chemistry like phosphor and Siloxane are being tested [7–9].

In recent years, plasma technologies have been involved in several industrial processes in materials, finishing and functionalization [4, 10]. These technologies offer the advantage to be low energy consumer, soft enough when applied to different materials and to have low environmental impact. In the textile field, plasma activation was found to be an efficient technique for the modification of natural and synthetic textile materials. Indeed, it has been successfully applied to enhance dyeability of various fibres [11]. In addition, it was able to replace several wet finishing processes. The plasma finishing applications are realized through surface activation, ablation, etching, cross-linking, functionalization, film deposition or by a combination of these effects [12]. Nowadays, a great attention is paid to the development of flame retardant textiles using plasma activation for better attachment of chemicals. An important

number of reports were published detailing the use of plasma to enhance finishing products attachment. In this context, atmospheric plasma technology has assumed a great attention since it is a dry and environmental method to achieve surface modification [13, 14]. Atmospheric plasma has been used as it could be integrated within an already established continuous process. Therefore, this eco-friendly technology will not induce significant decrease of the productivity that makes it acceptable by industries in an economic point of view. In this paper, we investigate the effect of a silicone coating applied with atmospheric pressure plasma jet technology on the comfort and flame retardant properties of cotton woven fabric. Comfort properties have been studied with draping and bending stiffness using Peirce cantilever. Flame resistance was evidenced by exposing the textile fabric to a flame and recording ignition time as well as flame propagation velocity.

MATERIALS AND METHODS

Material

The fabric used is plain woven cotton with 57 threads per centimetre in warp and weft. Its surface mass is 123.5 gsm. Weft and warp threads are 13.44 Tex and 14.22 Tex respectively.

Atmospheric Pressure Plasma Jet

Figure 1 illustrates the atmospheric pressure plasma jet technology system from Plasmatreat Company (Plasmatreater AS400) used for the deposition of SiO_x thin films at atmospheric pressure. A high-frequency (23 kHz) pulsed voltage was applied between two tubular electrodes separated by a dielectric material. The PT400 generator delivers a pulse-pause modulated current.

The current modulation is controlled by adjusting the plasma cycle time (PCT). With a PCT of 100%, the pulse duration is equal to the pause duration. The main gas flow consists of dry air, which was introduced through the torch at a pressure of 5 Bar. Cotton samples were treated at a moving speed of 10 m/min over a surface of 5 mm² Hexamethyldisiloxane (HMDSO, $(\text{CH}_3)_3\text{SiOSi}(\text{CH}_3)_3$, purity 98.5%, Sigma–Aldrich) was vaporized at 130 °C, mixed with nitrogen, and introduced into the plasma jet in a downstream region. The flow of the HMDSO was of 20 g/h for thin film and of 60 g/h for thick coating film. This variation induces a change in the concentration of Siloxane deposited onto the treated surface. The torch can be moved in the x- and y-directions, to deposit films over large surfaces, with a typical velocity and substrate to nozzle distance of 5 m/min and 30 mm, respectively.

Scanning Electron Microscopy (SEM)

Scanning Electron Microscope (Model HITACHI TM 3000) was used for morphological characterization of the cotton fibre surface at high magnification. The metallized specimens were analysed in partial vacuum conditions (0.1–0.15 torr), and under an accelerating

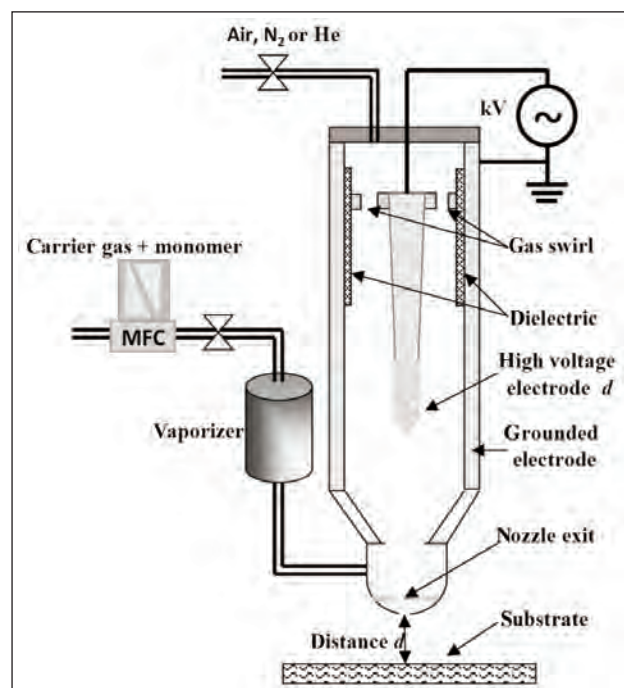


Fig. 1. Atmospheric pressure plasma jet technology system

voltage of 15 kV. Scanning Electron Microscopy with Energy Dispersive X-Ray (SEM-EDX) analyses are performed to determine the elementary chemical composition or to present cartography of the distribution of the elements in the form of an image.

Draping

Standardized tests, according to the French standard of draping NF G 07-109, were performed to determine how a textile fabric fall under its own weight into wavy structures. These structures are quantified objectively to give the draping factor of the fabric. The methods of determining the draping characteristics of a fabric use a circular support on which a circular shaped fabric sample is placed with a protruding section of the support. A ruler is used to record the vertical projection of the contour of the textile specimen falling from the base in 16 positions all around. In our case, the specimen was cut with a diameter of 25 cm and the support diameter was of 15 cm. The Drape factor, F , will then be calculated according to the equation 1 where “ d_i ” is the diameter associated to the projection of the textile vertically on a parallel plan to the circular support of the drape meter:

$$F = (d_i^2 - 225) / 400 \quad (1)$$

where $i = 1$ to 16. F is comprised between 0 and 1. The more F approaches 0, the more textile fabric is flexible. $F = 0$ corresponds to extremely flexible fabric. $F = 1$ corresponds to rigid fabric which does not fall apart the circular support.

This factor also reflects the shear stiffness of a textile material and its comfort when oriented to the clothing industry.

Bending stiffness

Standardized (ISO 9073-714005) flexibility tests are performed with the Peirce flexi-meter to determine the bending stiffness of our fabric. In his attempt to evaluate a fabric hand, Peirce introduced the principle of cantilever deformation in textiles to characterize fabric bending [15]. The fabric is made to deform under its own weight and the cantilever length necessary to produce a predetermined deflection angle is measured. As shown in the figure 2, a strip of fabric with well-defined dimensions is moved forward on a horizontal board to project as a cantilever. As soon as the extreme point of the curved fabric touch the inclined board regulated on 41.5° relative to the horizontal one, the cantilever length L is recorded. This length is then used to calculate the bending length C and the bending rigidity G of the fabric according to equations 2 and 3:

$$C = L * (\cos(\alpha/2) / 8 \tan \alpha)^{1/3} \sim L/2 \quad (2)$$

$$G = w * C^3 \quad (3)$$

where w is the fabric mass per unit area.

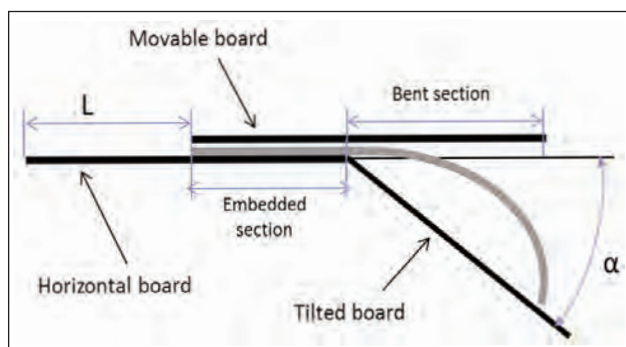


Fig. 2. Peirce cantilever tests for fabrics

Flame propagation

Tests were performed according to the French standard NF G 07-182 in order to determine the ignition time of the fabric and the flame propagation velocity for fabrics put on 45° inclined plane. The flame was 40 mm height, ignited with propane gas and placed perpendicular to the sample holder. The sample has been chosen 200 mm far from the edge of the entire woven fabric and has dimensions of 160 mm \times 600 mm.

RESULTS AND DISCUSSIONS

Morphology of the coating

The SEM micrographs show the normal spiral structure of cotton fibre. The untreated surface was found relatively smooth. After flame retardant treatment, the surface of the cotton becomes rougher with the presence of micro particles, which is suggested to be the HMDSO.

EDX analysis shows that they are associated to Siloxane functional groups that represent 35% of the global surface composition of the fibre in the case of the thick film and 22% in the case of the thin film. This result is in agreement with previous studies showing that Siloxane is detected on the surface of the coatings elaborated from a solution containing HMDSO. The Si ratio depends on the volumetric ratio of HMDSO [16].

Meanwhile, these microscopic observations on the figure 3 don't give idea whether the treatment penetrated the whole fibres or form a coating to the apparent surfaces exposed to plasma activation. For that reason, the treated cotton fibres sections have been observed under SEM-EDX technique to give composition cartography of the treated fibres section.

Experimentally, when the cotton yarns are cut with scissors or a blade at room temperature, the section at the edge is altered and could not be representative of the whole fibres section within the yarn. To overcome this disadvantage, the fabric has been cut after cooling the whole textile at -120°C with liquid nitrogen then making a sharp fracture that allows maintaining a realistic fibre section. The element Si has been isolated and represented with the blue colour whereas the fibre components (almost Carbon and Oxygen) with green colour. We observe that the Siloxane coating is concentrated on the external surface of the fibres which are exclusively exposed to the plasma jet.

A simple method was used to confirm the coating formation. The adhesion was evaluated as percent weight add on the samples by substitution in equation 4:

$$\text{weight add on (\%)} = 100 \frac{W_t - W_0}{W_0} \quad (4)$$

where W_0 is initial weight of test sample, and W_t – final weight of test sample. Tests were realized following

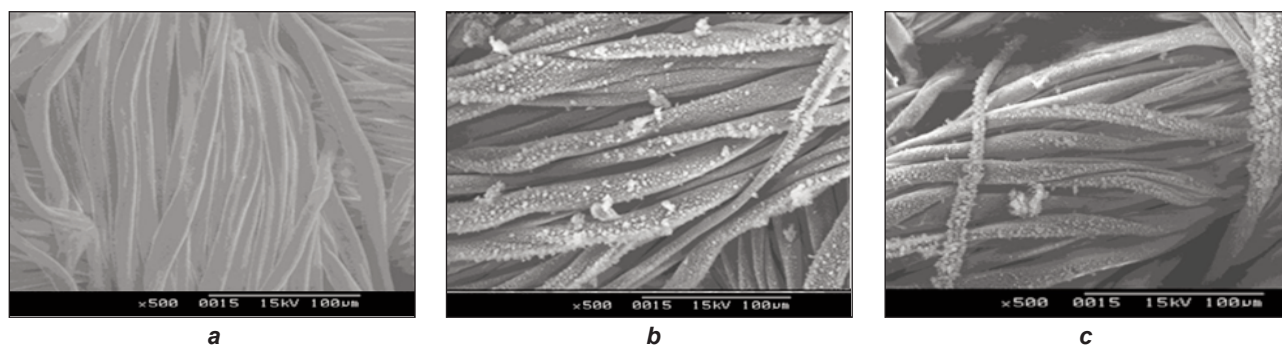
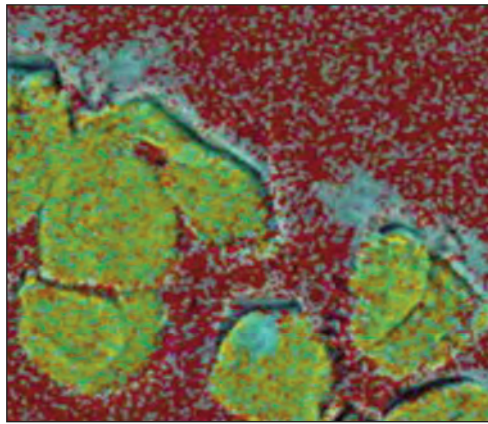
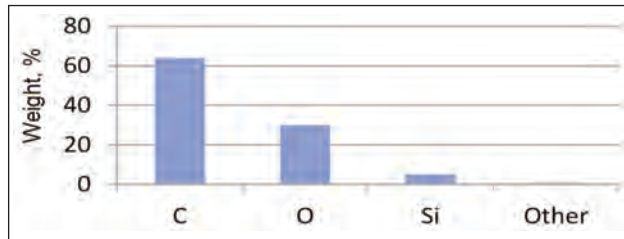


Fig. 3. SEM Micrographs associated to: a – non treated cotton fibres; b – treated with plasma deposited HMDSO in thick coating; c – treated with plasma deposited HMDSO in thin coating



a



b

Fig. 4. Graphical representations of: a – cotton fabric treated with thick plasma coating observed from the section; b – plasma coating's elementary chemical composition

samples preconditioning in a standard atmosphere ($20 \pm 2^\circ\text{C}$, $65 \pm 2\%$ RH).

Coated cotton (thick coating) showed a weight add on of about 7%. This result reveals that the plasma modification have made the fabric receptive to Siloxane which usually has reduced affinity to cellulose fibres.

Draping and bending stiffness

Draping factor increases by 16% and 21% for thin and thick coating respectively. Bending under own weight gravity shows the same tendencies for weft and warp yarns. These results prove that the application of Siloxane coating assisted with plasma jet technology is accompanied with an isotropic decrease of the fabric softness (table 1).

Table 1

DRAPING FACTOR AND BENDING RIGIDITY ASSOCIATED TO THE COTTON FABRIC AT RAW STATE AND TREATED WITH THICK AND THIN COATING			
Characteristics	Raw cotton	Thin coating	Thick coating
Draping Factor	0.71	0.83	0.86
Weft Bending stiffness (N/mm)	842	966	999
Warp Bending stiffness (N/mm)	273	308	315

The important increase in values compared with the control fabric is also attributed to the fact that, during the coating process, only the outer surface of the fibres is treated. This method is often accompanied by excessive weight add on, loss of drape and reduced comfort [17].

As the rigidity of the fabric is generally attributed to the macromolecular structure of fibres coupled with the friction between the fibres [18, 19], it could be deduced that the coating enhances the surface fibre friction probably by creating Siloxane bridges between fibres exposed to the plasma jet. This rigidification could not be attributed to the thermal effect induced to the fabric by plasma. In fact, we exposed the fabric to high temperature reaching 105°C for 30 minutes without Siloxane deposition and we obtained flexibility and draping factors similar to non-treated cotton.

Resistance to flame

In this study we are interested to different parameters related to the behaviour of the fabric when exposed to flame. First we investigated the time laps needed to ensure the ignition of the fabric after being in contact with the flame. Then, we investigated the velocity of the flame after ignition. Thereafter, we studied the final structure remaining after ignition being finished. All these data could determine the flame resistance class and orient the final applications associated to the treated textile. Table 2 summarizes the

Table 2

BEHAVIOUR OF COTTON FABRIC EXPOSED TO FLAME AT RAW STATE, AND TREATED WITH SILOXANE BEFORE AND AFTER WASHING				
Samples	Ignition time (s)	Flame propagation velocity (cm/s)	Surface remaining (%)	Residue
Raw cotton fabric	0.3	1.7	0	ashes
Thin Siloxane coating	1	1.1	70	structure conserved but carbonized
Thick Siloxane coating	1.3	0.8	85	structure conserved but carbonized
Thin Siloxane coating after washing	1	1.1	70	structure conserved but carbonized
Thick Siloxane coating after washing	1	1.1	70	structure conserved but carbonized

results obtained for the flame resistance performances of the raw and treated cotton fabric.

The resistance to the treatment against domestic washing has been tested according to ISO 6330:2000 [20], procedure 8A (delicate cycle, 30°C) in an automatic washing machine. For the washing process, the sample was stitched onto a piece of ballast.

Compared to the non-treated cotton fabric, Siloxane deposition on the surface improves significantly the textile flame resistance. In fact, the ignition time increases from 0.3 s to 1 s for thin coating then to 1.3 s for thick treatment. Moreover, the velocity of the flame on the fabric after ignition decreases by 35% and almost to the half for thin and thick coating, respectively. These delay in ignition and lowliness in propagation are very important in case of conflagration as it gives more time for rescue and intervention. In another hand, the conservation of the fabric structure after total burning is of high importance especially for house curtains. Actually, in case of fire starting in the curtains, the structure will be maintained and flammable textile will not fall down on carpets which inhibit the propagation of fire in the whole room. After washing, fabric treated with thin coating conserves its properties versus flame exposition whereas the thick coating was not totally permanent to washing and its behaviour becomes similar to that of thin coating fabric. This could be explained by the fact that in thin coating, Siloxane was strongly deposited on the active sites of cotton until saturation of these sites. Thick coating seems to be a superposition of Siloxane films that are not deposited directly on cotton but tethered, with physical affinity, to already deposited film. This physical tethering forms weak bonds which desorbed with washing in only one cycle.

CONCLUSIONS

Applying Siloxane coating on the cotton fabric surface upgrades the protective properties of the textile

to ignition as it postpone the ignition time, slows the propagation of the flame and conserve almost the whole structure of the burned fabric. The application of the Siloxane deposition using plasma technology presents evenly many ecological advantages. In fact, the technology itself is green as it consumes exclusively electrical energy but does not generate wastes that will be ejected in the nature like conventional treatment techniques which need post-industrial waste treatments. The dust generated from the samples facing the plasma is removed using a system that allows the collection and transport of dust particles in a vacuum environment. The particles are charged, floated and collected due to an electrostatic attraction. Moreover, plasma technology could be integrated in already implemented machines as the plasma torch is not bulky and could be hanged between industrial machines or moved using robots. The Siloxane molecules applied are respectful to toxicity guidelines like Reach and RoHS as they do not imply diseases for end-user and within factories. We showed that the Siloxane deposition assisted with plasma jet technology is mainly a surface treatment that does not reach the yarn cores for better flame resistant properties. A thin Siloxane coating film is strongly deposited on the cotton fabric, which conserves its properties after one cycle of domestic washing. Nevertheless, the application of Siloxane with plasma jet technology induces a significant decrease in the fabric softness which could be evidenced with draping and bending stiffness experiments. These draping and bending factors are very important for textile comfort when applied to clothing.

ACKNOWLEDGMENTS

This work was funded by the Tunisian Ministry of Higher Education and Scientific Research in the framework of the PROJECT 18PJEC12-22.

REFERENCES

- [1] Peng, Y., Cui, Y., *Advanced Textiles for Personal Thermal Management and Energy*, In: Joule, 2020, 4, 1–19
- [2] Keawploy, N., Venkatkarthick, R., Wangyao, P., Zhang, X., Liu, R., Qin, J., *Eco-Friendly Conductive Cotton-Based Textile Electrodes Using Silver- and Carbon-Coated Fabrics for Advanced Flexible Supercapacitors*, In: Energy Fuels, 2020, 34, 7, 8977–8986
- [3] Scopece, P., Viaro, A., Sulcis, R., Kulyk, I., Patelli, A., Guglielmi, M., *Plasma Process*, In: Polym., 2009, 6, S705
- [4] Chapple, S., Anandjiwala, R., *Flammability of Natural Fiber-reinforced Composites and Strategies for Fire Retardancy: A Review*, In: Journal of Thermoplastic Composite Materials, 2010, 23, 6, 871–893, <https://doi.org/10.1177/0892705709356338>
- [5] Samanta, K.K., Basak, S., Chattopadhyay, S., *Sustainable Flame-Retardant Finishing of Textiles: Advancement in Technology*, In: Handbook of Sustainable Apparel Production, CRC Press: Boca Raton, FL, USA, 2015, 64–89
- [6] Lu, S.Y., Hamerton, I., *Recent developments in the chemistry of halogen-free flame retardant polymers*, In: Prog. Polym. Sci. Oxf., 2002, 27, 8, 1661–1712
- [7] Khan, F., *Characterization of methyl methacrylate grafting onto preirradiated biodegradable lignocellulose fiber by γ -radiation*, In: Macromol. Biosci., 2005, 5, 1
- [8] Ragoubi, M., Bienaimé, D., Molina, S., George, B., Merlin, A., *Impact of corona treated hemp fibres onto mechanical properties of polypropylene composites made thereof*, In: Industrial Crops Prod., 2010, 31, 2, 344–349

- [9] Baltazar-y-Jimenez, A., Bistriz, M., Schulz, E., Bismarck, A., *Atmospheric air pressure plasma treatment of lignocellulosic fibres: impact on mechanical properties and adhesion to cellulose acetate butyrate*, In: Compos. Sci. Technol., 2008, 68, 1
- [10] Gargoubi, S., Saghrouni, F., Chevallier, P., Tolouei, R., Boudokhane, C., Ladhari, N., Mantovani, D., *Polydopamine-modified interface improves the immobilization of natural bioactive-dye onto textile and enhances antifungal activity*, In: Biointerphases, 2020, 15, 4, <https://doi.org/10.1116/6.0000295>
- [11] Agnhagea, T., Perwuelz, A., Behary, N., *Eco-innovative coloration and surface modification of woven polyester fabric using bio-based materials and plasma technology*, In: Industrial Crops and Products, 2016, 86, 334–341
- [12] Abd Jelil, R., *A review of low-temperature plasma treatment of textile materials*, In: Journal of Materials Science, 2015, 50, 5913–5943
- [13] Puytel, J., Kumar, V., Peng, P., Micheli, V., Laidani, N., Arefi-Khonsari, F., *Deposition of Organosilicon by a Non-Equilibrium Atmospheric Pressure Plasma Jet: Design, Analysis and Macroscopic Scaling Law of the Process*, In: Plasma Processes and Polymers, 2011, 8, 664–675
- [14] Fridman, A., Kennedy, L.A. (Eds.), *Plasma Physics and Engineering*, Taylor and Francis, New York, 2004
- [15] Peirce, F.T., *The "Handle" of Cloth as a Measurable Quantity*, In: J. Text. Inst., 1930, 21, T377
- [16] Hilt, F., Gherardi, N., Duday, D., Berne, A., Choquet, P., *Efficient Flame Retardant Thin Films Synthesized by Atmospheric Pressure PECVD through the High Co-deposition Rate of Hexamethyldisiloxane and Triethylphosphate on Polycarbonate and Polyamide-6 Substrates*, In: ACS Applied Materials & Interfaces, 2016, 8, 12422–12433
- [17] Gupta, D., *Emerging techniques for functional finishing of textiles*, In: Indian Journal of Fibre and Textile Research, 2011, 36, 4, 388
- [18] Ghosh, T.K., Zhou, N., *Characterizaion of fabric bending behavior: A review of measurement principles*, In: Indian Journal of Fibre & Textile Research, 2003, 28, 471–476
- [19] Boisse, P., Hamila, N., Vidal-Sallé, E., Dumont, F., *Simulation of wrinkling during textile composite reinforcement forming. Influence of tensile, in-plane shear and bending stiffnesses*, In: Composites Science and Technology, Elsevier, 2011, 71, 5, 683
- [20] Reifler, F.A., Fortunato, G., Gerhardt, L.-C., Seeger, S., *A Simple, One-Step Approach to Durable and Robust Superhydrophobic Textiles*, In: Advanced Functional materials, 2008, 18, 3662-3669

Authors:

RIADH ZOUARI¹, SONDES GARGOUBI¹, EMILIA VISILEANU²

¹Textile Engineering Laboratory – LGTex, University of Monastir,
Av Haj Ali Soua, BP68, 5070 Ksar Hellal – Tunisia

²The National Research and Development Institute for Textiles and Leather,
16, Lucretiu patrascanu Street, Bucharest, Romania
e-mail: e.visileanu@incdtp.ro

Corresponding author:

RIADH ZOUARI
e-mail: Riadh.Zouari@ksarhelal.r-iset.tn